UNIVERSIDADE FEDERAL DE MINAS GERAIS
Instituto de Ciências Biológicas
Programa de Pós-graduação em Biologia Celular

Graziela de Paula Ferreira Dantas

AVALIAÇÃO DOS EFEITOS DE NANOPARTÍCULAS INORGÂNICAS NA TOXICOLOGIA REPRODUTIVA MURINA

Belo Horizonte
2024

Graziela de Paula Ferreira Dantas

AVALIAÇÃO DOS EFEITOS DE NANOPARTÍCULAS INORGÂNICAS NA TOXICOLOGIA REPRODUTIVA MURINA

Tese apresentada ao Programa de Pós-Graduação em Biologia Celular da Universidade Federal de Minas Gerais, como requisito parcial para obtenção do título de Doutora em Ciências.

Orientador: Prof. Dr. Guilherme Mattos Jardim Costa

Coorientadora: Profª. Dra. Lídia Maria de Andrade

Belo Horizonte

2024

043 Dantas, Graziela de Paula Ferreira.
Avaliação dos efeitos de nanopartículas inorgânicas na toxicologia reprodutiva murina [manuscrito] / Graziela de Paula Ferreira Dantas. – 2024.
90 f. : il. ; 29,5 cm.

Orientador: Prof. Dr. Guilherme Mattos Jardim Costa. Coorientadora: Profa. Dra. Lídia Maria de Andrade.
Tese (doutorado) – Universidade Federal de Minas Gerais, Instituto de Ciências Biológicas. Programa de Pós-Graduação em Biologia Celular.

1. Biologia Celular. 2. Nanotecnologia. 3. Nanopartículas. 4. Células Intersticiais do Testículo. 5. Espermatozoides. 6. Toxicidade. I. Costa, Guilherme Mattos Jardim. II. Andrade, Lídia Maria de. III. Universidade Federal de Minas Gerais. Instituto de Ciências Biológicas. IV. Título.

CDU: 576

Ficha catalográfica elaborada pela bibliotecária Fabiane C M Reis – CRB 6 – 2680

UNIVERSIDADE FEDERAL DE MINAS GERAIS
ICB - COLEGIADO DE PÓS-GRADUAÇÃO EM BIOLOGIA CELULAR - SECRETARIA

ATA DE DEFESA DE DISSERTAÇÃO/TESE

ATA DA DEFESA DE TESE DE DOUTORADO DE

GRAZIELA DE PAULA FERREIRA DANTAS

2024
entrada
1º/2020
2020706738

Às **quatorze horas** do dia **28 de junho de 2024**, reuniu-se, no Instituto de Ciências Biológicas da UFMG, a Comissão Examinadora da Tese, indicada pelo Colegiado do Programa, para julgar, em exame final, o trabalho final intitulado: **"AVALIAÇÃO DOS EFEITOS DE NANOPARTÍCULAS INORGÂNICAS NA TOXICOLOGIA REPRODUTIVA MURINA"**, requisito final para obtenção do grau de Doutora em Biologia Celular. Abrindo a sessão, o Presidente da Comissão, **Dr. Guilherme Mattos Jardim Costa**, após dar a conhecer aos presentes o teor das Normas Regulamentares do Trabalho Final, passou a palavra à candidata, para apresentação de seu trabalho. Seguiu-se a arguição pelos examinadores, com a respectiva defesa da candidata. Logo após, a Comissão se reuniu, sem a presença da candidata e do público, para julgamento e expedição de resultado final. Foram atribuídas as seguintes indicações:

Prof./Pesq.	Instituição	Indicação
Dr. Guilherme Mattos Jardim Costa	UFMG	APROVADA
Dra. Lídia Maria de Andrade	UFMG	APROVADA
Dr. Ralph Santos-Oliveira	UFRJ	APROVADA
Dr. Diego Stéfani Teodoro Martinez	LNNano/CNPEM	APROVADA
Dr. ª Alice Freitas Versiani	University of Texas Medical Branch at Galveston	APROVADA
Dra. Ângela Leão Andrade	UFOP	APROVADA

Pelas indicações, a candidata foi considerada: APROVADA
O resultado final foi comunicado publicamente à candidata pelo Presidente da Comissão. Nada mais havendo a tratar, o Presidente encerrou a reunião e lavrou a presente ATA, que será assinada por todos os membros participantes da Comissão Examinadora. **Belo Horizonte, 28 de junho de 2024.**

Dr. Guilherme Mattos Jardim Costa (Orientador)_____

Drª. Lídia Maria de Andrade (Coorientador)_____

Dr. Ralph Santos-Oliveira_____

Dr. Diego Stéfani Teodoro Martinez_____

Dr.ª Alice Freitas Versiani_____

Dra. Ângela Leão Andrade _____

Documento assinado eletronicamente por **Guilherme Mattos Jardim Costa**, **Professor do Magistério Superior**, em 01/07/2024, às 10:44, conforme horário oficial de Brasília, com fundamento no art. 5º do Decreto nº 10.543, de 13 de novembro de 2020.

Documento assinado eletronicamente por **Lidia Maria de Andrade**, **Usuário Externo**, em 02/07/2024, às 08:58, conforme horário oficial de Brasília, com fundamento no art. 5º do Decreto nº 10.543, de 13 de novembro de 2020.

Documento assinado eletronicamente por **Ângela Leão Andrade**, **Usuária Externa**, em 02/07/2024, às 09:32, conforme horário oficial de Brasília, com fundamento no art. 5º do Decreto nº 10.543, de 13 de novembro de 2020.

Documento assinado eletronicamente por **Alice Freitas Versiani**, **Usuária Externa**, em 02/07/2024, às 22:01, conforme horário oficial de Brasília, com fundamento no art. 5º do Decreto nº 10.543, de 13 de novembro de 2020.

Documento assinado eletronicamente por **Ralph Santos Oliveira**, **Usuário Externo**, em 12/07/2024, às 12:33, conforme horário oficial de Brasília, com fundamento no art. 5º do Decreto nº 10.543, de 13 de novembro de 2020.

Documento assinado eletronicamente por **Diego Stéfani Teodoro Martinez**, **Usuário Externo**, em 12/07/2024, às 14:41, conforme horário oficial de Brasília, com fundamento no art. 5º do Decreto nº 10.543, de 13 de novembro de 2020.

A autenticidade deste documento pode ser conferida no site https://sei.ufmg.br/sei/controlador_externo.php?acao=documento_conferir&id_orgao_acesso_externo=0, informando o código verificador **3335667** e o código CRC **AC91012B**.

AGRADECIMENTOS

Gostaria de agradecer a todos que contribuíram e permitiram que esse trabalho fosse concretizado com êxito:

A Deus, por ter me dado força e sabedoria para alcançar meus objetivos;

Ao meu esposo Paulo, por estar comigo em todos os momentos incondicionalmente, me ajudando e incentivando;

Aos meus filhos, Paula e Lucas, que são o meu orgulho e a razão da minha vida, pelo carinho e constante parceria;

Aos meus amados pais, Maria e Vicente, por todo incentivo, apoio, conselhos e orações;

Ao meu orientador Guilherme, que é uma pessoa extraordinária! Muito acolhedor e solícito em todos os momentos. Gostaria de agradecê-lo pelo acolhimento, atenção, confiança e ensinamentos passados;

À minha coorientadora Lídia, pela paciência, dedicação e estímulo, principalmente durante a escrita dos artigos;

À Estefânia, que foi a maior incentivadora para que eu fizesse o doutorado;

À prof.ª Samyra pelas contribuições nos trabalhos ao longo dessa jornada;

Aos amigos Mara e Chicó, pela parceria, amizade e principalmente por toda ajuda;

Aos amigos do Laboratório de Biologia Celular, pelo companheirismo, troca de conhecimentos e momentos de descontração na hora do almoço;

Ao meu amigo John Lennon, que é minha dupla de trabalho preferida! Obrigada pela parceria de sempre, apoio, confiança, amizade, e principalmente pelas conversas e risadas. Você é muito especial e deixa os meus dias mais leves;

Aos colaboradores e co-autores dos artigos, que não pouparam esforços para que esses trabalhos fossem publicados;

Ao prof. Ralph Santos-Oliveira da Universidade do Estado do Rio de Janeiro e à prof.a Ângela Leão da Universidade Federal de Ouro Preto, pela parceria e contribuições;

Ao programa de pós-graduação em Biologia Celular (ICB/UFMG) e a todos os professores que contribuíram fortemente para minha formação acadêmica;

E por fim, à banca examinadora, pelas sugestões e contribuições.

Esta tese foi realizada no Laboratório de Biologia Celular do Departamento de Morfologia, Instituto de Ciências Biológicas da Universidade Federal de Minas Gerais, sob a orientação do Prof. Dr. Guilherme Mattos Jardim Costa e coorientação da Dr.ª Lídia Maria de Andrade.

Agradecemos o apoio financeiro das seguintes instituições:

- Coordenação de Aperfeiçoamento de Pessoal de Nível Superior (CAPES)
- Conselho Nacional de Desenvolvimento Científico e Tecnológico (CNPq- 422405/2018-3)
- Fundação de Amparo à Pesquisa de Minas Gerais (FAPEMIG- Rede Mineira de Nanomedicina Teranóstica - **RED-** 00079-22)

RESUMO

Nanotecnologia é uma das áreas da pesquisa em constante expansão e tem colaborado para vários campos da ciência, principalmente para área biomédica. O uso de nanomateriais (NMs) tem contribuído imensamente para biotecnologias voltadas para reprodução. Nos últimos anos, as nanopartículas (NPs) inorgânicas tem sido uma das classes de NMs mais pesquisados, devido às suas propriedades físico-químicas, o que permite sua exploração como uma ferramenta teranóstica em várias aplicações biomédicas. Nesse contexto, e dentre elas, as NPs de óxido de ferro superparamagnéticas (SPIONs) têm se destacado, devido à sua alta biocompatibilidade, estabilidade e propriedade magnética intrínseca (superparamagnetismo). Entretanto, a exposição à diferentes tipos de NPs têm sido relacionadas a uma série de efeitos nocivos na espermatogênese. Assim, o objetivo do nosso estudo foi investigar os dados na literatura sobre a toxicidade reprodutiva causada por NPs inorgânicas em células testiculares de roedores. Ainda, objetivamos investigar a toxicidade de SPIONs *in vitro* e *in vivo*, em células testiculares e espermatozoides de camundongos. Embora haja uma ampla visão da toxicidade de diferentes NPs inorgânicas nos artigos avaliados em nossa revisão sistemática, os resultados são muito variáveis devido à falta de padronização dos protocolos. Apesar de focar no efeito de diferentes nanopartículas na reprodução masculina, os mecanismos e vias relacionadas à toxicidade celular foram pouco discutidos. Nossos estudos *in vitro* e *in vivo* mostraram que as células de Leydig e os espermatozoides são sensíveis às SPIONs. *In vitro*, observamos citotoxicidade, acúmulo de NPs e aumento do volume citoplasmático das células de Leydig. Nos espermatozoides, foram identificadas alterações na motilidade, viabilidade e integridade do DNA, na atividade mitocondrial e peroxidação lipídica após exposição *in vitro* a SPIONs. *In vivo*, observamos alterações morfológicas em células de Leydig e no epitélio seminífero, acúmulo de NPs principalmente nas células de Leydig, diminuição dos níveis de testosterona, alteração de túbulos seminíferos e diminuição da produção diária de espermatozoides e danos no DNA de espermátides alongadas. Essas descobertas ajudarão no desenvolvimento e aplicação clínica eficaz de tecnologias baseadas em nanotecnologia.

Palavras-chave: Nanotecnologia; nanopartículas inorgânicas; nanopartículas superparamagnéticas de óxido de ferro; células Leydig; espermatozoides; toxicidade.

ABSTRACT

Nanotechnology is one of the rapidly expanding research areas and has significantly contributed to various fields of science, particularly in the biomedical area. Nanomaterials (NMs) have immensely aided biotechnologies aimed at reproduction. In recent years, inorganic nanoparticles (NPs) have been one of the most researched classes of NMs due to their physicochemical properties, which allow their exploration as a theranostic tool in various biomedical applications. In this context, superparamagnetic iron oxide nanoparticles (SPIONs) have gained attention due to their high biocompatibility, stability, and intrinsic magnetic property (superparamagnetism). However, exposure to different types of NPs has been linked to a range of harmful effects on spermatogenesis. Thus, the objective of our study was to investigate the data in the literature regarding reproductive toxicity caused by inorganic NPs in rodent testicular cells. Additionally, we aimed to investigate the toxicity of SPIONs in vitro and in vivo in mouse testicular cells and spermatozoa. Although there is a broad understanding of the toxicity of different inorganic NPs in the articles evaluated in our systematic review, the results are highly variable due to the lack of standardization of protocols. Despite focusing on the effect of different nanoparticles on male reproduction, the mechanisms and pathways related to cellular toxicity still need to be discussed. Our in vitro and in vivo studies showed that Leydig cells and spermatozoa are sensitive to SPIONs. In vitro, we observed cytotoxicity, NP accumulation, and increased cytoplasmic volume in Leydig cells. In spermatozoa, alterations in motility, viability, DNA integrity, mitochondrial activity, and lipid peroxidation were identified after in vitro exposure to SPIONs. In vivo, we observed morphological changes in Leydig cells and the seminiferous epithelium, NP accumulation primarily in Leydig cells, decreased testosterone levels, altered seminiferous tubules, reduced daily sperm production, and DNA damage in elongated spermatids. These findings will aid in the effective development and clinical application of nanotechnology-based technologies.

Keywords: Nanotechnology; inorganic nanoparticles; superparamagnetic iron oxide nanoparticles; Leydig cells; spermatozoa; toxicity.

LISTA DE ABREVIATURAS E SIGLAS

AgNPs - Nanopartículas de prata

AuNPs - Nanopartículas de ouro

Cit_SPIONs - Nanopartículas de óxido de ferro revestidas com citrato de sódio

CMC - concentração micelar crítica

DLS - Espalhamento dinâmico de luz

EGF - Fator de crescimento epidérmico

EROs - Espécies reativas do oxigênio

EUA - Estados Unidos da América

FDA - Food and Drug Administration

HER2 - Fator de crescimento epidérmico humano 2

ISTs - Infecções sexualmente transmissíveis

NiNPs - Nanopartículas de níquel

NMs - Nanomateriais

NPMs - Nanopartículas magnéticas

NPs - Nanopartículas

PBS - Tampão fosfato-salina

PI3K/AKT/mTOR - fosfoinositídeo 3-quinase/ serina/treonina quinase/ alvo mecanístico da rapamicina

RM - Ressonância magnética

SPIONs - Nanopartículas de Óxido de Ferro Superparamagnéticas

ST - Túbulos seminíferos

TEM - Microscopia eletrônica de transmissão

TiO2 NPs - Nanopartículas de dióxido de titânio

VSM - Magnetometria de amostra vibratória

XRD - Difração de Raio-X

ZnONPs - Nanopartículas de óxido de zinc

SUMÁRIO

INTRODUÇÃO

A nanotecnologia é uma das áreas mais promissoras do século XXI, e baseia-se na utilização de estruturas, dispositivos e sistemas com novas propriedades e funções, devido ao arranjo de seus átomos em escala nanométrica (Mansoori and Soelaiman, 2005; Bayda et al., 2020; Malik et al., 2023). Esse avanço tecnológico tem contribuído para vários campos da ciência, como física, ciências dos materiais, química, ciências da computação e principalmente para a biomedicina (Bayda et al., 2020; Malik et al., 2023). Por décadas, vários estudos vêm demonstrando o enorme potencial que nanomateriais (NM) desempenham como plataforma teranóstica (tratamento e diagnóstico simultaneamente) para muitas doenças (Chen et al., 2008; Sack et al., 2014 Kinnear et al., 2017; Wu and Kong, 2020; Abbasi Kajani et al., 2021). A utilização de NM em áreas relacionadas à biomedicina, como diagnóstico, administração de medicamentos, imagem molecular e nanofarmacêuticos estão sendo intensamente pesquisadas e têm oferecido excelentes resultados (Aminabad et al., 2018; Vangijzegem et al., 2019; Wu and Kong, 2020). Em biologia reprodutiva, o uso dessas ferramentas tem contribuído para o desenvolvimento de tecnologias voltadas para preservação da fertilidade, diagnóstico e tratamento de infertilidade, endometriose, infecções sexualmente transmissíveis (ISTs) e cânceres do trato reprodutivo (Shandilya et al., 2020).

NMs incluem nanopartículas (NPs) orgânicas (micelas, dendrímeros, lipossomas, nanogéis, biopolímeros,etc) e NPs inorgânicas (metais, óxidos, carbono e polímeros, etc), com pelo menos uma de suas dimensões abaixo de 100 nm (Ratner, 2019; Bayda et al., 2020). As nanopartículas apresentam diferentes tamanhos e formatos, como cubos, esferas, bastões, estrela, micelas e agulha (Contera et al., 2021). Nos últimos anos, as NPs inorgânicas atraíram a atenção de pesquisadores e se tornaram um dos NMs mais amplamente pesquisados, devido ao seu tamanho ajustável, possibilidade de manipulação da forma, cristalinidade, alta área de superfície e facilidade de funcionalização (Meena et al., 2014; Khalid et al., 2020) Além disso,

possuem propriedades ópticas, magnéticas, catalíticas, termodinâmicas e eletroquímicas únicas, que são exploradas em várias aplicações biomédicas (Meena et al., 2014; Khalid et al., 2020)

Dentre os vários tipos de NPs inorgânicas, as NPs de óxido de ferro superparamagnéticas (SPIONs) são uma das partículas mais investigadas em vários campos científicos e(Yan Cheng and Mruk, 2012; Anselmo e Mitragotri, 2015; Vangijzegem et al., 2019). No campo biomédico, devido à sua alta biocompatibilidade, estabilidade e propriedade magnética intrínseca (superparamagnetismo), as SPIONs são usadas como agentes de contraste para ressonância magnética (RM) (Fatima e Kim, 2018), na entrega direcionada de fármacos, como veículos em terapias gênicas (Sosa-Acosta et al., 2020; Vallabani et al., 2018) e em terapias tumorais através da hipertermia magnética (Kolosnjaj-Tabi and Wilhelm, 2017; Pham et al., 2017). Em medicina reprodutiva, as SPIONs estão sendo investigadas para a seleção de espermatozoides de alta qualidade para fertilização *in vitro* (Durfey et al., 2019) e *in vivo* (Feugang, 2017; Odhiambo et al., 2014) através da ligação de SPIONs revestidas com lectinas ou anexina V aos glicanos expostos pelas membranas acrossomais danificadas ou pelos espermatozoides apoptóticos. Além disso, estão sendo utilizadas como agente antimicrobiológico durante a criopreservação do sêmen(Tsakmakidis et al., 2020), na produção de animais transgênicos (Kim et al., 2010) e em técnicas de esterilização ou contracepção (Ding et al., 2021; Jivago et al., 2021).

Embora o uso de NPs tenha demonstrado bons resultados para o desenvolvimento de novas tecnologias voltadas para o campo biomédico, vários estudos têm evidenciado que as propriedades estruturais das NPs podem causar efeitos tóxicos e impactos negativos na saúde e no meio ambiente (Cypriyana et al., 2021; Egbuna et al., 2021). Diferentes NPs são capazes de se ligarem com a matéria biológica, e causar efeitos adversos em vários órgãos, como pulmão, fígado, rim, coração e cérebro (Wang et al., 2009; Yang et al., 2009; Li et al., 2012; Manke et al., 2013; Ahamed, 2013; Hadrup e Lam, 2014). Recentemente, estudos demonstraram que

algumas NPs são capazes de atravessar a barreira hematotesticular e causar citotoxicidade, estresse oxidativo e danos genotóxicos nos órgãos reprodutivos masculinos de roedores (Wang et al., 2018; Jia et al., 2020; Souza et al., 2021;). A exposição a diferentes tipos de NMs, como NPs de prata (AgNPs), ouro (AuNPs), óxido de zinco (ZnONPs), dióxido de titânio (TiO_2 NPs) e níquel (NiNPs), têm sido relacionadas a uma série de efeitos nocivos na esteroidogênese, espermatogênese e fertilidade em mamíferos (Li et al., 2012; Kong et al., 2019; Shen et al., 2019; Liu et al., 2020; Olugbodi et al., 2020).

O sistema reprodutivo dos mamíferos envolve uma série de processos fisiológicos complexos que são altamente sensíveis (Mima et al., 2018; Habas et al., 2021; Souza et al., 2021). Os testículos, são responsáveis pela gametogênese e pela secreção dos hormônios sexuais masculinos. O órgão é subdividido em compartimentos tubular e intertubular. O compartimento tubular é composto pelos túbulos seminíferos, que apresentam células germinativas em diferentes estágios de desenvolvimento, além das células de Sertoli e células peritubulares mioides (Svingen e Koopman, 2013; França et al., 2016). O compartimento intertubular é composto, principalmente, pelas células de Leydig, macrófagos, células endoteliais vasculares, células perivasculares, fibroblastos, células dendríticas e espaço linfático (França et al., 2016; Heinrich and DeFalco, 2020a).

As células de Sertoli são essenciais para o desenvolvimento das células germinativas, regulando a espermatogênese desde manutenção do nicho de células-tronco espermatogoniais até a liberação final de espermátides (Schulz e Nóbrega, 2011; Mruk e Cheng, 2015; O'Donnell et al., 2022;). Desempenham diversas funções na produção espermática, tais como suporte físico, nutricional, regulação da produção de andrógenos nos testículos e fagocitose de células germinativas degeneradas (França et al., 2016). Além disso, formam a barreira hematotesticular, criando um ambiente favorável para a diferenciação das células geminativas haploides, contribuindo para o privilégio imunológico testicular (Mruk e Cheng, 2015;

O’Donnell et al., 2022). As células de Leydig são as principais produtoras de hormônios esteroides, sendo responsáveis pela secreção da testosterona (Heinrich e DeFalco, 2020b). Além disso, elas participam de complexas interações de sinalização parácrina com populações de células testiculares como os macrófagos, as células de Sertoli e as células peritubulares mióides. Essas interações são extremamente necessárias para os processos de esteroidogênese, regulação imunológica, função das células de Sertoli e espermatogênese.

Nesse contexto, visto que diferentes NPs são amplamente estudadas para o tratamento de distúrbios reprodutivos e desempenham um papel essencial em aplicações biomédicas, o objetivo deste estudo foi, primeiramente, investigar os dados disponíveis na literatura sobre a toxicidade reprodutiva causada por NPs inorgânicas (prata, ouro, ferro, zinco, titânio e níquel) em células testiculares de roedores, discutindo os efeitos dessas NPs em células germinativas (em diferentes estágios de desenvolvimento), células de Sertoli e células de Leydig. Na sequencia, objetivamos investigar, experimentalmente, a toxicidade de SPIONs *in vitro* e *in vivo*, em células testiculares e espermatozoides de camundongos.

JUSTIFICATIVA

A reatividade de sistemas biológicos à exposição de diferentes NPs, *in vitro* e *in vivo*, é bem documentada e mostra vários efeitos adversos para a saúde humana e para o meio ambiente. Entretanto, no contexto reprodutivo, os mecanismos pelos quais as NPs interagem com as células testiculares não são totalmente compreendidos e são pouco explorados. Dessa forma, essa pesquisa aborda, primeiramente, os efeitos de diferentes NPs inorgânicas em células testiculares de camundongos, trazendo uma visão geral dos efeitos adversos que essas NPs podem causar nas células reprodutivas. Além disso, uma investigação da toxicidade de SPIONs, *in vitro e in vivo*, também foi realizada, para caracterizar a biocompatibilidade e segurança biológica dessas nanoestruturas emergentes, no sistema reprodutor masculino. Essas

descobertas ajudarão no desenvolvimento e aplicação clínica eficaz de tecnologias baseadas em nanotecnologia e auxiliaram em futuras regulamentações para a prevenção dos riscos inerentes ao uso dos nanomateriais.

OBJETIVOS

Objetivo Geral

Discutir os efeitos da toxicidade reprodutiva de NPs inorgânicas (prata, ouro, ferro, zinco, titânio e níquel) em células de Sertoli, Leydig e células germinativas de roedores, *in vitro* e *in vivo* (Capítulo 1) e investigar a toxicidade de nanopartículas de óxido de ferro superparamagnéticas (SPIONs) *in vitro* (Capítulo 2) e *in vivo* (Capítulo 3), em células testiculares e espermatozoides de camundongos.

Objetivos Específicos

Artigo 1: Male reproductive toxicity of inorganic nanoparticles in rodent models: A systematic review

- Analisar e discutir as os impactos da interação de NPs inorgânicas com as células testiculares, de acordo com dados disponíveis nos últimos 20 anos;
- Comparar os efeitos comuns e específicos decorrentes da exposição das células testiculares às diferentes NPs inorgânicas.

Artigo 2: The toxicity of superparamagnetic iron oxide nanoparticles induced on the testicular cells: *in vitro* study

- Caracterizar físico-quimicamente as amostras de nanopartículas de óxido de ferro superparamagnéticas (magnetita, Fe_3O_4) revestidas com citrato de sódio (Cit_SPIONs);

- Avaliar a viabilidade celular de culturas primárias de células de Leydig, células de Sertoli e células germinativas, após exposição às Cit_SPIONs.
- Avaliar a citoarquitetura do explante testicular, mantido em cultura, após a exposição às Cit_SPIONs;
- Determinar, a localização celular das Cit_SPIONs na cultura de tecido testicular;
- Avaliar os impactos da exposição *in vitro* de espermatozoides às Cit_SPIONs.

Artigo 3: Effects of superparamagnetic iron oxide nanoparticles (SPIONs) testicular injection on Leydig cell function and sperm production in a murine model

- Avaliar a distribuição celular das Cit_SPIONs após injeção direta nos testículos;
- Avaliar as alterações morfológicas dos testículos de camundongos expostos às Cit_SPIONs;
- Avaliar os efeitos da injeção testicular direta das Cit_SPIONs nos níveis séricos de testosterona dos camundongos;
- Avaliar as alterações ultraestruturais testiculares, a duração da espermatogênese e a produção espermática diária de camundongos, após injeção direta de Cit_SPIONs nos testículos;
- Investigar as alterações morfológicas dos espermatozoides, após os 56 dias de exposição às Cit_SPIONs.

RESULTADOS

CAPÍTULO 1

Artigo 1 **-** **"**Male reproductive toxicity of inorganic nanoparticles in rodent models: A systematic review"

Publicado na revista: Chemico-Biological Interactions

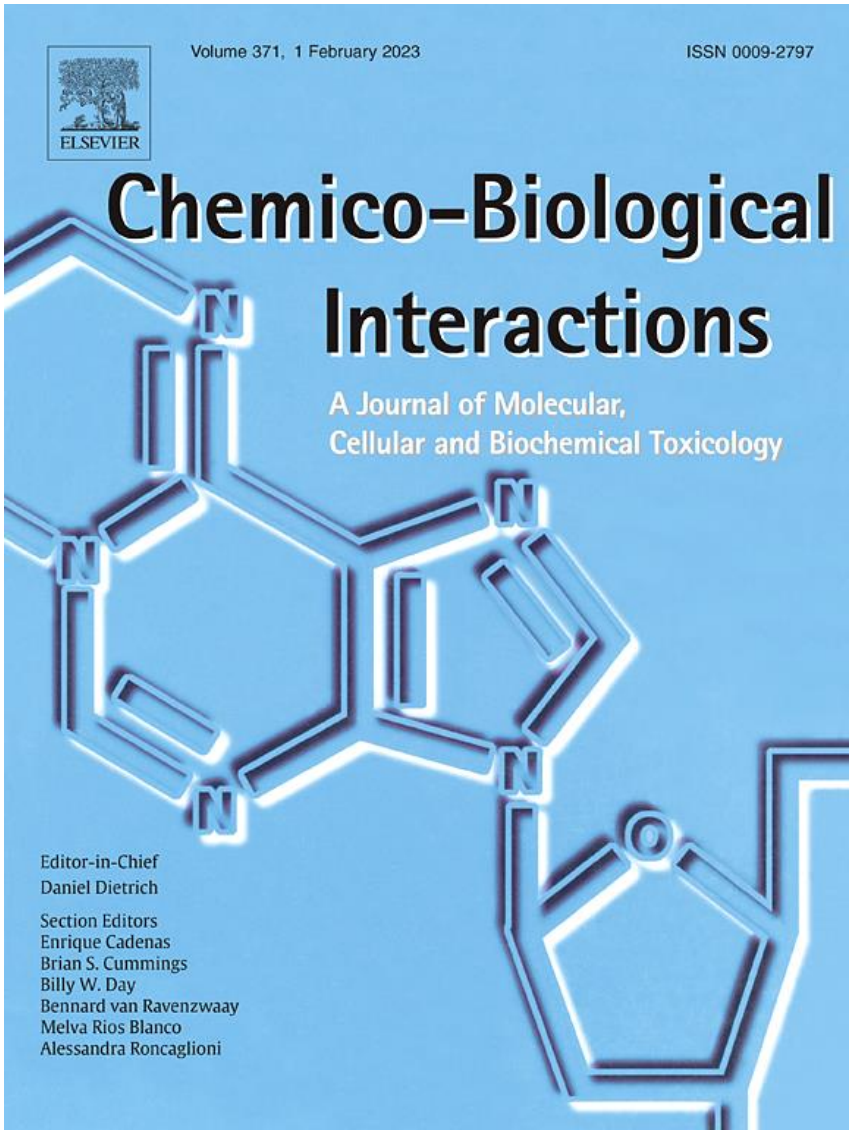

Chemico-Biological Interactions 363 (2022) 110023

Contents lists available at ScienceDirect

Chemico-Biological Interactions

journal homepage: www.elsevier.com/locate/chembioint

Book Review

Male reproductive toxicity of inorganic nanoparticles in rodent models: A systematic review

Graziela P.F. Dantas [a], Fausto S. Ferraz [a], Lídia M. Andrade [b], Guilherme M.J. Costa [a,*]

[a] Laboratory of Cellular Biology, Department of Morphology, Institute of Biological Sciences, Federal University of Minas Gerais, Belo Horizonte, MG, Brazil
[b] Nanobiomedical Research Group, Department of Physics, Federal University of Minas Gerais, Belo Horizonte, MG, Brazil

ARTICLE INFO

Keywords:
Inorganic nanoparticles
Testis
Reproductive toxicology
Nanotoxicology
Oxidative stress
Apoptosis

ABSTRACT

The use of nanoscale materials for different biomedical applications has grown a lot in the last years and raised several concerns about toxic effects on human health. Several studies have shown that different types of NPs may exert toxic effects on organs such as the brain, the liver and the kidney. However, The toxicological effects of inorganic NPs on reproductive organs only recently has attracted attention. This systematic review selected data published in the last twelve years assessing rodent-male *in vitro* and *in vivo* reproductive toxicity caused by different types of inorganic nanoparticles (AgNPs, AuNPs, IONPs, ZnONPs, TiO2NPs and NiNPs). Structural and functional alterations were commonly observed in Sertoli, Leydig, germ and sperm cells *in vitro* and *in vivo*. Oxidative stress, apoptosis, and/or necrosis were the most common findings after inorganic nanoparticle exposure. The toxicity of different NPs depends strongly on their physicochemical characteristics and intrinsic properties. Although a broad overview of the toxicity of different inorganic NPs was found in the papers evaluated, the results are highly variable due to the lack of standardization of protocols, regarding NPs sizes, concentration/doses, and routes of administration. Despite focusing on the effect of different nanoparticles on male reproduction, the mechanisms and pathways related to cellular and/or organ toxicity were poorly discussed. Understanding the specific molecular interactions between NPs and male testicular cells is crucial for developing nanobiotechnologies related to reproductive medicine.

1. Introduction

In the last decades, nanotechnology has emerged as a new tool for numerous technological and biological applications, which has raised a growing interest of researchers in the development of nanoparticles and nanomaterials of different types (metal, oxide, carbon, semiconductors, etc.) for the treatment and diagnosis of several diseases [1–3]. A nanoparticle (NP) is a particle whose size varies between 1 and 100 nm in diameter in at least one of its dimensions [4]. Due to their unique size and innumerable other physical and chemical properties (thermal, optical, electrical charge and biological properties), more than a few types of nanoparticles (NPs) have been explored in the target delivery of drugs to tissues/organs, in the imaging of molecular markers for genetic and autoimmune diseases, as well as in the treatment of tumors [5,6]. In addition, diagnostic and therapeutic approaches based on nanomaterials have been investigated and evaluated as research tools for various reproductive applications, such as assisted reproduction, biomarkers for reproductive disorders, gene therapy for reproductive dysfunctions, treatment of diseases associated with erectile dysfunction and contraception, among others [7].

The increasing use of NPs raises many concerns regarding adverse effects on human health and the environment. A number of scientists have shown that many NPs can cross biological barriers, for example, blood-brain and blood-testis barriers and penetrate tiny capillaries, accumulating and causing unwanted effects, such as cytotoxicity, oxidative stress, DNA and cell membrane damages, impaired mitochondrial function, inflammation and decreased cell proliferation [4,7–10]. The mechanisms of biological interactions are determined by NPs' physical and chemical characteristics, such as size, shape, specific surface area, charge, catalytic activity, and the presence of functional groups on their surfaces [11]. These properties define absorption, distribution, metabolism and elimination from the body and cells after NPs internalization [12].

Previous studies have shown that several NPs can exert toxic effects on organs such as the brain, the liver and the kidney [13,14] and recently, attention has been given to reproductive organ toxicities [9]. These adverse effects on male reproductive health have attracted

* Corresponding author.
E-mail address: gmjc@ufmg.br (G.M.J. Costa).

https://doi.org/10.1016/j.cbi.2022.110023
Received 5 May 2022; Received in revised form 6 June 2022; Accepted 20 June 2022
Available online 25 June 2022

Abbreviations

NPs	nanoparticles
DNA	deoxyribonucleic acid
DLS	dynamic light scattering
IL-1a	interleukin-1-alpha
IL-6	Interleukin-6
IL- 8	Interleukin-8
NF-ǩB	factor nuclear kappa B
ROS	Reactive Oxygen Species
AgNPs	Silver Nanoparticles
SSC	Spermatogonial stem cell
AuNPs	Gold nanoparticles
GNRs	gold nanorods
ZO-1	Zonula occludens-1
IONPs	Iron Oxide Nanoparticles
MR	Magnetic Resonance
SPIONs	Superparamagnetic iron oxide nanoparticles
TPGS	α-tocopheryl-polyethylene glycol-succinate
DMAB	dodecyl-dimethyl-ammonium-bromide
ZnONPs	Zinc Oxide Nanoparticles
StAR	Steroidogenic Acute Regulatory Protein
TiO_2NPs	Titanium dioxide nanoparticles
LH	luteinizing hormone
FSH	follicle-stimulating hormone
NiNPs	Nickel nanoparticles
BTB	blood-testis barrier
CTAB	Cetrimonium bromide
PLGA	Poly Lactic-*co*-Glycolic Acid
UV–Vis	Ultraviolet–visible
SOD	Superoxide dismutase
MDA	Malondialdehyde
CAT	Catalase
GSH-px	Glutathione peroxidase
NO	Nitric oxide

scientific interest as to mechanisms of toxicity and potential effects on reproduction and fertility [3,5]. It is reported that the male reproductive system is more sensitive and vulnerable to stress than other organic systems [15,16] and several data have shown that most NPs can reach male reproductive organs in mice, such as testis, affecting the spermatogenic process [9,17].

Testicles are responsible for gametogenesis and secretion of male sex hormones, mainly testosterone [18]. Thus, this hormone is necessary for maintaining the hematotesticular barrier, spermatogenesis, and fertility [19,20]. Spermatogenesis is a complex biological process of cell transformation, producing haploid germ cells through highly organized seminiferous epithelium cycles [9,19]. Sertoli cells, for instance, play an essential role in this process and provide support and protection to germ cells by maintaining the hematotesticular barrier [21]. Furthermore, these cells recognize and react to pathogens, controlling local immune cells through anti-inflammatory cytokines [22]. Testosterone and other androgens, produced by Leydig cells, can also inhibit pro-inflammatory cytokines, and strengthen the integrity of the blood-testis barrier, providing a more immune-privileged environment [21].

Several studies have shown that exposure to inorganic NPs during spermatogenesis can destabilize the hematotesticular barrier and affect sperm morphology and production due to ROS generation and/or induction of inflammatory response [21–24]. Likewise, inflammation can compromise Leydig cells, causing a reduction in serum testosterone levels, and weakening the blood-testis barrier [21]. Despite these findings, the molecular mechanisms involved in the toxicity of NPs in the reproductive system are still not fully elucidated.

In this context, this systematic review aims at compiling available data on reproductive toxicity caused by inorganic NPs (e.g., silver, gold, iron, zinc, titanium, and nickel) in testicular cells. These nanoparticles are widely studied to treat and diagnose several diseases and play an essential role in industrial and biological enterprises. Herein, we discuss the effects of these NPs on germ cells (at different stages), Sertoli cells and Leydig cells.

2. Methodology

The scientific articles chosen were obtained from the PubMed (NCBI) and Google Academic (related articles) databases. The inclusion and exclusion criteria are detailed in Fig. 1. The following keywords were used in our search:

- “Nanoparticles toxicity and testis";
- “Adverse effects of nanoparticles in testis";

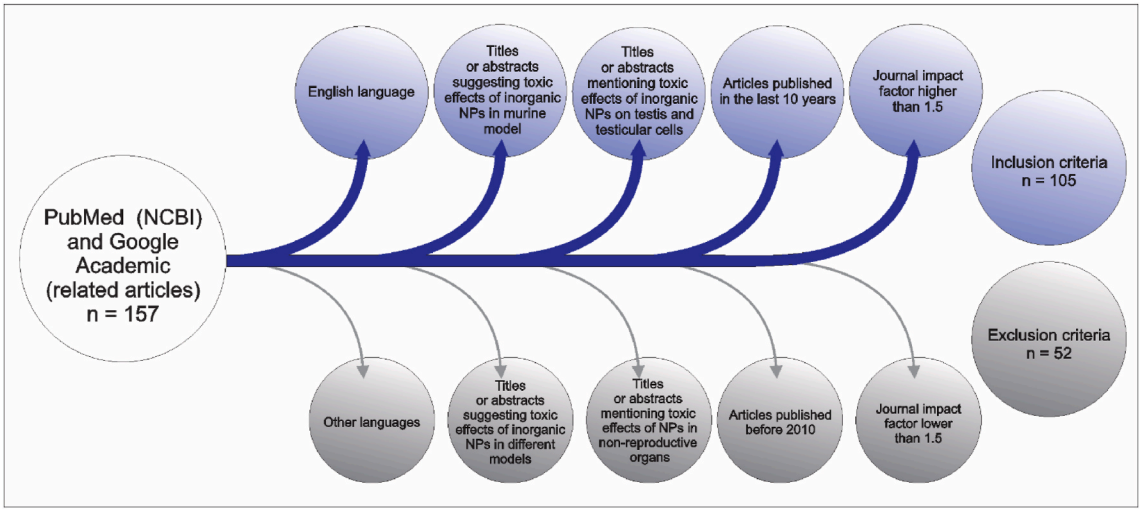

Fig. 1. Flow diagram representing the inclusion and exclusion criteria. The articles were obtained from PubMed (NCBI) and Google Academic (related articles) sources and selected according to the established criteria.

- “Nanoparticle toxicity in the male reproductive system".
- “Silver nanoparticles toxicity in testis"
- “Gold nanoparticles toxicity in testis"
- “Iron oxide nanoparticles toxicity in testis"
- “Zinc oxide nanoparticles toxicity in testis"
- “Titanium nanoparticle toxicity in testis"
- “Nickel nanoparticles toxicity in testis"

One hundred and fifty-seven articles published from 2010 to 2022 were selected. One hundred and five were used for this review, and fifty-two were excluded. All works were organized by type of NPs addressed, author, and publication date.

3. Silver nanoparticles (AgNPs)

Silver nanoparticles (AgNPs) have gained substantial popularity among researchers in recent years, being explored in several commercial and biomedical applications due to their unique physicochemical properties, such as high electrical and optical conductivity, chemical stability, and catalytic activity [25,26]. They have been used to manufacture antimicrobials, antifungals, antivirals, dressings, drug carriers, and anti-tumor agents [27–29].

The toxic effects of AgNPs have been reported in both prokaryotic and eukaryotic systems [26]. The toxicity depends on many factors associated with size, shape, surface charge, coating, solubility, concentration/dose, surface functionalization, mode of application, the mechanism of action, exposure time and cell type [5,26,30]. Studies have shown that AgNPs can enter the nucleus, leading to changes in DNA integrity, affecting its synthesis process and resulting in cell mutation [4,31,32]. These NPs can also lead to mitochondrial dysfunction and generate reactive oxygen species (ROS), causing impairment to proteins, nucleic acids, and cell proliferation [12,33,34].

In reproductive cells, these disorders can cause changes in spermatogenesis, fertility, and offspring development [4,31,35]. AgNPs can alter reproductive parameters in male rats, resulting in reduced sperm production and compromised testicular structure [36]. The *in vitro* and *in vivo* studies on AgNPs toxicity are summarized in the following topics and Table 1 and Table 2.

3.1. In vitro studies of silver nanoparticles (AgNPs)

The evaluation of hydrocarbon-coated AgNPs and Polysaccharide-coated AgNPs (10, 15, 25 and 80 nm) in C18-4 mouse spermatogonial stem cell lines (SSCs) for 24 h demonstrated a significant decrease in cell proliferation at concentrations higher than 10 μg/mL. Adverse effects were also observed in the signaling mediated by the glial cell-derived neurotrophic factor (GDNF), impairing the proliferation of the SSCs [37].

The exposure of two different sizes of non-coated AgNPs (10 and 20 nm/UV–vis: 410 nm and 395 nm) in somatic Leydig cells (TM3), Sertoli cells (TM4) and SSCs for 24 h resulted in diminished cell viability and proliferation. These NPs promoted damage in cell membranes and induced the generation of reactive oxygen species (ROS) in both cells. Likewise, AgNPs were detected in the cytoplasm and nucleus of TM3 and TM4 cells. The small AgNPs (10 nm) promoted mitochondrial damage and cell death by apoptosis/necrosis and increased the formation of autosomes and autolysosomes. In addition, AgNPs have significantly regulated genes related to testosterone synthesis and occlusion junction proteins of the blood-testis barrier [38].

The internalization of non-coated AgNPs (34–46 nm/DLS ~ 61,51 nm) in mouse sperm was evaluated by Yoisungnern and collaborators (2015). The internalized AgNPs inhibit sperm viability and acrosome reaction at higher concentrations. A significant increase in mitochondria abnormalities and cell mortality was also observed due to ROS increase. Sperm abnormalities significantly decreased the rate of fertilization, also affecting embryonic development.

Han and colleagues (2015) evaluated the toxic effect of non-coated AgNPs (20 nm/DLS: ~60 nm) in Sertoli cells (TM4) for 24 h. Their results showed decreased cell viability, increased generation of ROS, and a rise in the formation of autophagosomes and autolysosomes. Zhang and colleagues (2015) also reported the toxicity of non-coated AgNPs (10–20 nm/UV–vis: 412 nm) in Leydig (TM3) and Sertoli (TM4) cells for 24 h showing that cytotoxicity and cell death increased in a concentration-dependent manner in both cells.

3.2. In vivo studies of silver nanoparticles (AgNPs)

3.2.1. Oral administration

Prepubertal Wistar rats exposed to non-coated AgNPs (60-nm) from PND23 to PND53 presented delayed puberty, altered reproductive development, and compromised spermatogenesis. In the 50 μg/kg dosage, there was a numerical reduction in daily sperm production, disorganization of seminiferous epithelium and sloughing of the germ cells. The authors suggest through evidence that the observed effects were not reversed after the end of treatment [41].

Sub-chronic exposure (once a day) of Wistar rats to non-coated AgNPs (5–20 nm/UV–vis: 397 nm) also showed significant effects on spermatogenesis. Reduced number of spermatogenic cells, atrophy of the seminiferous tubules, germ cell sloughing (mainly spermatocytes and spermatids), reduced tubular lumen, and sperm cell necrosis were observed [30].

The toxic effects of non-coated AgNPs (DLS: 86.1 and 87 nm) in male prepubertal Wistar rats (from PND23 to PND58) were assessed by Mathias et al. [36]. They observed that AgNPs decreased the acrosome and plasma membrane integrities in this study, diminished mitochondrial activity, and increased sperm abnormalities. Moreover, there was a delay in the onset of puberty without compromising body growth, sexual behavior, and serum hormone (FSH, LH, testosterone and estradiol) concentrations. Interestingly, sperm cells seemed to be more sensitive to lower doses of AgNPs.

Elsharkawy and collaborators (2019) investigated the potential testicular toxicity induced by non-coated AgNPs (8.93–33.4 nm), giving them to Sprague Dawley rats twice per week for six months. The results showed that AgNPs caused more cytotoxicity in a high dose (13.4 mg/kg), promoting vacuolization in Sertoli cells, inactivating Leydig cells, decreasing sperm counts and changing sperm parameters. Furthermore, a decrease in SOD activity was accompanied by a significant increase in MDA level in testis.

3.2.2. Intravenous administration

Short-term *in vivo* exposure of citrate-coated AgNPs (10 nm/DLS.: 14 nm) at a dose of 1 mg/kg (5 injections on days 0, 3, 6, 9, and 12) in male CD1 mice promoted morphological damages in testes. Altered seminiferous epithelium induced germ cell apoptosis, changed Leydig cell size, and increased serum testosterone levels were observed in these mice [14].

Han and colleagues (2015) evaluated the reproductive toxicity of non-coated AgNPs (20 nm/DLS.: ~60 nm) in male ICR mice by single intravenous injection. They observed a significant loss of germ cells and an increase in pro-inflammatory cytokines, including tumor necrosis factor α (TNF- α), interferon-γ, IL-6, IL-1β, and monocyte chemoattractant protein-1 (MCP-1).

3.2.3. Intraperitoneal administration

The evaluation of non-coated AgNPs (20 nm/DLS.: 90 nm/ζP: 135 mV), administered in adult Balb/C mice every day (for 9 days), showed that AgNPs have the potential to induce toxicity in testis. These NPs, at concentrations higher than 0.25 mg/kg, led to testicular degeneration and necrosis in spermatogonial cells and promoted a significant reduction in sperm count, viability, and motility. Furthermore, increased sperm abnormalities were detected mainly in the head and tail [45].

In Wistar rats, Fathi and collaborators (2019), applying a single

Table 1
In vitro assessments using silver nanoparticles.

Assay	NP	Functionalization	Size	Cell line/animal model	Method of exposition/ administration	Exposure time	Concentration/dose	Main findings	Reference
in vitro	AgNPs	Hydrocarbon-coated	15 nm; 25 nm; 80 nm	SSC (C18-4 cell line)	incubation	24 h	5, 10, 25, 50 and 100 μg/mL	• Reduced SSCs proliferation (concentrations ≥10 μg/mL)	[37]
		Polysaccharide-coated	10 nm; 25 nm; 80 nm		incubation	24 h	5, 10, 25, 50 and 100 μg/mL	• Down - regulation GDNF signaling pathway	
in vitro	AgNPs	non-functionalized	10 nm; 20 nm	SSC (primary culture)	incubation	24 h	0, 10, 20, 30, 40, 50, 60, 80, 90 and 100 μg/mL	• Inhibition of proliferation and differentiation	[38]
		non-functionalized	10 nm; 20 nm	Sertoli cell (TM4)	incubation	24 h	0, 10, 20, 30, 40, 50, 60, 80, 90 and 100 μg/mL	• Decreased cell viability • ROS production • Autophagy, apoptosis • Mitochondrial damage • Reduced expression of BTB genes	
		non-functionalized	10 nm; 20 nm	Leydig cell (TM3)	incubation	24 h	0, 10, 20, 30, 40, 50, 60, 80, 90 and 100 μg/mL	• Decreased cell viability • ROS production • Autophagy, apoptosis • Mitochondrial damage • Reduced expression of steroidogenic genes	
In vitro	AgNPs	non-functionalized	34 nm–46 nm	Spermatozoa (vas deferens of BDF1 mice)	incubation	3 h	0.1, 1, 10 and 50 μg/mL	• Reduced viability • Mitochondrial damage • ROS production • Abnormal morphology • Reduced acrosomal reaction • Decreased fertilization • Reduced embryonic development	[39]
in vitro	AgNPs	non-functionalized	20 nm	Sertoli cell (TM4)	incubation	24 h	0, 3.0625, 6.125, 12.5, 25 and 50 μg/mL	• Cytotoxicity • ROS production • Accumulation of Autophagosomes and autolysosomes • Apoptosis and expression of pro-inflammatory cytokines	[40]
In vitro	AgNPs	non-functionalized	10 nm–20 nm	Leydig cell (TM3) Sertoli cell (TM4)	incubation incubation	24 h 24 h	0,10,20,30,40 and 50 μg/mL 0,10,20,30,40 and 50 μg/mL	• Cytotoxic effect • Cytotoxic effect	[29]

Table 2
In vivo assessments using silver nanoparticles.

Assay	NP	Functionalization	Size	Cell line/animal model	Method of exposition/ administration	Exposure time	Concentration/dose	Main findings	Reference
in vivo	AgNPs	non-functionalized	60 nm	Wistar rats	Oral administration (Gavage)	PND23 to PND53	0, 15, or 50 μg/kg	• Delay in the beginning of puberty • Reduced daily sperm production • Disorganization of seminiferous epithelium • Cellular debris in the seminiferous lumen • Sloughing of germ cells	[41]
in vivo	AgNPs	non-functionalized	86.1 nm; 87 nm	Wistar rat male offspring	Oral administration (Gavage)	PND23 to PND58	0, 15 or 30 mg/kg	• Delay in the beginning of puberty • Reduction in acrosome integrity • Reduction in plasma membrane integriy • Reduced mitochondrial activity	[36]
in vivo	AgNPs	non-functionalized	8.93 nm–33.4 nm	Sprague Dawley rats	Oral administration (Gavage)	twice per week for six months	5.36 mg/kg and 13.4 mg/kg	• Reduced serum testosterone levels • Increased LH levels • Decreased activity of SOD. • Lipid peroxidation • Decreased sperm viability • Decreased DNA chromatin integrity • Vacuolation in Sertoli cells • Decreased spermatid numbers • Reduced sperm numbers	[42]
in vivo	AgNPs	non-functionalized	5 nm–20 nm	Wistar rats	Oral administration (Gavage)	once a day for 90 days.	20 μg/kg/day	• Atrophy of seminiferous tubules • Loss of spermatogenic cells (spermatocytes and spermatids) • Sloughing of germinal cells • Reduced sperm numbers • Germ cell degeneration and/or necrosis • Sertoli cell vacuolization	[30]
in vivo	AgNPs	non-functionalized	~20 nm	Sprague-Dawley rats	Intratracheal instillation	Single instillation	50 μg/animal	• Changes in the expression of genes encoding oxidative stress-related enzymes (Gpx1, SOD, FMO2 and GAPDH.)	[43]
in vivo	AgNPs	non-functionalized	~250 nm	Wistar rats	Intraperitoneal administration	Single injection	30, 125 and 300 mg/kg	• Reduced sperm vitality • Reduced number of spermatogonia, Sertoli and Leydig cells • Reduced tubular diameter	[44]
in vivo	AgNPs	non-functionalized	14 nm	Male and female CD1 mice	Intravenous administration	5 injections on days 0, 3, 6, 9, and 12	1 mg/kg/dose	• Accumulation in testes • Increased luminal volume • Increased tubular diameter • Reduction of the seminiferous epithelium • Increased apoptotic germ cells • Increased serum and intratesticular testosterone levels • Increased Leydig cell size • Up-regulation of steroidogenic genes.	[14]
in vivo	AgNPs	non-functionalized	90 nm	BALB/c mice	Intraperitoneal administration	every day lasted for 9 days	0.25, 0.50 and 1 mg/kg	• Testicular degeneration • Spermatogonial cell death • Cytotoxic effects on sperm • Reduced sperm count, viability and mobility • Increased sperm abnormalities (mainly in heads).	[45]
in vivo	AgNPs	non-functionalized	10 nm; 40 nm	neonatal mice	Subcutaneous administration	Five injections (interval of 3 days from PND8–21)	0, 1, and 5 mg/kg	• Reduced GSI in the group treated with 5 mg/kg • Reduced seminiferous tubule diameter at PND28 and PND42 • Increased abnormal sperm at PND42, PND60, and PND100	[29]
in vivo	AgNPs	non-functionalized	20 nm	ICR mice	Intravenous administration	single injection and left untreated for 15 days	0.5 and 1.0 mg/kg	• Cytotoxicity • ROS production • Accumulation of autophagosomes and autolysosomes in Sertoli cells • Apoptosis • Expression of pro-inflammatory cytokines.	[40]

Table 3
In vitro and *in vivo* data using gold nanoparticles.

Assay	NP	Functionalization	Size	Cell line/animal model	Method of exposition/ administration	Exposure time	Concentration/dose	Main findings	Reference
in vitro	AuNPs (GNRs)	non-functionalized	(9–11) nm; (34–42) nm	Spermatocyte-derived cells GC-2	Incubation	24 and 48 h	0.1, 1, 10, 100, 200, 500, 1000 and 1500 nM	• Cytotoxic effects (higher doses)	[57]
				Sertoli cell (TM-4)	Incubation	24 and 48 h	0.1, 1, 10, 100 nM	• Cytotoxic effects (higher doses) • Metabolic changes in TM-4 cells • Decreased membrane permeability • Decreased mitochondrial membrane potential • Decreased glycine levels, altering BTB proteins	
in vitro	AuNPs (sphere)	non-functionalized	5–10 nm	Leydig cell (TM3)	Incubation	24, 48, 72 and 96 h	1.67, 5 and 12.5 μg/mL	• Cytotoxic effects (higher doses) • DNA Damage • ROS production • Autophagosomes • Disrupted the cell cycle in S phase	[58]
in vivo	AuNPs (sphere)	non-functionalized	~2.5 nm	Hybrid mice (CBA × C57Bl/6)	Intraperitoneal injection	4 days	0.2 mL of non-diluted gold hydrosol in 1×10^{15} particles/mL	• Seminiferous tubules without alterations • Chromosomal abnormalities in round spermatids	[59]
in vivo	AuNPs (sphere)	methoxy poly (ethylene glycol)	20 nm	ICR mice	Intravenous administration	One injection (evaluation on days 1, 7, 14, 21 and 30)	45 and 225 mg/kg	• Accumulation in testis • No effect on male fertility	[16]
		aminoethyl poly (ethylene glycol)					45 mg/kg	• Accumulation in testis • Increase plasma T levels • No effect on male fertility	
in vivo	AuNPs (sphere)	polyethylene glycol	34.4; 22.5; 29.3; 36.1 nm	Male and female C57 mice	Intraperitoneal administration	One injection (evaluation on day 28)	4000 μg/kg	• Without toxicity	[60]
in vivo	AuNPs (sphere)	non-functionalized	5–10 nm	Balb/c mice	Intravenous administration	once a day for 14 consecutive days	0.17 and 0.5 mg/kg	• Decreased serum testosterone levels • Decreased expression of 17α-hydroxylase	[58]
in vivo	AuNPs (sphere)	non-functionalized	50 nm	Wistar male rats	Intraperitoneal administration	Injection for 3 consecutive days	Toxic and non-toxic doses of GNPs (based on the IC50)	• Hyperemia • Decreased seminiferous tubules volume density (toxic dose) • Germ cell sloughing (toxic dose)	[61]

Table 4
In vivo data using iron oxide nanoparticles.

Assay	NP	Functionalization	Size	Cell line/animal model	Method of exposition/ administration	Exposure time	Concentration/dose	Main findings	Reference
in vivo	IONPs	α- tocopheryl-polyetheleneglycol-succinate (TPGS)	30 nm; 180 nm	Swiss albino mice	Oral administration (Gavage)	5 consecutive days (examination on the 7th and 21st days)	12.5 μg of Fe/kg	• Accumulation in testis • DNA damage • Oxidative stress • Abnormal shape of sperm heads (hook, pinhead, banana and amorphous)	[76]
		didodecyl-dimethyl-ammonium-bromide (DMAB)						• Accumulation in testis • DNA damage • Oxidative stress	
in vivo	IONPs	non-functionalized	<50 nm	Albino mice	Intraperitoneal injection	once a week for 4 weeks	25 and 50 mg/kg	• Accumulation in testis • ROS production • Lipid peroxidation • Apoptosis • Increased serum testosterone levels • Sertoli cell vacuolization • Germ cell sloughing	[77]
in vivo	IONPs	Polyethyleneimine poly (acrylic acid)	28 nm; 30 nm	Male and female CD-1 mice	Intraperitoneal injection	One injection in pregnant mice (on days 8, 9 or 10 of gestation)	Low (10 mg/kg) or high (100 mg/kg) dose	• Reduced seminiferous epithelium (100 mg/kg) • Germ cell loss in a high dose (100 mg/kg)	[78]

injection of non-coated AgNPs (60–80 nm/DLS~250 nm), obtained similar results. Moreover, a substantial reduction in spermatogonia, Sertoli and Leydig cells was observed in high concentrations.

3.2.4. Respiratory and subcutaneous administration

Sprague-Dawley rats exposed to non-coated AgNPs (DLS: 10–20 nm/ζP: −15 mV) through the respiratory route (Single installation of 50 μg/rat) had their testis investigated for oxidative stress, protein folding, cell cycle arrest, and cell death, for 28 days post-instillation. The results showed changes in the expression of genes encoding oxidative stress-related enzymes (Gpx1, SOD, FMO2 and GAPDH) in testicular tissues. On the other hand, genes related to metal toxicity (Mt1), apoptosis/cell cycle (casp 3, p53), and protein-folding (Hsp 70) processes were not modified [43]. The authors suggest that the effects were reversible, as the changes were observed only on day 7, but not on day 28.

The subcutaneous injection of non-coated AgNPs (10–40 nm/UV–vis: 412 nm) in mice, administered from PND8 to PND21, showed a decreased seminiferous tubules and a significant increase in the rate of abnormal sperm, especially in a high dose (5 mg/mL). In addition, down-regulation of Amh, Cx43, and Claudin-11 genes and up-regulation of E1f1ay, Gsta4, and Fdx 1 genes were observed (Zhang et al., 2015).

4. Gold nanoparticles (AuNPs)

Gold nanoparticles (AuNPs) have been widely explored for biomedical and scientific purposes due to their excellent physicochemical characteristics, such as electronic, optical, magnetic, and catalytic properties [46,47]. They are promising agents for diagnosis and treatment, being used as drug/gene deliverers, imaging, and cancer photothermal therapy [48–51].

The increase in AuNPs in biomedical applications has also raised concerns about their fate and potential toxic effects on living organisms, including humans [16]. Nevertheless, AuNPs are highly biocompatible in biological systems [2], and they show colloidal physical stability for at least two years when conjugated with biological molecules [52]. Concerns regarding AuNPs cytotoxicity came from studies showing that AuNPs can easily cross the cell membrane and nucleus, attaching to DNA and accumulating in different organs [53–55]. However, the AuNPs' adverse effects are related to size, dose, shape, mode of penetration into cells, period of exposure, metabolism, and immune responses [56]. Few studies were developed focusing on the reproductive organs. The following topics and Table 3 summarize the *in vitro* and *in vivo* AuNPs data.

4.1. In vitro studies of gold nanoparticles (AuNPs)

The toxic effects and the molecular mechanisms by which gold nanorods (GNRs) measuring 9–11 × 34–42 nm affect male reproduction was evaluated in cell lines derived from spermatocytes (GC-2) and Sertoli cells (TM-4) for 24 and 48 h. The results showed that GNRs could induce toxic effects on the mitochondria at even low concentrations, decreasing their membrane potential. The Sertoli cell barrier in TM-4 cells was also altered, interrupting ZO-1, occludin, claudin-5, and connexin-43. In GC-2 cells, however, no significant alteration was observed [57].

Liu and colleagues (2020) evaluated the effects of non-coated AuNPs (DLS.: 5–10 nm/ζP: −27 mV) on Leydig Cells (TM3) for 24, 48, 72, and 96 h. The NPs internalized into the endosomes/lysosomes of TM3 cells induced the formation of autophagosomes, increased the production of reactive oxygen species (ROS), and disrupted the cell cycle in the S phase, resulting in concentration-dependent cytotoxicity and DNA damage.

4.2. In vivo studies of gold nanoparticles (AuNPs)

4.2.1. Intraperitoneal administration

Zakhidov and collaborators (2012) evaluated the response of male mice (F1- hybrid: CBA × C57Bl/6) germ cells after exposure to non-coated AuNPs (DLS: ~2.5 nm) for four days. The results showed that the exposure did not cause damage to the spermatogenic epithelium and did not induce chromosomal abnormalities in SSCs. However, the cytogenetic evaluation showed that AuNPs could affect the chromosomes of round spermatids.

In another study, the *in vivo* toxicological effects of a single injection of PEG-coated AuNPs (4.4, 22.5, 29.3, and 36.1 nm/ζP: −6.01, −1.92, −1.89, and −0.98 mV) were investigated in C57 mice (male and female). Although the authors aimed to assess sex differences in the toxicity of gold nanoparticles, no significant toxicological response was observed in male and female genital organs [60].

Recently, Yahyaei and collaborators (2019) evaluated the toxicity of non-coated AuNPs (50 nm) administered for three consecutive days in different organs of Wistar rats, including testis. Their results showed a decrease in the seminiferous tubule cross-sections and vacuolization of the seminiferous epithelial at high doses.

4.2.2. Intravenous administration

The distribution and toxicity of a single injection of two types of functionalized AuNPs (ω-methoxy and ω-aminoethyl polyethylene glycol) of size 14 nm (DLS: 28.2 and 28 nm) were examined in adult male ICR mice. The two AuNPs crossed the hematotesticular barrier, entered germ cells, and accumulated in testis without affecting fertility, fetal survival, or development. However, testosterone levels were increased in the group treated with AuNPs functionalized with only ω-aminoethyl polyethylene glycol [16].

Non-coated AuNPs (DLS.: 5–10 nm/ζP: −27 mV) were administered once a day for 14 consecutive days in male mice. The data showed that AuNPs gradually accumulated in the testes, even though no histopathological changes were observed in germ and intestinal cells. The researchers only observed that AuNPs decreased plasma testosterone levels and 17αhydroxylase expression without affecting fertility [58].

5. Iron oxide nanoparticles (IONPs)

Iron oxide nanoparticles (IONPs) have been extensively investigated among the different magnetic nanoparticles due to their unique intrinsic magnetic properties, the so-called superparamagnetism [1]. These properties allow their use in several scientific areas, such as electronics, environment, and biomedicine [62,63]. The IONPs have been used in Magnetic Resonance (M.R.) (contrast agents), drug delivery systems, treatment of tumors (by hyperthermia), gene therapy and tissue repair [63–66].

Due to their similarity to endogenous iron in the body, IONPs were initially considered biocompatible and non-toxic [67]. However, many studies have shown that IONPs can cross physiological barriers in mice and can quickly accumulate in different tissues, inducing toxicity [63, 68–71]. The most common cellular and molecular effects induced by IONPs were oxidative and DNA damages, mitochondrial changes and cell membrane disruptions [71–75]. Few studies have demonstrated the effects of these NPs on the reproductive organs and the available *in vivo* toxicological studies using IONPs are discussed on the following topics and summarized in Table 4.

5.1. In vitro studies of iron oxide nanoparticles (IONPs)

In vitro data regarding the adverse effects of IONPs on the male reproductive system and sperm cells are still scarce.

5.2. In vivo studies of iron oxide nanoparticles (IONPs)

5.2.1. Intraperitoneal administration

Di Bona and colleagues (2015) investigated the influence of surface load and two doses (10 mg/kg and 100 mg/kg) of polyethyleneimine-coated (PEI-NPs) and poly (acrylic acid)-coated (PAA-NPs) iron oxide NPs, on testis development. CDI mice were exposed to positively charged PEI-NPs (28 nm) and to negatively charged PAA-NPs (30 nm) in the uterus (one injection on pregnant mice on days 8, 9, or 10 of gestation). The exposure to positively charged PEI-NPs altered testis morphology, showing a significant decrease in the seminiferous epithelium and germ cell numbers. Interestingly, no significant morphological changes were observed in the testis of mice exposed to negatively charged PAA-NPs.

The evaluation of the adverse effects of Fe_2O_3-NPs (<50 nm), administered on mice once a week for four weeks, showed that Fe_2O_3-NPs could cross the hematotesticular barrier and accumulate in the testis. While ROS, SOD, and vitamin C levels increased, the levels of CAT and GSH decreased. It was also observed increased apoptosis/degeneration of spermatogenic cells, desquamation of germ cells, and vacuolization of seminiferous tubules. The authors suggested that testicular toxicity may be associated with the accumulation of NPs, leading to oxidative stress and apoptosis [77]. It is worth mentioning that an increase in serum testosterone levels occurred at a concentration of 50 mg/kg, probably occurring in a dose-dependent manner.

5.2.2. Oral administration

Ghosh and colleagues (2020) showed the effects of two functionalized SPIONs with α-tocopheryl-polyethylene glycol-succinate-TPGS (30 nm/DLS: 178.6 nm/ζP: +35.6 mV) and dodecyl-dimethyl-ammonium-bromide-DMAB (180 nm/DLS: 67.14 nm/ζP: +53.3 mV) on sperm morphologies of albino Swiss mice after administration for five consecutive days. The animals treated, by gavage, with SPIONs-TPGS showed significant abnormalities in sperm heads, such as hook, pinhead, banana, and amorphous. Animals treated with SPIONs-DMAB, on the other hand, did not show differences in the sperm head. The authors suggested that the sub-micron size of the nanoparticles may be related to these abnormalities observed.

6. Zinc oxide nanoparticles (ZnONPs)

Zinc oxide nanoparticles (ZnONPs) have become one of the most used nanoparticles in various biological applications. Due to their excellent biocompatibility, low production cost and low toxicity, they have been used in drug delivery systems, bioimaging, molecular diagnosis and cancer therapy [79–81]. However, studies have shown that ZnONPs can accumulate in various organs and induce cytotoxicity [82, 83].

In vitro studies have revealed oxidative stress, lipid peroxidation, oxidative DNA damage, increased intracellular calcium release and cytotoxicity in different cell lines, including male reproductive cells [17, 84,85]. Most *in vitro* studies have focused on the effects of ZnONPs on spermatogenesis, describing the cytotoxicity in different cell types. The following topics and Table 5 summarize the *in vitro* and *in vivo* studies regarding ZnONPs toxicity in germ and testicular somatic cells.

6.1. In vitro studies of zinc oxide nanoparticles (ZnONPs)

Liu and colleagues (2016) used Sertoli cells (TM-4) and spermatocytes (GC2-spd) to explore the reproductive effects of non-coated ZnONPs (50 nm/DLS.: in water 177 nm and medium 331 nm) at sub-lethal doses for 24 h. *In vitro* exposure to NPs induced ROS generation, decreased glutathione level, increased MDA level, damaged DNA, and downregulated hematotesticular barrier protein expressions in TM-4 cells.

Another study investigated the adverse effects of non-coated ZnONPs

Table 5
Data using zinc oxide nanoparticles.

Assay	NP	Functionalization	Size	Cell line/animal model	Method of exposition/ administration	Exposure time	Concentration	Main findings	Reference
in vitro	ZnONPs	non-functionalized	50 nm	Sertoli cell line (TM-4)	incubation	24 h	0, 0.04, 0.08, 0.4, 0.8, 4, 8 and 16 μg/mL	• Decreased cell viability (dose of 8 μg/mL) • ROS production • Increased membrane permeability • Reduced expression of tight junction proteins • Increased TNF-α levels	[86]
				Spermatocyte cell line (GC2-spd)	incubation	24 h	0, 0.04, 0.08, 0.4, 0.8, 4, 8 and 16 μg/mL	• Decreased cell viability (dose of 8 μg/mL) • DNA damage • S phase arrest in GC2-spd cells • Increased ROS levels	
in vitro	ZnONPs	non-functionalized	20 nm–40 nm	Leydig cell line (TM3)	incubation	1, 4 and 12 h	0,1,2,5,10, 20, 50, 100, 150, 200 μg/mL	• Cytotoxicity • High number of autophagosomes and autolysosomes • Damages in mitochondria • Apoptosis • Increased SOD. activity • Increased expressions of steroidogenic genes • Increased testosterone	[87]
in vitro	ZnONPs	non-functionalized	<100 nm	GC-1 cell line	incubation	6 and 12 h	0, 1, 5, 8, 10, and 20 μg/mL	• Cytotoxicity • ROS production • DNA damage • Cytoskeleton and nucleoskeleton dynamic alterations	[23,84]
in vitro	ZnONPs	non-functionalized	70 nm	Leydig cell line (TM3)	incubation	12 and 24 h	0, 5, 10, 15 and 20 μg/mL	• Accumulation • Cytotoxicity • Induction of apoptosis • DNA damage • ROS production • Loss of mitochondrial membrane potential	[17]
				Sertoli cell line (TM-4)	incubation	12 and 24 h	0, 5, 10, 15 and 20 μg/mL	• Accumulation • Cytotoxicity • Induction of apoptosis • DNA damage • ROS production • Loss of mitochondrial membrane potential • Disorganization of the seminiferous epithelium • Sperm abnormalities (double head, small head, unshaped head, double tail)	
in vitro	ZnONPs	non-functionalized	30 nm	Leydig cell line (TM3)	incubation	24 h	0, 0.5, 1, 2, 3, 4, 8 μg/mL	• Oxidative stress • Apoptosis • Autophagy	[85]
in vivo	ZnONPs	non-functionalized	30 nm	Kunming mice	Oral administration (gavage)	for 28 days	100, 200, and 400 mg/kg/day	• Disorganization of the seminiferous epithelium • Germ cell loss • Reduction in round spermatids • Oxidative stress • Apoptosis • Autophagy	[85]

(*continued on next page*)

Table 5 (*continued*)

Assay	NP	Functionalization	Size	Cell line/animal model	Method of exposition/ administration	Exposure time	Concentration	Main findings	Reference
in vivo	ZnONPs	non-functionalized	30 nm	Kunming mice	Oral administration (gavage)	for 14 days	50, 150 and 450 mg/kg	• Accumulation in testis • Atrophy and vacuolization of germ cells • Reduced testosterone • Increased apoptosis • up-regulation of stress-related gene in the endoplasmic reticulum (ER.) • Negative regulation of the StAR gene	[24]
in vivo	ZnONPs	non-functionalized	70 nm	CD-1 mice	Intravenous injection	single dose	1 and 5 mg/kg	• Induction of apoptosis • DNA damage • ROS production • Loss of mitochondrial membrane potential • Reduction of the seminiferous epithelium • Sperm head abnormalities (double head, small head, unshaped head, double tail)	[17]

(<100 nm/GBET = 88 nm/ζP: −15 mV at pH = 6 and −55 mV at pH = 12) for 6 and 12 h, on mouse-derived spermatogonia (GC-1). The data indicated that higher concentrations compromise the progression of spermatogenesis. Moreover, ZnONPs increased the intracellular levels of ROS and caused double-strand DNA breaks. Also, changes in cytoskeleton and nucleoskeleton dynamics, with consequent cell death, mainly due to necrosis, were observed [85].

Han and collaborators (2016) evaluated the toxicity of non-coated ZnONPs (~70 nm/DLS.: between 20 and 110 nm) in Leydig and Sertoli cell lines for 12 h and 24 h. The results showed that NPs were internalized into cells and caused cytotoxicity in a time-dependent and dose-dependent manner. In this study, apoptosis was observed, probably due to DNA damage caused by ROS.

Bara and Kaul [87] evaluated the toxicity of non-coated ZnONPs (20–40 nm/DLS.: 75 nm) for 24 h, using Leydig cells (TM3). The results showed that ZnONPs cause direct and indirect effects on steroidogenesis. Cell morphological changes were reported in mitochondria and cytoplasm with the accumulation of autophagosomes/autolysosomes. Also, a significant increase in testosterone levels was observed in TM3 cells.

Shen and colleagues (2019) evaluated the toxicity of non-coated ZnONPs (30 nm/DLS: 66.36 nm/ζP: 38.25 mV) in Leydig cells (TM3). Their results demonstrated reduced cell viability, increased apoptosis and autophagy, and generation of oxidative stress (ROS) and MDA levels increased along with an increment in dose. In contrast, the content of GSH and the activities of the antioxidant enzymes SOD and GSH-PX decreased.

6.2. In vivo studies of zinc oxide nanoparticles (ZnONPs)

6.2.1. Intravenous administration

The intravenous injection (single dose) of non-coated ZnONPs (~70 nm/DLS.: between 20 and 110 nm) caused testicular histopathological changes in CD-1 mice. The data showed a significant reduction in the seminiferous epithelium height after the injection of ZnONPs (5 mg/kg) in the PND28 and PND42. A decrease in the seminiferous tubule diameter was also observed in the group treated with ZnONPs (1 mg/kg). Besides, abnormalities in sperm morphology (double head, small head, shapeless head, double tail) were identified 49 days after treatment with ZnONPs [17].

6.2.2. Oral administration

The adverse effects of non-coated ZnONPs (30 nm) administered for 14 days were evaluated on male reproductive systems in Kunming mice. Germ cell apoptosis and seminiferous tubule atrophy and vacuolization were observed in these animals. Furthermore, changes in the regulation of stress-related genes (in the endoplasmic reticulum) and the StAR gene occurred in Leydig cells, resulting in a significant decrease in testosterone levels. In this study, degeneration of seminiferous tubules, vacuolization of Sertoli cells, necrosis of germ cells and vacuolization of Leydig cells occurred along with an increment in dose [24].

In another study, using Kunming mice, it was observed that the intragastric exposure of non-coated ZnONPs (30 nm/DLS.; 66.36 nm/ζP: 38.25 mV) for 28 days resulted in alterations of the seminiferous epithelium, depletion of germ cells and reduction of round spermatids [85].

7. Titanium dioxide (TiO_2NPs) nanoparticles

Titanium dioxide (TiO_2NPs) nanoparticles are widely used due to their high stability, anti-corrosion, and photocatalytic properties. These NPs are used in consumable products, such as cosmetics, medicines, and sunscreens [16,20,88].

Recent studies have shown that TiO_2NPs can enter cells, initiating inflammatory pathways and apoptosis [89,90]. Furthermore, it is reported that TiO_2NPs form reactive oxygen species, causing DNA damage

Table 6
Data using titanium oxide nanoparticles.

Assay	NP	Functionalization	Size	Cell line/animal model	Method of exposition/ administration	Exposure time	Concentration	Main findings	Reference
in vitro	TiO_2NPs	non-functionalized	__	Primary culture of Leydig cells (LCs)	Incubation	24 h	0, 10, 20 and 40 μg/mL	• Viability reduction • Ultrastructural changes (vacuolization and nuclear condensation) • Mitochondrial damage • Reduced testosterone levels	[96]
in vivo	TiO_2NPs	non-functionalized	25 nm	Kunming mice	Oral administration	1 day	0, 10, 50 or 250 mg/kg	• Vacuoles in seminiferous tubules (higher doses) • Reduced number of germ cells • Reduced testosterone levels • Down-regulation of steroidogenic genes	[97]
in vivo	TiO_2NPs	non-functionalized	5–6 nm	CD-1 mice	Oral administration	90 consecutive days	2.5, 5, and 10 mg/kg	• Testis mass reduction • Accumulation in testes • Sperm number reduction • Sperm morphological alteration • Sertoli cell apoptosis • Decreased height of seminiferous epithelium • Sertoli cell vacuolization • Reduced LH, FSH and testosterone levels • Increase in E2 and P4 levels • Altered spermatogenic and oxidative stress gene expression	[94]
in vivo	TiO_2NPs	non-functionalized	6 nm	ICR mice	Oral administration	60 days	2.5, 5 or 10 mg/kg	• Reduced testicular weight • Reduced seminiferous epithelium height • Reductions in Leydig cell numbers • Lower sperm counts • Sperm morphological alteration • Germ cell death • Decreased activity of LDH, SODH, SDH and G6PD • ROS production	[92]
in vivo	TiO_2NPs	non-functionalized	5–10 nm	ICR mice	Oral administration (Gavage)	per day for 28 days	10, 50, or 100 mg/kg	• Sperm malformation and sperm cell MN rate increased • Reduction in germ cell number • Spherospermia • Vacuolization in spermatogenic cells • ROS production • Decreased SOD activity • Increased MDA activity	[98]
in vivo	TiO_2NPs	non-functionalized	__	C57BL/6 J gpt delta mice	Intravenous injection	Once per week for four weeks	0, 2 or 10 mg/kg	• Reduced sperm numbers • Decreased sperm motility	[99]
in vivo	TiO_2NPs	non-functionalized	20.6 nm	Pregnant females C57BL/6 J mice	Inhalation	1 h/day from gestation day 8 to gestation day 18	42 mg/m^3 aerosolized powder	• F1 male: reduced sperm production	[100]
				Mating of F1 generation with CBA/J mice to produce F2 generation	__	__	__	• F2 male: reduced sperm production	

(*continued on next page*)

Table 6 (*continued*)

Assay	NP	Functionalization	Size	Cell line/animal model	Method of exposition/ administration	Exposure time	Concentration	Main findings	Reference
in vivo	TiO_2NPs	non-functionalized	<25 nm	Wistar rat	Oral administration (Gavage)	3 weeks	50 mg/kg/day	• Reduced testicular weight • Increase the activity of the testicular marker enzyme γ-GT • Increase in testicular MDA level • Deregulation of testicular GSH levels • Significative increase testicular TNF-α level • Decline in StAR gene expression • Reduced testicular c-kit • Reduced serum testosterone levels • Elevations in serum estradiol levels • Increases in serum FSH and LH Levels • Cell apoptosis • Degeneration spermatogenic • Atrophy of seminiferous tubules	[101]
in vivo	TiO_2NPs	non-functionalized	21 nm	Wistar rats	Intravenous injection	30 days	0, 5, 25 and 50 mg/kg	• Accumulation in testis • DNA damage • Cell apoptosis • Reduced testosterone levels • Oxidative stress • Cytotoxicity and genotoxicity in sperm	[93]

and cellular function alterations [91–94]. Some studies have shown that the male reproductive system is sensitive to TiO_2NPs and that the testis is affected through several routes, such as intragastric, intraperitoneal and intravenous administration [95]. The *in vitro* and *in vivo* studies concerning the toxicity of TiO_2NPs are summarized in the following topics and Table 6.

7.1. *In vitro studies of titanium dioxide (TiO_2NPs) nanoparticles*

Li and colleagues (2018) evaluated the adverse effects of non-coated TiO_2NP (DLS: 42.36 nm/ζP: 42.8 mV) in primary cultures of Leydig cells for 24 h. The results revealed that TiO_2NP could cross cell membranes, causing vacuolization and nuclear condensation. Also, the exposure caused a reduction in cell viability in a time-dependent manner. Furthermore, suppression of testosterone was observed by regulating ERK1/2-PKA-PKC signaling pathways.

7.2. *In vivo studies of titanium dioxide (TiO_2NPs) nanoparticles*

7.2.1. *Oral administration*

The effects of non-coated TiO_2NPs (25 nm) were evaluated in male Kunming mice treated from the 28th postnatal day (PND 28) to PND 70. No histological changes were found in the testicles of mice exposed to a dose of 10 mg/kg/day. However, at doses of 50 and 250 mg/kg/day, vacuoles and reduced germ cell layers were observed in seminiferous tubules. Likewise, there was a reduction in testosterone levels in a dose-dependent manner, downregulating the genes related to steroidogenesis [97].

Gao and collaborators (2013) investigated the toxicity of non-coated TiO_2NPs (5–6 nm/DLS.: 294 nm) in CD-1 mice. These mice were sub-chronically exposed to different doses of this NP. The results showed that TiO_2NPs could cross the blood-testis barrier, accumulating in the testis. This NP reduced the seminiferous epithelium height and promoted vacuolization and irregular arrangement of Sertoli cells in this epithelium. The serum levels of sex hormones were significantly altered, presenting an increase in estradiol (E2) and progesterone (P4) values, while a marked decrease occurred in luteinizing hormone (LH), follicle-stimulating hormone (FSH) and testosterone levels. It was also reported that these nanoparticles could contribute to sperm malformations.

Shahin and Moramed [101] investigated the testicular effects of short-term oral exposure to non-coated TiO_2NPs (<25 nm) on Wistar rats for three weeks. Treated rats exhibited altered glutathione levels, elevated TNF-α levels, and up-regulated expressions of Fas, Bax, and caspase-3 genes. Moreover, intragastric administration increased testicular gamma-glutamyltransferase (γ-GT) activity, decreased StAR and c-kit gene expressions, reduced serum testosterone levels, lowered sperm counts, and high prevalence of defective sperms.

Toxic Effects of TiO_2NPs (5–10 nm) were also investigated on male ICR Mice testes. Results showed that TiO_2NPs induced sperm malformation and increased the rate of sperm cell micronucleus. These NPs also reduced the germ cell number and promoted the vacuolization of spermatogenic cells, as well as ROS and MDA content also increased while the SOD activity decreased [98].

7.2.2. *Intravenous administration*

Meena and collaborators (2014) investigated the intravenous administration of non-coated TiO_2NPs (~10–20 nm) in Wistar rats for 30 days at weekly intervals. These nanoparticles accumulated in testicular cells, mainly in lysosomes and mitochondria. In a broad view, the NPs promoted disorganization of seminiferous tubules, increased ROS, induced apoptosis, and cytotoxic and genotoxic changes in sperm. Furthermore, the activity of antioxidative enzymes (SOD and GPx) decreased with increment in dose, and a significant decrease in testosterone synthesis was also observed. The effects of intravenous injection of non-coated TiO_2NPs administered once per week for four weeks were also evaluated in male C57BL/6 J mice by Miura and collaborators

Table 7
Data using nickel nanoparticles.

Assay	NP	Functionalization	Size	Cell line/animal model	Method of exposition/ administration	Exposure time	Concentration	Main findings	Reference
in vitro	NiNPs	non-functionalized	90 nm	GC-1 cells line	incubation	24 h	0, 25, 50, 75,100 and 200 μg/mL	• Inhibition of cell proliferation • Cell shrinkage • Lost of intercellular connections • Reduced cell volume • Cell death/apoptosis • Agglutination of chromatin • Alteration in cytoskeleton • Enlarged endoplasmic reticulum • Cell cycle arrest	[109]
in vivo	NiNPs	non-functionalized	90 nm	Male and female Sprague-Dawley	Oral administration (Gavage)	during 10 weeks	0, 15 and 45 mg/kg/day	• Cell apoptosis • Decreased sperm motility • Decreased serum FSH and T concentrations.	[102]
in vivo	NiNPs	non-functionalized	90 nm	ICR mice	oral administration (Gavage)	during 30 days	0, 5, 15 and 45 mg/kg/day	• Disorganization of seminiferous epithelium • Cell apoptosis • Decreased sperm motility	[107]

(2014). They observed an evident reduction in testicular function, reducing sperm number and motility in a dose-dependent manner.

7.2.3. Respiratory administration

Kyjovska and collaborators (2013) investigated the influence of maternal exposure to non-coated TiO_2NPs (20.6 nm) by inhalation 1 h a day, from gestation day 8–18. The offspring's male reproductive organs were investigated. Maternal exposure did not severely affect spermatogenesis in the F1 generation; however, a decreased sperm count was observed. Also, there was a delay in the production of the F2 generation, which also presented a reduced sperm production.

8. Nickel nanoparticles (NiNPs)

Nickel is a natural element used in various applications, such as metallurgical processes and electrical components [102,103]. Due to their physicochemical properties, such as the high surface energy level, high magnetism, low melting point, high surface area, and low combustion point, NiNPs are constantly being utilized in different scientific areas [99,100]. These nanoparticles are being used in drug delivery systems and contrasting agents for different therapies [104,105]).

The applications of these NPs raise several concerns related to their potential toxic effects [102,106]. According to the International Agency for Research on Cancer, nickel compounds are classified as carcinogens [100]. Also, some experimental animal studies suggest the toxic potentials of nickel metallic nanoparticles in different biological systems [104,105,107,108], and recent studies have shown that NiNPs can cause toxicity in the male reproductive system of rats [102,107]. The *in vitro* and *in vivo* studies on toxicities of NiNPs in the male reproductive system are displayed in the following topics and summarized in Table 7.

8.1. In vitro studies of nickel nanoparticles (NiNPs)

There are few *in vitro* studies applying NiNPs. Wu and collaborators (2020) evaluated the toxicity effects induced by non-coated NiNPs (90 nm) in a mouse sperm cell line (GC-1) for 24 h. The results showed a significant decrease in cell proliferation, changes in cell morphology (cell shrinkage and loss of intercellular connections), alterations of cell ultrastructural components, cell pycnosis and interruption of the cell cycle in phase G1. It also demonstrated apoptosis activation by inhibiting the PI3K/AKT/mTOR signaling pathway.

8.2. In vivo studies of nickel nanoparticles (NiNPs)

8.2.1. Oral administration

Kong and collaborators (2014) evaluated the toxicity of non-coated NiNPs (90 nm) in the reproductive system of adult Sprague-Dawley rats, administering these NPs by gavage for ten weeks. A decreased level of FSH, testosterone and antioxidant enzymes such as SOD, CAT and GSH were observed, while NO, MDA and ROS were increased. Additionally, changes in sperm motility, germ cell impairment in the seminiferous epithelium, and apoptosis resulted in lower reproductive indexes and poor offspring development.

Hu and colleagues (2019) also evaluated the toxicity of NiNPs with the same concentrations and methods in male ICR mice. Similar results were found, such as a decreased sperm motility index and increased germ cell apoptosis in the groups exposed to high doses.

9. Discussion

The use of inorganic NPs for different medical applications has increased considerably in recent years. These NPs can be used in reproductive medicine, assisted reproduction, cryopreservation, transgenesis, and contraception [7,110]. Hence, there is a need to assess the potential adverse effects that NPs can bring to various organs and systems, and international regulatory uses should be established for their

use in reproductive medicine. Nowadays, several studies have demonstrated the specific interactions of these NPs with the reproductive system through different routes of administration [9,11,12]. This systematic review selected data published in the last 12 years, assessing the reproductive toxicity caused by different types of inorganic NPs. The *in vitro* and *in vivo* toxic data in germ cells, Sertoli cells, and Leydig cells were described according to the type of each NPs.

9.1. In vitro

Among the selected studies, AgNPs and ZnONPs were the most investigated NPs. In contrast, AuNPs, IONPs, TiO2NPs, and NiNPs had fewer data to broadly understand their effects, mainly in cellular signaling pathways. Most studies with testicular somatic cells (Sertoli and Leydig cells), germ cells (at different stages of differentiation) and sperm cells showed adverse effects when in contact with the NPs. Depending on the size and concentration of NPs, cytotoxicity, mitochondrial alterations, damage to DNA, oxidative stress, increased apoptosis, and necrosis were frequently observed.

At nanoscale dimensions, size plays a pivotal role in biological interactions since the toxic effects are significantly associated with small-sized NPs and their distribution and large surface/area ratio [2,30,111]. The sizes of some NPs are comparable to the size of different cell constituents, such as protein globules, the diameter of DNA helix, and the thickness of cell membranes, allowing them to enter cells and organelles [2]. Gold NPs no larger than 6 nm, for example, can effectively enter the cell nucleus, whereas large NPs only penetrate through the cell membrane and are found only in the cytoplasm [112]. NPs with smaller sizes are more toxic than larger NPs, which can not enter the nucleus. NPs smaller than 5 nm usually pass through cell barriers nonspecifically, while larger particles enter cells by phagocytosis, macropinocytosis, and specific and nonspecific transport mechanisms.

The surface charge of NPs also plays a vital role in their toxicity because it largely determines the interactions of NPs with biological systems. The zeta potential (ζP) is considered an electrical potential produced by the association between charged groups with the surface of a particle and the suspension medium [113]. The ζP may influence the degree of interaction between a particle and a cell surface once cell membranes are negatively charged [114]. *In vitro* data have shown that surface-functionalized cationic NPs may be more cytotoxic than neutral or anionic NPs by causing lysosomal damage [115]. Positively charged NPs can opsonize protein adsorption, facilitating the phagocytosis of antibodies and complement components from blood and biological fluids [2,116]. In addition, the adsorbed proteins may also affect the surface properties of NPs, altering the surface charge, aggregation characteristics, and/or hydrodynamic diameter of NPs [2,117].

Braydich-Stolle and colleagues (2010) demonstrated that (hydrocarbon and polysaccharide) functionalized AgNPs induced toxicity in

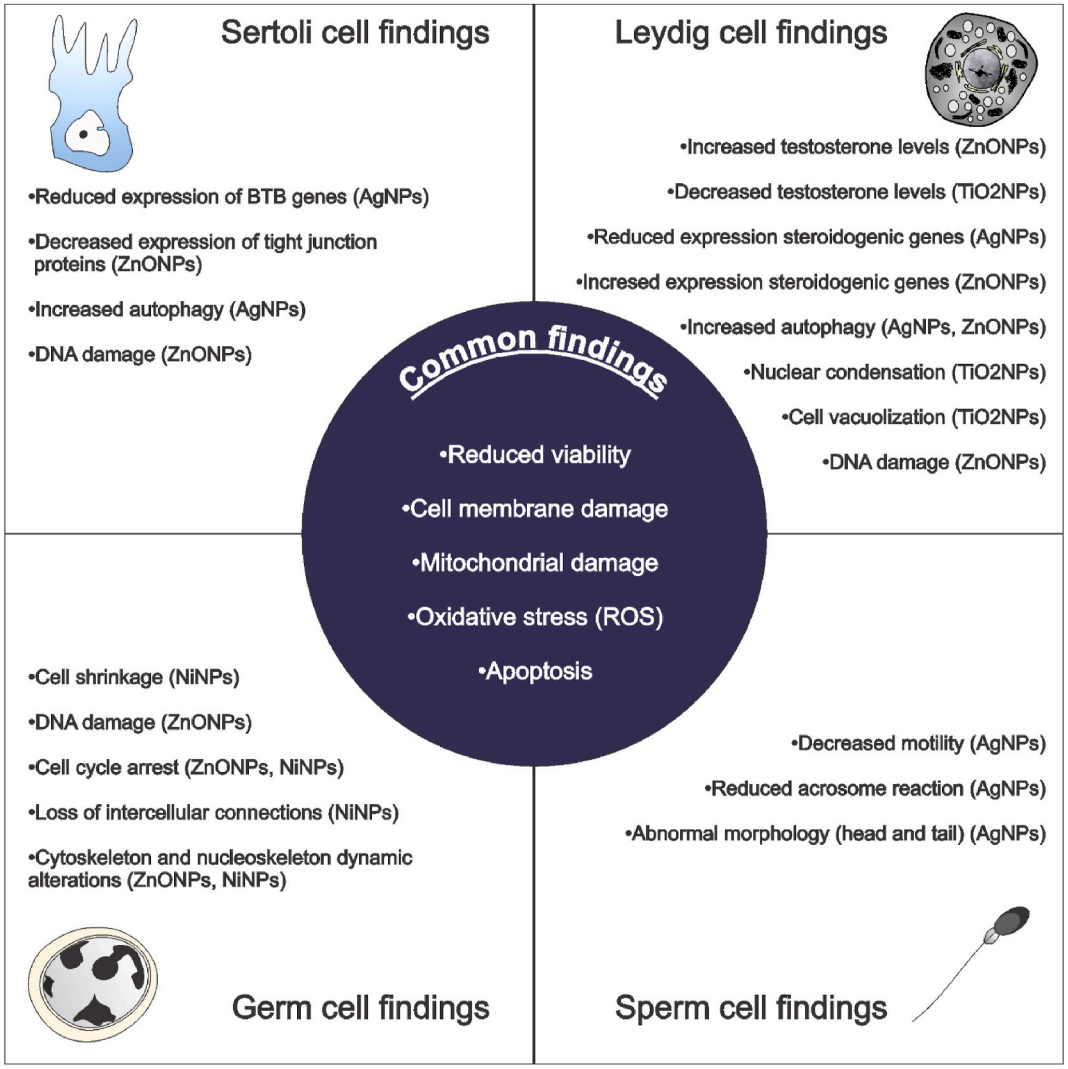

Fig. 2. Main toxic effects of inorganic nanoparticles in testicular cells *in vitro*. The common findings for all cells (circled in blue) and the main data for each cell type (Sertoli, Leydig, Germ and Sperm) are depicted in this scheme.

SSC, mainly due to size and concentration. Since the coating was degraded along with the exposure time, it does not influence toxicity. In addition, greater surface area and high concentrations/dose can provide higher chemical reactivity, inducing the production of reactive oxygen species (ROS), leading to enhanced toxicity of NPs. Likewise, germ cells, including sperm, show morphological and functional alterations when exposed to high concentrations of nanoparticles [44].

As demonstrated in Fig. 2, testicular somatic and germ cells diminished their viability when exposed to nanoparticles. Specifically, Sertoli cells presented alterations in BTB proteins, DNA damages, and increased autophagy incidence. For Leydig cells, alterations in steroidogenic gene expressions were commonly observed in the presence of inorganic nanoparticles beyond autophagy. Some nanoparticles stimulated testosterone production, while others inhibited this synthesis. Some hypotheses suggest increasing or decreasing testosterone levels after *in vitro* exposure to nanoparticles. Bara e Kaul [87] hypothesized that the increase in expression of genes related to testosterone synthesis (Star and P450scc) lead to altered testosterone production after exposure to ZnNPs. On the other hand, Li e colleagues (2018) suggested that inhibition of testosterone biosynthesis by TiO2NPs is achieved by regulating testosterone-related factors through the ERK1/2–PKA–PKC signaling pathways in LCs.

For germ cells, loss of intercellular connections, cytoskeleton, and nuclear alterations were common findings. Concerning sperm, loss of motility and morphological alterations were seen after exposure to nanoparticles. Cell membrane and mitochondria damage were frequently observed in an *in vitro* system. Furthermore, ROS production, resulting in apoptosis, seems to be a common consequence after exposure to inorganic nanoparticles.

9.2. *In vivo*

Regarding *in vivo* studies, the most frequently investigated NPs were AgNPs, ZnONPs, and TiO_2NPs. Interestingly, all the NPs examined in this review showed a great potential to penetrate the hematotesticular barrier, independent of the routes of administration. The organ/system (exposition route) to which NPs are administered will influence their biodistribution, tissue/cell uptake, clearance/bioaccumulation, and reproductive toxicity [11]. It is worth mentioning that TiO_2NPs demonstrated more toxicity compared to AgNPs and ZnONPs. In mice, the oral administration of non-coated TiO_2NPs (5–6 nm) showed that they could cross the blood-testis barrier, accumulating in the testis [94]. Several *in vivo* studies have shown that metallic NPs can penetrate the blood-testis barrier due to their size or induce an inflammatory response, compromising barrier integrity [19,21,24]). Changes in the hematotesticular barrier represent a risk for spermatogenesis since it controls the environment in which germ cells develop [19,24]). Considering inflammation, inorganic NPs activate nuclear kappa B (NF-ǩB) signaling by upregulating the transcription of several pro-inflammatory genes. Tumor necrosis factor-α, IL-1, IL-6, and IL-8 were frequently upregulated. These pro-inflammatory factors can promote oxidative stress, DNA damage, and apoptosis [12,118]. The NP size largely determines how the NPs interact with proteins and immune cells in the body. This interaction, in turn, affects the kinetics of their distribution and accumulation in different organs.

This review showed that NPs accumulation is a frequent finding that significantly impairs the different animal's spermatogenic processes (Fig. 3). The AuNPs seem to be the most biocompatible inorganic nanoparticle for reproductive organs, even though most AgNPs, ZnNPs, IONPs, TiO2NPs, and NiNPs studies reported morphological changes in testis. The most common findings were structural changes in Sertoli, Leydig and germ cells (including sperm cells), oxidative stress, apoptosis, and/or necrosis. Reduced seminiferous tubules, disorganized seminiferous epithelium, and diminished sperm production were observed in experimental studies. Sertoli cells showed vacuoles and weakened blood-testis barrier, while germ cells presented a high incidence of apoptosis. Leydig cells' steroidogenic genes were altered, influencing the secretion of testosterone and other steroidogenic hormones. Garcia and colleagues (2014) suggested that the elevated testosterone levels after exposure to AgNPs are due to the increase in Leydig cell size and expression of CYP11A1 and Hsdb31.

Li et al. [16] also proposed that the increase in testosterone levels after exposure to AuNPs would be related to testicular function since pituitary FSH and LH remained unchanged. On the other hand, Sundarraj and collaborators (2016) mentioned that Fe_2O_3-NPs might interfere with the hypothalamic-pituitary-testicular axis, acting as a potential endocrine disruptor and contributing to the increase in serum testosterone levels. Jia e colleagues (2014) showed that serum testosterone levels decrease after exposure to TiO_2NPs due to changes in the synthesis and the conversion of testosterone to estradiol. Therefore, Gao and collaborators (2013) also showed that testosterone levels decrease after Leydig cell exposure to TiO_2NPs.

9.3. *Oxidative stress*

In both systems (*in vitro* and *in vivo*), an increase in ROS generation was observed, with consequent oxidative stress. The production of ROS (hydrogen peroxide, H_2O_2), reactive superoxide anion radicals (O_2), and hydroxyl radicals (• OH) have an essential role in several cell signaling pathways. In a physiological context, it can activate several signaling cascades such as epidermal growth factor receptor (EGF), mitogen-activated protein kinase (MAPK) cascades, and transcription factor

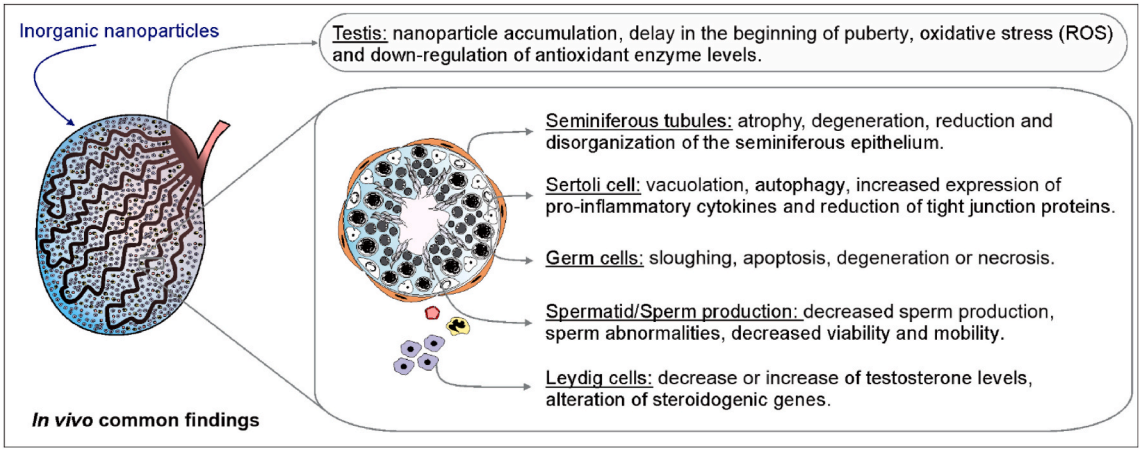

Fig. 3. Main toxic effects of inorganic nanoparticles in testis observed *in vivo*. The common findings seen in testis and for each testicular cell type are depicted in this illustration.

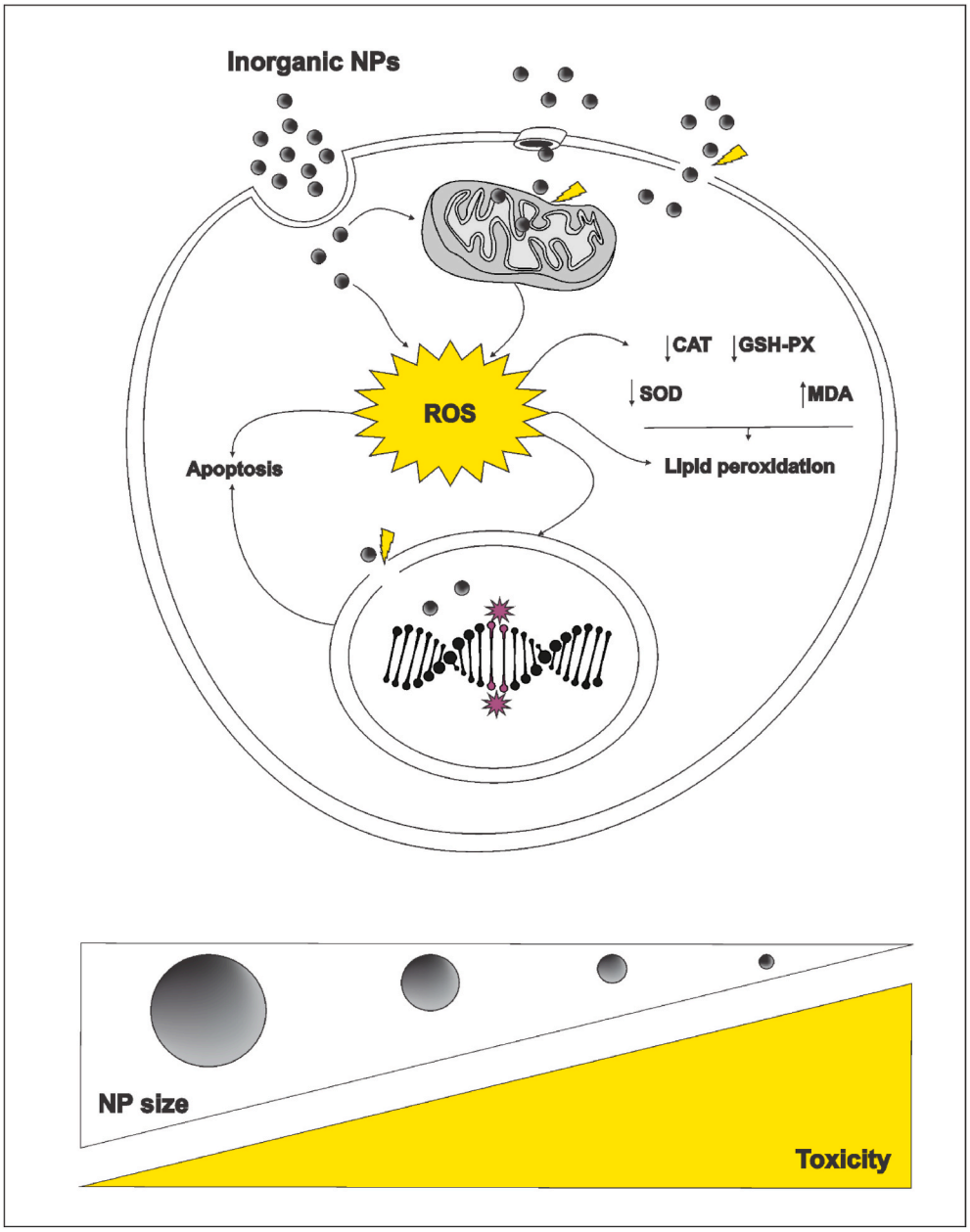

Fig. 4. Oxidative stress caused by inorganic nanoparticles in testicular cells. ROS = reactive oxygen species; SOD = Dismutase Superoxide; CAT = Catalase; GSH-Px = glutathione peroxidase; MDA = Malondialdehyde. Inorganic NPs with different physicochemical properties are taken up by cells through endocytosis, transmembrane proteins or plasmatic membrane pores. NPs can cross the mitochondrial membrane and increase the generation of ROS. In the presence of NPs, the protective factors (SOD, CAT and GSH-Px) are reduced, while free oxygen radicals lead to lipid peroxidation, increasing the levels of MDA. Inorganic NPs also may enter the nucleus, leading to changes in DNA integrity and apoptosis. NPs with smaller sizes are more toxic than larger NPs, reflecting their potential in entering the nucleus.

activating protein-1 (AP-1), and nuclear factor-κB (NF-κB) [119].

Studies with different cell types have shown that metal ions released by NPs promote intracellular ROS overexpression and accumulation by disturbing the electron transfer process [35,110], increasing the NADP+/NADPH ratio [33], and interfering with mitochondrial function.

Mitochondrial-derived ROS may cause cell and tissue destruction through DNA damage, lipid peroxidation, protein oxidation, carbonylation, depletion of cellular thiols, and activation of pro-inflammatory cytokine release. Different inorganic NPs can increase intracellular levels of ROS and reduce antioxidant enzymes, such as glutathione peroxidase (GSH) and superoxide dismutase (SOD), resulting in the formation of DNA adducts (Fig. 4) [29,120]. Inorganic NPs can also modulate genes involved in oxidative stress, such as Gpx1, SOD, FMO2 and GAPDH [43].

Other studies have suggested that metal NPs mixes into redox cycling ROS and chemocatalysis via the Fenton reaction [$H_2O_2 + Fe^{2+} \rightarrow Fe^{3+} + HO^- + \bullet OH$] or Fenton-like reaction [$Ag + H_2O_2 + H+ = Ag+ + \bullet OH + H_2O$] forming free radicals (i.e. hydroxyl radicals) [119,121]. The excessive generation of free radicals alters the homeostatic redox state and promotes tissue inflammation, and cell damage strongly affects testicular functions essential for spermatogenesis [12,111,118].

9.4. Nanoparticle functionalization

In addition to the dose and size of the nanoparticles, other factors such as the duration of exposure, the route of administration, the surface chemistry, among others, may be accountable for the wide variation in the toxicity profile of NPs [30,35]. Additionally, the same NP can present different behaviors depending on the cell types [122]. The modification of surface chemistry or functionalization aims to improve biocompatibility, delay aggregation in body fluids, and stabilize them for biomedical applications [123]. On the other hand, this chemistry surface modification can be associated with NPs toxicity. Notably, the kind of stabilizer agent used plays a role in the level of toxicity. For instance, Cetrimonium bromide (CTAB), commonly used for GNR

synthesis, presents cytotoxicity, even at low concentrations [50]. It is essential to mention that most reproductive toxicological studies evaluated in this systematic review did not use functionalized nanoparticles.

Functionalized AuNPs showed high biocompatibility and, even accumulating in the testis, they did not cause any relevant negative effect on spermatogenesis. A similar result was observed in a study by Ghosh and collaborators [76], using superparamagnetic iron oxide nanoparticles (SPIONs) functionalized with a biodegradable polymer (PLGA) with the surfactant dodecyl-dimethyl-ammonium-bromide (DMAB). The nanoparticle formulation did not induce abnormalities in sperm, and the authors suggested that NPs encapsulation was responsible for reducing cytotoxicity and genotoxicity caused by uncoated SPION.

9.5. General overview

This systemic review showed a good correlation between *in vivo* and *in vitro* findings. Due to the pivotal role of oxidative stress as a second messenger and its link with several other cellular signaling pathways, the role of pure and functionalized inorganic nanoparticles should be considered for future studies. In this review, some studies have shown that NPs with biocompatible polymers seem to be an exciting strategy to reduce toxic effects. Particular attention should be given to AuNPs and IONPs, because they showed more outstanding biocompatibility in reproductive organs when functionalized. However, few studies have focused on the coating and functionalization of NPs. It should be mentioned that the exact mechanisms by which NPs penetrate the blood-testis barrier, the cells, and organelles and their roles in cell signaling alterations are not yet fully understood, described, or proposed in-depth. Despite this broad overview of the toxic effects of several inorganic NPs, the results are highly different because of the lack of standard protocols, distinct NPs sizes, concentration/doses, and routes of administration. Due to this variability, it is hard to highlight the unique or common toxicities related to different subclasses of NPs. These statements are crucial because they can affect the comparisons, making it difficult to determine the most biocompatible NPs in reproductive organs precisely.

In addition, the studies did not clarify whether the route of exposure alters the toxicity of nanoparticles. Furthermore, in most studies, there is a lack of discussions regarding the long-term effect of each type of nanoparticle on male reproduction. Even though *in vivo* studies present strength data, they do not provide detailed information about cellular and/or organ toxicity pathways. Also, most studies focused on investigating the toxicity of NPs in pubertal or adult individuals, and little attention was given to fetal development or infancy. Paternal or maternal exposure to NPs can also lead to fetal toxicity and has been little explored in nanomaterial toxicity studies. Over these years, several discoveries related to the interactions of inorganic NPs with the male reproductive system have been established, but many gaps related to the mechanisms of toxicity of these MPs still need to be filled.

10. Conclusion

The reproductive toxicity of different NPs depends on their physical-chemical characteristics and intrinsic properties, such as size, shape, electrical charge, concentration/dose, and chemical compositions. Significant developments have been made in reporting the main adverse effects in cells; however, future investigations are needed to clarify the exact molecular pathways involved in inorganic NPs toxicity. Understanding the specific molecular interaction between NPs and male testicular cells is essential and deserves significant attention, especially for developing biotechnologies related to reproductive medicine.

Funding

This work was supported by the Coordination for the Improvement of Higher Education Personnel (CAPES, Brazil)for the scholarship granted to GPFD, the National Council for Scientific and Technological Development (CNPq, 422405/2018-3, Brazil), and the Foundation to Support Research of the State of Minas Gerais (FAPEMIG, RED-00079-22, Brazil).

Financial support

CNPq (422405/2018-3) FAPEMIG (RED-00079-22) and CAPES.

CRediT authorship contribution statement

Graziela P.F. Dantas: Funding acquisition, Writing – review & editing. **Fausto S. Ferraz:** Writing – review & editing. **Lídia M. Andrade:** Funding acquisition, Writing – review & editing. **Guilherme M.J. Costa:** Funding acquisition, Roles/Writing - original draft, Writing – review & editing.

Declaration of competing interest

The authors declare that they have no known competing financial interests or personal relationships that could have appeared to influence the work reported in this paper.

Acknowledgments

The support from CAPES, FAPEMIG (REDE MINEIRA DE NANOMEDICINA TERANÓSTICA) and CNPq was of great importance.

References

[1] T. Vangijzegem, D. Stanicki, S. Laurent, Magnetic iron oxide nanoparticles for drug delivery: applications and characteristics, Expet Opin. Drug Deliv. 16 (1) (2019) 69–78, https://doi.org/10.1080/17425247.2019.1554647.
[2] A. Sukhanova, S. Bozrova, P. Sokolov, M. Berestovoy, A. Karaulov, I. Nabiev, Dependence of nanoparticle toxicity on their physical and chemical properties, Nanoscale Res. Lett. 13 (2018) 44, https://doi.org/10.1186/s11671-018-2457-x.
[3] A.H. Yoshikawa, L. Possebon, S.D.S. Costa, Adverse effects of metal-based nanoparticles on male reproductive cells, Top 10 Contributions on Environmental Health (2018) 1–19.
[4] N. Asare, C. Instanes, W.J. Sandberg, M. Refsnes, P. Schwarze, M. Kruszewski, G. Brunborg, Cytotoxic and genotoxic effects of silver nanoparticles in testicular cells, Toxicology 291 (1–3) (2012) 65–72, https://doi.org/10.1016/j.tox.2011.10.022.
[5] J.O. Olugbodi, O. David, E.N. Oketa, B. Lawal, B.J. Okoli, F. Mtunzi, Silver nanoparticles stimulates spermatogenesis impairments and hematological alterations in testis and epididymis of Male rats, Molecules 25 (5) (2020) 1063, https://doi.org/10.3390/molecules25051063.
[6] M. Sack, L. Alili, E. Karaman, S. Das, A. Gupta, S. Seal, P. Brenneisen, Combination of conventional chemotherapeutics with redox-active cerium oxide nanoparticles - a novel aspect in cancer therapy, Mol. Cancer Therapeut. 13 (7) (2014) 1740–1749, https://doi.org/10.1158/1535-7163.MCT-13-0950.
[7] R. Shandilya, P.K. Mishra, N. Pathak, N.K. Lohiya, R.S. Sharma, Nanotechnology in reproductive medicine: opportunities for clinical translation, Clinical and Experimental Reproductive Medicine 47 (4) (2020) 245–262, https://doi.org/10.5653/cerm.2020.03650.
[8] J. Jia, Z. Wang, T. Yue, G. Su, C. Teng, B. Yan, Crossing biological barriers by engineered nanoparticles, Chem. Res. Toxicol. 33 (5) (2020) 1055–1060, https://doi.org/10.1021/acs.chemrestox.9b00483.
[9] R. Wang, B. Song, J. Wu, Y. Zhang, A. Chen, L. Shao, Potential adverse effects of nanoparticles on the reproductive system, Int. J. Nanomed. 13 (2018) 8487–8506, https://doi.org/10.2147/IJN.S170723.
[10] A. Kumar, P. Kumar, A. Anandan, T.F. Fernandes, G.A. Ayoko, G. Biskos, Engineered Nanomaterials: Knowledge Gaps in Fate, Exposure, Toxicity, and Future Directions, vol. 16, Hindawi Publishing Corporation: Journal of Nanomaterials, 2014, https://doi.org/10.1155/2014/130198, 2014.
[11] M.R. Souza, R. Mazaro-Costa, T.L. Rocha, Can nanomaterials induce reproductive toxicity in male mammals? A historical and critical review, Sci. Total Environ. 769 (2021), 144354, https://doi.org/10.1016/j.scitotenv.2020.144354.
[12] R.D. Brohi, L. Wang, H.S. Talpur, D. Wu, F.A. Khan, D. Bhattarai, L.J. Huo, Toxicity of nanoparticles on the reproductive system in animal models: a review, Front. Pharmacol. 8 (2017) 1–22, https://doi.org/10.3389/fphar.2017.00606.
[13] N. Hadrup, H.R. Lam, Oral toxicity of silver ions, silver nanoparticles and colloidal silver - a review, Regul. Toxicol. Pharmacol. 68 (1) (2014) 1–7, https://doi.org/10.1016/j.yrtph.2013.11.002.
[14] T.X. Garcia, G.M.J. Costa, L.R. França, M.C. Hofmann, Sub-acute intravenous administration of silver nanoparticles in male mice alters Leydig cell function and testosterone levels, Reprod. Toxicol. 45 (2014) 59–70, https://doi.org/10.1016/j.reprotox.2014.01.006.

[15] X. Zhang, Z. Yue, H. Zhang, L. Liu, X. Zhou, Repeated administrations of Mn3O4 nanoparticles cause testis damage and fertility decrease through PPAR-signaling pathway, Nanotoxicology 14 (3) (2020) 326–340, https://doi.org/10.1080/17435390.2019.1695976.

[16] W.Q. Li, F. Wang, Z.M. Liu, Y.C. Wang, J. Wang, F. Sun, Gold nanoparticles elevate plasma testosterone levels in male mice without affecting fertility, Small 9 (9–10) (2013) 1708–1714, https://doi.org/10.1002/smll.201201079.

[17] Z. Han, Q. Yan, W. Ge, Z.G. Liu, S. Gurunathan, M. De Felici, X.F. Zhang, Cytotoxic effects of ZnO nanoparticles on mouse testicular cells, Int. J. Nanomed. 11 (2016) 5187–5203, https://doi.org/10.2147/IJN.S111447.

[18] L.R. França, R.A. Hess, J.M. Dufour, M.C. Hofmann, M.D. Griswold, The Sertoli cell: one hundred fifty years of beauty and plasticity, Andrology 4 (2) (2016) 189–212, https://doi.org/10.1111/andr.12165.

[19] D.D. Mruk, C.Y. Cheng, The mammalian blood-testis barrier: its biology and regulation, Endocr. Rev. 36 (5) (2015) 564–591, https://doi.org/10.1210/er.2014-1101.

[20] M.A. Smith, R. Michael, R.G. Aravindan, S. Dash, S.I. Shah, D.S. Galileo, P. A. Martin-DeLeon, Anatase titanium dioxide nanoparticles in mice: evidence for induced structural and functional sperm defects after short-, but not long-, term exposure, Asian J. Androl. 17 (2) (2015) 261–268, https://doi.org/10.4103/1008-682X.143247.

[21] Z. Lan, W.X. Yang, Nanoparticles and spermatogenesis: how do nanoparticles affect spermatogenesis and penetrate the blood-testis barrier, Nanomedicine 7 (4) (2012) 579–596, https://doi.org/10.2217/nnm.12.20.

[22] S.A. Krawetz, D.G. De Rooij, M.P. Hedger, Molecular aspects of male fertility. International workshop on molecular andrology, EMBO Rep. 10 (10) (2009) 1087–1092, https://doi.org/10.1038/embor.2009.211.

[23] A.R. Pinho, S. Rebelo, M. de Lourdes Pereira, The impact of zinc oxide nanoparticles on male (In)fertility, Materials 13 (4) (2020) 1–18, https://doi.org/10.3390/ma13040849.

[24] Y. Tang, B. Chen, W. Hong, L. Chen, L. Yao, Y. Zhao, H. Xu, ZnO nanoparticles induced male reproductive toxicity based on the effects on the endoplasmic reticulum stress signaling pathway, Int. J. Nanomed. 14 (2019) 9563–9576, https://doi.org/10.2147/IJN.S223318.

[25] Z. Ferdous, A. Nemmar, Health impact of silver nanoparticles: a review of the biodistribution and toxicity following various routes of exposure, Int. J. Mol. Sci. 21 (2020) 2375, https://doi.org/10.3390/ijms21072375.

[26] X.F. Zhang, W. Shen, S. Gurunathan, Silver nanoparticle-mediated cellular responses in various cell lines: an in vitro model, Int. J. Mol. Sci. 17 (10) (2016) 1–26, https://doi.org/10.3390/ijms17101603.

[27] C. Liao, Y. Li, S.C. Tjong, Bactericidal and cytotoxic properties of silver nanoparticles, Int. J. Mol. Sci. 20 (2) (2019) 449, https://doi.org/10.3390/ijms20020449.

[28] S.J. Cameron, F. Hosseinian, W.G. Willmore, A current overview of the biological and cellular effects of nanosilver, Int. J. Mol. Sci. 19 (7) (2018) 1–40, https://doi.org/10.3390/ijms19072030.

[29] X.F. Zhang, S. Gurunathan, J.H. Kim, Effects of silver nanoparticles on neonatal testis development in mice, Int. J. Nanomed. 10 (2015) 6243–6256, https://doi.org/10.2147/IJN.S90733.

[30] M. Thakur, H. Gupta, D. Singh, I.R. Mohanty, U. Maheswari, G. Vanage, D. Joshi, Histopathological and ultra structural effects of nanoparticles on rat testis following 90 days (Chronic study) of repeated oral administration, J. Nanobiotechnol. 12 (1) (2014) 1–13, https://doi.org/10.1186/s12951-014-0042-8.

[31] N. Asare, N. Duale, H.H. Slagsvold, B. Lindeman, A.K. Olsen, J. Gromadzka-Ostrowska, C. Instanes, Genotoxicity and gene expression modulation of silver and titanium dioxide nanoparticles in mice, Nanotoxicology 10 (3) (2016) 312–321, https://doi.org/10.3109/17435390.2015.1071443.

[32] K.S. Butler, D.J. Peeler, B.J. Casey, B.J. Dair, R.K. Elespuru, Silver nanoparticles: correlating nanoparticle size and cellular uptake with genotoxicity, Mutagenesis 30 (4) (2015) 577–591, https://doi.org/10.1093/mutage/gev020.

[33] A. Haase, S. Rott, A. Mantion, P. Graf, J. Plendl, A.F. Thünemann, G. Reiser, Effects of silver nanoparticles on primary mixed neural cell cultures: uptake, oxidative stress and acute calcium responses, Toxicol. Sci. 126 (2) (2012) 457–468, https://doi.org/10.1093/toxsci/kfs003.

[34] Danielle McShan, Paresh Ray, H. Yu, Molecular toxicity mechanism of nanosilver danielle McShan, paresh C. Ray, and hongtao yu department of chemistry and biochemistry, jackson state university, jackson, J. Food Drug Anal. 22 (1) (2014) 116–127, https://doi.org/10.1016/j.jfda.2014.01.010.Molecular.

[35] M. Ema, N. Kobayashi, M. Naya, S. Hanai, J. Nakanishi, Reproductive and developmental toxicity studies of manufactured nanomaterials, Reprod. Toxicol. 30 (3) (2010) 343–352, https://doi.org/10.1016/j.reprotox.2010.06.002.

[36] F.T. Mathias, R.M. Romano, M.M.L. Kizys, T. Kasamatsu, G. Giannocco, M. I. Chiamolera, M.A. Romano, Daily exposure to silver nanoparticles during prepubertal development decreases adult sperm and reproductive parameters, Nanotoxicology 9 (1) (2014) 64–70, https://doi.org/10.3109/17435390.2014.889237.

[37] L.K. Braydich-Stolle, B. Lucas, A. Schrand, R.C. Murdock, T. Lee, J.J. Schlager, M. C. Hofmann, Silver nanoparticles disrupt GDNF/Fyn kinase signaling in spermatogonial stem cells, Toxicol. Sci. 116 (2) (2010) 577–589, https://doi.org/10.1093/toxsci/kfq148.

[38] X.F. Zhang, Y.J. Choi, J.W. Han, E. Kim, J.H. Park, S. Gurunathan, J.H. Kim, Differential nanoreprotoxicity of silver nanoparticles in male somatic cells and spermatogonial stem cells, Int. J. Nanomed. 10 (2015) 1335–1357, https://doi.org/10.2147/IJN.S76062.

[39] T. Yoisungnern, Y.J. Choi, J. Woong Han, M.H. Kang, J. Das, S. Gurunathan, J. H. Kim, Internalization of silver nanoparticles into mouse spermatozoa results in poor fertilization and compromised embryo development, Sci. Rep. 5 (6) (2015) 1–13, https://doi.org/10.1038/srep11170.

[40] J.W. Han, J.K. Jeong, S. Gurunathan, Y.J. Choi, J. Das, D.N. Kwon, J.H. Kim, Male- and female-derived somatic and germ cell-specific toxicity of silver nanoparticles in mouse, Nanotoxicology 10 (3) (2015) 361–373, https://doi.org/10.3109/17435390.2015.1073396.

[41] H.K. Sleiman, R.M. Romano, C. A. De Oliveira, M.A. Romano, Effects of prepubertal exposure to silver nanoparticles on reproductive parameters in adult male wistar rats, J. Toxicol. Environ. Health 76 (17) (2013) 1023–1032, https://doi.org/10.1080/15287394.2013.831723.

[42] E.E. Elsharkawy, M. Abd El-Nasser, H.F. Kamaly, Silver nanoparticles testicular toxicity in rat, Environ. Toxicol. Pharmacol. 70 (2019), 103194, https://doi.org/10.1016/j.etap.2019.103194.

[43] T. Coccini, R. Gornati, F. Rossi, E. Signoretto, I. Vanetti, G. Bernardini, L. Manzo, Gene expression changes in rat liver and testes after lung instillation of a low dose of silver nanoparticles, J. Nanomed. Nanotechnol. 5 (5) (2014) 227, https://doi.org/10.4172/2157-7439.1000227.

[44] N. Fathi, S.M. Hoseinipanah, Z. Alizadeh, M.J. Assari, A. Moghimbeigi, M. Mortazavi, M. Bahmanzadeh, The effect of silver nanoparticles on the reproductive system of adult male rats: a morphological, histological and DNA integrity study, Adv. Clin. Exp. Med. 28 (3) (2019) 299–305, https://doi.org/10.17219/acem/81607.

[45] H. Moradi-Sardareh, H.R.G. Basir, Z.M. Hassan, M. Davoudi, F. Amidi, M. Paknejad, Toxicity of silver nanoparticles on different tissues of Balb/C mice, Life Sci. 211 (2018) 81–90, https://doi.org/10.1016/j.lfs.2018.09.001.

[46] A.M. Alkilany, C.J. Murphy, Toxicity and cellular uptake of gold nanoparticles: what we have learned so far? J. Nanoparticle Res. 12 (7) (2010) 2313–2333, https://doi.org/10.1007/s11051-010-9911-8.

[47] D.S. Reis, V.L. de Oliveira, M.L. Silva, R.M. Paniago, L.O. Ladeira, L.M. Andrade, Gold nanoparticles enhance fluorescence signals by flow cytometry at low antibody concentrations, J. Mater. Chem. B 9 (2021) 1414–1423, https://doi.org/10.1039/d0tb02309d.

[48] N.S. Aminabad, M. Farshbaf, A. Akbarzadeh, Recent advances of gold nanoparticles in biomedical applications: state of the art, Cell Biochem. Biophys. 77 (2) (2018) 123–137, https://doi.org/10.1007/s12013-018-0863-4.

[49] A.T. Haine, T. Niidome, Gold nanorods as nanodevices for bioimaging, photothermal therapeutics, and drug delivery, Chem. Pharm. Bull. 65 (7) (2017) 625–628, https://doi.org/10.1248/cpb.c17-00102.

[50] A.F. Versiani, L.M. Andrade, E.M.N. Martins, S. Scalzo, J.M. Geraldo, C.R. Chaves, F.G. Da Fonseca, Gold nanoparticles and their applications in biomedicine, Future Virol. 11 (4) (2016) 293–309, https://doi.org/10.2217/fvl-2015-0010.

[51] S. Fraga, A. Brandão, M.E. Soares, T. Morais, J.A. Duarte, L. Pereira, H. Carmo, Short- and long-term distribution and toxicity of gold nanoparticles in the rat after a single-dose intravenous administration, Nanomed. Nanotechnol. Biol. Med. 10 (8) (2014) 1757–1766, https://doi.org/10.1016/j.nano.2014.06.005.

[52] L.M. Andrade, E.M.N. Martins, A.F. Versiani, D.S. Reis, F.G. da Fonseca, I.P. d. Souza, L.O. Ladeira, The physicochemical and biological characterization of a 24-month-stored nanocomplex based on gold nanoparticles conjugated with cetuximab demonstrated long-term stability, EGFR affinity and cancer cell death due to apoptosis, Mater. Sci. Eng. C 107 (2020), 110203, https://doi.org/10.1016/j.msec.2019.110203.

[53] A. Sani, C. Cao, D. Cui, Toxicity of gold nanoparticles (AuNPs): a review, Biochemistry and Biophysics Reports 26 (2021), 100991, https://doi.org/10.1016/j.bbrep.2021.100991.

[54] C. Lopez-Chaves, J. Soto-Alvaredo, M. Montes-Bayon, J. Bettmer, J. Llopis, C. Sanchez-Gonzalez, Gold nanoparticles: distribution, bioaccumulation and toxicity. In vitro and in vivo studies, Nanomed. Nanotechnol. Biol. Med. 14 (1) (2018) 1–12, https://doi.org/10.1016/j.nano.2017.08.011.

[55] S.K. Balasubramanian, J. Jittiwat, J. Manikandan, C.N. Ong, L.E. Yu, W.Y. Ong, Biodistribution of gold nanoparticles and gene expression changes in the liver and spleen after intravenous administration in rats, Biomaterials 31 (8) (2010) 2034–2042, https://doi.org/10.1016/j.biomaterials.2009.11.079.

[56] X.D. Zhang, H.Y. Wu, D. Wu, Y.Y. Wang, J.H. Chang, Z. Bin Zhai, F.Y. Fan, Toxicologic effects of gold nanoparticles in vivo by different administration routes, Int. J. Nanomed. 5 (1) (2010) 771–781, https://doi.org/10.2147/IJN.S8428.

[57] B. Xu, M. Chen, X. Ji, Z. Mao, X. Zhang, X. Wang, Y. Xia, Metabolomic profiles delineate the potential role of glycine in gold nanorod-induced disruption of mitochondria and blood-testis barrier factors in TM-4 cells, Nanoscale 6 (14) (2014) 8265–8273, https://doi.org/10.1039/c4nr01035c.

[58] Y. Liu, X. Li, S. Xiao, X. Liu, X. Chen, Q. Xia, K. Xiao, The effects of gold nanoparticles on leydig cells and male reproductive function in mice, Int. J. Nanomed. 15 (2020) 9499–9514, https://doi.org/10.2147/IJN.S276606.

[59] S.T. Zakhidov, S.M. Pavlyuchenkova, T.L. Marshak, V.M. Rudoy, O. V. Dement'eva, I.A. Zelenina, Y.M. Evdokimov, Effect of gold nanoparticles on mouse spermatogenesis, Biol. Bull. 39 (3) (2012) 229–236, https://doi.org/10.1134/S1062359012030156.

[60] J. Chen, H. Wang, W. Long, X. Shen, D. Wu, S.S. Song, X.D. Zhang, Sex differences in the toxicity of polyethylene glycol-coated gold nanoparticles in mice, Int. J. Nanomed. 8 (2013) 2409–2419, https://doi.org/10.2147/IJN.S46376.

[61] B. Yahyaei, M. Nouri, S. Bakherad, M. Hassani, P. Pourali, Effects of biologically produced gold nanoparticles: toxicity assessment in different rat organs after intraperitoneal injection, Amb. Express 9 (1) (2019) 38, https://doi.org/10.1186/s13568-019-0762-0.

[62] N.M. Dissanayake, K.M. Current, S.O. Obare, Mutagenic effects of Iron oxide nanoparticles on biological cells, Int. J. Mol. Sci. 16 (10) (2015) 23482–23516, https://doi.org/10.3390/ijms161023482.
[63] B. Laffon, N. Fernández-Bertólez, C. Costa, F. Brandão, J.P. Teixeira, E. Pásaro, V. Valdiglesias, Cellular and molecular toxicity of iron oxide nanoparticles, Adv. Exp. Med. Biol. 1048 (2018) 199–213, https://doi.org/10.1007/978-3-319-72041-8_12.
[64] J.R. Sosa-Acosta, C. Iriarte-Mesa, G.A. Ortega, A.M. Díaz-García, DNA–Iron oxide nanoparticles conjugates: functional magnetic nanoplatforms in biomedical applications, Top. Curr. Chem. 378 (1) (2020) 1–29, https://doi.org/10.1007/s41061-019-0277-9.
[65] N.V.S. Vallabani, S. Singh, A.S. Karakoti, Magnetic nanoparticles: current trends and future aspects in diagnostics and nanomedicine, Curr. Drug Metabol. 20 (6) (2018) 457–472, https://doi.org/10.2174/1389200220666181122124458.
[66] R.A. Revia, M. Zhang, Magnetite nanoparticles for cancer diagnosis, treatment, and treatment monitoring: recent advances, Mater. Today 19 (3) (2016) 157–168, https://doi.org/10.1016/j.mattod.2015.08.022.
[67] U.S. Patil, S. Adireddy, A. Jaiswal, S. Mandava, B.R. Lee, D.B. Chrisey, In vitro/in vivo toxicity evaluation and quantification of iron oxide nanoparticles, Int. J. Mol. Sci. 16 (2015) 24417–24450, https://doi.org/10.3390/ijms161024417.
[68] S. Nasri, S. Rezai-Zarchi, P. Kerishchi, S. Sadeghi, The effect of iron oxide nanoparticles on sperm numbers and mobility in male mice, Zahedan Journal of Research in Medical Sciences 17 (10) (2015) e2185, https://doi.org/10.17795/zjrms-2185.
[69] M. Radu, Exposure to iron oxide nanoparticles coated with phospholipid-based polymeric micelles induces biochemical and histopathological pulmonary changes in mice, Int. J. Mol. Sci. 16 (12) (2015) 29417–29435, https://doi.org/10.3390/ijms161226173.
[70] M. Kumari, S. Rajak, S.P. Singh, U.S.N. Murty, M. Mahboob, P. Grover, M. F. Rahman, Biochemical alterations induced by acute oral doses of iron oxide nanoparticles in Wistar rats, Drug Chem. Toxicol. 36 (3) (2013) 296–305, https://doi.org/10.3109/01480545.2012.720988.
[71] N. Singh, G.J.S. Jenkins, R. Asadi, S.H. Doak, Potential toxicity of superparamagnetic iron oxide nanoparticles (SPION), Nano Rev. 1 (1) (2010) 5358, https://doi.org/10.3402/nano.v1i0.5358.
[72] M. Watanabe, M. Yoneda, A. Morohashi, Y. Hori, D. Okamoto, A. Sato, Y. Totsuka, Effects of Fe3O4 magnetic nanoparticles on A549 cells, Int. J. Mol. Sci. 14 (8) (2013) 15546–15560, https://doi.org/10.3390/ijms140815546.
[73] M.I. Khan, A. Mohammad, G. Patil, S.A.H. Naqvi, L.K.S. Chauhan, I. Ahmad, Induction of ROS, mitochondrial damage and autophagy in lung epithelial cancer cells by iron oxide nanoparticles, Biomaterials 33 (5) (2012) 1477–1488, https://doi.org/10.1016/j.biomaterials.2011.10.080.
[74] N. Singh, G.J.S. Jenkins, B.C. Nelson, B.J. Marquis, T.G.G. Maffeis, A.P. Brown, S. H. Doak, The role of iron redox state in the genotoxicity of ultrafine superparamagnetic iron oxide nanoparticles, Biomaterials 33 (1) (2012) 163–170, https://doi.org/10.1016/j.biomaterials.2011.09.087.
[75] B. Szalay, E. Tátrai, G. Nyíro, T. Vezér, G. Dura, Potential toxic effects of iron oxide nanoparticles in in vivo and in vitro experiments, J. Appl. Toxicol. 32 (6) (2012) 446–453, https://doi.org/10.1002/jat.1779.
[76] S. Ghosh, I. Ghosh, M. Chakrabarti, A. Mukherjee, Genotoxicity and biocompatibility of superparamagnetic iron oxide nanoparticles: influence of surface modification on biodistribution, retention, DNA damage and oxidative stress, Food Chem. Toxicol. 136 (2020), 110989, https://doi.org/10.1016/j.fct.2019.110989.
[77] V.K. Sundarraj, A. Manickam, M. Raghunath, M.P. Periyasamy, E.P. Viswanathan, Repeated exposure to iron oxide nanoparticles causes testicular toxicity in mice, Environ. Toxicol. 32 (2) (2016) 594–608, https://doi.org/10.1002/tox.22262.
[78] K.R. Di Bona, Y. Xu, M. Gray, D. Fair, H. Hayles, L. Milad, J.F. Rasco, Short- and long-term effects of prenatal exposure to iron oxide nanoparticles: influence of surface charge and dose on developmental and reproductive toxicity, Int. J. Mol. Sci. 16 (12) (2015) 30251–30268, https://doi.org/10.3390/ijms161226231.
[79] J. Jiang, J. Pi, J. Cai, The advancing of zinc oxide nanoparticles for biomedical applications, Hindawi Bioinorganic Chemistry and Applications 18 (2018), https://doi.org/10.1155/2018/1062562, 2018.
[80] G. Madhumitha, G. Elango, S.M. Roopan, Biotechnological aspects of ZnO nanoparticles: overview on synthesis and its applications, Appl. Microbiol. Biotechnol. 100 (2) (2016) 571–581, https://doi.org/10.1007/s00253-015-7108-x.
[81] H. Sharma, K. Kumar, C. Choudhary, P.K. Mishra, B. Vaidya, Development and characterization of metal oxide nanoparticles for the delivery of anticancer drug, Artif. Cell Nanomed. Biotechnol. 44 (2) (2016) 672–679, https://doi.org/10.3109/21691401.2014.978980.
[82] R. Abbasalipourkabir, H. Moradi, S. Zarei, S. Asadi, A. Salehzadeh, A. Ghafourikhosroshahi, N. Ziamajidi, Toxicity of zinc oxide nanoparticles on adult male Wistar rats, Food Chem. Toxicol. 84 (2015) 154–160, https://doi.org/10.1016/j.fct.2015.08.019.
[83] Y.F. Lin, I.J. Chiu, F.Y. Cheng, Y.H. Lee, Y.J. Wang, Y.H. Hsu, H.W. Chiu, The role of hypoxia-inducible factor-1α in zinc oxide nanoparticle-induced nephrotoxicity in vitro and in vivo, Part. Fibre Toxicol. 13 (1) (2016) 1–14, https://doi.org/10.1186/s12989-016-0163-3.
[84] A.R. Pinho, F. Martins, M.E.V. Costa, A.M.R. Senos, Odete A B da Cruz E Silva, M. L. Pereira, S. Rebelo, In vitro cytotoxicity effects of zinc oxide nanoparticles on spermatogonia cells, Cells 9 (5) (2020) 1–25, https://doi.org/10.3390/cells9051081.
[85] J. Shen, D. Yang, X. Zhou, Y. Wang, S. Tang, H. Yin, J. Chen, Role of autophagy in zinc oxide nanoparticles-induced apoptosis of mouse LEYDIG cells, Int. J. Mol. Sci. 20 (16) (2019) 4042, https://doi.org/10.3390/ijms20164042.
[86] Q. Liu, C. Xu, G. Ji, H. Liu, Y. Mo, D.J. Tollerud, Q. Zhang, Sublethal effects of zinc oxide nanoparticles on male reproductive cells, Toxicol. Vitro 35 (2016) 131–138, https://doi.org/10.1016/j.tiv.2016.05.017.
[87] N. Bara, G. Kaul, Enhanced steroidogenic and altered antioxidant response by ZnO nanoparticles in mouse testis Leydig cells, Toxicol. Ind. Health 34 (8) (2018) 571–588, https://doi.org/10.1177/0748233718774220.
[88] E. Rollerova, J. Tulinska, A. Liskova, M. Kuricova, J. Kovriznych, A. Mlynarcikova, S. Scsukova, Titanium dioxide nanoparticles: some aspects of toxicity/focus on the development, Endocr. Regul. 49 (2) (2015) 97–112, https://doi.org/10.4149/endo_2015_02_97.
[89] S. Kongseng, K. Yoovathaworn, K. Wongprasert, R. Chunhabundit, P. Sukwong, D. Pissuwan, Cytotoxic and inflammatory responses of TiO2 nanoparticles on human peripheral blood mononuclear cells, J. Appl. Toxicol. 36 (10) (2016) 1364–1373, https://doi.org/10.1002/jat.3342.
[90] M. Tsugita, N. Morimoto, M. Nakayama, SiO2 and TiO2 nanoparticles synergistically trigger macrophage inflammatory responses, Part. Fibre Toxicol. 14 (1) (2017) 1–9, https://doi.org/10.1186/s12989-017-0192-6.
[91] F.M. Fartkhoon, A. Noori, A. Mohammadi, Effects of titanium dioxide nanoparticles toxicity on the kidney of male rats, Int. J. Life Sci. 10 (1) (2016) 65–69, https://doi.org/10.3126/ijls.v10i1.14513.
[92] F. Hong, W. Si, X. Zhao, L. Wang, Y. Zhou, M. Chen, J. Zhang, TiO2 nanoparticle exposure decreases spermatogenesis via biochemical dysfunctions in the testis of male mice, J. Agric. Food Chem. 63 (31) (2015) 7084–7092, https://doi.org/10.1021/acs.jafc.5b02652.
[93] R. Meena, K. Kajal, P. R, Cytotoxic and genotoxic effects of titanium dioxide nanoparticles in testicular cells of male wistar rat, Appl. Biochem. Biotechnol. 175 (2) (2014) 825–840, https://doi.org/10.1007/s12010-014-1299-y.
[94] G. Gao, Y. Ze, X. Zhao, X. Sang, L. Zheng, X. Ze, X. Zhang, Titanium dioxide nanoparticle-induced testicular damage, spermatogenesis suppression, and gene expression alterations in male mice, J. Hazard Mater. 258–259 (2013) 133–143, https://doi.org/10.1016/j.jhazmat.2013.04.046.
[95] N. Miura, K. Ohtani, T. Hasegawa, H. Yoshioka, G.W. Hwang, High sensitivity of testicular function to titanium nanoparticles, J. Toxicol. Sci. 42 (3) (2017) 359–366, https://doi.org/10.2131/jts.42.359.
[96] L. Li, X. Mu, L. Ye, Y. Ze, F. Hong, Suppression of testosterone production by nanoparticulate TiO 2 is associated with ERK1/2-PKA-PKC signaling pathways in rat primary cultured leydig cells, Int. J. Nanomed. 13 (2018) 5909–5924, https://doi.org/10.2147/IJN.S175608.
[97] F. Jia, Z. Sun, X. Yan, B. Zhou, J. Wang, Effect of pubertal nano-TiO2 exposure on testosterone synthesis and spermatogenesis in mice, Arch. Toxicol. 88 (3) (2014) 781–788, https://doi.org/10.1007/s00204-013-1167-5.
[98] G. Song, L. Lin, L. Liu, K. Wang, Y. Ding, Q. Niu, S. Guo, Toxic effects of anatase titanium dioxide nanoparticles on spermatogenesis and testicles in male mice, Pol. J. Environ. Stud. 26 (6) (2017) 2739–2746, https://doi.org/10.15244/pjoes/70807.
[99] N. Miura, K. Ohtani, T. Hasegawa, R. Hoj, Y. Yanagiba, T. Suzuki, R.-S. Wang, Hazardous effects of titanium dioxide nanoparticles on testicular function in mice, Fundamental Toxicological Sciences 1 (3) (2014) 81–85, https://doi.org/10.2131/fts.1.81.
[100] Z.O. Kyjovska, A.M.Z. Boisen, P. Jackson, H. Wallin, U. Vogel, K.S. Hougaard, Daily sperm production: application in studies of prenatal exposure to nanoparticles in mice, Reprod. Toxicol. 36 (2013) 88–97, https://doi.org/10.1016/j.reprotox.2012.12.005.
[101] N.N. Shahin, M.M. Mohamed, Nano-sized titanium dioxide toxicity in rat prostate and testis: possible ameliorative effect of morin, Toxicol. Appl. Pharmacol. 334 (2017) 129–141, https://doi.org/10.1016/j.taap.2017.08.014.
[102] L. Kong, M. Tang, T. Zhang, D. Wang, K. Hu, W. Lu, Y. Pu, Nickel nanoparticles exposure and reproductive toxicity in healthy adult rats, Int. J. Mol. Sci. 15 (11) (2014) 21253–21269, https://doi.org/10.3390/ijms151121253.
[103] J.Z. Kročková, P. Massányi, A.V. Sirotkin, J. Pivko, A.V. Makarevich, N. Lukáč, Z. Poláková, Nickel induced structural and functional alterations in mouse Leydig cells in vitro, J. Trace Elem. Med. Biol. 25 (1) (2011) 14–18, https://doi.org/10.1016/j.jtemb.2010.11.003.
[104] R.R. Magaye, X. Yue, B. Zou, H. Shi, H. Yu, K. Liu, J. Zhao, Acute toxicity of nickel nanoparticles in rats after intravenous injection, Int. J. Nanomed. 9 (1) (2014) 1393–1402, https://doi.org/10.2147/IJN.S56212.
[105] R. Magaye, J. Zhao, Recent progress in studies of metallic nickel and nickel-based nanoparticles' genotoxicity and carcinogenicity, Environ. Toxicol. Pharmacol. 34 (3) (2012) 644–650, https://doi.org/10.1016/j.etap.2012.08.012.
[106] L. Kong, W. Hu, C. Lu, K. Cheng, M. Tang, Mechanisms underlying nickel nanoparticle induced reproductive toxicity and chemo-protective effects of vitamin C in male rats, Chemosphere 218 (2019) 259–265, https://doi.org/10.1016/j.chemosphere.2018.11.128.
[107] W. Hu, Z. Yu, X. Gao, Y. Wu, M. Tang, L. Kong, Study on the damage of sperm induced by nickel nanoparticle exposure, Environ. Geochem. Health 42 (6) (2019) 1715–1724, https://doi.org/10.1007/s10653-019-00364-w.
[108] E.E. Glista-Baker, A.J. Taylor, B.C. Sayers, E.A. Thompson, J.C. Bonner, Nickel Nanoparticles cause exaggerated lung and airway remodeling in mice lacking the T-box transcription factor, TBX21 (T-bet), Part. Fibre Toxicol. 11 (1) (2014) 1–16, https://doi.org/10.1186/1743-8977-11-7.
[109] Y. Wu, J. Ma, Y. Sun, M. Tang, L. Kong, Effect and mechanism of PI3K/AKT/mTOR signaling pathway in the apoptosis of GC-1 cells induced by nickel

nanoparticles, Chemosphere 255 (2020), 126913, https://doi.org/10.1016/j.chemosphere.2020.126913.
[110] I.M. Saadeldin, W.A. Khalil, M.G. Alharbi, S.H. Lee, The current trends in using nanoparticles, liposomes, and exosomes for semen cryopreservation, Animals 10 (12) (2020) 1–16, https://doi.org/10.3390/ani10122281.
[111] S. Bakand, A. Hayes, Toxicological considerations, toxicity assessment, and risk management of inhaled nanoparticles, Int. J. Mol. Sci. 17 (6) (2016) 1–17, https://doi.org/10.3390/ijms17060929.
[112] S. Huo, S. Jin, X. Ma, X. Xue, K. Yang, A. Kumar, X.J. Liang, Ultrasmall gold nanoparticles as carriers for nucleus-based gene therapy due to size-dependent nuclear entry, ACS Nano 8 (6) (2014) 5852–5862, https://doi.org/10.1021/nn5008572.
[113] W.S. Cho, R. Duffin, F. Thielbeer, M. Bradley, I.L. Megson, W. MacNee, K. Donaldson, Zeta potential and solubility to toxic ions as mechanisms of lung inflammation caused by metal/metal oxide nanoparticles, Toxicol. Sci. 126 (2) (2012) 469–477, https://doi.org/10.1093/toxsci/kfs006.
[114] C. McGuinnes, R. Duffin, S. Brown, N.L. Mills, I.L. Megson, W. MacNee, K. Donaldson, Surface derivatization state of polystyrene latex nanoparticles determines both their potency and their mechanism of causing human platelet aggregation in vitro, Toxicol. Sci. 119 (2) (2011) 359–368, https://doi.org/10.1093/toxsci/kfq349.
[115] A. Asati, S. Santra, C. Kaittanis, J.M. Perez, Localization, surface-charge-dependent cell nanoparticles, cerium oxide, ACS Nano 4 (9) (2011) 5321–5331, https://doi.org/10.1021/nn100816s.
[116] F. Alexis, E. Pridgen, L.K. Molnar, O.C. Farokhzad, Factors affecting the clearance and biodistribution of polymeric nanoparticles, Mol. Pharm. 5 (4) (2008) 505–515, https://doi.org/10.1021/mp800051m.
[117] C. Gunawan, M. Lim, C.P. Marquis, R. Amal, Nanoparticle-protein corona complexes govern the biological fates and functions of nanoparticles, J. Mater. Chem. B 2 (15) (2014) 2060–2083, https://doi.org/10.1039/c3tb21526a.
[118] P. Khanna, C. Ong, B.H. Bay, G.H. Baeg, Nanotoxicity: an interplay of oxidative stress, inflammation and cell death, Nanomaterials 5 (3) (2015) 1163–1180, https://doi.org/10.3390/nano5031163.
[119] Z. Yu, Q. Li, J. Wang, Y. Yu, Y. Wang, Q. Zhou, P. Li, Reactive oxygen species-related nanoparticle toxicity in the biomedical field, Nanoscale Res. Lett. 15 (1) (2020) 115, https://doi.org/10.1186/s11671-020-03344-7.
[120] C. Carlson, S.M. Hussein, A.M. Schrand, L.K. Braydich-Stolle, K.L. Hess, R. L. Jones, J.J. Schlager, Unique cellular interaction of silver nanoparticles: size-dependent generation of reactive oxygen species, J. Phys. Chem. B 112 (43) (2008) 13608–13619, https://doi.org/10.1021/jp712087m.
[121] W. He, Y.T. Zhou, W.G. Wamer, M.D. Boudreau, J.J. Yin, Mechanisms of the pH dependent generation of hydroxyl radicals and oxygen induced by Ag nanoparticles, Biomaterials 33 (30) (2012) 7547–7555, https://doi.org/10.1016/j.biomaterials.2012.06.076.
[122] F.S. Ferraz, J.L. López, S.M.S.N. Lacerda, M.S. Procópio, A.F.A. Figueiredo, E.M. N. Martins, G.M.J. Costa, Biotechnological approach to induce human fibroblast apoptosis using superparamagnetic iron oxide nanoparticles, J. Inorg. Biochem. 206 (2020), 111017, https://doi.org/10.1016/j.jinorgbio.2020.111017.
[123] G. Sanità, B. Carrese, A. Lamberti, Nanoparticle surface functionalization: how to improve biocompatibility and cellular internalization, Front. Mol. Biosci. 7 (2020), 587012, https://doi.org/10.3389/fmolb.2020.587012.

CAPÍTULO 2

Artigo 2 – "The toxicity of superparamagnetic iron oxide nanoparticles induced on the testicular cells: in vitro study"

Aceito para publicação na revista: NanoImpact

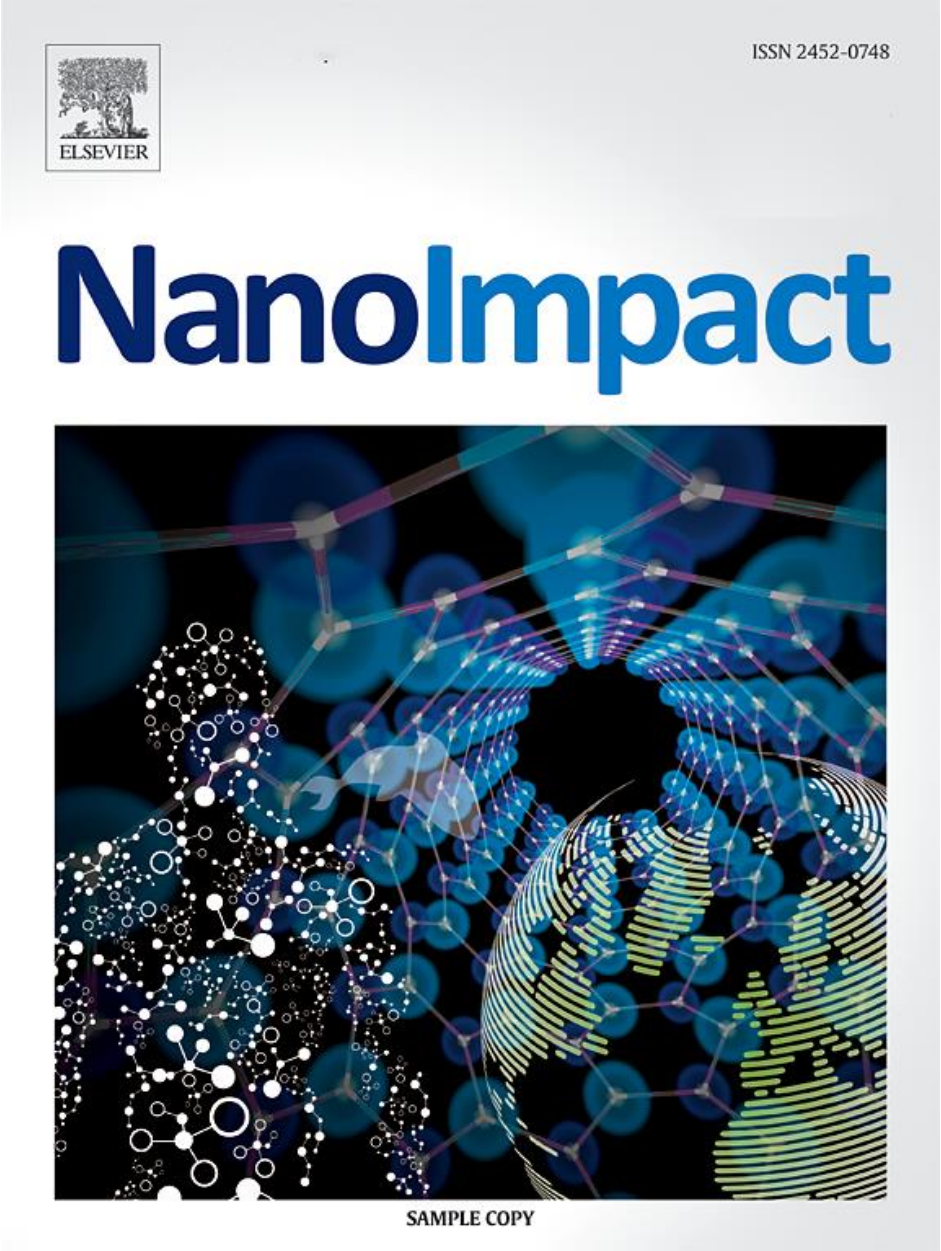

NanoImpact 35 (2024) 100517

Contents lists available at ScienceDirect

NanoImpact

journal homepage: www.elsevier.com/locate/nanoimpact

The toxicity of superparamagnetic iron oxide nanoparticles induced on the testicular cells: In vitro study

Graziela de P.F. Dantas [a], Fausto S. Ferraz [a], John L.P. Coimbra [a], Roberto M. Paniago [b], Maria S.S. Dantas [c], Samyra M.S.N. Lacerda [a], Marcela S. Procópio [a], Matheus F. Gonçalves [a], Marcelo H. Furtado [a,d], Bárbara P. Mendes [d], Jorge L. López [e], Alisson C. Krohling [f], Estefânia M.N. Martins [f], Lídia M. Andrade [a,b], Luiz O. Ladeira [c], Ângela L. Andrade [g], Guilherme M.J. Costa [a,*]

[a] Department of Morphology, ICB, Federal University of Minas Gerais, Belo Horizonte, MG, Brazil
[b] Department of Physics, ICEx, Federal University of Minas Gerais, Belo Horizonte, MG, Brazil
[c] Metallurgical and Materials Engineering Department, EE, Federal University of Minas Gerais, Belo Horizonte, MG, Brazil
[d] Clínica MF Fertilidade Masculina, Belo Horizonte, MG, Brazil
[e] Center for Biological and Natural Sciences, Federal University of Acre, Rio Branco, Acre, Brazil
[f] Centro de Desenvolvimento da Tecnologia Nuclear, CDTN, 31270-901, Belo Horizonte, MG, Brazil
[g] Department of Chemistry, ICEB, Federal University of Ouro Preto, Ouro Preto, MG, Brazil

ARTICLE INFO

Editor: Ruibin Li

Keywords:
SPIONs
Nanotoxicity
Testicular cells
Oxidative stress
Ultrastructural alterations

ABSTRACT

Superparamagnetic iron oxide nanoparticles (SPIONs) have gained significant attention in biomedical research due to their potential applications. However, little is known about their impact and toxicity on testicular cells. To address this issue, we conducted an *in vitro* study using primary mouse testicular cells, testis fragments, and sperm to investigate the cytotoxic effects of sodium citrate-coated SPIONs (Cit_SPIONs). Herein, we synthesized and physiochemically characterized the Cit_SPIONs and observed that the sodium citrate diminished the size and improved the stability of nanoparticles in solution during the experimental time. The sodium citrate (measured by thermogravimetry) was biocompatible with testicular cells at the used concentration (3%). Despite these favorable physicochemical properties, the *in vitro* experiments demonstrated the cytotoxicity of Cit_SPIONs, particularly towards testicular somatic cells and sperm cells. Transmission electron microscopy analysis confirmed that Leydig cells preferentially internalized Cit_SPIONs in the organotypic culture system, which resulted in alterations in their cytoplasmic size. Additionally, we found that Cit_SPIONs exposure had detrimental effects on various parameters of sperm cells, including motility, viability, DNA integrity, mitochondrial activity, lipid peroxidation (LPO), and ROS production. Our findings suggest that testicular somatic cells and sperm cells are highly sensitive and vulnerable to Cit_SPIONs and induced oxidative stress. This study emphasizes the potential toxicity of SPIONs, indicating significant threats to the male reproductive system. Our findings highlight the need for detailed development of iron oxide nanoparticles to enhance reproductive nanosafety.

1. Introduction

Different Nanoparticles (NPs) have been used in various applications such as biomedicine, sensing, and agriculture due to their small size, large surface area, and high reactivity (Valdiglesias et al., 2015; Vassal et al., 2021). Superparamagnetic iron oxide NPs (SPIONs) are formed by small iron oxide crystals, commonly called magnetite (Fe_3O_4), maghemite (Fe_2O_3) or hematite (α-Fe_2O_3), and have received particular importance because they are highly sensitive to magnetism (Suciu et al., 2020; Sharma et al., 2016). The unique characteristics of SPIONs, such as their magnetic guidance capability towards specific organs or tissues when exposed to a magnetic field, have positioned them as highly promising tools in biomedical applications (Vangijzegem et al., 2019; Ghosh et al., 2020; Ye et al., 2014).

These characteristics of SPIONs make them excellent tools, especially for obtaining magnetic resonance imaging (Llenas et al., 2019; Dulińska-

* Corresponding author.
E-mail address: gmjc@ufmg.br (G.M.J. Costa).

https://doi.org/10.1016/j.impact.2024.100517
Received 14 August 2023; Received in revised form 12 April 2024; Accepted 2 June 2024
Available online 6 June 2024

Litewka et al., 2019) and in therapies for hyperthermia (Caizer, 2021; Datta et al., 2016). To ensure their colloidal stability in aqueous environments, SPIONs can be functionalized with organic acids (e.g., citric acid), hydrophilic polymers (e.g., polyethylene glycol), or polysaccharides (Dulińska-Litewka et al., 2019). The surface modification of SPIONs with various molecules such as DNA, antibodies, peptides, aptamers, and carbohydrates enables their versatile utilization in various biological applications, such as targeted drug delivery, diagnostics (sensing), and imaging (Suciu et al., 2020; Laurent et al., 2008; Kaczyńska et al., 2016). In the field of reproductive medicine, researchers have explored the potential of SPIONs in various applications such as enhancing male fertility *in vivo* or *in vitro* (Durfey et al., 2019; Feugang, 2017; Makhluf et al., 2006), gene therapy for reproductive disorders (Kim et al., 2015; Farini et al., 2016), treatment of diseases associated with erectile dysfunction (Kim et al., 2015), contraception (Jivago et al., 2021; Ding et al., 2021), among others (Shandilya et al., 2020).

Numerous studies have shown that SPIONs have great potential in the biomedical field. However, there is still a need for a clear understanding of the risks that these nanoparticles pose to reproductive health. Some studies have demonstrated the vulnerability of testicular cells to various types of nanoparticles (Dantas et al., 2022; Meena and Kajal, 2014; Han et al., 2011; Habas et al., 2018; Elsharkawy et al., 2019). The route of administration, dosage, and properties such as size, shape, chemical composition, and surface charge play significant roles (Malhotra et al., 2020; Ganguly et al., 2018; Sengupta et al., 2014). Studies have shown that SPIONs can cross biological barriers in mice and accumulate quickly in various tissues, which can result in toxic effects (Malhotra et al., 2020; Ganguly et al., 2018; Sengupta et al., 2014; Sundarraj et al., 2017). In a previous study conducted by our research group, it was found that SPIONs could cross the blood-testis barrier, accumulating in germ cells (Ferraz et al., 2024).

The accumulation of nanoparticles (NPs) in the testis can affect the quality of gametes, leading to disruptions in reproductive function and interference with embryogenesis (Yoisungnern et al., 2015; Campagnolo et al., 2012; Di Bona et al., 2015). *In vivo* studies have shown that different ways of exposure to SPIONs can cause harmful effects on spermatogenesis, resulting in decreased spermatozoa motility, viability, and increased morphological abnormalities (Ghosh et al., 2020; Sundarraj et al., 2017; Di Bona et al., 2015; Nasri et al., 2015; Younus et al., 2020a). The primary mechanism proposed to explain these adverse effects is oxidative stress (Younus et al., 2020a; Sati and Huszar, 2015a; Mahmoudi et al., 2009). In this context, this study's primary objective was to assess in detail the potentially toxic effects of the direct exposition of testicular cells to sodium citrate-coated superparamagnetic iron oxide nanoparticles (SPIONs).

The use of nanomaterials for developing contraceptives and sterilizing agents is gaining attention as a promising tool (Ferraz et al., 2024; Coimbra et al., 2023). However, it is crucial to conduct in-depth investigations to evaluate the interaction of nanoparticles with reproductive cells for biotechnological developments. In this context, we have examined the cytotoxicity of citrate-coated SPIONs (Cit_SPIONs) on primary cultures of different testicular cells and organotypic cultures of testes. Moreover, we have evaluated the impact of Cit_SPIONs on spermatozoa and focused on parameters such as motility, viability, morphology, DNA integrity, and ROS production.

2. Materials and methods

2.1. Nanoparticle synthesis

The Cit_SPIONs were synthesized using a modified method based on the original procedure proposed by Qu et al. (Qu et al., 1999). In brief, a solution of $FeCl_3{\cdot}6H_2O$ (2 M) dissolved in 0.5 M HCl (30 mL) was combined with a Na_2SO_3 solution (1 M) (20 mL). This mixture was subjected to a vacuum ($\sim 10^{-2}$ Torr) for 30 s. Initially, the solution colour changed from yellow to red, and after a few minutes, it reverted back to yellow. Subsequently, a diluted ammonia solution (50.8 mL of NH_4OH diluted to a total volume of 800 mL) was rapidly added to the flask under vigorous stirring. The reaction medium was once again subjected to vacuum for 30 s, resulting in the formation of a black precipitate. The resulting suspension was stirred for an additional 30 min and then centrifuged at 2.000 rpm for 3 min to remove the supernatant. The washing process was repeated five times until a supernatant with a neutral pH value was obtained. The resulting precipitate, designated as M0, was kept under vacuum.

The precipitate of nanoparticulate iron oxide was then dispersed in water using ultrasonication in a closed system under a nitrogen atmosphere. The NPs were coated with a 0.2 M tri-sodium citrate solution at 80 °C for 40 min. This process was used to ensure the chemical stability of the NPs in aqueous solutions and reduce aggregation (Cândido et al., 2022). Sodium citrate is a commonly used compound to coat magnetic NPs and is known to be safe for cells (Sarimov et al., 2022a; Nosrati et al., 2018; Sarimov et al., 2022b; Kristianto et al., 2020; Patel et al., 2018). After coating, the NPs were lyophilized.

2.2. Nanoparticle characterization

SPIONs and Cit_SPIONs were characterized by transmission electron microscopy (TEM) to visualize their morphology. The average diameter of the nanoparticles was determined using the Image J v.1.45 s software for image processing and analysis. The zeta potential was evaluated using Particle Analyzer Litesizer™ 500 AntonPaar. Thermogravimetric analyses, TGA and DTG, were also carried out to calculate the composition of the sodium citrate coating on the Cit_SPIONs. TGA and DTG thermograms were obtained with a DTG60H Shimadzu analyzer, under an air flow rate of 50 mL min-1 with a heating rate of 10 °C min-1 up to 900 °C, alumina crucible and sample mass of approximately 8.0 mg.

The X-ray diffraction (XRD) experiments of powder samples were acquired on an Empyrean Panalytical diffractometer using Cu Kα radiation ($\lambda = 1.5406$ Å) operated at 45 kV/40 mA and using a PIXcel3D area detector. Raman spectra were obtained with a LabRam-HR 800 (Horiba/Jobin Yvon) spectrograph equipped with an Olympus BX-41 Microscope and a 632.8 nm excitation from a helium-neon laser. The back-scattered light collected was dispersed by a monochromator and detected by a LN2 cooled CCD system. The magnetic hysteresis response of the nanoparticles was investigated by vibrating sample magnetometry using the Lake Shore 7400 Series Spectrometer. We used 12 mg of powder with the sample at room temperature.

Mössbauer spectroscopy measurements were performed using a setup that included a multichannel analyzer, function generator, speed driver, gamma ray detector, and a ^{57}Co radioactive source embedded in a rhodium matrix (RITVERC Isotope Products, Germany). The Mössbauer spectroscopy of ^{57}Fe was conducted in the standard transmission geometry (absorption), with the drive operated in constant acceleration mode using a triangular velocity waveform. The obtained data were analyzed and fitted using the NORMOS-SITE program (Brand, 1994). The resulting hyperfine parameters are reported relative to natural iron.

Photoelectron Spectroscopy (XPS) was carried out using monochromatic Al-Kα radiation (1486.6 eV) at room temperature. A Thermo Fisher Escalab-220-ixL spectrometer equipped with a hemispherical energy analyzer was utilized for the measurements. The XPS survey spectrum was acquired with an Epass energy of 50 eV, providing an overview of the elemental composition. Furthermore, high-resolution spectra of the Fe2p, C1s, O1s, and N1s lines were obtained at a higher resolution by setting the Epass energy to 20 eV (Artemenko et al., 2021a).

2.3. Animals

A total of twelve Balb/c mice, sourced from the central vivarium of

the Institute of Biological Sciences (UFMG), were utilized in this study. Two mice were dedicated to the primary culture of testicular cells and subsequent viability assessments, while the remaining ten mice were allocated for testicular tissue culture and sperm analysis. The mice were provided unlimited food and water access and subjected to a 12-h light/dark cycle. The experimental procedures followed the guidelines set forth by the Ethics Committee in Animal Experimentation of the Federal University of Minas Gerais - CEUA/UFMG (approval no. 183/2018).

2.4. Primary culture of testicular cells

Following the orchiectomy of two mice, their testes were collected and transferred to Petri dishes. The testicles were decapsulated and subjected to enzymatic solutions to isolate the various testicular cell types (Bhushan et al., 2016; Chang et al., 2011a). For the enrichment of Leydig cells, the testicular tissue underwent enzymatic digestion using collagenase 2 mg/mL (C0130, Merck, Brazil) and hyaluronidase 2 mg/mL (H2126, Merck, Brazil). Subsequently, an enriched fraction of Leydig cells was obtained from the supernatant after sedimentation of the seminiferous tubules (Bhushan et al., 2016; Chang et al., 2011a). These Leydig cells were then incubated in 96-well cell culture plates (Kasvi).

The seminiferous tubules underwent enzymatic digestion using trypsin (0.25% *v*/v) with 1 mM EDTA (T4049, Merck, Brazil) to isolate Sertoli and germ cells. The resulting cell suspension was incubated in 6-well culture plates (Kasvi, Brazil) coated with Geltrex® (A1413302, Thermo Fisher Scientific, USA). After an overnight culture, non-adherent cells (germ cells) were collected from the supernatant and incubated in 96-well cell culture plates (Kasvi, Brazil). Adherent cells were subjected to a hypotonic solution (0.3× HBSS) to lyse contaminating germ cells. Following this step, Sertoli cells (which are resistant to hypotonic treatment) were also cultured in 96-well cell culture plates (Kasvi, Brazil).

Leydig, germ, and Sertoli cells were maintained in DMEM/F-12 Culture Medium (Dulbecco's Modified Eagle's Medium: F-12 Nutrient Mix; 12,491,015, Gibco®, USA) supplemented with 10% FBS, 100 IU/mL Penicillin (P4458, Merck, Brazil), 100 μg/mL Streptomycin (S6501, Merck, Brazil), and 100 IU/mL amphotericin (A2942, Merck, Brazil) under a humid atmosphere containing 5% CO_2 at a temperature of 35 °C.

2.5. Immunofluorescence on isolated testicular cells

Immunofluorescence reactions were conducted to verify the enriched cell fractions of germ, Sertoli, and Leydig cells using specific molecular markers. To begin, aliquots of each cell fraction were fixed in a methacarn solution for 5 min and allowed to dry on histological slides treated with Poly-L-Lysine (P8920, Merck, Brazil) to enhance adherence. Non-specific binding blocking was performed by incubating the cells with 10% serum for 1 h, followed by washing with PBS for 5 min (Chang et al., 2011b) Next, the cells were incubated overnight at 4 °C with primary antibodies diluted in 3% serum in PBS.

On the following day, slides were washed with PBS for 5 min, and the cells were incubated with fluorescent secondary antibodies diluted in 3% serum in PBS. Following incubation with the secondary antibodies, the cells were washed with PBS for 5 min, and the slides were mounted using Fluoromount™ Aqueous Mounting Medium (F4680, Merck, Brazil). Imaging was performed using a Nikon Eclipse TE2000-U fluorescence microscope (Nikon Eclipse Ti—S, Nikon Instruments Inc., USA).

Specific primary and secondary antibodies were used for the identification of Leydig, Sertoli, and germ cells. Leydig cells were labeled using an anti-3βHSD primary antibody (goat anti-3βHSD 1:100, SC-30820 - Santa Cruz) and an AlexaFluor546® secondary antibody (donkey anti-goat, 1:1000, a11056 - Invitrogen). Sertoli cells were identified using a primary anti-GATA4 antibody (mouse anti-GATA4, 1:100, SC-25310 – Santa Cruz) and an AlexaFluor633® secondary antibody (rabbit anti-mouse, 1:1000, A21063 - Invitrogen). Germ cells were detected using a primary anti-VASA antibody (rabbit anti-VASA, 1:100, ab13840 - Abcam) and an AlexaFluor488® secondary antibody (donkey anti-rabbit, 1:1000, A21206 - Invitrogen).

2.6. Cell viability

Different types of testicular cells (10^5 cells per well) were exposed to Cit_SPIONs in two different concentrations (8×10^{-2} and 8×10^{-3} mg/mL) for three periods of time. The selection of concentrations was based on earlier studies conducted by Ferraz et al. (Ferraz et al., 2020), which indicated that Cit_SPIONs had low cytotoxicity in MRC-5 human lung fibroblast cells at concentrations lower than 8×10^{-2} mg/mL. Another study conducted by Ferraz et al. (Ferraz et al., 2024) revealed significant effects of intratesticular injections of Cit_SPIONs on the testis at the concentration of 8×10^{-2} mg/mL. The control group cells were cultured in a medium without any nanoparticles.

In addition, we evaluated the toxicity potential of sodium citrate. The sodium citrate concentration was chosen according to the TGA analysis. Different testicular cells (10^5 cells per well) were exposed to DMEM/F12 supplemented with sodium citrate (3%) for 24, 48, and 72 h. In addition, the sperm retrieved from the epididymis were incubated with DMEM/F12 supplemented with sodium citrate (3%) for 4 h. The control media of these cells (DMEM) was not supplemented with sodium citrate.

In cell viability experiments, viable cells were analyzed based on their ability to convert a redox dye called resazurin into a fluorescent product known as resorufin. To perform this analysis, 20 μL of CellTiter-Blue® (a reagent for cell viability assays, CTB, Promega) was added to each well, followed by a 4-h incubation period. Fluorescence measurements were taken using a VarioskanFlash spectrophotometer (Thermo Scientific, Skanlt Software 2.4.3 RE) with an excitation wavelength of 530 nm and an emission wavelength of 590 nm. The obtained data were normalized based on the control groups and represented as fluorescence units proportional to the number of viable cells.

2.7. Testis tissue culture

Testes from a total of ten mice ($n = 20$ testicles) were dissected, with the tunica albuginea carefully removed. The testicles were then placed on the surface of an agarose block soaked in 2 mL of enriched culture medium. The culture medium consisted of DMEM supplemented with antibiotics, 10% FBS, 1 mM sodium pyruvate, 4 mM glutamine, 100 ng/mL of vitamin A, 200 ng/mL of vitamin E, 50 ng/mL of vitamin C, 10 μg/mL of insulin, and 5 μg/mL of transferrin. Additionally, 200 ng/mL of FSH/LH (Pulset®, CEVA) and 1 IU/mL of HCG (Vetecor, Hertape Calier) were added to the medium (Yokonishi et al., 2013).

Half of the testes received a concentration of 8×10^{-2} mg/mL of Cit_SPIONs, while the other half served as the control group. The testes were cultured in this system for 24 and 48 h, under a humid atmosphere containing 5% CO_2 at a temperature of 35 °C. For further analysis, the testicular explants were fixed in bouin solution for morphometric analysis and in 4% glutaraldehyde for the detection of internalized Cit_SPIONs using transmission electron microscopy (TEM).

Subsequently, fragments of these organs were dehydrated using increasing concentrations of alcohol (70°, 80°, 90°, 95°, 100° ABS I, and 100° ABS II) and embedded in a plastic resin based on glycol methacrylate using the Leica Historesin Embedding Kit (14,702,231,731, Leica Instruments, USA). Histological sections with a thickness of 5 μm were obtained using a rotating microtome equipped with a glass razor. These sections were stained with a 1% toluidine blue-sodium borate solution and mounted with glass coverslips and Entellan (100,869, Merck, Brazil). Finally, the sections were analyzed using an Olympus BX 60 microscope.

2.8. Morphometric analysis in testis fragments

Morphometric analyses were developed according to (Costa et al., 2018). Briefly, the volumetric densities of the testicular tissue components, tubular diameter, the height of the seminiferous epithelium, nuclear diameters, and the number of testicular cells were evaluated using an Olympus BX-60 light microscope (Center Valley, PA, USA) and analyzed using ImageJ software (National Institute of Health, Bethesda, MA, USA).

2.9. Transmission electron microscopy

Testicular fragments were fixed for 1 h using a modified Karnovsky fixative, consisting of 2% paraformaldehyde and 2.5% glutaraldehyde in a 0.1 M sodium phosphate buffer at pH 7.4. Following fixation, the samples were washed three times, each for 5 min, using a 0.1 M sodium phosphate buffer containing 0.15 M NaCl and buffered saline solution at 4 °C. Subsequently, they were fixed in 2% osmium tetroxide for 30 min at room temperature. To enhance contrast, the samples were block stained with 2% uranyl acetate (EMS) for 20 min in the dark.

The samples were then subjected to a dehydration process using a graded series of ethanol and acetone. After dehydration, they were infiltrated with a mixture of acetone and Epon resin (1:3 ratio; EMBed 812 Resin, EMS) for 30 min and subsequently embedded in pure Epon resin. Ultrathin sections were obtained using a diamond knife on a Leica EM UC6 ultramicrotome (Leica Microsystems). These sections were mounted on 200-mesh copper grids (Ted Pella), stained with lead citrate (Merck), and examined using a Tecnai G2–12 transmission electron microscope (Thermo Fisher Scientific / FEI) at the Microscopy Center of the Federal University of Minas Gerais.

2.10. Sperm analysis

The cauda epididymides of ten mice ($n = 20$) were dissected and macerated in a Petri dish containing 500 μL of DMEM/F12 medium to release the sperm. Half of the samples ($n = 10$) were exposed to Cit_SPIONs at concentrations of 8×10^{-3} and 8×10^{-2} mg/mL, while the other half (n = 10) were kept in DMEM/F12 as a negative control. The spermatozoa were then incubated at 37 °C in a 5% CO_2 atmosphere three times for 30 min, 1 h, and 2 h.

2.10.1. Sperm motility and viability

After each incubation period, 10 μL of seminal fluid was placed on a glass slide and covered with a coverslip for motility evaluation. Motility was assessed based on three parameters: progressive motile, non-progressive motile, and immotile. Viability analysis was conducted by staining 5 μL of seminal fluid with 5 μL of eosin on glass slides, followed by counting stained (dead) and unstained (live) spermatozoa under a light microscope with 400× magnification. Both analyses were performed on 200 spermatozoa (Nazari et al., 2016).

2.10.2. Sperm DNA fragmentation

To DNA fragmentation analysis, smears previously prepared on glass slides were fixed with 95% alcohol for 5 min. The slides were then stained with Acridine Orange dye solution (Acridine Orange (0.1%), Citric acid (0.1 M), and Na_2HPO_4 (0.3 M)) in a dark environment for 5 min. Intact DNA was labeled in green, while fragmented DNA was labeled in red. Excess dye was removed with water, and approximately 300 spermatozoa were analyzed using a fluorescence microscope with excitation/emission filters of 490 and 530 nm. The percentage of spermatozoa with intact DNA was calculated by dividing the number of green-stained spermatozoa by the total number of spermatozoa and multiplying the result by 100 (Tomov et al., 2020).

2.10.3. Sperm mitochondrial activity and lipid peroxidation (LPO)

Half of the sperm samples ($n = 10$) were exposed to Cit_SPIONs at a concentration of 8×10^{-3} mg/mL, while the other half (n = 10) were kept in DMEM/F12 as a negative control. The spermatozoa were then incubated at 37 °C in a 5% CO_2 atmosphere for 2 h.

Mitochondrial activity was measured using the probe MitoTracker™ Green FM Dye (M7514, Invitrogen, EUA). After incubation, suspensions of 1×10^7/mL spermatozoa/tube from the treated and control groups were washed by centrifugation with 2 mL of PBS 1×. The supernatant was discarded, and the pellet was resuspended in 200 μL of PBS 1×. The probe was added to each sample at a final concentration of 20 nM. The samples were shielded from light and incubated at 37 °C for 20 min. After incubation, the samples were centrifuged again with 2 mL of PBS 1× to remove the unbound probe. A flow cytometer (FACScan, Becton Dickinson) and Flow Jo software were used to examine the labeled sperm (Amaral and Ramalho-Santos, 2010).

LPO was measured using the probe BODIPY581/591-C11 (D3861 Invitrogen, EUA). After the incubation period, suspensions of 4×10^6/mL spermatozoa/tube from the treated and control groups were washed by centrifugation with 2 mL of PBS 1×. The supernatant was discarded, and the pellet was resuspended in 200 μL of PBS 1×. Each sample was loaded with the probe at a final concentration of 5 μM and incubated at 37 °C for 30 min, protected from light. After incubation, the samples were rewashed by centrifugation to remove the unbound probe. The labeled sperm were analyzed using a flow cytometer (FACScan, Becton Dickinson) and Flow Jo software (Ortega Ferrusola et al., 2009).

2.10.4. Measurement of reactive oxygen species (ROS)

To quantify intracellular ROS production, a DCFDA/H2DCFDA Cellular ROS Assay Kit (ab113851, Abcam, USA) was utilized according to the manufacturer's instructions. Approximately 1×10^6 sperm/mL from treated and control groups were stained with a diluted DCFDA solution and incubated at 37 °C for 30 min in the dark. The fluorescence intensity was measured at 485/535 nm using a Cytation 5 Cell Imaging plate reader (Biotek, USA).

Furthermore, the generation of intracellular superoxide anions ($O_2^{\cdot-}$) was assessed using a MitoSOX™ Red Mitochondrial Superoxide Indicator kit (M36008, Thermo Fisher Scientific, USA) and performed per manufacturer instructions. The labeled sperm were analyzed using a Cytation 5 Cell Imaging (Biotek, USA) plate reader at 531/593 nm.

2.11. Statistical analysis

Quantitative data were assessed for normality using the Kolmogorov-Smirnov (Dallal-Wilkinson-Lilliefor) test, while the homogeneity of variances was examined using the Bartlett test. The results were expressed as mean ± SEM (standard error of the mean).

For data with a normal distribution, analysis of variance (ANOVA) was conducted, followed by the Newman-Keuls' test or two-way analysis of variance (Two-way ANOVA) for post hoc comparisons of means. Non-parametric data were analyzed using the Kruskal-Wallis test for analysis of variance, and the Dunns' test was employed for mean comparisons.

To compare the control group with the treated group, Student's *t*-test was used, taking into consideration the parametric or non-parametric distribution of the data. All statistical analyses were performed using the GraphPad Prism 8.4.2 software (GraphPad Software, Inc.), and a significance level of $p < 0.05$ was considered statistically significant.

3. Results

3.1. Synthesis, coating and characterization of Cit_SPIONs

The cuboidal/spherical morphologies and the interatomic space of SPIONs and Cit_SPIONs are evident in Fig. 1A-B'. While the average diameter of SPIONs was 13 ± 4.1 nm (Fig. 1C), the mean diameter of Cit_SPIONs was 8.0 ± 1.8 nm (Fig. 1D). The zeta potential of SPIONs was positive (+11.8 ± 0.4 mV) during the two weeks evaluated. Differently, the zeta potential of Cit_SPIONs was negative in the two time points

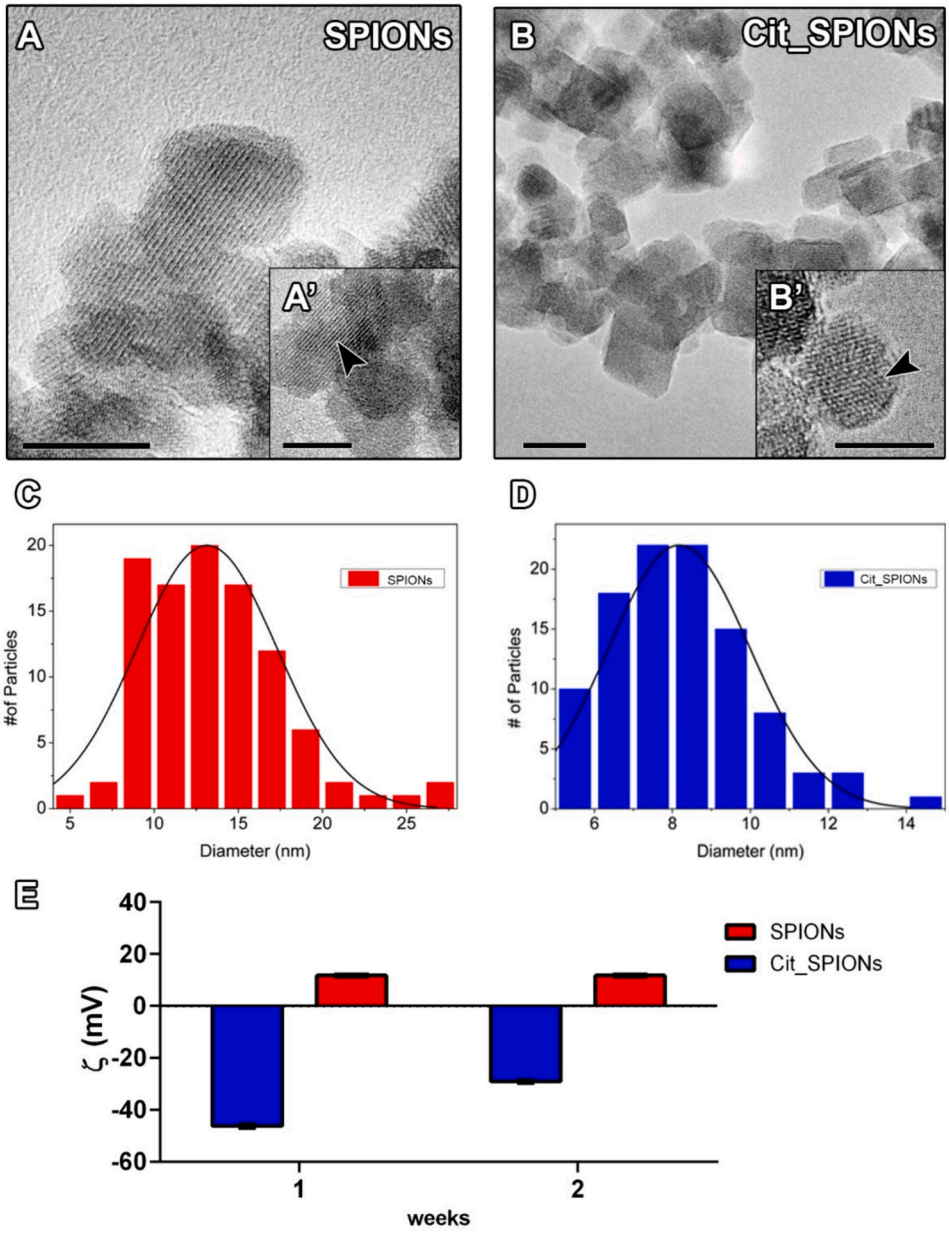

Fig. 1. Morphological and zeta potential analyses of SPIONs and Cit_SPIONs. (A-B′) Transmission electron microscopy (TEM) micrograph showing the morphology of SPIONs (A-A') and Cit_SPIONs (B-B′). (A' and B′) TEM micrograph representing the diameter and the interatomic spaces of isolated nanoparticles. (C—D) Histograms of nanoparticle size distributions from SPIONs and Cit_SPIONs. (E) Zeta potential data from SPIONs and Cit_SPIONs during two weeks of evaluation. Scale bar = 10 nm.

evaluated. Notably, the zeta potential value of Cit_SPIONs increased from the first week (−46.2 ± 0.9 mV) to the second week (−29.0 ± 0.6 mV).

The TGA and DTG thermograms of sodium citrate, SPIONs, and Cit_SPIONs samples are shown in Fig. 2A-C. From these data, the content of sodium citrate coating on the Cit_SPIONs was calculated. The TGA curve of sodium citrate has three stages of weight loss (Fig. 2A). The weight loss was about 11.7 wt% in the first stage, starting at 155 °C up to 180 °C, which is related to the water loss of crystallization [ref]. The second stage, which occurs between 290 °C and 325 °C, corresponds to the partial degradation of the sodium citrate (13.4%). The last stage is from approximately 330 °C to 460 °C due to the oxidation of the residues (11.7%) from the previous step (Bai et al., 2010).

The TGA curve of the SPIONs sample shows a continuous weight loss from the initial temperature to the end (Fig. 2B). The thermal degradation process consisted of two stages: 1) loss of physically adsorbed water molecules (3.1%) between 20 °C and 140 °C, and 2) mass loss attributed to the elimination of the strong-bonded water molecules from the surface of nanoparticles (3.8%), which occurs between 140 °C and 700 °C (Mohammed et al., 2021). The TGA plot of Cit_SPIONs exhibits two mass loss steps (Fig. 2C). The first loss of ~2.9% occurred between 20 °C and 140 °C. The second one of ~3.2% occurred from 140 °C to 460 °C (Fig. 2C). Then, as sodium citrate lost approximately 36.8% of mass, SPIONs lost about 5.1% (related to water), and Cit_ SPIONs lost about 6.2% of mass up to a temperature of 460 °C, we can consider that the Cit_SPIONs sample contains approximately 3% of citrate.

DTG curves (Fig. 2A-C) provide more insights into the thermal decomposition peaks. Comparing the decomposition peaks of magnetite in the DTG curve for the SPIONs (Fig. 2B) and Cit_SPIONs (Fig. 2C) samples, the values remained at approximately 40 °C and 555 °C. The sodium citrate decomposition peak at about 164 °C was shifted to 250 °C in the Cit_SPIONs, indicating higher thermal stability of citrate-loaded

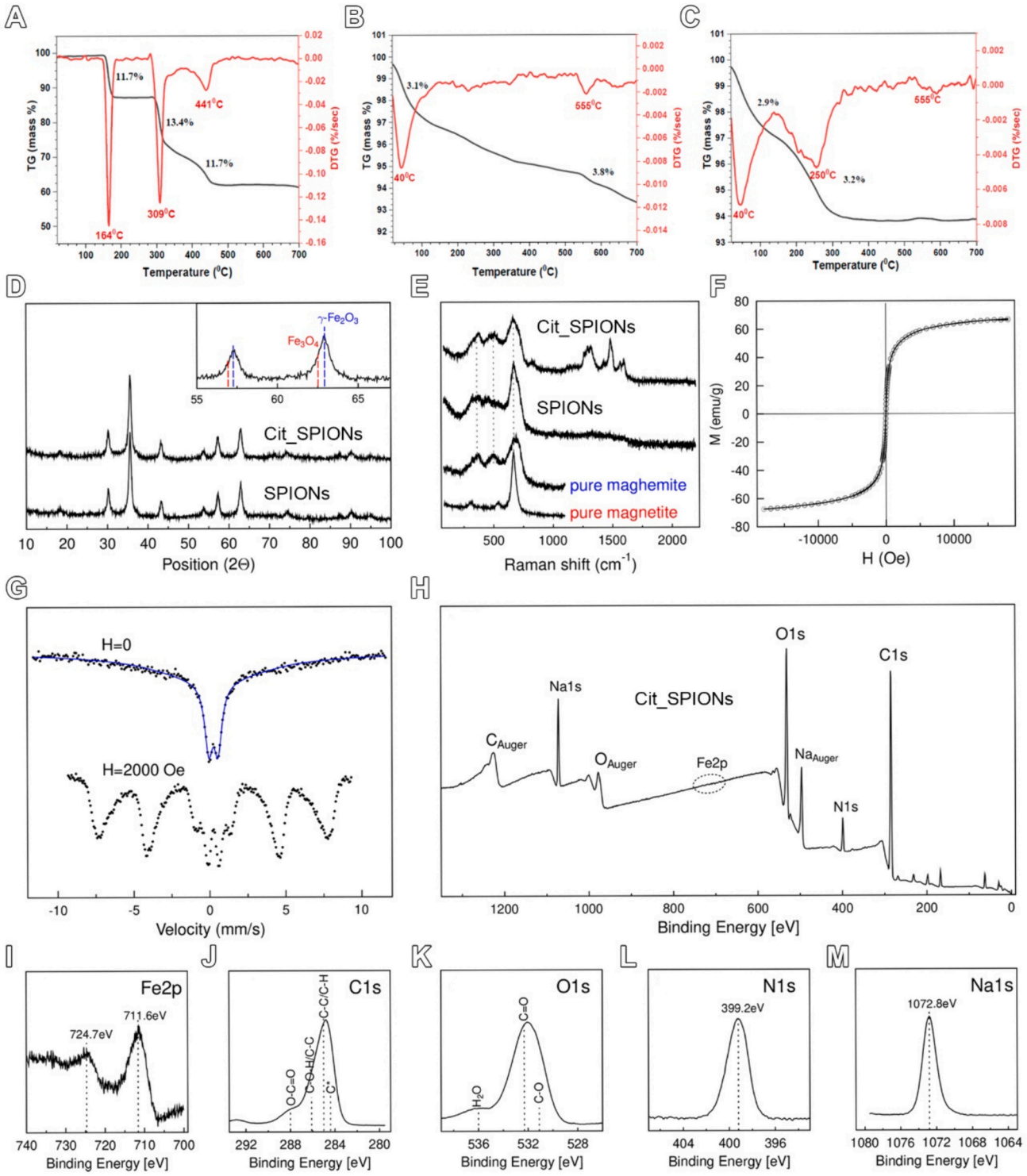

Fig. 2. Physico-chemical characterization of Cit_SPIONs. (A-C) TGA and DTG curves for the decomposition of: (A) sodium citrate, (B) SPIONs, and (C) Cit_SPIONs. (D) X-ray diffraction of Cit_SPIONs. (E) Raman spectra of SPIONs and Cit_SPOINs. (F) VSM magnetometry of Cit_SPIONs. (G) Mössbauer spectra of Cit_SPIONs. (H-M) Photoelectron Spectroscopy (XPS) spectra providing insights into the chemical species present in the Cit_SPIONs.

SPIONs than pure citrate.

The X-ray diffraction results shown in Fig. 2D demonstrated that the sodium citrate coating does not alter the structure of the nanoparticles since both patterns are indistinguishable. Moreover, according to ref. (Vassal et al., 2021), our XRD data show peak positions closer to the expected ones for the maghemite phase. This data is the first indication that our Cit_SPIONs are closer to the structure of maghemite.

Raman spectra of SPIONs and Cit_SPOINs are shown in Fig. 2E and compared to pure maghemite and magnetite samples. The prominent Raman bands of magnetite are known to be located at 668, 538, and 306 cm − 1 (Fig. 2E, dotted lines) (Suciu et al., 2020). The main peak (668 cm^{-1}) perfectly matches our SPIONs and Cit_SPIONs samples. However, the main line of both is very broad, and the lower frequencies are also broader and slightly shifted towards the values of pure maghemite (γ-Fe2O3), which may be a result of magnetite oxidation (Testa-Anta et al., 2019). Peaks at 1300-1600 cm − 1 are related to the sodium

citrate.

Fig. 2F contains the VSM magnetometry result of the powder sample. As expected for nanoparticulated oxide, there is no hysteresis (open) loop. This "superparamagnetic behavior" occurs because when the magnetic field is removed, the magnetization of each nanoparticle randomly flips its direction under the influence of room temperature, and no remanence or coercive field is observed. The saturation magnetization, MS =67 emu/g at Hmax = 18,000 Oe, is a low value even for maghemite. However, lower values are also expected in nanoparticulate oxides due to surface effects and defects.

Two Mössbauer spectra are shown in Fig. 2G. Without applying a magnetic field to sample one, a broad spectrum (upper spectrum, H = 0) is observed, clearly evidencing a superparamagnetic iron oxide, with its particles having an average diameter of <10 nm. The particle size distribution of Cit_SPIONs and the various types of surrounding crystallography of the iron atoms cause the broadening of the sextet lines into a relaxed spectrum plus a doublet. The ion state of iron atoms (Fe2+ and Fe3+) cannot be distinguished at room temperature due to the fast electron-hopping process. The fitted spectrum has an average isomer shift of 0.36(1) mm/s, closer to Fe3+, suggesting maghemite formation. However, it is also known that the maghemite phase (γ-Fe2O3) can coexist with magnetite (Fe3O4) during synthesis or appear due to partial oxidation. Applying a magnetic field to the sample makes the spectrum more static (lower spectrum, H = 2000 Oe), and the sextet lines appear, even though some smaller particles remain superparamagnetic. That spectrum also indicates the magnetite/maghemite formation.

Fig. 2H shows the XPS-Survey spectrum. First, the Fe2p lines are barely visible in the survey spectrum. This indicates that a very efficient functionalization of the oxide nanoparticles took place since XPS is a surface-sensitive method that probes only ca. 2 nm. The XPS main peaks are due to the presence of oxygen, carbon, nitrogen, and sodium at the surface of the SPIONs. Nitrogen comes from the culture medium, while sodium comes from the coating with the stabilizing sodium citrate.

Figs. 2I-M show high-resolution spectra of the most important transitions: Fe2p, C1s, O1s, N1s, and Na1s. The estimated binding energies consider a tolerance of ±0.1 eV. Since the SPIONs were coated with sodium citrate, even the main Fe-peaks exhibit a very small signal; therefore, they have been measured with a much higher accumulation time than the other lines. As shown in Fig. 2I, the Fe2p3/2 and Fe2p1/2 lines are observed at 711.6 and 724.7 eV, respectively. These binding energies are in accordance with the presence of ferrimagnetic iron oxide, corroborating the Mössbauer result. The satellite peak at around 719 eV is characteristic of Fe3+ in γ-Fe2O3; however, it is relatively weak, suggesting coexistence with magnetite. In summary, a mixture of maghemite and magnetite is most likely.

Fig. 2J exhibits a C1s structure due to a convolution of peaks mainly related to chemical groups on the surface of the NPs. We attribute them to C—C and C—H at 285.0 eV, C-O-H and C-O-C at 286.1 eV, O–C=O at 288.0 eV, and adventious carbon at 284.4 eV. Fig. 2K shows the O1s transition, consisting of at least three peaks. We relate them to C=O (531.1 eV), C-OH (532.3 eV), and H2O (536 eV). The N1s peak in Fig. 2L was found at 399.2 eV, which we attribute to unionized nitrogen (NH2, C=NH) (Artemenko et al., 2021b). Fig. 2M shows a single Na1s peak at 1072.8 eV, which may be mainly from the sodium citrate and partly from the NaOH used as a precipitating agent during the Cit_SPIONs synthesis.

3.2. Cit_SPIONs is highly toxic for Sertoli and Leydig cells in vitro

Prior to exposing the testicular cells to nanoparticles, we verified the effective enrichment of testicular cell fractions (Fig. 3A-C). Germ cells, characterized by their rounded morphology and abundant presence in bright field microscopy, exhibited the expression of the VASA protein (Fig. 3A). Sertoli cells, which demonstrated resistance to the osmotic test, were identified based on the expression of the GATA4 transcription factor (Fig. 3B). Additionally, Leydig cells displayed a granular appearance and exhibited expression of the steroidogenic factor 3βHSD (Fig. 3C).

To assess the cytotoxicity of Cit_SPIONs in testicular cells, we employed the cell viability assay using the CTB® kit. Two concentrations of Cit_SPIONs were evaluated for cytotoxic effects over 24, 48, and 72 h (Fig. 3D). Following a 24 h exposure to Cit_SPIONs, we observed that Leydig cells were particularly susceptible to the lowest concentration (Fig. 3E). In the subsequent time points examined (48 and 72 h), both Sertoli and Leydig cells demonstrated decreased viability in the presence of Cit_SPIONs (Fig. 3F-G). The reduction in cell viability was more pronounced when the higher concentration of Cit_SPIONs was utilized (Fig. 3F-G). Intriguingly, VASA-positive germ cells exposed to Cit_SPIONs maintained cell viability comparable to the control group (Fig. 3E-G).

In addition to evaluating Cit_SPIONs, we evaluated the cytotoxicity of the sodium citrate (3%) according to the data obtained in the TGA analysis. Our data indicated that the different testicular cells presented higher than 75% cell viability in all time points evaluated (24, 48, and 72 h) (Supplemental Fig. 1). The sperm viability was not altered in the presence of sodium citrate (Supplemental Fig. 2). These data indicate a good biocompatibility of the sodium citrate.

3.3. High internalization of Cit_SPIONs by Leydig cells

Following exposure of Cit_SPIONs (at a concentration of 8×10^{-2} mg/mL) in a testis culture on an agarose block, the samples were collected at 24 and 48 h for further histological analysis (Fig. 4A, B). Subsequently, the testis was processed to assess its structural features (Fig. 4C-F). Notably, there were no significant differences observed in terms of tubular diameter and the volumetric density of both tubular and intertubular compartments (Fig. 4G-I).

Further analysis through transmission electron microscopy (Fig. 4J-K, K') revealed that Cit_SPIONs were primarily located within phagocytic vesicles within peritubular macrophages (Fig. 4J) and displayed a preferential localization within vesicles in Leydig cells (Fig. 4K-K'-indicated by red arrows). While the nuclear volume of Leydig cells remained unchanged, exposure to Cit_SPIONs induced significant alteration in the cytoplasmic volume of Leydig cells (Fig. 4L-M).

3.4. Cit_SPIONs changed the sperm motility, viability and DNA integrity

Exposure to Cit_SPIONs at a concentration of 8×10^{-2} mg/mL for 30 min resulted in significant alterations in sperm motility across all three evaluated parameters (progressive motile, non-progressive motile, and immotile) (Fig. 5A-C). Furthermore, a negative impact on sperm viability was observed, with all sperm being stained as non-viable during analysis. Similar significant changes in the three sperm parameters were observed at various time points (30 min, 1 h, and 2 h) following exposure to Cit_SPIONs at a concentration of 8×10^{-3} mg/mL (Fig. 5D-F). Motility and viability were also affected by this treatment (Fig. 5G).

After a two-hour exposure to Cit_SPIONs (at a concentration of 8×10^{-3} mg/mL), a significant increase was observed in the percentage of spermatozoa exhibiting fragmented DNA (Fig. 5H). Staining with Acridine Orange revealed spermatozoa with fragmented DNA, exhibiting fluorescence in a spectrum ranging from yellow to orange and red (Fig. 5I-J).

3.5. Cit_SPIONs altered sperm mitochondrial activity and induced lipid peroxidation

MitoTracker Green probe was employed to assess mitochondrial activity. Mitotracker dyes passively diffuse across the plasma membrane and accumulate in active mitochondria, emitting a green fluorescence (Fig. 6A-D). Sperm with low active mitochondria lack green fluorescence (Fig. 6E-H). Notably, the group treated with Cit_SPIONs displayed a significant decrease in low mitochondrial activity (Fig. 6I-L).

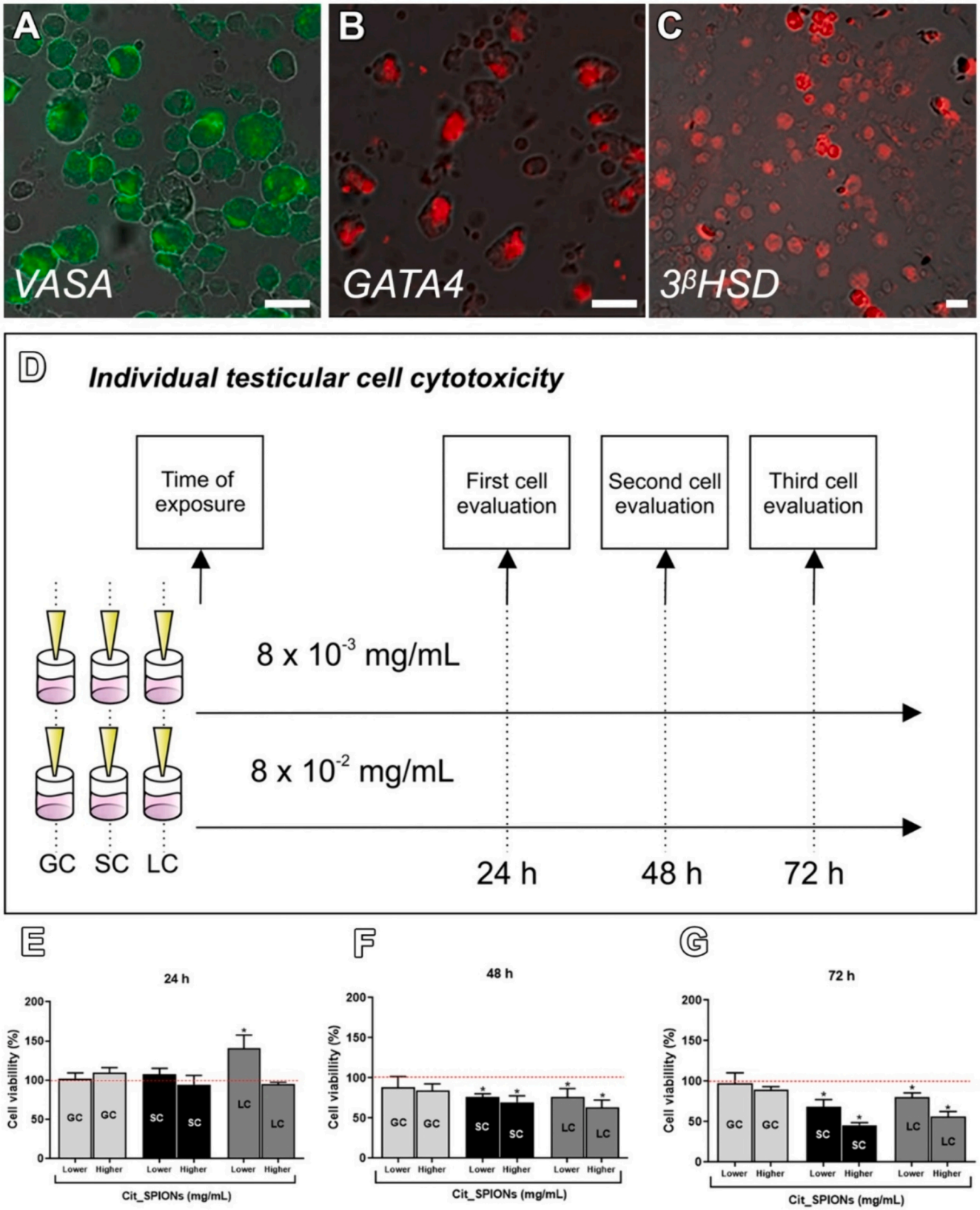

Fig. 3. Cytotoxicity of Cit_SPIONs in Different Testicular Cells. (A) Immunofluorescence staining for VASA protein to identify germ cells (GC). (B) Immunofluorescence staining for GATA4 transcription factor to identify Sertoli cells (SC) after the osmotic test. (C) Immunofluorescence staining for 3βHSD to identify Leydig cells (LC). (D) Cell viability assessment using the Cell Titer Blue® (CTB) assay. Two concentrations of Cit_SPIONs (8×10^{-2} and 8×10^{-3} mg/mL) were employed, and viability was evaluated at three time points: 24 h (e), 48 h (f), and 72 h (g). Scale bar = 10 μm. Statistical significance was determined at $^{*}p < 0.05$. (For interpretation of the references to colour in this figure legend, the reader is referred to the web version of this article.)

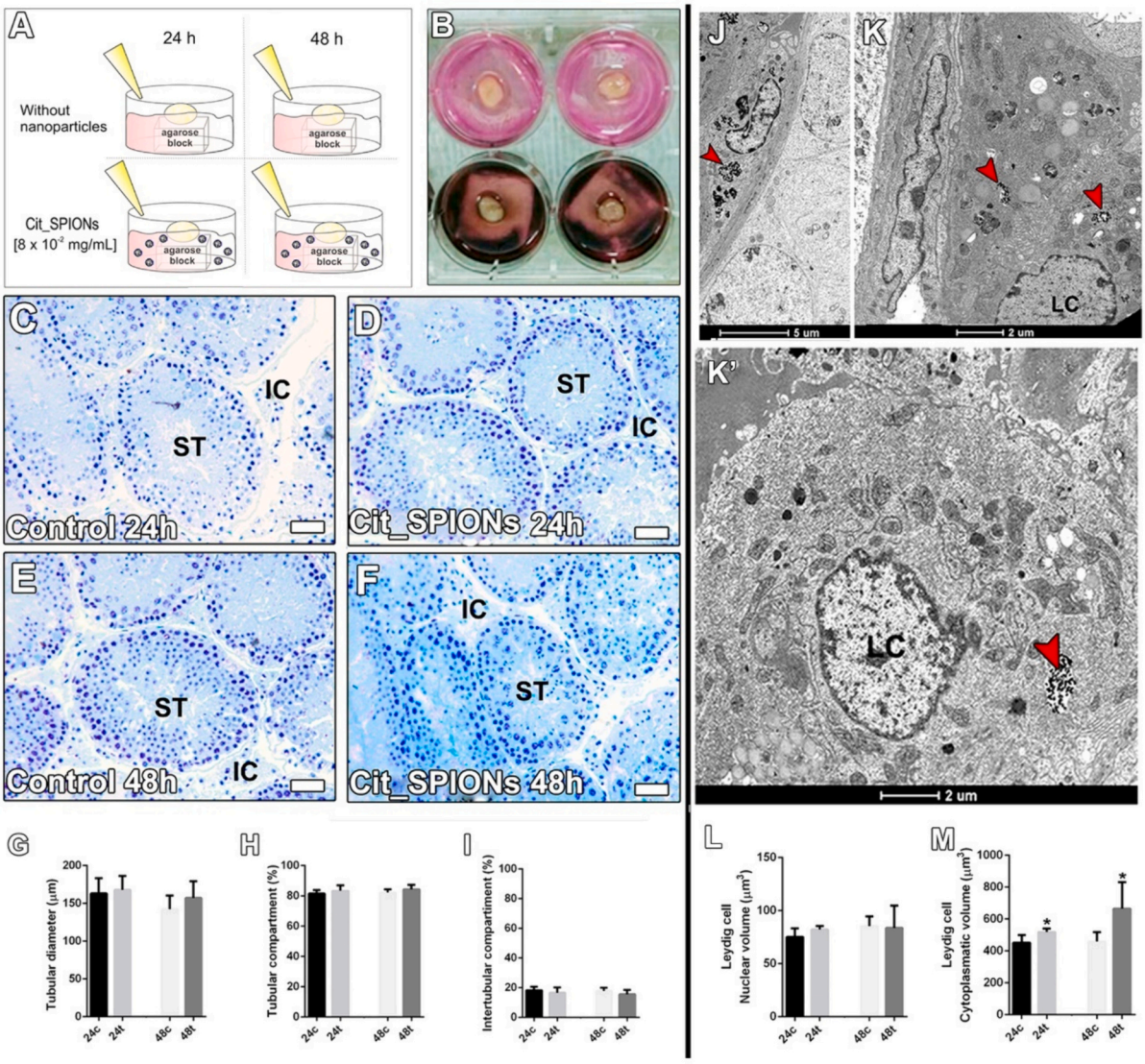

Fig. 4. Effects of Cit_SPIONs on Testis Organotypic Culture. (A) Schematic representation of the experimental design for *in vitro* assays. (B) Representative image showing a testicular explant in contact with culture medium containing Cit_SPIONs. (C—F) Histological images of the testicular tissue following *in vitro* assays. (G) Analysis of tubular diameter revealing no significant changes. (H—I) Proportion of the tubular and intertubular compartments showing no significant alterations. (J-K') Identification of Cit_SPIONs within endocytic vesicles in the cytoplasm of macrophages (J) and Leydig cells (K-K') indicated by red arrowheads. (l) No changes observed in Leydig cell nuclear volume. (M) Alteration observed in Leydig cell cytoplasmic volume. Seminiferous tubules (ST), interstitial compartment (IC). Scale bar = 50 µm; black scale bar = 5 cm. Statistical significance was determined at $*p < 0.05$. (For interpretation of the references to colour in this figure legend, the reader is referred to the web version of this article.)

In the analysis of lipid peroxidation (LPO), unperoxidized spermatozoa exhibited red fluorescence (Fig. 6M-O). Conversely, peroxidized spermatozoa were characterized by green fluorescence, primarily observed in the midpiece and tail regions (Fig. 6P-R). Spermatozoa exposed to Cit_SPIONs demonstrated a substantial increase in LPO levels (Fig. 6S-U).

3.6. Cit_SPIONs increases ROS production in spermatozoa

DCFDA - Cellular ROS Assay Kit (Abcam, USA) and MitoSOX™ (Invitrogen™, USA) were used to evaluate the ROS production in sperm. The DCFDA - Cellular ROS Assay Kit quantitatively assesses reactive oxygen species (ROS) in live cell samples (Fig. 7A-B). DCFDA labeling showed a significant increase in the generation of total intracellular ROS (Fig. 7C) in the sperm exposed to Cit_SPIONs compared to the control group. MitoSOX™ is a fluorogenic dye used to detect superoxide anion ($O2^{\bullet-}$) in the mitochondria of living cells (Fig. 7D-E). Spermatozoa exposed to Cit_SPIONs demonstrated a substantial increase in mitochondrial superoxide anion production (Fig. 7F).

4. Discussion

In vitro investigations examining the impact of superparamagnetic iron oxide nanoparticles (SPIONs) on testicular cells remain limited (Dantas et al., 2022; Younus et al., 2020b). Therefore, further research exploring nanoparticles' biocompatibility, biological effects, and potential biomedical applications in reproductive contexts is crucial (Durfey et al., 2019). A comprehensive understanding of how nanostructures affect testicular cells has the potential to guide the development of targeted therapies for male infertility, hypogonadism, and contraception (Yan Cheng and Mruk, 2012). In light of these considerations, this study aimed to assess the toxicity of Cit_SPIONs in mouse testicular cells using an *in vitro* model. The results of the current study showed the *in vitro* toxicity of Cit_SPIONs to testicular somatic cells and

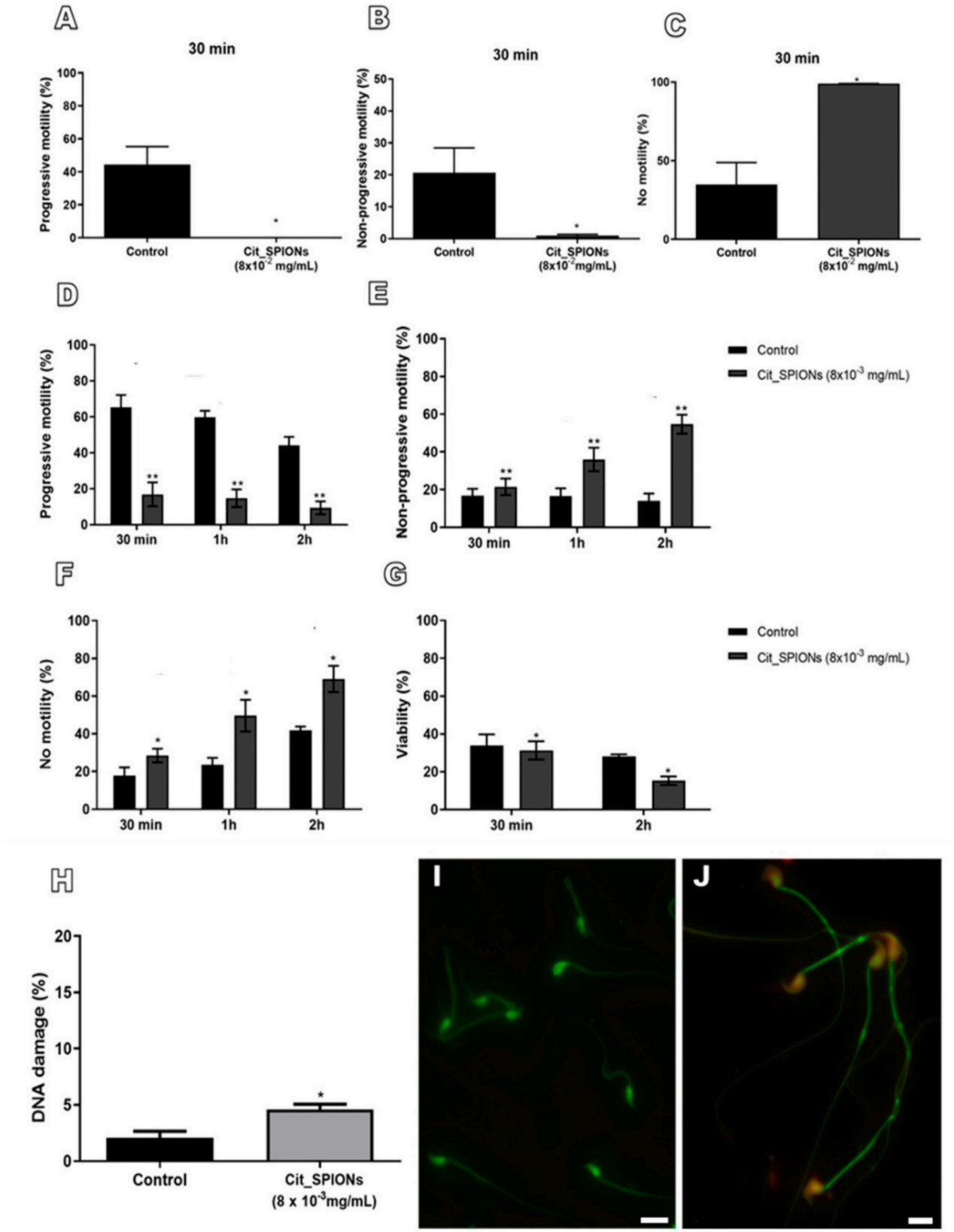

Fig. 5. Effects of Cit_SPIONs on Sperm Motility, Viability, and DNA Damage. (A-C) Sperm motility analysis after exposure to Cit_SPIONs at a concentration of 8×10^{-2} mg/mL for 30 min. (D—F) Sperm motility analysis following exposure to Cit_SPIONs at a concentration of 8×10^{-3} mg/mL for 30 min, 1 h, and 2 h. (G) Sperm viability assessment after exposure to Cit_SPIONs at a concentration of 8×10^{-3} mg/mL for 30 min and 2 h. (H) Percentage of fragmented DNA in spermatozoa exposed to Cit_SPIONs at a concentration of 8×10^{-3} mg/mL for 2 h. (I) Representative image of spermatozoa without fragmented DNA. (J) Representative image of spermatozoa with fragmented DNA. Scale bar = 5 μm. Values are presented as mean ± SEM. $^{**}P < 0.01$ $^{*}P < 0.05$.

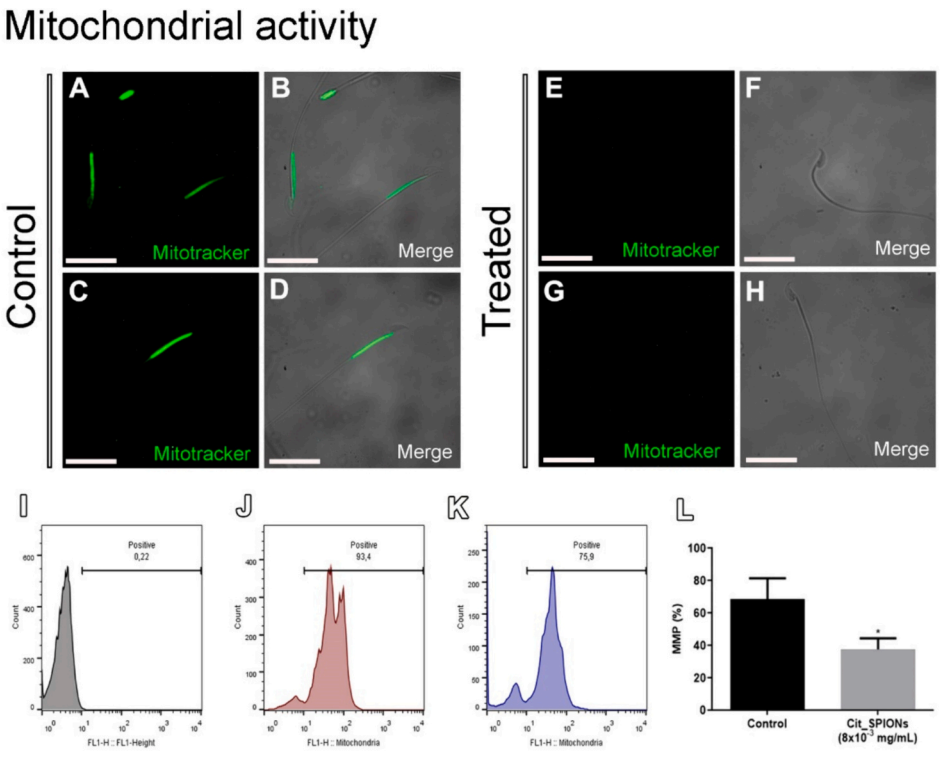

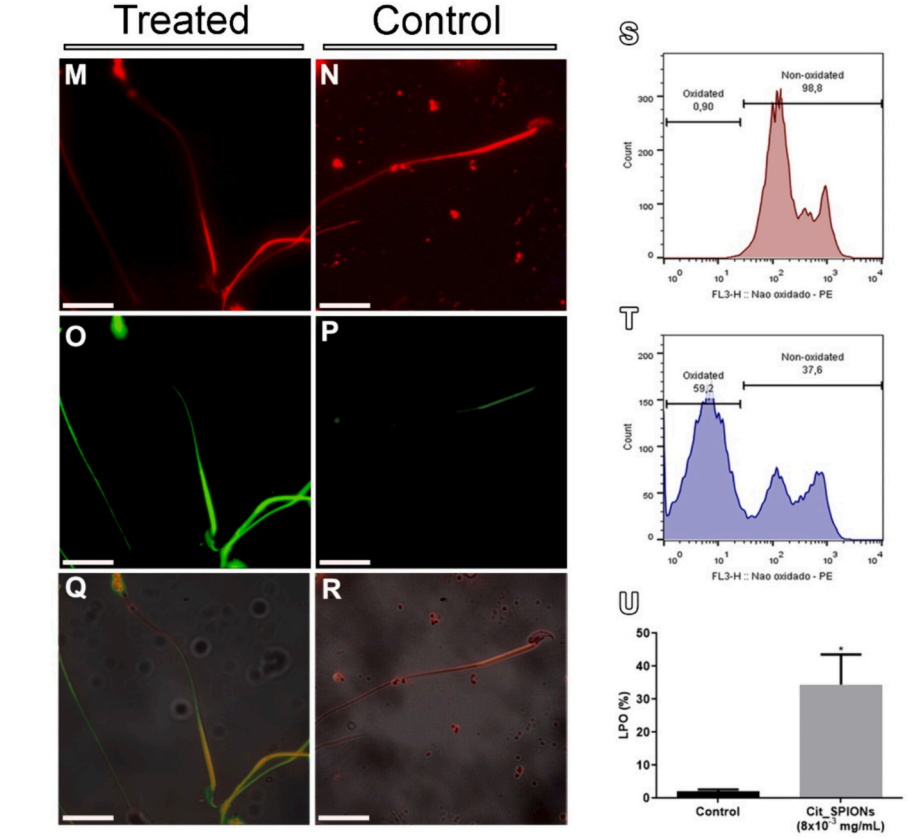

(caption on next page)

Fig. 6. Effects of Cit_SPIONs on Sperm Mitochondrial activity and Lipid Peroxidation. (A-D) Fluorescence microscopy images of spermatozoa loaded with Mitotracker Green probe. Green fluorescence emission in the midpiece indicates a mitochondrial activity in viable sperm. (E-H) Fluorescence microscopy images of spermatozoa without fluorescence emission in the midpiece, indicating low mitochondrial activity in non-viable sperm. (I-L) Percentage of spermatozoa exhibiting changes in mitochondrial activity following exposure to Cit_SPIONs at a concentration of 8×10^{-3} mg/mL for 2 h. (M-R) Fluorescence microscopy images of spermatozoa loaded with BODIPY-C11 probe. (M and N) Red fluorescence corresponds to the non-oxidized probe in spermatozoa. (O and P) Green fluorescence indicates the oxidized probe in spermatozoa. (Q and R) Merged images. (S—U) Percentage of peroxidized and unperoxidized spermatozoa after exposure to Cit_SPIONs. All images were acquired using the Eclipse Ti2 Series - Nikon fluorescence microscope. Magnification: 100×. Scale bar = 20 μm. Statistical significance was determined at $*p < 0.05$. (For interpretation of the references to colour in this figure legend, the reader is referred to the web version of this article.)

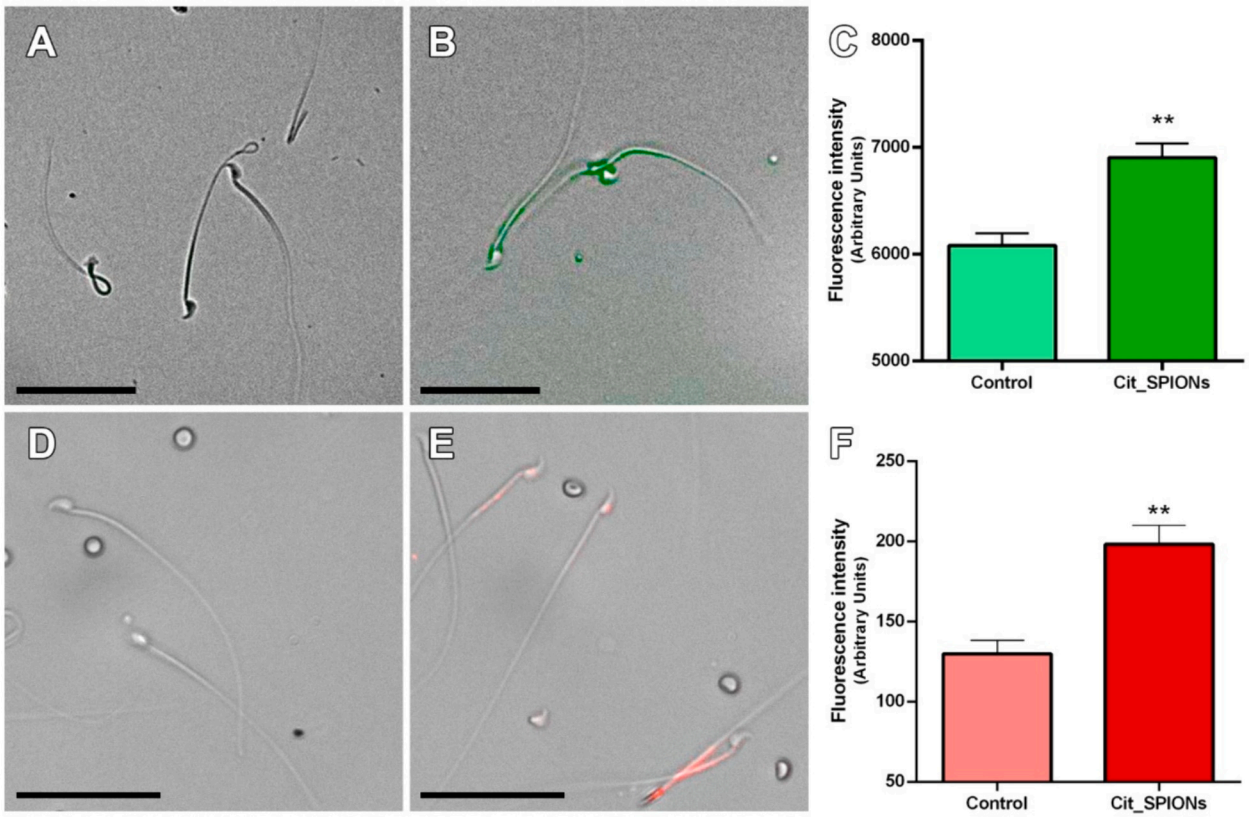

Fig. 7. Free radicals in sperm after exposition to Cit_SPIONs. A-C) DCFDA - Cellular ROS Assay in (A) control and (B) sperm exposed to Cit_SPIONs. C) Quantitative data of total ROS production. D—F) MitoSOX™ assay in (D) control and (E) sperm exposed to Cit_SPIONs. F) Quantitative data of mitochondrial superoxide anion ($O2^{\bullet-}$) production.

spermatozoa. The data support the findings of Ferraz et al. (Ferraz et al., 2024), which suggest that Cit_SPIONs can aid in the creation of contraceptive or sterilizing agents. These nanoparticles have been shown to have adverse effects on the endocrine functions of the testes, specifically the Leydig cells and testosterone, as well as on the exocrine functions related to gamete production and functionality.

In this study, we conducted a characterization setup of Cit_SPIONs, revealing that the sodium citrate diminished the nanoparticle size and improved the dispersion in culture media and the stability in the solution during the experimental time. In this study, the characterization by TEM revealed polydispersity of Cit_SPIONs in terms of nanoparticle size distribution (6–9 nm). The co-precipitation method is one of the most widely used and successful for synthesizing SPIONs; however, one of its limitations is the wide particle size distribution (Wu et al., 2015; Dadfar et al., 2020). Particle growth is kinetically controlled and depends on various experimental parameters, such as the types of iron salts, Fe (II) / Fe (III) ratio, pH value, and ionic strength of the medium (Wu et al., 2015). Refining the size distribution of SPIONs substantially improves performance in different biomedical applications (Dadfar et al., 2020).

Various studies have shown that not only the size of the NPs but also other physicochemical characteristics such as shape, concentration, surface chemistry, surface charge, catalytic activity, among others, play a fundamental role in biological interactions (Dantas et al., 2022; Bakand and Hayes, 2016; Sukhanova et al., 2018; Souza et al., 2021; Barua and Mitragotri, 2014; Thakur et al., 2014). Furthermore, biological changes depend on the time of exposure to NPs, the stability of the NP in biological fluids, and its ability to accumulate in tissues and organs (Dantas et al., 2022; Bakand and Hayes, 2016; Sukhanova et al., 2018; Souza et al., 2021; Thakur et al., 2014). The toxic effects are more significantly associated with small NPs and their distribution and large surface/area ratio. Smaller NPs can more easily cross epithelial and endothelial barriers and accumulate in different organs. Due to their small size and large surface area, NPs can interact with cellular organelles, for example, mitochondria and nuclei, and this can alter cellular metabolism, cause DNA damage, mutations, and cell death (Dantas et al., 2022; Souza et al., 2021; Barua and Mitragotri, 2014).

The XRD, Raman spectroscopy, and Mössbauer analyses indicated that the iron oxide nanoparticle resembles better maghemite (γ-Fe2O3). However, it is important to note that maghemite can coexist with magnetite (Fe3O4) during synthesis (Coimbra et al., 2023). VSM demonstrated the superparamagnetic characteristic of Cit_SPIONs. The particle size distribution of Cit_SPIONs and the distinct crystallographic configurations of iron atoms contribute to broadening the sextet lines, resulting in a relaxed spectrum and a doublet (Brand, 1994). The XPS-

Survey spectrum revealed the effective coating of oxide nanoparticles with sodium citrate, as evidenced by the absence of the Fe2p line in the survey spectrum. XPS, being a surface-sensitive technique with a probing depth of approximately 2 nm, confirmed the presence of oxygen, carbon, nitrogen, and sodium on the surface of the Cit_SPIONs. Nitrogen likely originated from the culture media, while sodium resulted from the sodium citrate coating for stabilization. The sodium citrate (measured by TGA) was biocompatible with testicular cells at the used concentration (3%). Despite these favorable physicochemical properties, the *in vitro* experiments demonstrated the cytotoxicity of Cit_SPIONs, particularly towards testicular somatic cells and sperm cells.

Leydig cells (LCs) in the testes are responsible for testosterone synthesis and secretion (Vassal et al., 2021; Bara and Kaul, 2018). Accumulation of metal oxide nanoparticles (MONPs) in the testes can have harmful effects on testosterone production, impacting reproductive function (Vassal et al., 2021; Liu et al., 2020). In our study, we observed concentration- and time-dependent cytotoxicity of Cit_SPIONs on Leydig cells. These nanoparticles were rapidly internalized by Leydig cells in the testicular tissue culture system, accumulating within cytoplasmic vesicles and potentially contributing to increased cytoplasmic volume. Interestingly, Leydig cells in the testes express high levels of mitochondrial ferritin (MtF), a protein known to be involved in regulating iron (Fe) homeostasis and toxicity (Santambrogio et al., 2007; Liu et al., 2022; Levi and Arosio, 2004). Given the known structural and functional similarities between MtF and cytoplasmic ferritin, it is plausible to suggest that MtF may play a role in sequestering excess Fe and protecting against oxidative damage, potentially by reducing Fenton's reactions (Liu et al., 2022; Levi and Arosio, 2004; Tvrda et al., 2015). However, further research is needed to fully elucidate the specific mechanisms and functions of MtF in Leydig cells.

Our findings revealed significant alterations in sperm motility, viability, DNA integrity, mitochondrial function changes, and lipid peroxidation (LPO) following *in vitro* exposure to Cit_SPIONs. Previous studies, both *in vivo* and *in vitro*, have highlighted the importance of iron (Fe) for the development of male reproductive cells, particularly germ cells (Liu et al., 2022; Tvrda et al., 2015; Tvrdá et al., 2012). Iron plays a crucial role in supporting sperm function by contributing to the proliferation, differentiation, and maintenance of motility and energy metabolism in germ cells (Liu et al., 2022; Tvrda et al., 2015; Wise et al., 2003). While further research is necessary, some studies suggest that SPIONs can access the lysosomal pathway and undergo metabolism, which may result in the release of iron in its free form (Ghosh et al., 2020; Chen and Hou, 2023; Wu et al., 2013; Singh et al., 2010; Lunov et al., 2010; Chen et al., 2010). The excessive iron levels can lead to increased production of reactive oxygen species (ROS) in spermatozoa, resulting in oxidative damage and potentially inducing ferroptosis (Liu et al., 2022; Tvrdá et al., 2012). Oxidative stress, arising from an imbalance between ROS production and antioxidant defense mechanisms, is a major contributor to sperm dysfunction, leading to effects on proteins, lipids, and DNA within the spermatozoa (Sati and Huszar, 2015b).

Oxidative stress can lead to a decrease in mitochondrial activity, which is crucial because sperm mitochondria play a vital role in various processes essential for successful fertilization, including sperm motility, hyperactivation, capacitation, acrosomal reaction, and fertilization (Barbagallo et al., 2020). Oxidative stress can also result in sperm cell DNA fragmentation, which has adverse effects on sperm concentration, motility, and morphology, ultimately affecting fertility outcomes (Nazari et al., 2016; Razavi et al., 2003; Morris et al., 2002; Hosseinalipour et al., 2021). Motility, a critical parameter for successful fertilization, can be compromised due to damage caused by elevated levels of reactive oxygen species (ROS) to the sperm plasma membranes (Doreswamy et al., 2004; Baker and Aitken, 2005; Smith et al., 2015). Sperm-specific polyunsaturated fatty acids (PUFAs), which are important components of cell membranes, are particularly susceptible to oxidative damage through lipid peroxidation. This oxidative damage to unsaturated fatty acids is associated with increased production of reactive oxygen species within the mitochondria (mROS) (Liu et al., 2022; Xu et al., 2019; Amaral et al., 2013).

Numerous studies investigating various types of nanoparticles (NPs) have highlighted the role of reactive oxygen species (ROS) in mediating effects on sperm cells. Yoisungnern et al. (Yoisungnern et al., 2015) demonstrated that silver nanoparticles (AgNPs) could be taken up by spermatozoa, leading to a dose-dependent reduction in sperm viability and impaired acrosomal reaction. Aziz et al. (Aziz et al., 2004) observed a correlation between ROS levels and sperm abnormalities, such as amorphous heads, damaged acrosomes, midpiece defects, cytoplasmic droplets, and tail defects, following exposure to different chemicals. Santonastaso et al. (Santonastaso et al., 2019) provided evidence for intracellular ROS production in human spermatozoa and highlighted its negative impact as a potential primary mechanism underlying the genotoxicity of titanium dioxide nanoparticles (TiO_2NPs).

Although we observed toxic effects on sperm cells at specific concentrations of Cit_SPIONs, it is worth noting that *in vitro* studies have demonstrated the biocompatibility of magnetic nanoparticles (NPs) with sperm (Shandilya et al., 2020). Magnetic NPs, such as superparamagnetic iron oxide nanoparticles (SPIONs), have been utilized to detect and remove non-viable spermatozoa from semen without compromising their motility and ability to undergo the acrosome reaction (Durfey et al., 2019; Feugang, 2017; Makhluf et al., 2006). In artificial insemination in wild boars, SPIONs have been used during semen processing, demonstrating an antimicrobial effect while preserving sperm characteristics (Tsakmakidis et al., 2020). Moreover, magnetic NPs loaded with DNA sequences can be transferred to the sperm plasma membrane, facilitating the delivery of exogenous DNA to the oocyte through *in vitro* fertilization (Kim et al., 2010). These findings highlight the potential applications of magnetic NPs in reproductive medicine.

The cytotoxic effects of Cit_SPIONs on Sertoli cells and VASA+ germ cells display differential susceptibilities. Sertoli cells exhibit higher susceptibility to the toxic effects of Cit_SPIONs at elevated concentrations, albeit with minimal alterations observed in the testis tissue culture system. In contrast, VASA+ germ cells demonstrate greater resistance to the presence of nanoparticles, both in isolated form and within testes explants. These findings suggest a potential resilience of the exocrine function of the testes, ensuring sperm production even in the presence of inorganic nanoparticles. Notably, both cell types are susceptible to the generation of free radicals and oxidative stress, as indicated by previous studies (Han et al., 2015; Han et al., 2016; Zhang et al., 2015). However, it is important to recognize that other research groups have reported disruptive effects of nanoparticles on the Sertoli cell barrier and disturbances in spermatogonial physiology and meiosis in murine models (Pinho et al., 2020; Salman, 2017; Mozaffari et al., 2015).

5. Conclusions

Although the use of SPIONs in various biological applications is well documented, there is still a great need to identify the possible cell damage associated with exposure to these nanoparticles. Currently, few studies have demonstrated the interaction of SPIONs with testicular cells and their potential risks to reproductive health. The results of our study provide evidence of the susceptibility of somatic testicular cells and sperm to exposure to iron oxide nanoparticles. We observed a pronounced internalization of Cit_SPIONs in Leydig cells, contributing to cell cytoplasmic volume change. Furthermore, our results demonstrate that spermatozoa present compromised motility, viability, DNA integrity, mitochondrial changes, and lipid peroxidation after exposure to Cit_SPIONs. The ROS increase in sperm cells suggests that Cit_SPIONs present relevant toxicity to testicular cells, inducing oxidative stress. Our findings highlight the need for detailed development of iron oxide nanoparticles to enhance reproductive nanosafety.

Financial support

CNPq (422405/2018–3 and 317259/2021–0), FAPEMIG (RED00079-22) and CAPES.

CRediT authorship contribution statement

Graziela de P.F. Dantas: Writing – review & editing, Writing – original draft, Investigation, Formal analysis, Data curation, Conceptualization. **Fausto S. Ferraz:** Writing – review & editing, Writing – original draft, Investigation, Formal analysis. **John L.P. Coimbra:** Writing – review & editing, Writing – original draft, Investigation, Formal analysis. **Roberto M. Paniago:** Writing – review & editing, Writing – original draft, Investigation, Formal analysis. **Maria S.S. Dantas:** Formal analysis, Investigation. **Samyra M.S.N. Lacerda:** Writing – review & editing, Writing – original draft, Formal analysis. **Matheus F. Gonçalves:** Writing – review & editing, Writing – original draft, Formal analysis. **Marcelo H. Furtado:** Writing – review & editing, Writing – original draft, Formal analysis. **Bárbara P. Mendes:** Writing – review & editing, Writing – original draft, Formal analysis. **Jorge L. López:** Writing – review & editing, Writing – original draft, Formal analysis. **Alisson C. Krohling:** Formal analysis, Investigation. **Estefânia M.N. Martins:** Formal analysis, Investigation. **Lídia M. Andrade:** Writing – review & editing, Writing – original draft, Formal analysis. **Luiz O. Ladeira:** Writing – review & editing, Writing – original draft, Formal analysis. **Ângela L. Andrade:** Writing – review & editing, Writing – original draft, Formal analysis. **Guilherme M.J. Costa:** Writing – review & editing, Writing – original draft, Supervision, Resources, Investigation, Formal analysis, Data curation, Conceptualization.

Declaration of competing interest

The authors declare that there is no conflict of interest regarding the publication of this manuscript.

Data availability

Data will be made available on request.

Acknowledgments

We would like to acknowledge the support received from CAPES (Coordination for the Improvement of Higher Education Personnel; GFD scholarship), FAPEMIG (Minas Gerais State Research Foundation) through the REDE MINEIRA DE NANOMEDICINA TERANÓSTICA - RED00079-22, and CNPq (National Council for Scientific and Technological Development - 422405/2018-3 and 317259/2021-0). We also extend our gratitude to Clínica MF Fertilidade Masculina, Laboratório de Caracterização de Nanomateriais (LCPNano), Laboratório LabCri/UFMG, Centro de Microscopia, and CAPI from UFMG for the use of their facilities.

Appendix A. Supplementary data

Supplementary data to this article can be found online at https://doi.org/10.1016/j.impact.2024.100517.

References

Amaral, A., Ramalho-Santos, J., 2010. Assessment of mitochondrial potential: implications for the correct monitoring of human sperm function. Int. J. Androl. 33, e180–e186. https://doi.org/10.1111/j.1365-2605.2009.00987.x.

Amaral, A., Lourenço, B., Marques, M., Ramalho-Santos, J., 2013. Mitochondria functionality and sperm quality. Reproduction 146, R163–R174. https://doi.org/10.1530/REP-13-0178.

Artemenko, A., Shchukarev, A., Štenclová, P., Wagberg, T., Segervald, J., Jia, X., Kromka, A., 2021a. Reference XPS spectra of amino acids. In: IOP Conf Ser Mater Sci Eng, 1050. IOP Publishing Ltd, p. 012001. https://doi.org/10.1088/1757-899X/1050/1/012001.

Artemenko, A., Shchukarev, A., Štenclová, P., Wagberg, T., Segervald, J., Jia, X., Kromka, A., 2021b. Reference XPS spectra of amino acids. In: IOP Conf Ser Mater Sci Eng, 1050. IOP Publishing Ltd, p. 012001. https://doi.org/10.1088/1757-899X/1050/1/012001.

Aziz, N., Saleh, R.A., Sharma, R.K., Lewis-Jones, I., Esfandiari, N., Thomas, A.J., Agarwal, A., 2004. Novel association between sperm reactive oxygen species production, sperm morphological defects, and the sperm deformity index. Fertil. Steril. 81, 349–354. https://doi.org/10.1016/j.fertnstert.2003.06.026.

Bai, Z., Yang, L., Zhang, J., Li, L., Hu, C., Lv, J., Guo, Y., 2010. High-efficiency carbon-supported platinum catalysts stabilized with sodium citrate for methanol oxidation. J. Power Sources 195, 2653–2658. https://doi.org/10.1016/j.jpowsour.2009.11.008.

Bakand, S., Hayes, A., 2016. Toxicological considerations, toxicity assessment, and risk management of inhaled nanoparticles. Int. J. Mol. Sci. 17, 1–17. https://doi.org/10.3390/ijms17060929.

Baker, M.A., Aitken, R.J., 2005. Reactive oxygen species in spermatozoa: methods for monitoring and significance for the origins of genetic disease and infertility. Reprod. Biol. Endocrinol. 3, 67. https://doi.org/10.1186/1477-7827-3-67.

Bara, N., Kaul, G., 2018. Enhanced steroidogenic and altered antioxidant response by ZnO nanoparticles in mouse testis Leydig cells. Toxicol. Ind. Health 34, 571–588. https://doi.org/10.1177/0748233718774220.

Barbagallo, F., La Vignera, S., Cannarella, R., Aversa, A., Calogero, A.E., Condorelli, R.A., 2020. Evaluation of sperm mitochondrial function: a key organelle for sperm motility. J. Clin. Med. 9, 363. https://doi.org/10.3390/jcm9020363.

Barua, S., Mitragotri, S., 2014. Challenges associated with penetration of nanoparticles across cell and tissue barriers: a review of current status and future prospects. Nano Today 9, 223–243. https://doi.org/10.1016/j.nantod.2014.04.008.

Bhushan, S., Aslani, F., Zhang, Z., Sebastian, T., Elsässer, H.P., Klug, J., 2016. Isolation of sertoli cells and peritubular cells from rat testes. J. Vis. Exp. 2016, 1–12. https://doi.org/10.3791/53389.

Brand, R.A., 1994. NORMOS 90, Laboratorium Für Angewandte Physik. Universität Duisburg, Germany.

Caizer, C., 2021. Optimization study on specific loss power in superparamagnetic hyperthermia with magnetite nanoparticles for high efficiency in alternative cancer therapy. Nanomaterials 11, 1–22. https://doi.org/10.3390/nano11010040.

Campagnolo, L., Massimiani, M., Magrini, A., Camaioni, A., Pietroiusti, A., 2012. Physico-Chemical Properties Mediating Reproductive and Developmental Toxicity of Engineered Nanomaterials, 19, pp. 4488–44894. http://www.euro.who.int/__data/assets/pdf_file/0010/73954/EN63.p.

Cândido, M.A., Rost, N.C.V., Ferreira, V.R., Raniero, L., 2022. Síntese de nanopartículas de óxido de ferro estabilizadas com citrato de sódio e TMAOH. Res. Soc. Developm. 11, e139111637698 https://doi.org/10.33448/rsd-v11i16.37698.

Chang, Y.F., Lee-Chang, J.S., Panneerdoss, S., MacLean, J.A., Rao, M.K., 2011a. Isolation of Sertoli, Leydig, and spermatogenic cells from the mouse testis. Biotechniques 51, 341–344. https://doi.org/10.2144/000113763.

Chang, Y.-F., Lee-Chang, J.S., Panneerdoss, S., MacLean, J.A., Rao, M.K., 2011b. Isolation of Sertoli, Leydig, and spermatogenic cells from the mouse testis. Biotechniques 51, 341–344. https://doi.org/10.2144/000113764.

Chen, Y., Hou, S., 2023. Recent progress in the effect of magnetic iron oxide nanoparticles on cells and extracellular vesicles. Cell Death Dis. 9, 195. https://doi.org/10.1038/s41420-023-01490-2.

Chen, Y.C., Hsiao, J.K., Liu, H.M., Lai, I.Y., Yao, M., Hsu, S.C., Ko, B.S., Chen, Y.C., Yang, C.S., Huang, D.M., 2010. The inhibitory effect of superparamagnetic iron oxide nanoparticle (Ferucarbotran) on osteogenic differentiation and its signaling mechanism in human mesenchymal stem cells. Toxicol. Appl. Pharmacol. 245, 272–279. https://doi.org/10.1016/j.taap.2010.03.011.

Coimbra, J.L.P., de PDantas, G.F., de Andrade, L.M., Brener, M.R.G., Viana, P.I.M., Lopes, R.A., Gontijo, D.O.G., Ervilha, L.O.G., Assis, M.Q., Barcelos, L.S., Szawka, R. E., Damasceno, D.C., Machado-Neves, M., Mota, A.P., Costa, G.M.J., 2023. Gold nanoparticle intratesticular injections as a potential animal sterilization tool: long-term reproductive and toxicological implications. Toxicology 492, 153543. https://doi.org/10.1016/j.tox.2023.153543.

Costa, G.M.J., Lacerda, S.M.S.N., Figueiredo, A.F.A., Leal, M.C., Rezende-Neto, J.V., França, L.R., 2018. Higher environmental temperatures promote acceleration of spermatogenesis in vivo in mice (Mus musculus). J. Therm. Biol. 77, 14–23. https://doi.org/10.1016/j.jtherbio.2018.07.010.

Dadfar, S.M., Camozzi, D., Darguzyte, M., Roemhild, K., Varvarà, P., Metselaar, J., Banala, S., Straub, M., Güvener, N., Engelmann, U., Slabu, I., Buhl, M., Van Leusen, J., Kögerler, P., Hermanns-Sachweh, B., Schulz, V., Kiessling, F., Lammers, T., 2020. Size-isolation of superparamagnetic iron oxide nanoparticles improves MRI, MPI and hyperthermia performance. J. Nanobiotechnol. 18, 22. https://doi.org/10.1186/s12951-020-0580-1.

Dantas, G.P.F., Ferraz, F.S., Andrade, L.M., Costa, G.M.J., 2022. Male reproductive toxicity of inorganic nanoparticles in rodent models: a systematic review. Chem. Biol. Interact. 363, 110023 https://doi.org/10.1016/j.cbi.2022.110023.

Datta, N.R., Krishnan, S., Speiser, D.E., Neufeld, E., Kuster, N., Bodis, S., Hofmann, H., 2016. Magnetic nanoparticle-induced hyperthermia with appropriate payloads: Paul Ehrlich's "magic (nano)bullet" for cancer theranostics? Cancer Treat. Rev. 50, 217–227. https://doi.org/10.1016/j.ctrv.2016.09.016.

Di Bona, K.R., Xu, Y., Gray, M., Fair, D., Hayles, H., Milad, L., Montes, A., Sherwood, J., Bao, Y., Rasco, J.F., 2015. Short- and long-term effects of prenatal exposure to iron oxide nanoparticles: influence of surface charge and dose on developmental and

reproductive toxicity. Int. J. Mol. Sci. 16, 30251–30268. https://doi.org/10.3390/ijms161226231.
Ding, W., Chen, Z., Gu, Y., Chen, Z., Zheng, Y., Sun, F., 2021. Magnetic testis targeting and magnetic hyperthermia for noninvasive, controllable male contraception via intravenous administration. Nano Lett. 21, 6289–6297. https://doi.org/10.1021/acs.nanolett.1c02181.
Doreswamy, K., Shrilatha, B., Rajeshkumar, T., 2004. Muralidhara, nickel-induced oxidative stress in testis of mice: evidence of DNA damage and genotoxic effects. J. Androl. 25, 996–1003. https://doi.org/10.1002/j.1939-4640.2004.tb03173.x.
Dulińska-Litewka, J., Łazarczyk, A., Hałubiec, P., Szafrański, O., Karnas, K., Karewicz, A., 2019. Superparamagnetic iron oxide nanoparticles-current and prospective medical applications. Materials 12. https://doi.org/10.3390/ma12040617.
Durfey, C.L., Swistek, S.E., Liao, S.F., Crenshaw, M.A., Clemente, H.J., Thirumalai, R.V.K. G., Steadman, C.S., Ryan, P.L., Willard, S.T., Feugang, J.M., 2019. Nanotechnology-based approach for safer enrichment of semen with best spermatozoa. J. Anim. Sci. Biotechnol. 10, 14. https://doi.org/10.1186/s40104-018-0307-4.
Elsharkawy, E.E., Abd El-Nasser, M., Kamaly, H.F., 2019. Silver nanoparticles testicular toxicity in rat. Environ. Toxicol. Pharmacol. 70, 103194 https://doi.org/10.1016/j.etap.2019.103194.
Farini, V.L., Camaño, C.V., Ybarra, G., Viale, D.L., Vichera, G., Yakisich, J.S., Radrizzani, M., 2016. Improvement of bovine semen quality by removal of membrane-damaged sperm cells with DNA aptamers and magnetic nanoparticles. J. Biotechnol. 229, 33–41. https://doi.org/10.1016/j.jbiotec.2016.05.008.
Ferraz, F.S., López, J.L., Lacerda, S.M.S.N., Procópio, M.S., Figueiredo, A.F.A., Martins, E. M.N., Guimarães, P.P.G., Ladeira, L.O., Kitten, G.T., Dias, F.F., Domingues, R.Z., Costa, G.M.J., 2020. Biotechnological approach to induce human fibroblast apoptosis using superparamagnetic iron oxide nanoparticles. J. Inorg. Biochem. 206, 111017 https://doi.org/10.1016/j.jinorgbio.2020.111017.
Ferraz, F.S., de Dantas, G.P.F., Coimbra, J.L.P., López, J.L., Lacerda, S.M.S.N., dos Santos, M.L., de Vieira, C.P., Lara, N.L.E.M., Viana, P.I.M., Ladeira, L.O., Guarnieri, L.O., Marçal, E.M.A., Moraes, M.F.D., Martins, E.M.N., Andrade, L.M., Costa, G.M.J., 2024. Effects of superparamagnetic iron oxide nanoparticles (SPIONS) testicular injection on Leydig cell function and sperm production in a murine model. Reprod. Toxicol. 126, 108584 https://doi.org/10.1016/j.reprotox.2024.108584.
Feugang, J.M., 2017. Novel agents for sperm purification, sorting, and imaging. Mol. Reprod. Dev. 84, 832–841. https://doi.org/10.1002/mrd.22831.
Ganguly, P., Breen, A., Pillai, S.C., 2018. Toxicity of nanomaterials: exposure, pathways, assessment, and recent advances. ACS Biomater. Sci. Eng. 4, 2237–2275. https://doi.org/10.1021/acsbiomaterials.8b00068.
Ghosh, S., Ghosh, I., Chakrabarti, M., Mukherjee, A., 2020. Genotoxicity and biocompatibility of superparamagnetic iron oxide nanoparticles: influence of surface modification on biodistribution, retention, DNA damage and oxidative stress. Food Chem. Toxicol. 136, 110989 https://doi.org/10.1016/j.fct.2019.110989.
Habas, K., Brinkworth, M.H., Anderson, D., 2018. Silver nanoparticle-mediated cellular responses in isolated primary Sertoli cells in vitro. Food Chem. Toxicol. 116, 182–188. https://doi.org/10.1016/j.fct.2018.04.030.
Han, D.-W., Hong, S.C., Lee, J.H., Lee, J., Kim, H.Y., Park, J.Y., Cho, J., Lee, D.-W. Han, 2011. Subtle cytotoxicity and genotoxicity differences in superparamagnetic iron oxide nanoparticles coated with various functional groups. Int. J. Nanomedicine 3219. https://doi.org/10.2147/ijn.s26355.
Han, J.W., Jeong, J.K., Gurunathan, S., Choi, Y.J., Das, J., Kwon, D.N., Cho, S.G., Park, C., Seo, H.G., Park, J.K., Kim, J.H., 2015. Male- and female-derived somatic and germ cell-specific toxicity of silver nanoparticles in mouse. Nanotoxicology 10, 361–373. https://doi.org/10.3109/17435390.2015.1073396.
Han, Z., Yan, Q., Ge, W., Liu, Z.G., Gurunathan, S., De Felici, M., Shen, W., Zhang, X.F., 2016. Cytotoxic effects of ZnO nanoparticles on mouse testicular cells. Int. J. Nanomedicine 11, 5187–5203. https://doi.org/10.2147/IJN.S111447.
Hosseinalipour, E., Karimipour, M., Ahmadi, A., 2021. Detrimental effects of cerium oxide nanoparticles on testis, sperm parameters quality, and in vitro fertilization in mice: an experimental study. Int. J. Reprod. Biomed. 19, 801–810. https://doi.org/10.18502/ijrm.v19i9.9712.
Jivago, J.L.P.R., Brito, J.L.M., Capistrano, G., Vinícius-Araújo, M., Verde, E.L., Bakuzis, A.F., Souza, P.E.N., Azevedo, R.B., Lucci, C.M., 2021. New prospects in neutering male animals using magnetic nanoparticle hyperthermia. Pharmaceutics 13, 1465. https://doi.org/10.3390/pharmaceutics13091465.
Kaczyńska, A., Guzdek, K., Derszniak, K., Karewicz, A., Lewandowska-Łańcucka, J., Mateuszuk, Ł., Skórka, T., Banasik, T., Jasiński, K., Kapusta, C., Chlopicki, S., Nowakowska, M., 2016. Novel nanostructural contrast for magnetic resonance imaging of endothelial inflammation: targeting SPIONs to vascular endothelium. RSC Adv. 6, 72586–72595. https://doi.org/10.1039/c6ra10994b.
Kim, T.S., Lee, S.H., Gang, G.T., Lee, Y.S., Kim, S.U., Koo, D.B., Shin, M.Y., Park, C.K., Lee, D.S., 2010. Exogenous DNA uptake of boar spermatozoa by a magnetic nanoparticle vector system. Reprod. Domest. Anim. 45, e201–e206. https://doi.org/10.1111/j.1439-0531.2009.01516.x.
Kim, J.H., Lee, H.J., Doo, S.H., Yang, W.J., Choi, D., Kim, J.H., Won, J.H., Song, Y.S., 2015. Use of nanoparticles to monitor human mesenchymal stem cells transplanted into penile cavernosum of rats with erectile dysfunction, Korean. J. Urol. 56, 280–287. https://doi.org/10.4111/kju.2015.56.4.280.
Kristianto, H., Reynaldi, E., Prasetyo, S., Sugih, A.K., 2020. Adsorbed leucaena protein on citrate modified Fe3O4 nanoparticles: synthesis, characterization, and its application as magnetic coagulant. Sustain. Environ. Res. 30, 32. https://doi.org/10.1186/s42834-020-00074-4.
Laurent, S., Forge, D., Port, M., Roch, A., Robic, C., Vander Elst, L., Muller, R.N., 2008. Magnetic iron oxide nanoparticles: synthesis, stabilization, vectorization, physicochemical characterizations and biological applications. Chem. Rev. 108, 2064–2110. https://doi.org/10.1021/cr068445e.
Levi, S., Arosio, P., 2004. Mitochondrial ferritin. Int. J. Biochem. Cell Biol. 36, 1887–1889. https://doi.org/10.1016/j.biocel.2003.10.020.
Liu, Y., Li, X., Xiao, S., Liu, X., Chen, X., Xia, Q., Lei, S., Li, H., Zhong, Z., Xiao, K., 2020. The effects of gold nanoparticles on leydig cells and male reproductive function in mice. Int. J. Nanomedicine 15, 9499–9514. https://doi.org/10.2147/IJN.S276606.
Liu, Y., Cao, X., He, C., Guo, X., Cai, H., Aierken, A., Hua, J., Peng, S., 2022. Effects of Ferroptosis on male reproduction. Int. J. Mol. Sci. 23, 7139. https://doi.org/10.3390/ijms23137139.
Llenas, M., Sandoval, S., Costa, P.M., Oró-Solé, J., Lope-Piedrafita, S., Ballesteros, B., Al-Jamal, K.T., Tobias, G., 2019. Microwave-assisted synthesis of SPION-reduced graphene oxide hybrids for magnetic resonance imaging (MRI). Nanomaterials 9. https://doi.org/10.3390/nano9101364.
Lunov, O., Syrovets, T., Büchele, B., Jiang, X., Röcker, C., Tron, K., Nienhaus, G.U., Walther, P., Mailänder, V., Landfester, K., Simmet, T., 2010. The effect of carboxydextran-coated superparamagnetic iron oxide nanoparticles on c-Jun N-terminal kinase-mediated apoptosis in human macrophages. Biomaterials 31, 5063–5071. https://doi.org/10.1016/j.biomaterials.2010.03.023.
Mahmoudi, M., Simchi, A., Milani, A.S., Stroeve, P., 2009. Cell toxicity of superparamagnetic iron oxide nanoparticles. J. Colloid Interface Sci. 336, 510–518. https://doi.org/10.1016/j.jcis.2009.04.046.
Makhluf, S.B.D., Qasem, R., Rubinstein, S., Gedanken, A., Breitbart, H., 2006. Loading magnetic nanoparticles into sperm cells does not affect their functionality. Langmuir 22, 9480–9482. https://doi.org/10.1021/la061988z.
Malhotra, N., Lee, J.S., Liman, R.A.D., Ruallo, J.M.S., Villaflore, O.B., Ger, T.R., Der Hsiao, C., 2020. Potential toxicity of iron oxide magnetic nanoparticles: a review. Molecules 25, 3159. https://doi.org/10.3390/molecules25143159.
Meena, R., Kajal, K., P. R, 2014. Cytotoxic and genotoxic effects of titanium dioxide nanoparticles in testicular cells of male Wistar rat. Appl. Biochem. Biotechnol. 175, 825–840. https://doi.org/10.1007/s12010-014-1299-y.
Mohammed, H.B., Rayyif, S.M.I., Curutiu, C., Birca, A.C., Oprea, O.C., Grumezescu, A.M., Ditu, L.M., Gheorghe, I., Chifiriuc, M.C., Mihaescu, G., Holban, A.M., 2021. Eugenol-functionalized magnetite nanoparticles modulate virulence and persistence in pseudomonas aeruginosa clinical strains. Molecules 26, 2189. https://doi.org/10.3390/molecules26082189.
Morris, I.D., Ilott, S., Dixon, L., Brison, D.R., 2002. The spectrum of DNA damage in human sperm assessed by single cell gel electrophoresis (comet assay) and its relationship to fertilization and embryo development. Hum. Reprod. 17, 990–998. https://doi.org/10.1093/humrep/17.4.990.
Mozaffari, Z., Parivar, K., Roodbari, N.H., Irani, S., 2015. Histopathological evaluation of the toxic effects of zinc oxide (ZnO) nanoparticles on testicular tissue of NMRI adult mice. Adv Stud. Biol. 7, 275–291. https://doi.org/10.12988/asb.2015.5425.
Nasri, S., Rezai-Zarchi, S., Kerishchi, P., Sadeghi, S., 2015. The effect of Iron oxide nanoparticles on sperm numbers and mobility in male mice. Zahedan J. Res. Med. Sci. 17, e2185 https://doi.org/10.17795/zjrms-2185.
Nazari, M., Talebi, A.R., Sharifabad, M.H., Abbasi, A., Khoradmehr, A., Danafar, A.H., 2016. Acute and chronic effects of gold nanoparticles on sperm parameters and chromatin structure in mice. Int. J. Reprod. Biomed. 14, 637–642. https://doi.org/10.29252/ijrm.14.10.637.
Nosrati, H., Adibtabar, M., Sharafi, A., Danafar, H., Hamidreza Kheiri, M., 2018. PAMAM-modified citric acid-coated magnetic nanoparticles as pH sensitive biocompatible carrier against human breast cancer cells. Drug Dev. Ind. Pharm. 44, 1377–1384. https://doi.org/10.1080/03639045.2018.1451881.
Ortega Ferrusola, C., González Fernández, L., Morrell, J.M., Salazar Sandoval, C., Macías García, B., Rodríguez-Martinez, H., Tapia, J.A., Peña, F.J., 2009. Lipid peroxidation, assessed with BODIPY-C 11, increases after cryopreservation of stallion spermatozoa, is stallion-dependent and is related to apoptotic-like changes. Reproduction 138, 55–63. https://doi.org/10.1530/REP-08-0484.
Patel, U., Chauhan, K., Gupte, S., 2018. Synthesis, characterization and application of lipase-conjugated citric acid-coated magnetic nanoparticles for ester synthesis using waste frying oil. 3 Biotech 8, 211. https://doi.org/10.1007/s13205-018-1228-9.
Pinho, A.R., Rebelo, S., de Lourdes Pereira, M., 2020. The impact of zinc oxide nanoparticles on male (in)fertility. Materials 13, 1–18. https://doi.org/10.3390/ma13040849.
Qu, S., Yang, H., Ren, D., Kan, S., Zou, G., Li, D., Li, M., 1999. NOTE Magnetite Nanoparticles Prepared by Precipitation from Partially Reduced Ferric Chloride Aqueous Solutions, 215, pp. 190–192. https://doi.org/10.1006/jcis.1999.6185.
Razavi, S., Nasr-Esfahani, M.H., Mardani, M., Mafi, A., Moghdam, A., 2003. Effect of human sperm chromatin anomalies on fertilization outcome post-ICSI. Andrologia 35, 238–243. https://doi.org/10.1046/j.1439-0272.2003.00566.x.
Salman, R.A., 2017. The influence of ZnO NPs on reproductive system tissues of albino male mice. Histopathological study. Int. J. Sci. Res. (IJSR) 6, 2021–2025. https://doi.org/10.21275/art20175455.
Santambrogio, P., Biasiotto, G., Sanvito, F., Olivieri, S., Arosio, P., Levi, S., 2007. Mitochondrial ferritin expression in adult mouse tissues. J. Histochem. Cytochem. 55, 1129–1137. https://doi.org/10.1369/jhc.7A7273.2007.
Santonastaso, M., Mottola, F., Colacurci, N., Iovine, C., Pacifico, S., Cammarota, M., Cesaroni, F., Rocco, L., 2019. In vitro genotoxic effects of titanium dioxide nanoparticles (n-TiO2) in human sperm cells. Mol. Reprod. Dev. 86, 1369–1377. https://doi.org/10.1002/mrd.23134.
Sarimov, R.M., Nagaev, E.I., Matveyeva, T.A., Binhi, V.N., Burmistrov, D.E., Serov, D.A., Astashev, M.E., Simakin, A.V., Uvarov, O.V., Khabatova, V.V., Akopdzhanov, A.G., Schimanowskii, N.L., Gudkov, S.V., 2022a. Investigation of aggregation and disaggregation of self-assembling Nano-sized clusters consisting of individual Iron oxide nanoparticles upon interaction with HEWL protein molecules. Nanomaterials 10, 3960. https://doi.org/10.3390/nano12223960.

Sarimov, R.M., Nagaev, E.I., Matveyeva, T.A., Binhi, V.N., Burmistrov, D.E., Serov, D.A., Astashev, M.E., Simakin, A.V., Uvarov, O.V., Khabatova, V.V., Akopdzhanov, A.G., Schimanowskii, N.L., Gudkov, S.V., 2022b. Investigation of aggregation and disaggregation of self-assembling Nano-sized clusters consisting of individual Iron oxide nanoparticles upon interaction with HEWL protein molecules. Nanomaterials 12, 3960. https://doi.org/10.3390/nano12223960.

Sati, L., Huszar, G., 2015a. Sperm motility and viability: overview of the cellular and physiological aspects that support these functions. EMJ Repro. 1, 74–80. https://doi.org/10.33590/emjreprohealth/10314360.

Sati, L., Huszar, G., 2015b. Sperm motility and viability: overview of the cellular and physiological aspects that support these functions. EMJ Repro. 1, 74–80. https://doi.org/10.33590/emjreprohealth/10314360.

Sengupta, J., Ghosh, S., Datta, P., Gomes, A., Gomes, A., 2014. Physiologically important metal nanoparticles and their toxicity. J. Nanosci. Nanotechnol. 14, 990–1006. https://doi.org/10.1166/jnn.2014.9078.

Shandilya, R., Mishra, P.K., Pathak, N., Lohiya, N.K., Sharma, R.S., 2020. Nanotechnology in reproductive medicine: opportunities for clinical translation. Clin. Exp. Reprod. Med. 47, 245–262. https://doi.org/10.5653/cerm.2020.03650.

Sharma, H., Kumar, K., Choudhary, C., Mishra, P.K., Vaidya, B., 2016. Development and characterization of metal oxide nanoparticles for the delivery of anticancer drug. Artif Cells Nanomed. Biotechnol. 44, 672–679. https://doi.org/10.3109/21691401.2014.978980.

Singh, N., Jenkins, G.J.S., Asadi, R., Doak, S.H., 2010. Potential toxicity of superparamagnetic iron oxide nanoparticles (SPION). Nanotechnol. Rev. 1, 5358. https://doi.org/10.3402/nano.v1i0.5358.

Smith, M.A., Michael, R., Aravindan, R.G., Dash, S., Shah, S.I., Galileo, D.S., Martin-DeLeon, P.A., 2015. Anatase titanium dioxide nanoparticles in mice: evidence for induced structural and functional sperm defects after short-, but not long-, term exposure. Asian J. Androl. 17, 261–268. https://doi.org/10.4103/1008-682X.143247.

Souza, M.R., Mazaro-Costa, R., Rocha, T.L., 2021. Can nanomaterials induce reproductive toxicity in male mammals? A historical and critical review. Sci. Total Environ. 769, 144354 https://doi.org/10.1016/j.scitotenv.2020.144354.

Suciu, M., Ionescu, C.M., Ciorita, A., Tripon, S.C., Nica, D., Al-Salami, H., Barbu-Tudoran, L., 2020. Applications of superparamagnetic iron oxide nanoparticles in drug and therapeutic delivery, and biotechnological advancements, Beilstein. J. Nanotechnol 11, 1092–1109. https://doi.org/10.3762/BJNANO.11.94.

Sukhanova, A., Bozrova, S., Sokolov, P., Berestovoy, M., Karaulov, A., Nabiev, I., 2018. Dependence of nanoparticle toxicity on their physical and chemical properties. Nanoscale Res. Lett. 13, 44. https://doi.org/10.1186/s11671-018-2457-x.

Sundarraj, K., Manickam, V., Raghunath, A., Periyasamy, M., Viswanathan, M.P., Perumal, E., 2017. Repeated exposure to iron oxide nanoparticles causes testicular toxicity in mice. Environ. Toxicol. 32, 594–608. https://doi.org/10.1002/tox.22262.

Testa-Anta, M., Ramos-Docampo, M.A., Comesaña-Hermo, M., Rivas-Murias, B., Salgueiriño, V., 2019. Raman spectroscopy to unravel the magnetic properties of iron oxide nanocrystals for bio-related applications. Nanoscale Adv. 1, 2086–2103. https://doi.org/10.1039/c9na00064j.

Thakur, M., Gupta, H., Singh, D., Mohanty, I.R., Maheswari, U., Vanage, G., Joshi, D., 2014. Histopathological and ultra structural effects of nanoparticles on rat testis following 90 days (chronic study) of repeated oral administration. J. Nanobiotechnol. 12, 42. https://doi.org/10.1186/s12951-014-0042-8.

Tomov, S.N., Stoyanova, R.S., Atanasova, P.K., Dechev, I.Y., 2020. Changes in the level of DNA fragmentation in sperm cells detected by Acridine Orange test in men with sub/infertility treated with nutritional supplement PAPA. Folia Med. (Plovdiv) 62, 112–116. https://doi.org/10.3897/folmed.62.e48001.

Tsakmakidis, I.A., Samaras, T., Anastasiadou, S., Basioura, A., Ntemka, A., Michos, I., Simeonidis, K., Karagiannis, I., Tsousis, G., Angelakeris, M., Boscos, C.M., 2020. Iron oxide nanoparticles as an alternative to antibiotics additive on extended boar semen. Nanomaterials 10, 1–16. https://doi.org/10.3390/nano10081568.

Tvrdá, E., Kňažická, Z., Lukáčová, J., Schneidgenová, M., Massányi, P., Goc, Z., Stawarz, R., Lukáč, N., 2012. Relationships Between Iron and Copper Content, Motility Characteristics and Antioxidant Status in Bovine Seminal Plasma 2, pp. 536–547. https://office2.jmbfs.org/index.php/JMBFS/article/view/7162.

Tvrda, E., Peer, R., Sikka, S.C., Agarwal, A., 2015. Iron and copper in male reproduction: a double-edged sword. J. Assist. Reprod. Genet. 32, 3–16. https://doi.org/10.1007/s10815-014-0344-7.

Valdiglesias, V., Kiliç, G., Costa, C., Fernández-Bertólez, N., Pásaro, E., Teixeira, J.P., Laffon, B., 2015. Effects of iron oxide nanoparticles: cytotoxicity, genotoxicity, developmental toxicity, and neurotoxicity. Environ. Mol. Mutagen. 56, 125–148. https://doi.org/10.1002/em.21909.

Vangijzegem, T., Stanicki, D., Laurent, S., 2019. Magnetic iron oxide nanoparticles for drug delivery: applications and characteristics. Expert Opin. Drug Deliv. 16, 69–78. https://doi.org/10.1080/17425247.2019.1554647.

Vassal, M., Rebelo, S., de Pereira, M.L., 2021. Metal oxide nanoparticles: evidence of adverse effects on the male reproductive system. Int. J. Mol. Sci. 22 https://doi.org/10.3390/ijms22158061.

Wise, T., Lunstra, D.D., Rohrer, G.A., Ford, J.J., 2003. Relationships of testicular iron and ferritin concentrations with testicular weight and sperm production in boars. J. Anim. Sci. 81, 503–511. https://doi.org/10.2527/2003.812503x.

Wu, H.Y., Chung, M.C., Wang, C.C., Huang, C.H., Liang, H.J., Jan, T.R., 2013. Iron oxide nanoparticles suppress the production of IL-1beta via the secretory lysosomal pathway in murine microglial cells. Part. Fibre Toxicol. 10, 46. https://doi.org/10.1186/1743-8977-10-46.

Wu, W., Wu, Z., Yu, T., Jiang, C., Kim, W.S., 2015. Recent progress on magnetic iron oxide nanoparticles: synthesis, surface functional strategies and biomedical applications. Sci. Technol. Adv. Mater. 16, 023501 https://doi.org/10.1088/1468-6996/16/2/023501.

Xu, T., Ding, W., Ji, X., Ao, X., Liu, Y., Yu, W., Wang, J., 2019. Molecular mechanisms of ferroptosis and its role in cancer therapy. J. Cell. Mol. Med. 23, 4900–4912. https://doi.org/10.1111/jcmm.14511.

Yan Cheng, C., Mruk, D.D., 2012. The blood-testis barrier and its implications for male contraception. Pharmacol. Rev. 64, 16–64. https://doi.org/10.1124/pr.110.002790.

Ye, F., Barrefelt, Å., Asem, H., Abedi-Valugerdi, M., El-Serafi, I., Saghafian, M., Abu-Salah, K., Alrokayan, S., Muhammed, M., Hassan, M., 2014. Biodegradable polymeric vesicles containing magnetic nanoparticles, quantum dots and anticancer drugs for drug delivery and imaging. Biomaterials 35, 3885–3894. https://doi.org/10.1016/j.biomaterials.2014.01.041.

Yoisungnern, T., Choi, Y.J., Woong Han, J., Kang, M.H., Das, J., Gurunathan, S., Kwon, D.N., Cho, S.G., Park, C., Kyung Chang, W., Chang, B.S., Parnpai, R., Kim, J. H., 2015. Internalization of silver nanoparticles into mouse spermatozoa results in poor fertilization and compromised embryo development. Sci. Rep. 5, 1–13. https://doi.org/10.1038/srep11170.

Yokonishi, T., Sato, T., Katagiri, K., Ogawa, T., 2013. In Vitro Spermatogenesis Using an Organ Culture Technique, 927, pp. 479–488. https://doi.org/10.1007/978-1-62703-038-0_41.

Younus, Ahmed Ibrahim, Yousef, Mokhtar Ibrahim, Abdel-NabiKamel, Maher, Alrawi, Rakhad, Abdulrahman, Jubran Mohammed, 2020a. Changes in semen characteristics and sex hormones of rats treated with iron oxide nanoparticles, silver nanoparticles and their mixture. GSC Biol. Pharmaceut. Sci. 12, 229–237. https://doi.org/10.30574/gscbps.2020.12.2.0272.

Younus, Ahmed Ibrahim, Yousef, Mokhtar Ibrahim, Abdel-NabiKamel, Maher, Alrawi, Rakhad, Abdulrahman, Jubran Mohammed, 2020b. Changes in semen characteristics and sex hormones of rats treated with iron oxide nanoparticles, silver nanoparticles and their mixture. GSC Biol. Pharmaceut. Sci. 12, 229–237. https://doi.org/10.30574/gscbps.2020.12.2.0272.

Zhang, X.F., Choi, Y.J., Han, J.W., Kim, E., Park, J.H., Gurunathan, S., Kim, J.H., 2015. Differential nanoreprotoxicity of silver nanoparticles in male somatic cells and spermatogonial stem cells. Int. J. Nanomedicine 10, 1335–1357. https://doi.org/10.2147/IJN.S76062.

CAPÍTULO 3

***Artigo 3* – "**Effects of superparamagnetic iron oxide nanoparticles (SPIONs) testicular injection on Leydig cell function and sperm production in a murine model".

Publicado na revista: Reproductive Toxicology

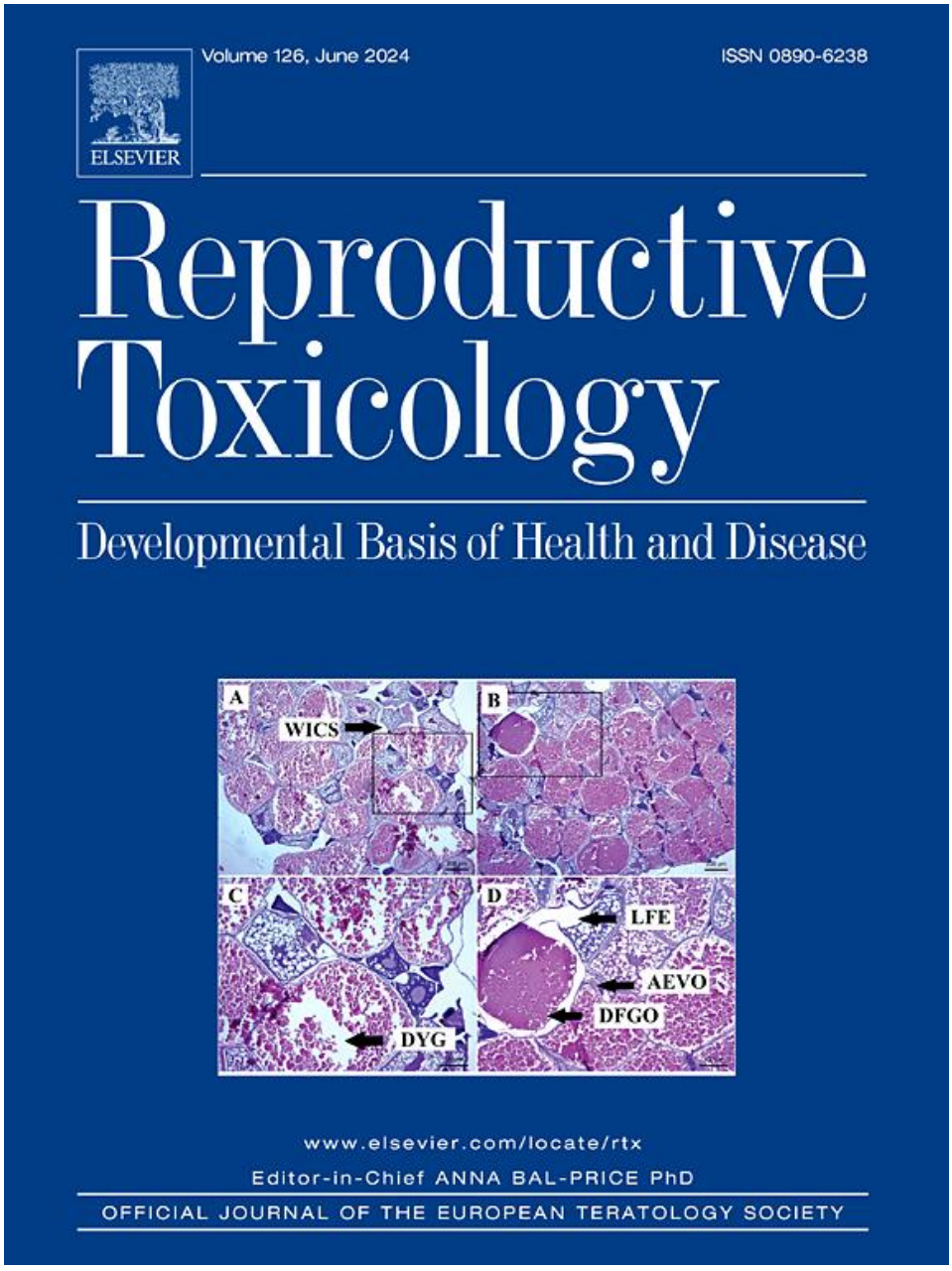

Reproductive Toxicology 126 (2024) 108584

Contents lists available at ScienceDirect

Reproductive Toxicology

journal homepage: www.elsevier.com/locate/reprotox

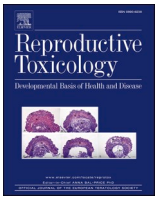

Effects of superparamagnetic iron oxide nanoparticles (SPIONS) testicular injection on Leydig cell function and sperm production in a murine model

Fausto S. Ferraz [a,1], Graziela de P.F. Dantas [a,1], John L.P. Coimbra [a], Jorge L. López [b], Samyra M. S.N. Lacerda [a], Mara L. dos Santos [a], Carolina P. Vieira [a], Nathália de L.E.M. Lara [a], Pedro I. M. Viana [a], Luiz O. Ladeira [c], Leonardo O. Guarnieri [d], Eduardo M.A. Marçal [d], Márcio F. D. Moraes [d], Estefânia M.N. Martins [e], Lídia M. Andrade [a,c], Guilherme M.J. Costa [a,*,2]

[a] Department of Morphology, ICB, Federal University of Minas Gerais, Belo Horizonte, MG, Brazil
[b] Center for Biological and Natural Sciences, Federal University of Acre, Rio Branco, AC, Brazil
[c] Department of Physics, ICEX, Federal University of Minas Gerais, Belo Horizonte, MG, Brazil
[d] Magnetic Resonance Center (CTPMag) of the Department of Electrical Engineering at the Federal University of Minas Gerais, Belo Horizonte, MG, Brazil
[e] Nuclear Technology Development Center (CDTN), National Nuclear Energy Commission (CNEN), Belo Horizonte, MG, Brazil

ARTICLE INFO

Handling Editor: Dr. Bal-Price Anna

Keywords:
Nanotechnology
Nanotoxicology
Reproductive toxicology
Superparamagnetic Iron Oxide Nanoparticles
Leydig cell
Spermatogenesis

ABSTRACT

In the domain of medical advancement, nanotechnology plays a pivotal role, especially in the synthesis of biocompatible materials for therapeutic use. Superparamagnetic Iron Oxide Nanoparticles (SPIONs), known for their magnetic properties and low toxicity, stand at the forefront of this innovation. This study explored the reproductive toxicological effects of Sodium Citrate-functionalized SPIONs (Cit_SPIONs) in adult male mice, an area of research that holds significant potential yet remains largely unknown. Our findings reveal that Cit_SPIONs induce notable morphological changes in interstitial cells and the seminiferous epithelium when introduced via intratesticular injection. This observation is critical in understanding the interactions of nanomaterials within reproductive biological systems. A striking feature of this study is the rapid localization of Cit_SPIONs in Leydig cells post-injection, a factor that appears to be closely linked with the observed decrease in steroidogenic activity and testosterone levels. This data suggests a possible application in developing nanostructured therapies targeting androgen-related processes. Over 56 days, these nanoparticles exhibited remarkable biological distribution in testis parenchyma, infiltrating various cells within the tubular and intertubular compartments. While the duration of spermatogenesis remained unchanged, there were many Tunel-positive germ cells, a notable reduction in daily sperm production, and reduced progressive sperm motility in the treated group. These insights not only shed light on the intricate mechanisms of Cit_SPIONs interaction with the male reproductive system but also highlight the potential of nanotechnology in developing advanced biomedical applications.

1. Introduction

The field of nanotechnology, a precursor of groundbreaking medical advancements, has enabled the synthesis of nanomaterials marked by exceptional biocompatibility and responsiveness. As highlighted in recent studies [1,46], this technological leap has paved the way for innovative medical applications. Nanoparticles (NPs), in particular, have transcended traditional boundaries, finding diverse and critical roles across various scientific domains, ranging from fundamental research to practical applications [1,13,46]. In reproductive medicine, the emergence of NPs has been nothing short of transformative. They are being increasingly recognized for their potential in a variety of roles, including serving as biomarkers for reproductive disorders, aiding in gene therapy, enhancing assisted reproduction techniques, treating erectile dysfunction, and as potential candidates in novel contraception approaches [13,60,7].

NPs, with a minute scale of one to a hundred nanometers, can be synthesized from various substances, each endowed with distinct

* Corresponding author.
E-mail address: gmjc@ufmg.br (G.M.J. Costa).
[1] These authors contributed equally
[2] +5531992744569

https://doi.org/10.1016/j.reprotox.2024.108584
Received 22 December 2023; Received in revised form 27 March 2024; Accepted 28 March 2024
Available online 30 March 2024

physicochemical properties [1,13]. Among these, Superparamagnetic Iron Oxide Nanoparticles (SPIONs), which consist of iron oxide cores like magnetite (Fe_3O_4), maghemite (γ-Fe_2O_3), or hematite (α-Fe_2O_3), stand out. Predominantly synthesized through co-precipitation methods (F. [77]), these SPIONs are lauded for their reduced toxicity, high biocompatibility, and unique magnetic properties, making them highly suitable for biological applications [64,71,74]. SPIONs are used as contrast agents for magnetic resonance imaging (MRI) [21,52,56] in targeted drug delivery [61,63,70] as vehicles in gene therapies ([61]; Sachdeva et al., 2022) and in tumor therapies through magnetic hyperthermia [40,53,73].

Recently, some researchers have proposed using SPIONs as a non-invasive, targeting, and controllable approach to male contraception [18,36]. In the presence of a magnetic field, SPIONs can convert magnetic energy into heat, causing structural and functional alterations in the testes [19,2,3,36,8]. Despite the promising applications of SPIONs, their interaction with biological systems has raised concerns about potential nanotoxicological risks [12,37,47,9]. Studies have pointed out issues such as genotoxicity [33,54,62] and the induction of oxidative stress [47,50]. associated with SPION exposure. In the context of reproductive health, adverse effects like abnormalities in sperm morphology, reduced motility, and decreased sperm count have been observed following intraperitoneal exposure in mice [51]. [65] demonstrated that intraperitoneal administration of SPIONs causes an increase in ROS and an imbalance of antioxidant enzymes in the testes, which leads to oxidative stress and apoptosis. Ghosh et al. [28] also demonstrated that orally administered SPIONs cause different abnormalities in the sperm of mice. However, there is a notable gap related to *in vivo* research, explicitly investigating the morpho-functional impacts of SPION exposure on male reproductive parameters. Moreover, studies evaluating the long-term effects of such exposure on the gonads are markedly scarce.

In response to this research gap, the current study explores the long-term toxicological consequences of bilateral intratesticular injections of superparamagnetic iron oxide nanoparticles functionalized with sodium citrate (Cit_SPIONs) in male gonads. This investigation involves a comprehensive assessment of post-nanoparticle testicular injection, focusing on Cit_SPIONs characterization and biodistribution, analysis of the spermatogenic cycle, morphological examination of testes, measurement of serum testosterone levels and steroidogenic enzymes, and evaluation of daily sperm production and sperm parameters in adult male mice. This study brings substantial knowledge about the interaction of SPIONs with the male reproductive system, which in the future could contribute to the development of new anti-androgen therapies.

2. Materials and methods

2.1. Synthesis, coating and characterization

Ferraz et al. [22] have previously reported the synthesis and characterization procedures of Cit_SPIONs utilized in this study. The SPIONs were synthesized using the chemical co-precipitation method from an acidified aqueous solution of HCl (2 M) (Cas. 7647–01, Merck, Brazil), containing iron chloride - FeCl3.6H2O (Cas. 10025–77–1, Merck, Brazil) and iron sulfate - FeSO4.7H2O (Cas. 7782–63–0, Merck, Brazil) in a molar ratio of Fe2+ to Fe3+ = 1:2. Under vacuum and stirring, an aqueous solution of NaOH (1 M) (Cas. 1310–73–2, Merck, Brazil) was added to the reaction in an argon atmosphere at 15°C. The reaction formed a black precipitate, and the suspension was centrifuged five times at 2,000 rpm for 3 min to remove the supernatant. The magnetite particles were then dispersed in water using ultrasound and subsequently coated with a 0.2 M trisodium citrate solution (Cas. 6132–04–3, Merck, Brazil) at 90 °C for 30 min to produce the Cit_SPIONs.

In this study, we assessed the morphological characteristics of Cit_SPIONs using Transmission Electron Microscopy. The average diameter was determined using Image J software (http://imagej.nih.gov/ij). Additionally, the hydrodynamic diameter (DLS), polydispersity (PDI), and zeta potential were measured using the Zetasizer Lab System (Malvern Panalytical, UK).

2.2. Animals

Sixteen Balb/c mice, with a mean body weight of 42.44 g ± 4.6 g, procured from the Central Animal Facility of the Institute of Biological Sciences (UFMG), were included in this study. A subset of four individuals underwent evaluation to explore the dynamics of testicular nanoparticle biodistribution employing magnetic resonance analysis. The remaining twelve animals were divided into control and treated groups for the experiment. Each animal was housed in an individual cage situated in a controlled environment, which included a 12-hour light/dark cycle. They had unrestricted access to food and water (ad libitum).

All procedures were conducted in accordance with the ARRIVE guidelines and were carried out in accordance with the U.K. Animals (Scientific Procedures) Act, 1986 and associated guidelines, the European Communities Council Directive of 24 November 1986 (86/609/EEC). The sample size, criteria for group formation, and experimental protocols adhered to the stipulations of Law No. 11,794 and the regulations set forth by the National Council for Animal Experimentation Control (CONCEA). The study was granted ethical approval by the Ethics Commission on Animal Use (CEUA; document 183/2018).

2.3. Intratesticular injections of Cit_SPIONs

The animals (n=12) were divided into control and treated groups. The control group received an intratesticular application of 30 μL of PBS/Testicle (10 mM phosphate buffer, pH 7.4, 140 mM NaCl) and was evaluated after 56 days. The treated group received a single intratesticular injection of 30 μL of Cit_SPIONs/Testicle [8×10^{-2} mg/mL]. We administered nanoparticles (NPs) directly into the testicles using intratesticular injection in an attempt to minimize systemic side effects, and the nanoparticle concentration was chosen based on prior *in vitro* studies conducted by our research group, demonstrating the biocompatibility in fibroblast cells [22]. After 56 days, the animals were euthanized by anesthetic overdose using ketamine (240 mg/kg) and xylazine (45 mg/kg), and blood was collected via cardiac puncture.

Inorganic nanoparticles tend to bioaccumulate in testis parenchyma [13]. Therefore, we monitored testis and gamete alterations after 56 days of the nanoparticle exposition. This time frame is longer than balb/c mice's spermatogenesis duration (~40 days) and subsequent 6-day sperm transit in the epididymis [14,25]. This time window allowed that sperm collected in the epididymal cauda were germ cells exposed to nanoparticles inside the testis. Furthermore, this time allowed the transit of sperm previously exposed as germ cells to reach the cauda epididymis.

We closely observed the animals throughout this period to detect any clinical signs indicating adverse systemic effects. The testes, epididymis, and seminal vesicles were excised, dissected, weighed, and fixed for further analysis. Histological and Magnetic Resonance Imaging (MRI) techniques were employed to assess the NPs' distribution in testes.

2.4. Magnetic resonance imaging

Magnetic resonance imaging (MRI) was employed to assess the dispersion of magnetic nanoparticles in the testicles of the animals. Four animals were anesthetized using Inactin (thiobutabarbital sodium) (100 mg/Kg) intraperitoneally, and subsequently, saline solution (PBS - 10 mM phosphate buffer, pH 7.4, 140 mM NaCl) was administered to the left testicle (control), while Cit_SPIONs [8×10^{-2} mg/mL] were applied to the right testis. The scrotum of the animals was exposed to the MRI equipment, and images were obtained at three time points: 30 min, 60 min, and 24 h after the testicular injections.

A 4.7 T NMR magnet (Oxford Systems) under the control of a UNITY Inova-200 imaging console (Varian) was utilized for image acquisition. The imaging protocol involved obtaining T2-weighted cross-sectional images (TR = 3000 ms, TE = 50 ms) with 20 contiguous slices of 1 mm thickness (512 × 256 voxels). Subsequently, the images were analyzed using the Bamboo Tablet Driver V5.2.5 WIN (WACOM Technology Corporation, USA) and MeVisLab (MeVis Medical Solutions AG, Fraunhofer) software to assess the dispersion of magnetic nanoparticles in the testes. These imaging and analysis procedures were conducted at the Magnetic Resonance Center (CTPMag) of the Department of Electrical Engineering at the Federal University of Minas Gerais.

2.5. Transmission electron microscopy

Testicular fragments were fixed for 1 h in a modified Karnovsky fixative (2% paraformaldehyde (Cas. 30525–89–4, Merck, Brazil) + 2.5% glutaraldehyde (Cas. 111–30–8, Merck, Brazil) in 0.1 M sodium phosphate buffer, pH 7.4). Following fixation, they underwent three 5-minute washes in 0.1 M sodium phosphate buffer / 0.15 M NaCl (Cas. 7647–14–5, Merck, Brazil) at 4 °C, and then were fixed in 2% osmium tetroxide (Sigma-Aldrich, USA) for 30 min at room temperature. Subsequently, samples were block-stained with 2% uranyl acetate (Cas. 541–09–3, EMS, USA) for 20 min in the dark, dehydrated in a graded series of ethanol (Cas. 64–17–5, Merck, Brazil) and acetone (Cas. 67–64–1, Merck, Brazil), infiltrated with acetone/Epon EMBed 812 Resin 1:3 (Cas. 14120, EMS, USA) for 30 min, and finally embedded in pure Epon.

Ultrathin sections were obtained using a diamond knife on a Leica EM UC6 ultramicrotome (Leica Microsystems, Brazil), mounted on 200-mesh copper grids (Ted Pella), stained with lead citrate (Cas. 6132–04–3, Merck, Brazil), and analyzed using transmission electron microscopy (Tecnai G2–12 Thermo Fisher Scientific / FEI, USA) at the Microscopy Center of the Federal University of Minas Gerais. Electron micrographs were randomly acquired at different magnifications to assess the ultrastructural characteristics of the testes.

2.6. Histology

Testes were fixed for histological analysis in Bouin (MFCD00146169, Merck, Brazil) and Glutaraldehyde (Cas. 111–30–8, Merck, Brazil). Subsequently, testis fragments were dehydrated in increasing series of alcohols (70º, 80º, 90º, 95º, 100º ABS I, and 100º ABS II) and embedded in plastic resin based on glycol methacrylate (Leica Historesin Embedding Kit, Leica Instruments, Brazil). Histological Section (5 μm) were obtained using a rotating microtome with a glass razor, stained with 1% toluidine blue-sodium borate solution and Prussian blue. The slides were mounted with glass coverslips and Entellan (Cas. 107960, Merck, Brazil) and analyzed under a light microscope (Olympus BX-60, USA).

2.7. Testicular histological analysis

Morphometric analyses were conducted following the protocol described by Costa et al. [11]. In brief, the volumetric density of testicular tissue components, the number and indices of testicular cells, the frequency analysis of seminiferous epithelium cycle stages, and the duration of spermatogenesis were assessed to determine daily sperm production. Images were acquired using a light microscope (Olympus BX-60, USA), and subsequent analyses were performed using ImageJ software (http://imagej.nih.gov/ij).

2.8. Prussian blue staining

The Prussian blue histological staining method was employed to detect the biodistribution of intratesticular injected iron oxide nanoparticles. In brief, histological sections were immersed in a Prussian blue solution (comprising equal volumes of 4% HCl (Cas. 7647–01–0, Merck, Brazil), 10% potassium ferrocyanide (Cas. 14459–95–1, Merck, Brazil) aqueous solution, and neutral red (Cas. 553–24–2, Merck, Brazil)) for 15 min. The presence of ferric ions (Fe^{3+}) in the testes, spleen, liver, kidney and lung was visualized as a blue pigment after staining. Additionally, the samples were counterstained with neutral red dye for 5 min to enhance visualization and differentiation between cellular structures and iron deposits.

2.9. 3βHSD analysis

The evaluation of the 3βHSD was performed by immunoperoxidase according to the protocol of [20]. Briefly, the slides were deparaffinized and dehydrated, and endogenous peroxidase was blocked using a hydrogen peroxide solution (Cas. 7722–84–1, Merck, Brazil). The antigen was retrieved using buffered sodium citrate (Cas. 6132–04–3, Merck, Brazil), pH 6.0 at 96°C for 10 min. The unspecific proteins were blocked using Ultra-V-Block (Cat. TA-060-UB, Thermo Scientific, USA). As a primary antibody, we incubated the slides overnight with the goat anti-rabbit 3βHSD (1:100, sc30820, Santa Cruz Biotechnology, USA). As a secondary antibody, we used the biotinylated anti-goat (1:200, ab6740, Abcam Inc, USA). Afterward, we incubated the slides with streptavidin peroxidase and used diaminobenzidine (DAB) substrate (Cas. 91–95–2, Merck, Brazil) as a chromogen.

The expression of the steroidogenic enzyme 3βHSD was evaluated through da Pixel Intensity Analysis. Ten random images (approximately 50 Leydig cells) were captured using an Olympus BX60 microscope with a coupled camera. After converting images to grayscale in Photoshop CS6 v13.0, pixel intensity measurements were obtained from the labeled cells. The ratio between the pixel intensity from the labeled cells and the background was used [20].

2.10. Testosterone levels

Blood samples were collected in a minimum volume of 0.5 mL per animal and centrifuged at 2000 rpm for 10 min to obtain serum, which was then stored at −20 °C. Testosterone levels were determined using the radioimmunoassay (RIA) method, following the protocol by Gonçalves et al. [30]. A commercial kit (Tecsa®, Belo Horizonte, MG, Brazil) was employed, and the analysis was conducted using an electrochemiluminescence assay on the automated Cobas 8000 platform (Roche Diagnostics Inc., Indianapolis, IN, USA). The intra- and inter-assay coefficients of variation (CV) for testosterone were 1.1% and 1.5%, respectively.

2.11. BrdU labeling

Two animals per group were intraperitoneally administered with 150 mg/kg of the 5-Bromo-2-deoxyuridine (Cas. 102212–99–7, Merck, Brazil) as a marker to assess the duration of spermatogenesis. BrdU labels cells actively synthesizing DNA at the time of injection [41]. In this study, BrdU application and evaluation were conducted at two distinct time points: 21 days and 1 h prior to animal euthanasia.

Following the histological processing of the testes, immunohistochemistry was performed using the anti-BrdU antibody (dilution 1:100; Pharmingen, # 347580) in combination with a biotinylated secondary antibody (dilution 1:200; Sigma, # B7264) [41].

2.12. Sperm analysis

The mice epididymides were carefully separated and placed in a Petri dish containing 500 μL of DMEM/F12 medium. Subsequently, the epididymis cauda was punctured with 24 G needles to release the sperm into the culture medium. After this procedure, the spermatozoa were transferred to Eppendorf tubes for accurate volume measurement and homogenization [23,30].

The sperm motility, classified as progressive motility, non-

progressive motility, and no motility, was evaluated according to previous studies [23,30]. A 5 μL aliquot of the sperm sample was stained with 5 μL of eosin, spread on glass slides, and mounted with 22 mm x 22 mm coverslips. We analyzed 200 spermatozoa, distinguishing stained (dead) and unstained (live) sperm, using light microscopy at 100x and 400x magnification.

Following the initial evaluation, an aliquot of semen (10μL) was diluted in 10% buffered formalin (2 mL), and sperm concentration was determined using a Neubauer chamber maintained at 35.5ºC. Percentages of normal and altered spermatozoa were assessed for each smear, and acrosome integrity was quantified. Morphological defects were determined and classified according to sperm regions, including the head, mid-piece (including cytoplasmic droplets), and tail (CBRA, 1998).

2.13. DNA fragmentation assessment

The Tunel assay (Terminal dUTP Nick-End Labeling) was used to detect cell's DNA fragmentation after exposure to Cit_SPIONs. The Tunel assay was performed using the "In situ Cell Death Detection Kit, Fluorescein" kit (Roche) in testicular cells after 56 days of exposure to Cit_SPIONs. Firstly, the histological sections were deparaffinized and rehydrated; next, they were digested in Proteinase K solution (20μg / mL in 10 mM Tris / HCl, pH 7.5) for 20 min at 37 °C. Then, they were washed twice in PBS 1x for 5 min and after incubated with a TUNEL reaction mixture 1:5 (enzyme solution + labeling solution) over 60 min at 37 °C in a humid chamber. Before incubation with the TUNEL reaction mixture, some sections were incubated with recombinant DNase I (40 U / mL in 50μM Tris / HCl and 1 mg/mL BSA, pH 7.5) and labeling solution for 10 min at 25 ° C, for positive and negative control, respectively.

After the incubation period of the mix, the sections were rewashed in PBS 1X thrice for 5 min. The slides were mounted with Fluoromount™ aqueous mounting medium (F4680, Merck, Brazil) and subsequently analyzed under a fluorescence microscope (Olympus BX-60, USA) [38]. Tunel-positive cells were counted using the ImageJ software (http://imagej.nih.gov/ij). Five images random/animal at 400X magnification were analyzed, and the total number of marked and unmarked cells in the tubular compartment was estimated in the seminiferous epithelium ([38]; C. [76]).

2.14. Statistical analysis

Before analysis, all quantitative data were assessed for normality and homoscedasticity of variances using the Kolmogorov-Smirnov (Dallal-Wilkinson-Lilliefor) and Bartlett tests, respectively. Comparisons between the control and treated groups were conducted using Student's t-test, considering the appropriate parametric and non-parametric distribution. The data are presented as mean ± SEM. All statistical analyses were performed using the GraphPad Prism 8 software (GraphPad Software, Inc), with a significance level set at $*p < 0.05$.

3. Results

3.1. Characterization of Cit_SPIONs

Cit_SPIONs presenting mean diameter of 8.9 ± 2.4 nm; Dynamic Light Scattering (DLS) revealed that the Cit_SPIONs possessed 167 nm in solution with a polydispersity index (PDI) of 0.279. Furthermore, the displayed zeta potential, at physiological pH, was −30.5 mV (Table 1). The other physicochemical characterizations of our nanoparticles can be accessed in the article of Ferraz et al. [22].

Table 1
Morphological characteristics of the Cit_SPIONs.

Morphological characteristics	
Average diameter	8.9 nm
Hydrodynamic diameter (DLS)	167 nm
Polydispersity (PDI)	0.279
Zeta potential (ζP)	-30.5 mV

3.2. Accumulation of Cit_SPIONs in Leydig cells one day after intratesticular administration

Comparing the control animals (Figure 1A1) that received an intratesticular injection of PBS (10 mM phosphate buffer, pH 7.4, 140 mM NaCl) with those administered with Cit_SPIONs (Figure 1A2), the testicular weight remained unchanged (control testis = 0.101 ± 0.001 g vs treated testis = 0.114 ± 0.004) (Supplemental Table 1).

Semi-thin sections of control animals revealed evident lipid droplets in Leydig cells (Fig. 1B, white arrowhead). In contrast, treated animals displayed darkened structures in the Leydig cell cytoplasm, suggesting the association of Cit_SPIONs with lipid vesicles (Fig. 1C – red arrowheads) 24 h post-injection. Prussian blue staining demonstrated preferential localization of Cit_SPIONs within Leydig cells (Fig. 1E - red arrowheads).

Magnetic resonance imaging (Fig. 1F) showed non-homogeneous dispersion of Cit_SPIONs 30 and 60 min after injection, concentrated in areas adjacent to the injection site. At 24 h post-administration, a homogeneous distribution of magnetic nanoparticles was observed throughout the testicular parenchyma, with no indication of their presence in the contralateral testis injected with PBS (Fig. 1F').

3.3. Cit_SPIONs exhibit high biodistribution in testis parenchyma after 56 days of intratesticular application

Through transmission electron microscopy analyses, it was identified that Cit_SPIONs were not restricted to Leydig cells after 56 days of intratesticular injections. This pattern was different from the data observed 24 h after application.

Cit_SPIONs were found to be distributed in various cellular compartments within the testis parenchyma, revealing their wide biodistribution. Notably, in the basal compartment of the seminiferous tubules, prominent accumulation of Cit_SPIONs was observed in Sertoli cells' cytoplasm (Fig. 2A-A′, black arrowhead) and peritubular myoid cells (Fig. 2B-B′, black arrowhead), forming small endocytic vesicles. Furthermore, Cit_SPIONs were detected in spermatogonia, within endocytic vacuoles (Fig. 2C-C′, black arrowhead). Although not quantified, MET analyses also showed ultrastructural alterations in germ cell mitochondria and depicted large endocytic vesicles in Sertoli cells in the treated group (Supplemental Fig. 1A-D).

In the intertubular compartment, macrophages were identified as key players in Cit_SPION uptake, displaying large phagocytic vesicles containing these nanoparticles (Fig. 2D-D′, black arrowhead). Leydig cells exhibited significant Cit_SPION accumulation in multiple endocytic vesicles within the cytoplasm (Fig. 2E-E′, black arrowhead), and mitochondrial localization of Cit_SPIONs was also observed in Leydig cells (Fig. 2F-F′, black arrowhead). MET analyses also showed enlarged lipid droplets containing Cit_SPIONs and morphologically altered mitochondria in the Leydig cells (Supplemental Fig. 1E-H).

Interestingly, Prussian blue staining did not reveal any Cit_SPION presence in the renal, lung, or liver parenchyma, indicating specific distribution within the testis tissue. To validate the staining technique, abundant Fe deposits were identified in the spleen parenchyma, serving as a positive control (Fig. 3A-D). In the treated group, organ morphology remained unaltered. Spleen analysis indicated regular white and red pulp morphology. Liver examination revealed standard hepatic lobe architecture. Kidney sections showed typical cortical and medullary characteristics. Lung structures, including bronchi, bronchioles, and alveoli, were normal (Fig. 3A-D). It is also important to mention that the treated animals exhibited no adverse clinical signs, including diarrhea, dehydration, weight loss, abdominal distension, or sporadic mortality.

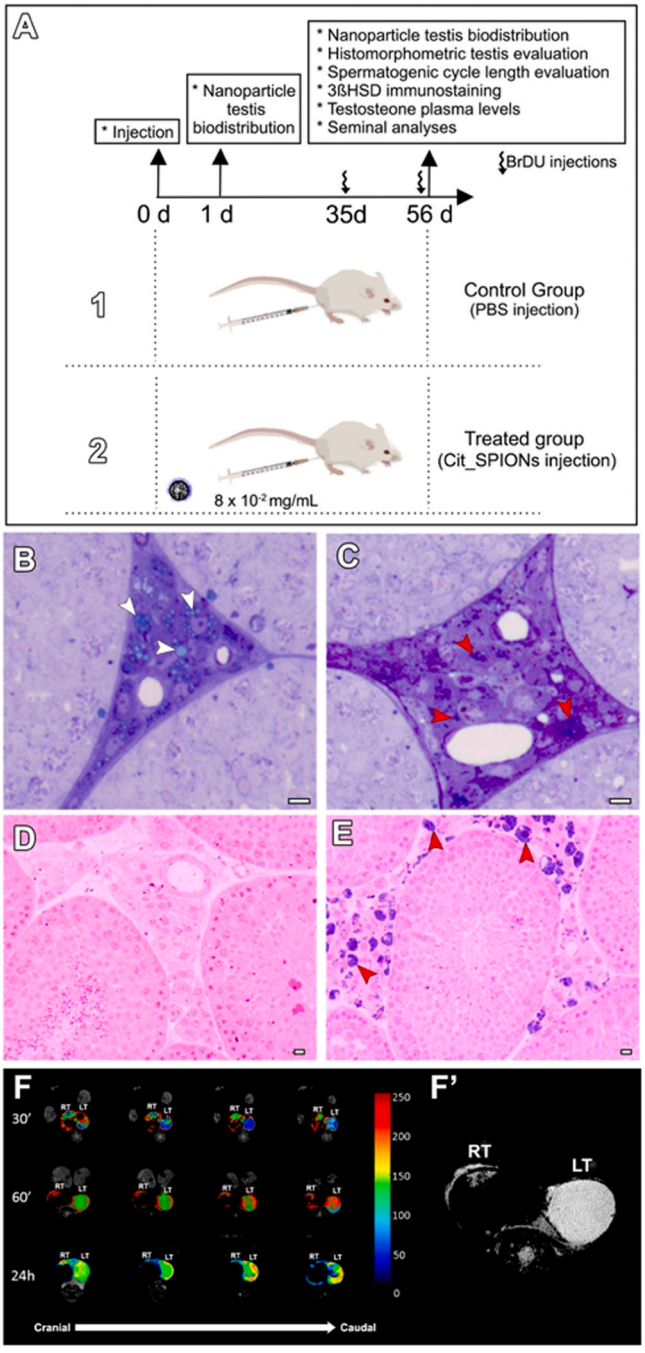

Fig. 1. Intratesticular Application of Cit_SPIONs in vivo. (A) Schematic representation of the *in vivo* experimental design. Histological analysis of intratesticular injections of PBS (B, D) and Cit_SPIONs (C, E) after one day. (B) Control animal testes showing clear lipid droplets (white arrowhead). (C) Treated animal testes displaying nanoparticle's clusters (red arrowheads) in Leydig cell cytoplasm. (D-E) Testicular histology of control (D) and treated (E) animals stained with Prussian blue. Leydig cells of treated animals exhibited intense staining, indicating intracellular iron presence (red arrowheads). (F) Magnetic resonance images of testes (in sequential 1 mm slices) taken after 30 min, 60 min, and 24 h following nanoparticles administration in the right testis (RT) and PBS in the left testis (LT). (F′) High magnification image of seminiferous tubule distribution (white area) in LT parenchyma, while the RT parenchyma is filled with nanoparticles (black area). Scale bar B, C = 20 μm; D, E = 10 μm.

3.4. Cit_SPIONs promoted morphological and functional changes in Leydig cells

Several Leydig cells containing Cit_SPIONs were identified through Prussian blue staining (Fig. 4A-B) and toluidine blue staining (Fig. 4C-D). Morphometric analyses revealed a significant increase ($P < 0.05$) in the intertubular compartment of the animals treated with Cit_SPIONs (Fig. 4E). Within this compartment, the volumetric proportion of Leydig cells ($P < 0.05$) and their nuclear, cytoplasmic, and individual ($P < 0.01$) volume were augmented (Fig. 4F-I).

Despite the larger volume of these cells, we observed a similar number of Leydig cells per gram of testis between the control and treated groups (Fig. 4J). Evaluating steroidogenesis, weaker staining for the 3βHSD enzyme in the Leydig cells was observed in the treated animals compared to the control group. Significant reductions ($P < 0.05$) in plasma testosterone levels (Fig. 4N) and seminal vesicle weight (Fig. 4O) were also noted in the treated group.

3.5. Cit_SPIONs did not alter spermatogenesis pace

Immunostaining for BrdU (Fig. 5A-D) allowed the identification of the most advanced stained germ cells at the investigated time points. One hour after BrdU application, primary spermatocytes in preleptotene (red arrows) were identified in stages VII-VIII of the seminiferous epithelium cycle in both the control (Fig. 5A-A′) and treated (Fig. 5B-B′) groups. Twenty-one days after BrdU application, elongated spermatids (green arrows) in the XII stage of the seminiferous epithelium cycle were identified in both the control (Fig. 5C-C′) and treated (Fig. 5D-D') groups.

The frequency of the seminiferous epithelium cycle stages did not differ between the control and treated groups (Fig. 5E). After associating these data, it was possible to conclude that the duration of the spermatogenic cycle remained unchanged (~8.7 days; Fig. 5F).

3.6. Cit_SPIONs reduced the tubular compartment volume and daily sperm production

Further histological investigation of the tubular compartment revealed focal tubular alterations in the testicular parenchyma caused by Cit_SPIONs (Fig. 6A-B). Approximately 20% of the seminiferous tubules showed a reduction ($P < 0.05$) in the number of germ cells in the epithelium (Fig. 6C). The presence of Cit_SPIONs resulted in a significant reduction in the tubular compartment volume (Fig. 6D; $P < 0.05$), as well as in the tubular diameter (Fig. 6E; $P < 0.05$) and the height of the seminiferous epithelium (Fig. 6F, $P < 0.01$). Interestingly, the diameter of the tubular lumen (Fig. 6G) and the length of the seminiferous tubules per gram (Fig. 6H) remained unchanged in the presence of Cit_SPIONs.

In treated animals, the reduction in germ cells led to lower ($P < 0.05$) meiotic indices (Fig. 6I) and a decrease ($P < 0.05$) in the Sertoli cell index (Fig. 6J). However, the number of Sertoli cells per gram of testis remained unchanged compared to the control group (Fig. 6K). The decreased spermatid number in treated animals also resulted in a lower ($P < 0.01$) daily sperm production per gram of testis (Fig. 6L). Consistent with these findings, a lower ($P < 0.05$) sperm concentration (Fig. 6M) was observed in the epididymis of treated animals. However, no significant changes were observed in sperm viability (Fig. 6N) and sperm morphology (Fig. 7 A-B), including the head, midpiece, and tail (Table 2).

3.7. Cit_SPIONs alter sperm motility and induce germ cell DNA fragmentation

Sperm from the treated group presented lower progressive motility ($P<0.01$) and higher non-progressive motility ($P<0.01$) compared to those from the control group (Fig. 7C-D). No differences were observed regarding sperm without motility (Fig. 7E).

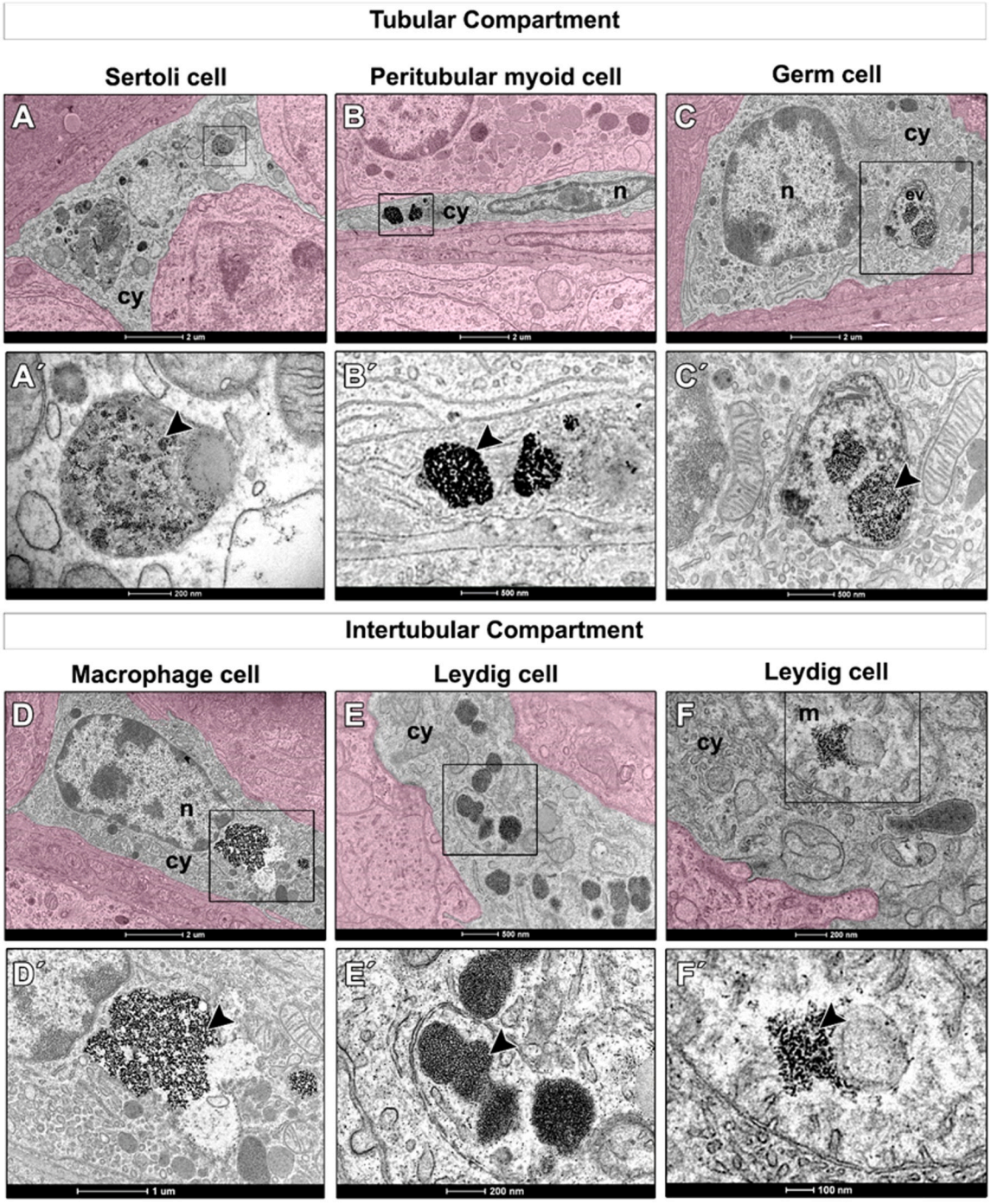

Fig. 2. Testicular distribution of Cit_SPIONs after 56 days of testicular application. Through transmission electron microscopy, Cit_SPIONs were identified in the tubular compartment in Sertoli cells (A-A'), peritubular myoid cells (B-B'), and germ cells (C-C'). Regarding the intertubular compartment, Cit_SPIONs were identified in macrophages (D-D') and Leydig cells (E-F), both in the cytoplasm (E-E') and in the mitochondria (F-F'). cy = cytoplasm, m = mitochondria, ev = endocytic vacuole, black boxes = areas selected to high magnification analysis, black arrowheads = identification of Cit_SPIONs.

The presence of Cit_SPIONs in the testis caused a significative increase ($P < 0.05$) in the number of Tunel-positive cells in the tubular compartment (Fig. 7F). The positive control showed intense staining of cells in the tubular and intertubular compartments (Fig. 7G). In the negative control (Fig. 7H), no labeling was observed. Compared to the control group (Fig. 7I), Tunel-positive cells were more frequent in the treated group, mainly in elongated spermatids (Fig. 7J).

4. Discussion

In our study, we delved into the effects of Cit_SPIONs on testicular tissue in a living organism, shedding new light on the interaction of nanoparticles with male reproductive systems. A fundamental discovery from our research is the detailed biodistribution of these nanoparticles across different testicular regions, with a notable concentration in the interstitial compartment. This observation is particularly significant, as it correlates with substantial morphological and functional changes in Leydig cells. The most striking of these changes is the marked decrease

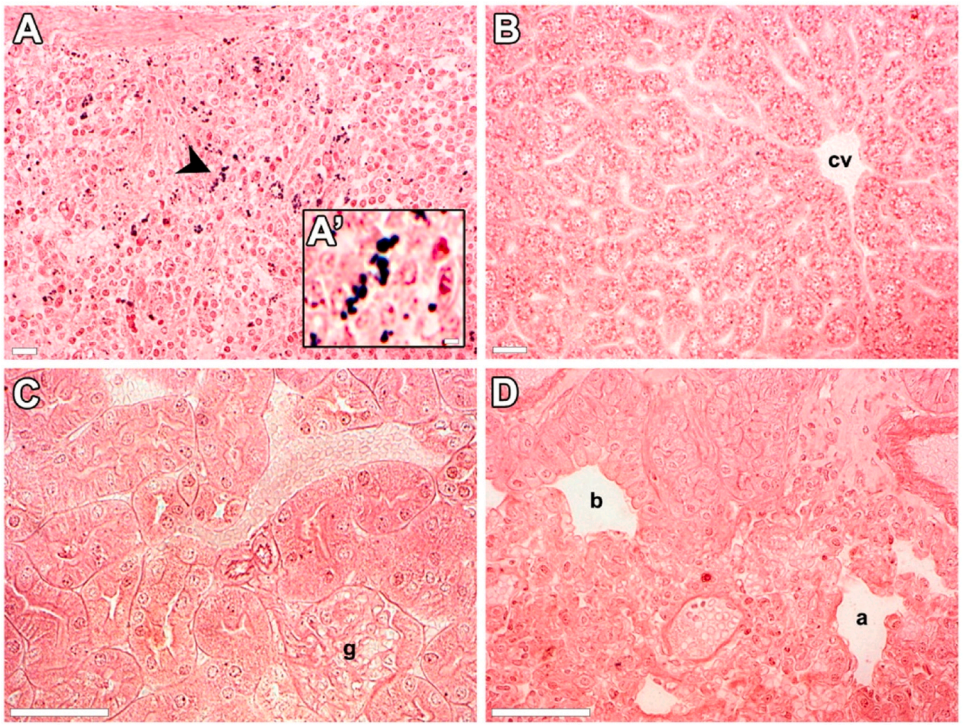

Fig. 3. Biodistribution of Cit_SPIONs after 56 days of intratesticular application. Prussian blue staining was used to detect the presence of iron (Fe) in various organs. (A) Fe was identified exclusively in the splenic parenchyma (black arrowhead). (A') Fe at higher magnification within the spleen. In contrast, no Fe was detected in the hepatic (B), renal (C), or pulmonary (D) parenchyma. cv = centrilobular vein; g = glomerulus; b = bronchus; a = alveoli; scale bar A' = 10 μm; A = 30 μm; B = 40 μm and C, D = 100 μm.

in steroidogenic activity and a reduction in serum testosterone levels. These findings are pivotal in understanding the mechanistic impact of nanoparticles on hormone regulation and reproductive function.

Furthermore, our study reveals a notable decrease in germ cell numbers within the tubular compartment. This reduction leads to diminished spermatogenic indices and daily sperm production in treated subjects. Furthermore, the treatment promoted the DNA fragmentation of germ cells and reduced the sperm progressive motility (as illustrated in Fig. 8). However, it is intriguing to note that, despite these considerable alterations in germ cell production, there were no observable changes in the duration of the spermatogenic cycle nor sperm viability or morphology. Our findings suggest a complex and nuanced response of the testicular environment to nanoparticle exposure, highlighting a selective vulnerability within the spermatogenic process. These insights contribute significantly to the field of reproductive toxicology and raise essential considerations for the future development and application of nanoparticle-based therapies in reproductive health.

In our innovative study, we meticulously charted the dispersion of Cit_SPIONs in testicular tissue, observing significant spread as early as one-hour post-injection. Magnetic resonance analysis revealed their presence from the caput to the cauda regions. The uniform particle size, negative zeta potential, and moderate stability of Cit_SPIONs, as discussed by [16]., likely facilitated this biodistribution, emphasizing their potential in biomedical applications. As suggested by [5,15], the incorporation of sodium citrate seems to have played a pivotal role in enhancing the colloidal stability and effective biodistribution of these SPIONs.

After 56 days of intratesticular injection, Cit_SPIONs were found to be specifically localized and widely spread within the testicular parenchyma. Notably, they were absent in other organs, including the kidney, lung, and liver. This selective distribution highlights the unique behavior of Cit_SPIONs in the testicular microenvironment. While various studies have reported the accumulation of different types of nanoparticles (NPs) in various organs [24,32,34,6], the targeted and restricted presence of Cit_SPIONs in the testicular tissue showcases their potential for specific and controlled biodistribution in the context of reproductive toxicology and biomedical applications.

Our findings particularly spotlight the affinity of Leydig cells for encapsulating Cit_SPIONs. These accumulated Cit_SPIONs were found to induce an increase in both nuclear and cytoplasmic volumes of Leydig cells. We speculate that the high presence of Mitochondrial Ferritin (MtF) in mouse Leydig cells [59] may contribute to these observed patterns. MtF, known for its role in iron storage and metabolism, serves to safeguard mitochondria and cells from oxidative stress [43,44,58,68,80].

In our investigation, we observed the accumulation of Cit_SPIONs in lipid droplets within Leydig cells one day after intratesticular injection. Sundarraj et al. [65] previously demonstrated that iron oxide nanoparticles (Fe_2O_3-NPs) can induce testicular toxicity through interactions with functional groups of lipids, proteins, and nucleic acids. This accumulation may have been a crucial factor contributing to the observed morpho-functional changes in Leydig cells. The reduction in immunolabeling of 3BHSD, a key enzyme involved in testosterone synthesis [78], further supports a potential connection between Cit_SPION accumulation and the decrease in serum testosterone levels.

Ultrastructural analyses showed significant changes in the mitochondrial morphology of Leydig cells. Mitochondria play an essential role in regulating the biosynthesis of steroid hormones through cholesterol metabolism [27,48]. The transfer of cholesterol from intracellular reserves to the inner mitochondrial membrane is the first and most limiting step in steroidogenesis [27,48]. Functional mitochondria are necessary to have efficient steroidogenesis in Leydig cells. Therefore, our findings agree that nanoparticle interactions within Leydig cells can significantly affect testicular function and hormone production. In this context, our results suggest that Cit_SPIONs present great possibilities for the development of anti-androgen therapies.

Testosterone is a crucial hormone that plays a vital role in maintaining the integrity of the Sertoli cell barrier and supporting the

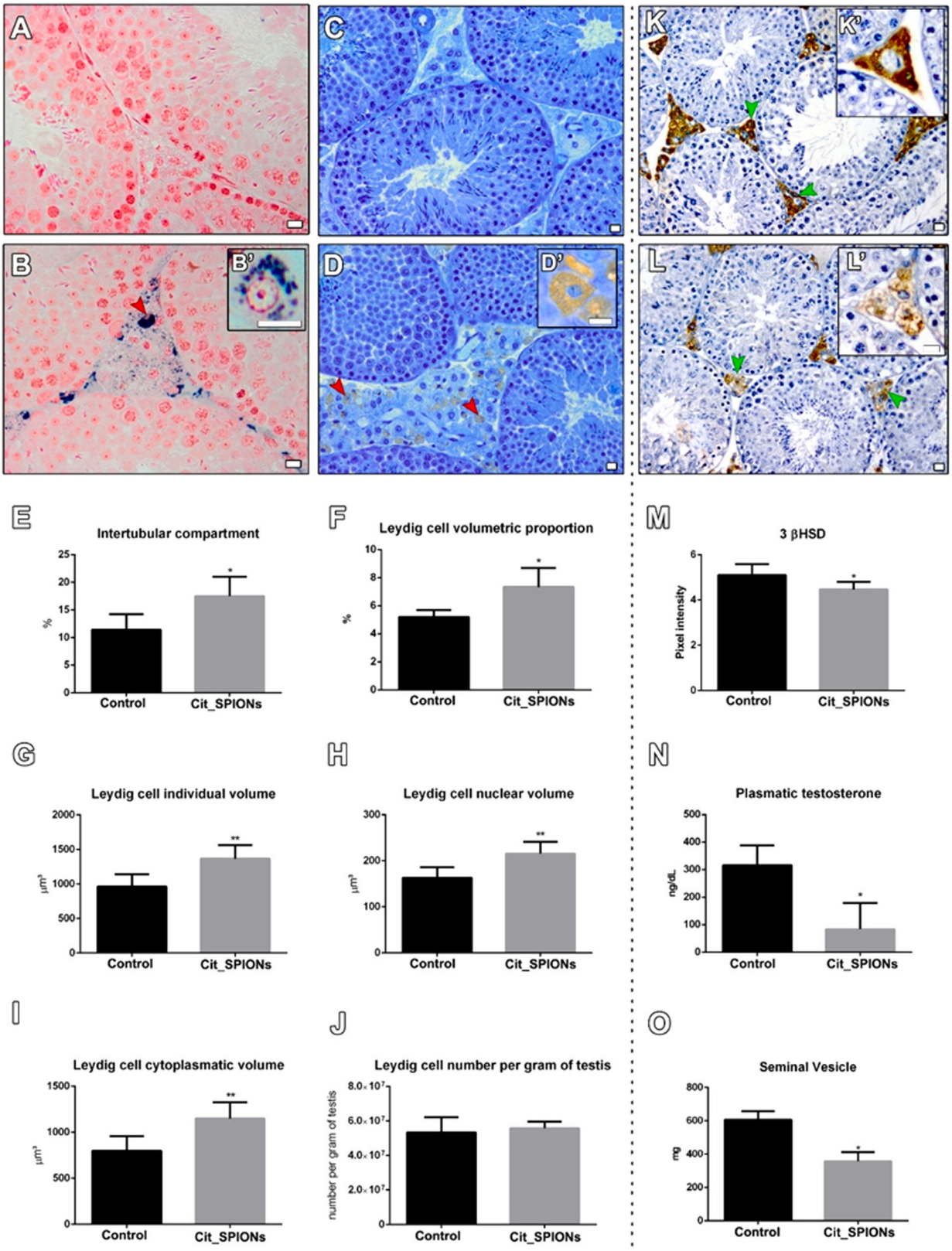

Fig. 4. Morphological and functional alterations in Leydig cells following intratesticular application of Cit_SPIONs. (A-D) Comparison of testis histology between control animals (A, C) and treated mice (B, D). Leydig cells containing Cit_SPIONs were identified using Prussian blue (B) and toluidine blue (D) staining. (E-I) Analyses of the intertubular compartment: (E) volumetric density, (F) volumetric proportion of Leydig cells, (G) individual volume of Leydig cells, and (H) nuclear and (I) cytoplasmic volume of Leydig cells. (J) The number of Leydig cells per gram of testis. (K-O) Assessment of Leydig cell steroidogenic activity. (K-M) Comparison of 3BHSD labeling intensity between control (K, M) and treated (L, M) animals. (N) Plasma testosterone levels in control and treated animals. (O) Seminal vesicle weight in control and treated animals. (B′, D′, K′, L′) Inserts showing Leydig cells at higher magnification. Scale bar = 10 µm. Values are expressed as mean ± SEM. * $P < 0.05$, ** $P < 0.01$.

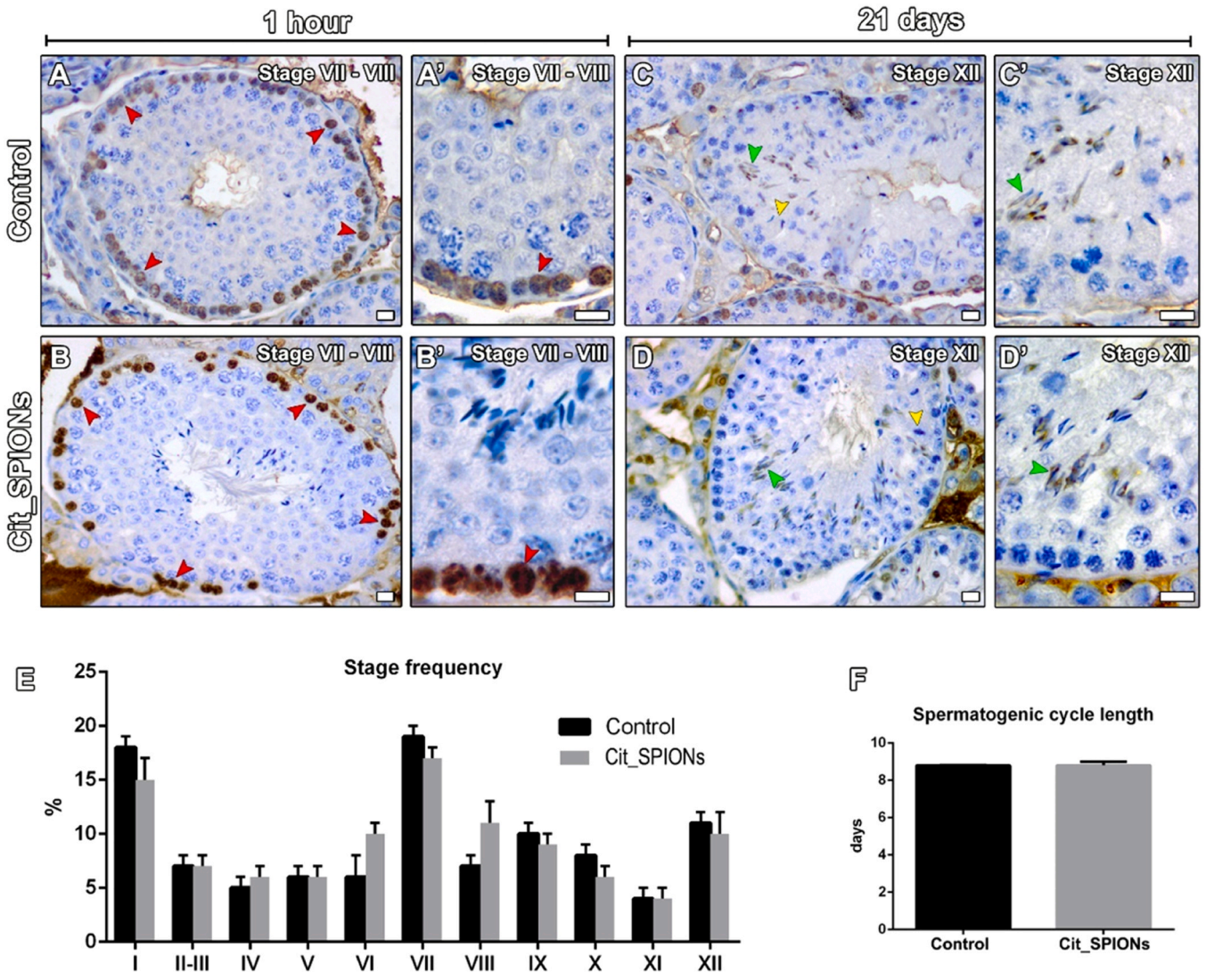

Fig. 5. Spermatogenic cycle duration after Cit_SPIONs treatment. (A-B′) Immunostaining for pre-leptotene spermatocytes (red arrowheads) at stages VII-VIII of the seminiferous epithelium cycle in control and treated animals, one hour after BrdU administration. (C-D′) Immunostaining for elongated spermatids (green arrowheads) at stage XII of the seminiferous epithelium cycle in control and treated animals, twenty-one days after BrdU injection. Yellow arrowheads = metaphase plate of the meiotic division. (E-F) The frequency (E) and duration (F) of the seminiferous epithelium cycle remain unchanged after the Cit_SPIONs treatment. Scale bar A, B, C and D = 10 μm, A', B', C' and D' = 20 μm.

development of germ cells [55,67]. As demonstrated in our study, the reduction of testosterone levels can negatively impact the efficiency of meiotic division in the seminiferous epithelium, resulting in a decrease in daily sperm production [75]. Previous data also confirm that the accumulation of metal oxide nanoparticles (NPs) in the testes can lead to a decrease in testosterone production, which in turn may impair sperm quality and fertility [26,35,45,66,72].

In the intertubular compartment, we observed peritubular macrophages containing phagocytic vesicles with Cit_SPIONs. Previous studies have extensively explored the immunomodulatory effects of SPIONs, particularly in tumor environments, focusing on the polarization and reprogramming of macrophages [31,49,83]. These studies suggested that SPION treatment can induce a pro-inflammatory phenotype in macrophages [39,42,57]. However, testicular macrophages serve additional roles beyond responding to infections; they also influence and regulate steroidogenesis ([29]; Chen et al., 2002).

Building upon our previous research [10], this study is the first to report unchanged spermatogenesis duration post-Cit_SPION injection. Although the spermatogenic pace did not change, the experimental time frame demonstrated that Cit_SPION bioaccumulation in the testis parenchyma could interfere with the development of germ cells, diminishing germ cell survival, sperm concentration, and progressive motility. Further studies would explore whether the impact on sperm motility was a consequence of the previous testicular cell exposure to Cit_SPIONs or a direct effect of nanoparticles on the epididymis physiology, affecting the sperm maturation during the transit in the epididymal duct (~6 days) [25].

The direct and indirect effects of Cit_SPIONs on the seminiferous epithelium, including accumulation in Sertoli and peritubular myoid cells and decreased testosterone levels, hint at a complex interplay within the testicular environment. While iron is essential for germ cell development, an iron overload can lead to ferroptosis, increasing reactive oxygen species (ROS) production [44]. In vivo studies have shown that the primary mechanisms of toxicity of SPIONs are related to increased ROS and, consequently, oxidative stress [69,79,81]. Excess iron combined with the inactivity of the antioxidant system can result in increased ROS, lipid peroxidation, protein damage, and DNA damage, interfere with signaling pathways, and modulate gene transcription, leading to cell death of various cell types [44,69,81].

In our study, we observed DNA fragmentation, mainly in elongated

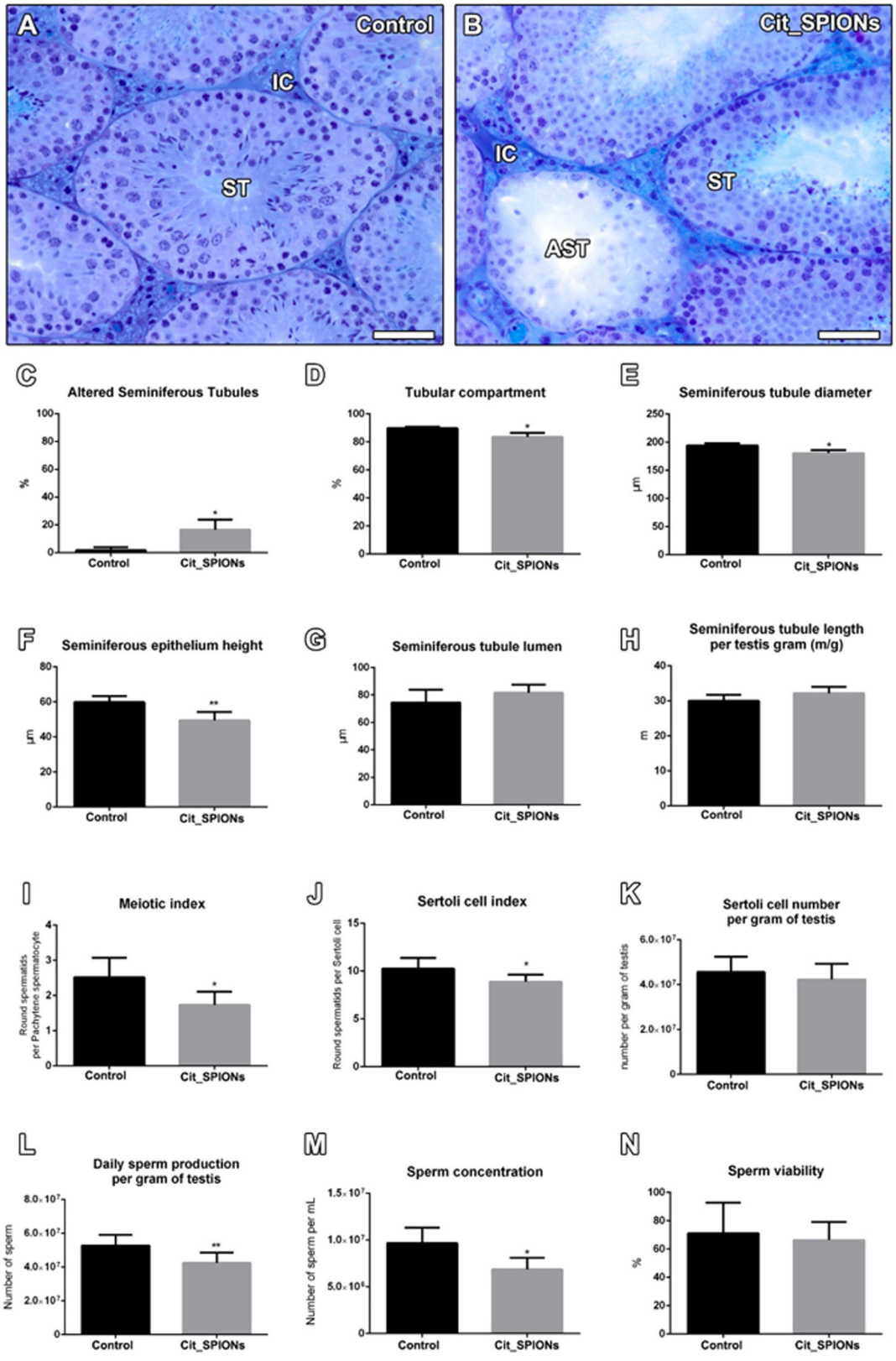

Fig. 6. Morphological and quantitative changes in the tubular compartment of animals treated with Cit_SPIONs. (A-B) Comparison of testicular histology between control (A) and treated (B) animals. (C) Quantification of seminiferous tubules with morphological alterations. (D) Tubular compartment volume density in control and treated animals. Evaluation of seminiferous tubule diameter (E), epithelium height (F), lumen size (G), and length (H) in control and treated animals. Analysis of meiotic (I) and Sertoli cell (J) indexes in control and treated animals. Determination of Sertoli cell number (K) and daily sperm production (L) per gram of testis in control and treated animals. Assessment of sperm concentration (M) and viability (N) in control and treated animals. ST = seminiferous tubule; IC = intertubular compartment; AST = morphologically altered seminiferous tubule. Scale bar = 50 µm. Values are expressed as mean ± SEM. * $P < 0.05$, ** $P < 0.01$.

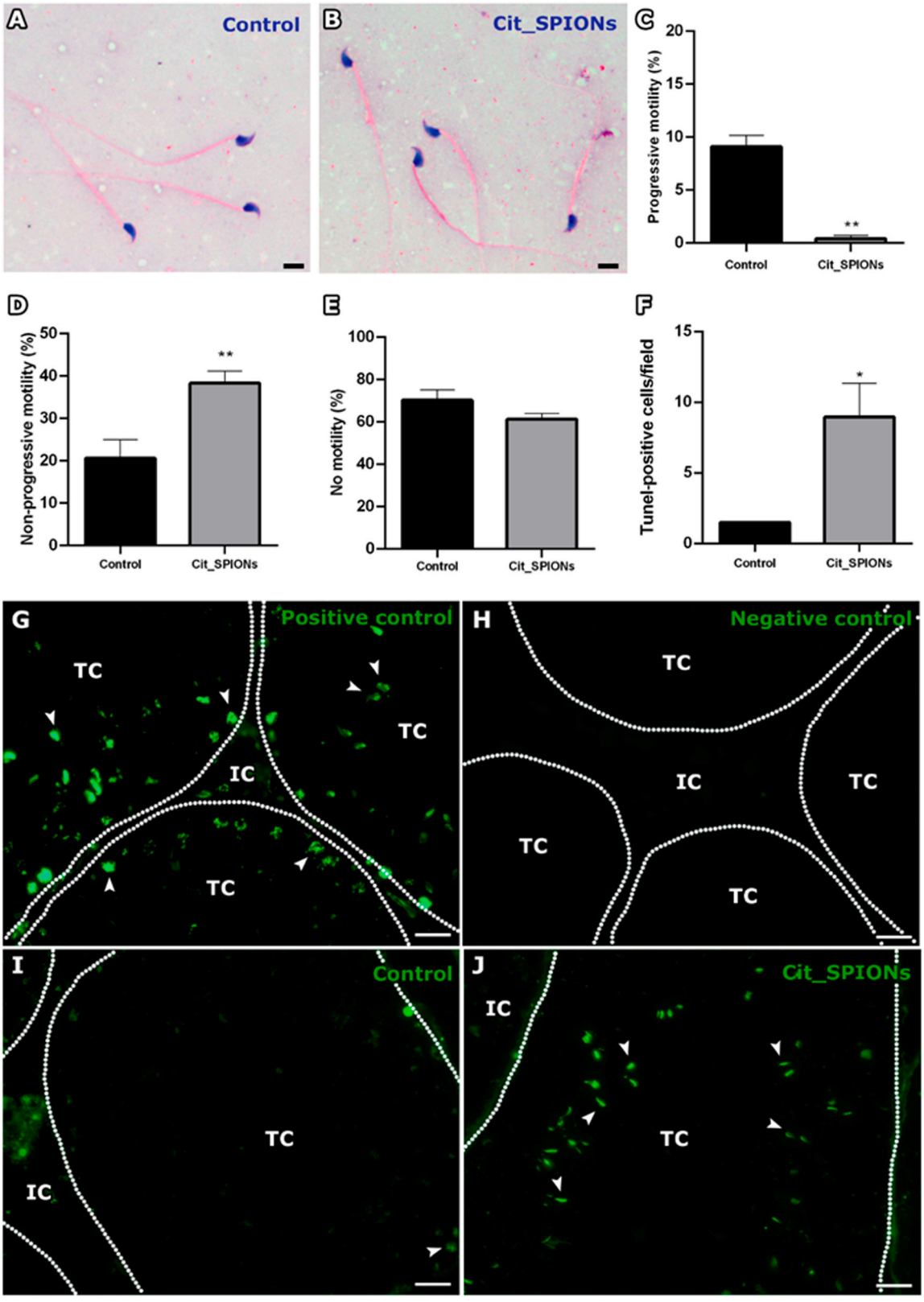

Fig. 7. Sperm cell features and DNA fragmentation after 56 days of exposure to Cit_SPIONs. (A-B) Sperm cell morphology in control and treated group. C-E) Sperm cell motility. (F) comparative analysis of the Tunel positive testicular cells between the treated and control groups. (G) Positive control of Tunel staining depicting several tunel-positive testicular cells (White arrowheads) in the tubular and intertubular compartments. (H) negative control of Tunel staining. (I) The control group depicted a few tunel-positive cells (white arrowhead). (J)The treated group showed several tunel-positive testicular cells, mainly elongated spermatids (White arrowheads). TC= tubular compartment; IC = intertubular compartment. Black scale bar = 10 μm; White scale bar = 20 μm. Values are expressed as mean ± SEM. * $P < 0.05$; **$P<0.01$.

Table 2
Morphological sperm profile in control (CT) and Cit_SPIONs treated mice (mean ± SEM).

Sperm characteristics (%)	CT	Cit_SPIONs
Head defects	53.46 ± 3.21	57.16 ± 8.47
Hookless	4.14 ± 1.4	1.41 ± 0.74
Banana-like	4.34 ± 1.6	1.66 ± 0.52
Narrow	2.46 ± 1.8	3.23 ± 1.69
Macrocephalous	1.38 ± 0.96	0.41 ± 0.58
Headless	3.55 ± 1.66	2.73 ± 2.01
Amorphous	37.39 ± 3.03	40.63 ± 8.94
Double headed	0.2 ± 0.27	0.08 ± 0.2
Midpiece defects	6.9 ± 0.97	5.39 ± 2.04
Midpiece only	0.3 ± 0.44	0.08 ± 0.2
Thicker	2.27 ± 0.75	1.74 ± 1.17
Smaller	0.89 ± 0.54	0.66 ± 0.41
Irregular insertion	3.45 ± 0.69	2.90 ± 1.5
Tail defects	11.43 ± 4.55	10.44 ± 3.03
Double tailed	0.20 ± 0.27	N/A
Folded	8.09 ± 2.68	6.96 ± 2.36
Coiled	3.15 ± 2.57	3.48 ± 0.83
Without midpiece and tail	5.82 ± 0.62	5.38 ± 2.47

spermatids. The accumulation of Cit_SPIONs in the tubular compartment and a decrease in testosterone levels may have increased the vulnerability of germ cells. Notably, previous studies by Yang et al [82], Awaad et al [4], and Di Bona et al [17] using different but close dosages support our findings. They also suggest that exposure to iron oxide nanoparticles (IONPs) can negatively impact male reproductive health, leading to a reduction in sperm quantity, increased oxidative stress, and apoptosis of cells in the tubular compartment. Although significant alterations were found in the present study, it is imperative to mention that further long-term evaluations related to gamete genetic and epigenetic alterations and the reversibility of the observed effects should be conducted.

5. Conclusions

In conclusion, our study presents groundbreaking insights into the toxic effects of Cit_SPIONs following intratesticular administration in mice, with significant implications for reproductive toxicology. We discovered pronounced intertubular impact, especially in Leydig cells, where Cit_SPION accumulation led to decreased steroidogenic activity and androgen support. This disruption resulted in secondary seminiferous tubular changes, leading to germ cell loss and reduced sperm production. Our findings illuminate the intricate responses of testicular tissues to nanoparticles and open new therapeutic avenues using SPIONs to modulate Leydig cell function. This study underscores the potential of nanotechnology in advancing male reproductive health treatments, marking a significant step forward in the field.

Financial support

Conselho Nacional de Desenvolvimento Científico e Tecnológico (CNPq - 422405/2018–3 and 317259/2021–0), Fundação de Amparo à Pesquisa do Estado de Minas Gerais (FAPEMIG - RED00079–22) and Fundação Coordenação de Aperfeiçoamento de Pessoal de Nível Superior (CAPES)

CRediT authorship contribution statement

Márcio F. D. Moraes: Writing – review & editing, Writing – original draft, Methodology, Investigation, Formal analysis. **Fausto S. Ferraz:** Writing – review & editing, Writing – original draft, Investigation, Formal analysis, Data curation, Conceptualization. **Estefânia M. N. Martins:** Writing – review & editing, Writing – original draft, Methodology, Investigation, Formal analysis. **Jorge L. López:** Writing – review & editing, Writing – original draft, Supervision, Methodology, Investigation. **Leonardo O. Guarnieri:** Writing – review & editing, Writing – original draft, Methodology, Investigation, Formal analysis. **Eduardo**

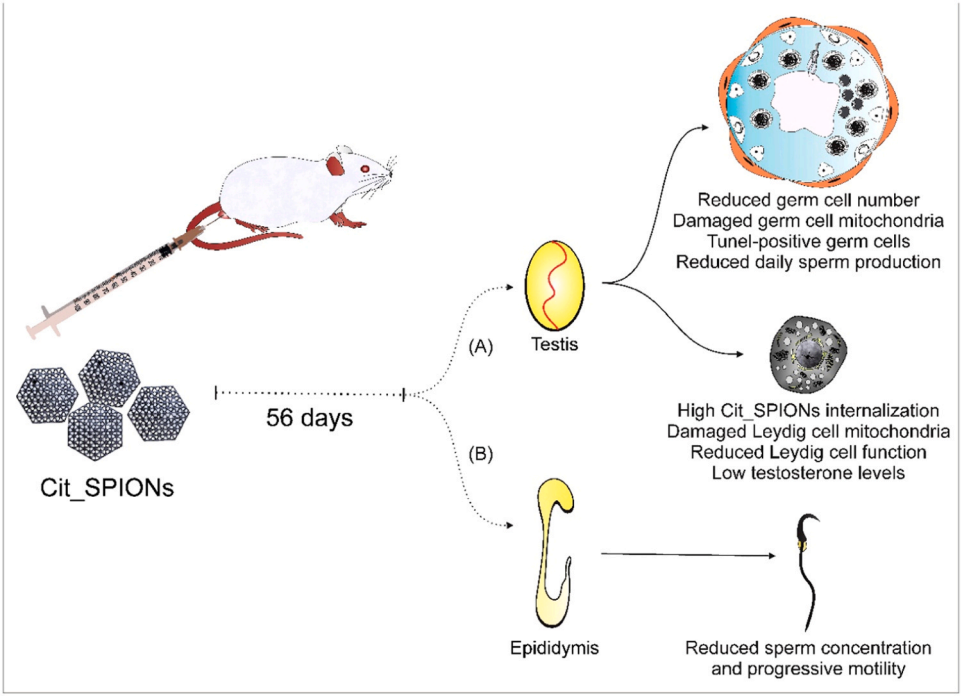

Fig. 8. Schematic drawing of the main effects observed after intratesticular injection of Cit_SPIONs in a murine model. After 56 days of injection, Cit_SPIONs promoted alterations in the gonads and sperm output. (A) In the testis, we observed a reduction in the number of germ cells, Tunel-positive germ cells, a decrease in spermatogenic indices, and reduced daily sperm production. Furthermore, we observed high Cit_SPIONs internalization, damaged Leydig cell mitochondria, reduced Leydig cell function, and low testosterone levels. (B) We evaluated the epididymis cauda and observed a reduced sperm concentration and progressive motility in the Cit_SPIONs treated animals.

M. A. Marçal: Writing – review & editing, Writing – original draft, Methodology, Investigation, Formal analysis. **Graziela de P. F. Dantas:** Writing – review & editing, Writing – original draft, Investigation, Formal analysis, Data curation, Conceptualization. **Luiz O. Ladeira:** Writing – review & editing, Writing – original draft, Supervision, Investigation, Formal analysis. **Nathália de L.E.M. Lara:** Writing – review & editing, Writing – original draft, Methodology, Investigation, Formal analysis. **Pedro I. M. Viana:** Writing – review & editing, Writing – original draft, Methodology, Investigation, Formal analysis. **Mara L. dos Santos:** Writing – review & editing, Writing – original draft, Methodology, Investigation, Formal analysis. **Carolina P. Vieira:** Writing – review & editing, Writing – original draft, Methodology, Investigation, Formal analysis. **Lídia M. Andrade:** Writing – review & editing, Writing – original draft, Supervision, Methodology, Investigation, Formal analysis. **John L. P. Coimbra:** Writing – review & editing, Writing – original draft, Methodology, Investigation, Formal analysis. **Guilherme M J Costa:** Writing – review & editing, Writing – original draft, Supervision, Resources, Project administration, Investigation, Funding acquisition, Conceptualization. **Samyra M. S. N. Lacerda:** Writing – review & editing, Writing – original draft, Methodology, Investigation, Formal analysis.

Declaration of Competing Interest

The authors declare that there is no conflict of interest regarding the publication of this manuscript.

Data availability

Data will be made available on request.

Acknowledgments

The support from CAPES, FAPEMIG (REDE MINEIRA DE NANOMEDICINA TERANÓSTICA; RED-00079–22) and CNPq (422405/2018–3 and 317259/2021–0) was of great importance, as well as Laboratório de Caracterização e Processamento de Nanomateriais (LCPNano), CAPI-UFMG, CTPMAG-UFMG and Centro de Microscopia da UFMG for the use of their facilities.

Appendix A. Supporting information

Supplementary data associated with this article can be found in the online version at doi:10.1016/j.reprotox.2024.108584.

References

[1] A. Abbasi Kajani, S. Haghjooy Javanmard, M. Asadnia, A. Razmjou, Recent Advances in Nanomaterials Development for Nanomedicine and Cancer, in: In ACS Applied Bio Materials, Vol. 4, American Chemical Society, 2021, pp. 5908–5925, https://doi.org/10.1021/acsabm.1c00591.

[2] E. Alphandéry, Biodistribution and Targeting Properties Of Iron Oxide Nanoparticles For Treatments Of Cancer And Iron Anemia Disease, in: In Nanotoxicology, Vol. 13, Taylor and Francis Ltd, 2019, pp. 573–596, https://doi.org/10.1080/17435390.2019.1572809.

[3] Alphandéry, E. (2020). Iron Oxide Nanoparticles for Therapeutic Applications. In Drug Discovery Today (Vol. 25, Issue 1, pp. 141–149). Elsevier Ltd. https://doi.org/10.1016/j.drudis.2019.09.020.

[4] A. Awaad, M.A. Adly, D. Hosny, Histological and histopathological studies on the protective role of Echinacea purpurea extract after intra-testicular injection of magnetic nanoparticles in male albino rats, J. Histotechnology *40* (4) (2017) 100–114, https://doi.org/10.1080/01478885.2017.1369210.

[5] Aziz, N., Saleh, R.A., Sharma, R.K., Lewis-Jones, I., Esfandiari, N., Thomas, A.J., & Agarwal, A. (n.d.). Novel Association between Sperm Reactive Oxygen Species Production, Sperm Morphological Defects, and the Sperm Deformity Index. https://doi.org/10.1016/j.fertnstert.2003.

[6] A.L. Bailly, F. Correard, A. Popov, G. Tselikov, F. Chaspoul, R. Appay, A. Al-Kattan, A.V. Kabashin, D. Braguer, M.A. Esteve, In vivo evaluation of safety, biodistribution and pharmacokinetics of laser-synthesized gold nanoparticles, Sci. Rep. *9* (1) (2019), https://doi.org/10.1038/s41598-019-48748-3.

[7] N. Barkalina, C. Charalambous, C. Jones, K. Coward, Nanotechnology in reproductive medicine: emerging applications of nanomaterials, Nanomed. Nanotechnol. Biol. Med. *10* (5) (2014) e921–e938, https://doi.org/10.1016/j.nano.2014.01.001.

[8] P. Cherukuri, E.S. Glazer, S.A. Curley, Targeted hyperthermia using metal nanoparticles, Adv. Drug Deliv. Rev. Vol. 62 (Issue 3) (2010) 339–345, https://doi.org/10.1016/j.addr.2009.11.006.

[9] V.V. Chrishtop, V.A. Mironov, A.Y. Prilepskii, V.G. Nikonorova, V.V. Vinogradov, Organ-specific toxicity of magnetic iron oxide-based nanoparticles, in: In Nanotoxicology, Vol. 15, Taylor and Francis Ltd, 2021, pp. 167–204, https://doi.org/10.1080/17435390.2020.1842934.

[10] J.L.P. Coimbra, G. Dantas, P.F. de, L.M. de Andrade, M.R.G. Brener, P.I.M. Viana, R.A. Lopes, D. O.G Gontijo, L.O.G. Ervilha, M.Q. Assis, L.S. Barcelos, R. E. Szawka, D.C. Damasceno, M. Machado-Neves, A.P. Mota, G.M.J. Costa, Gold nanoparticle intratesticular injections as a potential animal sterilization tool: long-term reproductive and toxicological implications, Toxicology *492* (2023), https://doi.org/10.1016/j.tox.2023.153543.

[11] G.M.J. Costa, S.M.S.N. Lacerda, A.F.A. Figueiredo, M.C. Leal, J.V. Rezende-Neto, L. R. França, Higher environmental temperatures promote acceleration of spermatogenesis in vivo in mice (Mus musculus), J. Therm. Biol. *77* (2018) 14–23, https://doi.org/10.1016/j.jtherbio.2018.07.010.

[12] P.J. Cypriyana, J. S, S. Angalene J, L.A. Samrot, A.V. Kumar S, S. Ponniah, P, S. Chakravarthi, Overview on tOxicity of Nanoparticles, It's Mechanism, Models Used in Toxicity Studies and Disposal Methods – A Review, in: In Biocatalysis and Agricultural Biotechnology, Vol. 36, Elsevier Ltd, 2021, https://doi.org/10.1016/j.bcab.2021.102117.

[13] G.P.F. Dantas, F.S. Ferraz, L.M. Andrade, G.M.J. Costa, Male Reproductive Toxicity of Inorganic Nanoparticles in Rodent Models: A Systematic Review, in: In Chemico-Biological Interactions, Vol. 363, Elsevier Ireland Ltd, 2022, https://doi.org/10.1016/j.cbi.2022.110023.

[14] A.F.C. De Oliveira, N. De Lima, M. Lara, B. Ramalho, L. Cardoso, Luiz, R. De França, G. Fernandes De Avelar, 2020, Comparative Testis Structure and Function in Three Representative Mice Strains.

[15] M.A. Dheyab, A.A. Aziz, M.S. Jameel, O.A. Noqta, P.M. Khaniabadi, B. Mehrdel, Simple rapid stabilization method through citric acid modification for magnetite nanoparticles, Sci. Rep. *10* (1) (2020), https://doi.org/10.1038/s41598-020-67869-8.

[16] M.A. Dheyab, A.A. Aziz, M.S. Jameel, O.A. Noqta, P.M. Khaniabadi, B. Mehrdel, Simple rapid stabilization method through citric acid modification for magnetite nanoparticles, Sci. Rep. *10* (1) (2020), https://doi.org/10.1038/s41598-020-67869-8.

[17] K.R. Di Bona, Y. Xu, M. Gray, D. Fair, H. Hayles, L. Milad, A. Montes, J. Sherwood, Y. Bao, J.F. Rasco, Short- and long-term effects of prenatal exposure to iron oxide nanoparticles: influence of surface charge and dose on developmental and reproductive toxicity, Int. J. Mol. Sci. *16* (12) (2015) 30251–30268, https://doi.org/10.3390/ijms161226231.

[18] W. Ding, Z. Chen, Y. Gu, Z. Chen, Y. Zheng, F. Sun, Magnetic testis targeting and magnetic hyperthermia for noninvasive, controllable male contraception via intravenous administration, Nano Lett. *21* (14) (2021) 6289–6297, https://doi.org/10.1021/acs.nanolett.1c02181.

[19] W. Ding, Z. Chen, Y. Gu, Z. Chen, Y. Zheng, F. Sun, Magnetic testis targeting and magnetic hyperthermia for noninvasive, controllable male contraception via intravenous administration, Nano Lett. *21* (14) (2021) 6289–6297, https://doi.org/10.1021/acs.nanolett.1c02181.

[20] T.D.O. Farias, A.F.A. Figueiredo, N.T. Wnuk, F.S. Ferraz, S.A. Talamoni, G.M. J. Costa, Male reproductive morphofunctional evaluation of a Neotropical sperm-storing vespertilionid bat (Myotis levis) in an environmental context, Cell Tissue Res. *382* (3) (2020) 639–656, https://doi.org/10.1007/s00441-020-03242-5.

[21] H. Fatima, K.S. Kim, Iron-based magnetic nanoparticles for magnetic resonance imaging, Adv. Powder Technol. *29* (11) (2018) 2678–2685, https://doi.org/10.1016/j.apt.2018.07.017.

[22] F.S. Ferraz, J.L. López, S.M.S.N. Lacerda, M.S. Procópio, A.F.A. Figueiredo, E.M. N. Martins, P.P.G. Guimarães, L.O. Ladeira, G.T. Kitten, F.F. Dias, R.Z. Domingues, G.M.J. Costa, Biotechnological approach to induce human fibroblast apoptosis using superparamagnetic iron oxide nanoparticles, J. Inorg. Biochem. *206* (August 2019) (2020) 111017, https://doi.org/10.1016/j.jinorgbio.2020.111017.

[23] A.F.A. Figueiredo, N.T. Wnuk, C.P. Vieira, M.F.F. Gonçalves, M.R.G. Brener, A. B. Diniz, M.M. Antunes, H.M. Castro-Oliveira, G.B. Menezes, G.M.J. Costa, Activation of C–C motif chemokine receptor 2 modulates testicular macrophages number, steroidogenesis, and spermatogenesis progression, Cell Tissue Res. *386* (1) (2021) 173–190, https://doi.org/10.1007/s00441-021-03504-w.

[24] J. Fonseca-Gomes, J.A. Loureiro, S.R. Tanqueiro, F.M. Mouro, P. Ruivo, T. Carvalho, A.M. Sebastião, M.J. Diógenes, M.C. Pereira, In vivo bio-distribution and toxicity evaluation of polymeric and lipid-based nanoparticles: a potential approach for chronic diseases treatment, Int. J. Nanomed. *15* (2020) 8609–8621, https://doi.org/10.2147/IJN.S267007.

[25] L.R. França, G.F. Avelar, F.F.L. Almeida, Spermatogenesis and sperm transit through the epididymis in mammals with emphasis on pigs, Theriogenology *63* (2 SPEC. ISS.) (2005) 300–318, https://doi.org/10.1016/j.theriogenology.2004.09.014.

[26] Y. Gao, D.D. Mruk, C.Y. Cheng, Sertoli Cells Are the Target of Environmental Toxicants in the Testis-a Mechanistic and Therapeutic Insight, in: In Expert Opinion on Therapeutic Targets, Vol. 19, Taylor and Francis Ltd, 2015, pp. 1073–1090, https://doi.org/10.1517/14728222.2015.1039513.

[27] S. Garza, L. Chen, M. Galano, G. Cheung, C. Sottas, L. Li, Y. Li, B.R. Zirkin, V. Papadopoulos, Mitochondrial dynamics, Leydig cell function, and age-related testosterone deficiency, FASEB J. *36* (12) (2022), https://doi.org/10.1096/fj.202201026R.

[28] S. Ghosh, I. Ghosh, M. Chakrabarti, A. Mukherjee, Genotoxicity and biocompatibility of superparamagnetic iron oxide nanoparticles: influence of surface modification on biodistribution, retention, DNA damage and oxidative stress, Food Chem. Toxicol. *136* (2020) 110989, https://doi.org/10.1016/j.fct.2019.110989.

[29] T. Goluža, A. Boscanin, J. Cvetko, V. Kozina, M. Kosović, M.M. Bernat, M. Kasum, Ž. Kaštelan, D. Ježek, Macrophages and leydig cells in testicular biopsies of azoospermic men, BioMed. Res. Int. *2014* (2014), https://doi.org/10.1155/2014/828697.

[30] M.F.F. Gonçalves, S.M. dos S.N. Lacerda, N. de L. e M. Lara, C.F.A. de Oliveira, A.F. A. Figueiredo, M.R.G. Brener, M.A. Cavalcante, A.K. Santos, G.H. Campolina-Silva, V.V. Costa, A.C.C. Santana, R.A. Lopes, R.E. Szawka, G.M.J. Costa, GATA-1 mutation alters the spermatogonial phase and steroidogenesis in adult mouse testis, Mol. Cell. Endocrinol. *542* (2022), https://doi.org/10.1016/j.mce.2021.111519.

[31] Z. Gu, T. Liu, J. Tang, Y. Yang, H. Song, Z.K. Tuong, J. Fu, C. Yu, Mechanism of iron oxide-induced macrophage activation: the impact of composition and the underlying signaling pathway, J. Am. Chem. Soc. *141* (15) (2019) 6122–6126, https://doi.org/10.1021/jacs.8b10904.

[32] Q. He, Z. Zhang, F. Gao, Y. Li, J. Shi, In vivo biodistribution and urinary excretion of mesoporous silica nanoparticles: effects of particle size and PEGylation, Small *7* (2) (2011) 271–280, https://doi.org/10.1002/smll.201001459.

[33] S.C. Hong, J.H. Lee, J. Lee, H.Y. Kim, J.Y. Park, J. Cho, J. Lee, D.W. Han, Subtle cytotoxicity and genotoxicity differences in superparamagnetic iron oxide nanoparticles coated with various functional groups, Int. J. Nanomed. *6* (2011) 3219–3231.

[34] N. Hoshyar, S. Gray, H. Han, G. Bao, The Effect of Nanoparticle Size on in Vivo Pharmacokinetics and Cellular Interaction, in: In Nanomedicine, Vol. 11, Future Medicine Ltd, 2016, pp. 673–692, https://doi.org/10.2217/nnm.16.5.

[35] J. Jia, Z. Wang, T. Yue, G. Su, C. Teng, B. Yan, Crossing biological barriers by engineered nanoparticles, Chem. Res. Toxicol. *33* (5) (2020) 1055–1060, https://doi.org/10.1021/acs.chemrestox.9b00483.

[36] J.L.P.R. Jivago, J.L.M. Brito, G. Capistrano, M. Vinícius-Araújo, E.L. Verde, A. F. Bakuzis, P.E.N. Souza, R.B. Azevedo, C.M. Lucci, New prospects in neutering male animals using magnetic nanoparticle hyperthermia, Pharmaceutics *13* (9) (2021), https://doi.org/10.3390/pharmaceutics13091465.

[37] M. Kaloyianni, A. Dimitriadi, M. Ovezik, D. Stamkopoulou, K. Feidantsis, G. Kastrinaki, G. Gallios, I. Tsiaoussis, G. Koumoundouros, D. Bobori, Magnetite nanoparticles effects on adverse responses of aquatic and terrestrial animal models, J. Hazard. Mater. *383* (2020), https://doi.org/10.1016/j.jhazmat.2019.121204.

[38] M.K. Kheirabad, Z. Khodabandeh, F. Rahmanifar, A. Tamadon, B.N. Jahromi, M. Owjfard, O. Koohi-Hosseinabadi, Testicular germ cells apoptosis following exposure to chronic stress in rats, Asian Pac. J. Reprod. *5* (5) (2016) 371–375, https://doi.org/10.1016/j.apjr.2016.07.005.

[39] V. Kodali, M.H. Littke, S.C. Tilton, J.G. Teeguarden, L. Shi, C.W. Frevert, W. Wang, J.G. Pounds, B.D. Thrall, Dysregulation of macrophage activation profiles by engineered nanoparticles, ACS Nano *7* (8) (2013) 6997–7010, https://doi.org/10.1021/nn402145t.

[40] J. Kolosnjaj-Tabi, C. Wilhelm, Magnetic Nanoparticles in Cancer Therapy: How Can Thermal Approaches Help?, in: In Nanomedicine, Vol. 12 Future Medicine Ltd, 2017, pp. 573–575, https://doi.org/10.2217/nnm-2017-0014.

[41] N.L.M. Lara, I.C. Santos, G.M.J. Costa, D.A. Cordeiro-Junior, A.C.G. Almeida, A. P. Madureira, M.S. Zanini, L.R. França, Duration of spermatogenesis and daily sperm production in the rodent Proechimys guyannensis, Zygote *24* (5) (2016) 783–793, https://doi.org/10.1017/S0967199416000137.

[42] A. Laskar, J. Eilertsen, W. Li, X.M. Yuan, SPION primes THP1 derived M2 macrophages towards M1-like macrophages, Biochem. Biophys. Res. Commun. *441* (4) (2013) 737–742, https://doi.org/10.1016/j.bbrc.2013.10.115.

[43] S. Levi, P. Arosio, Mitochondrial ferritin, Int. J. Biochem. Cell Biol. Vol. 36 (Issue 10) (2004) 1887–1889, https://doi.org/10.1016/j.biocel.2003.10.020.

[44] Y. Liu, X. Cao, C. He, X. Guo, H. Cai, A. Aierken, J. Hua, S. Peng, Effects of ferroptosis on male reproduction, Int. J. Mol. Sci. Vol. 23 (Issue 13) (2022), https://doi.org/10.3390/ijms23137139.

[45] Y. Liu, X. Li, S. Xiao, X. Liu, X. Chen, Q. Xia, S. Lei, H. Li, Z. Zhong, K. Xiao, The effects of gold nanoparticles on leydig cells and male reproductive function in mice, Int. J. Nanomed. *15* (2020) 9499–9514, https://doi.org/10.2147/IJN.S276606.

[46] M. Mabrouk, D.B. Das, Z.A. Salem, H.H. Beherei, Nanomaterials for biomedical applications: production, characterisations, recent trends and difficulties, Molecules Vol. 26 (Issue 4) (2021), https://doi.org/10.3390/molecules26041077.

[47] M. Mahmoudi, A. Simchi, A.S. Milani, P. Stroeve, Cell toxicity of superparamagnetic iron oxide nanoparticles, J. Colloid Interface Sci. *336* (2) (2009) 510–518, https://doi.org/10.1016/j.jcis.2009.04.046.

[48] M.L.J. Medar, D.Z. Marinkovic, Z. Kojic, A.P. Becin, I.M. Starovlah, T. Kravic-Stevovic, S.A. Andric, T.S. Kostic, Dependence of leydig cell's mitochondrial physiology on luteinizing hormone signaling, Life *11* (1) (2021) 1–17, https://doi.org/10.3390/life11010019.

[49] V. Mulens-Arias, J.M. Rojas, D.F. Barber, The use of iron oxide nanoparticles to reprogram macrophage responses and the immunological tumor microenvironment, Front. Immunol. Vol. 12 (2021), https://doi.org/10.3389/fimmu.2021.693709.

[50] A.R. Murray, E. Kisin, A. Inman, S.H. Young, M. Muhammed, T. Burks, A. Uheida, A. Tkach, M. Waltz, V. Castranova, B. Fadeel, V.E. Kagan, J.E. Riviere, N. Monteiro-Riviere, A.A. Shvedova, Oxidative stress and dermal toxicity of iron oxide nanoparticles in vitro, Cell Biochem. Biophys. *67* (2) (2013) 461–476, https://doi.org/10.1007/s12013-012-9367-9.

[51] S. Nasri, S. Rezai-Zarchi, P. Kerishchi, S. Sadeghi, The effect of iron oxide nanoparticles on sperm numbers and mobility in male mice, Zahedan J. Res. Med. Sci. *17* (10) (2015), https://doi.org/10.17795/zjrms-2185.

[52] S.D. Oberdick, K.V. Jordanova, J.T. Lundstrom, G. Parigi, M.E. Poorman, G. Zabow, K.E. Keenan, Iron oxide nanoparticles as positive T1 contrast agents for low-field magnetic resonance imaging at 64 mT, Sci. Rep. *13* (1) (2023), https://doi.org/10.1038/s41598-023-38222-6.

[53] J. Palzer, L. Eckstein, I. Slabu, O. Reisen, U.P. Neumann, A.A. Roeth, Iron oxide nanoparticle-based hyperthermia as a treatment option in various gastrointestinal malignancies, Nanomaterials Vol. 11 (Issue 11) (2021), https://doi.org/10.3390/nano11113013.

[54] M. Pöttler, A. Staicu, J. Zaloga, H. Unterweger, B. Weigel, E. Schreiber, S. Hofmann, I. Wiest, U. Jeschke, C. Alexiou, C. Janko, Genotoxicity of superparamagnetic iron oxide nanoparticles in granulosa cells, Int. J. Mol. Sci. *16* (11) (2015) 26280–26290, https://doi.org/10.3390/ijms161125960.

[55] F. Qin, T. Shen, J. Li, J. Qian, J. Zhang, G. Zhou, J. Tong, SF-1 mediates reproductive toxicity induced by Cerium oxide nanoparticles in male mice, J. Nanobiotechnology *17* (1) (2019), https://doi.org/10.1186/s12951-019-0474-2.

[56] Rahman, M. (2023). Magnetic Resonance Imaging and Iron-oxide Nanoparticles in the Era of Personalized Medicine. In Nanotheranostics (Vol. 7, Issue 4, pp. 424–449). Ivyspring International Publisher. https://doi.org/10.7150/ntno.86467.

[57] J.M. Rojas, L. Sanz-Ortega, V. Mulens-Arias, L. Gutiérrez, S. Pérez-Yagüe, D. F. Barber, Superparamagnetic iron oxide nanoparticle uptake alters M2 macrophage phenotype, iron metabolism, migration and invasion, Nanomed. Nanotechnol. Biol. Med. *12* (4) (2016) 1127–1138, https://doi.org/10.1016/j.nano.2015.11.020.

[58] P. Santambrogio, G. Biasiotto, F. Sanvito, S. Olivieri, P. Arosio, S. Levi, Mitochondrial ferritin expression in adult mouse tissues, J. Histochem. Cytochem. *55* (11) (2007) 1129–1137, https://doi.org/10.1369/jhc.7A7273.2007.

[59] P. Santambrogio, G. Biasiotto, F. Sanvito, S. Olivieri, P. Arosio, S. Levi, Mitochondrial ferritin expression in adult mouse tissues, J. Histochem. Cytochem. *55* (11) (2007) 1129–1137, https://doi.org/10.1369/jhc.7A7273.2007.

[60] R. Shandilya, P.K. Mishra, N. Pathak, N.K. Lohiya, R.S. Sharma, Nanotechnology in reproductive medicine: opportunities for clinical translation, Clin. Exp. Reprod. Med. *47* (4) (2020) 245–262, https://doi.org/10.5653/cerm.2020.03650.

[61] L. Shen, B. Li, Y. Qiao, Fe3O4 nanoparticles in targeted drug/gene delivery systems, Materials Vol. 11 (Issue 2) (2018), https://doi.org/10.3390/ma11020324.

[62] N. Singh, G.J.S. Jenkins, B.C. Nelson, B.J. Marquis, T.G.G. Maffeis, A.P. Brown, P. M. Williams, C.J. Wright, S.H. Doak, The role of iron redox state in the genotoxicity of ultrafine superparamagnetic iron oxide nanoparticles, Biomaterials *33* (1) (2012) 163–170, https://doi.org/10.1016/j.biomaterials.2011.09.087.

[63] J.R. Sosa-Acosta, C. Iriarte-Mesa, G.A. Ortega, A.M. Díaz-García, DNA–Iron Oxide Nanoparticles Conjugates: Functional Magnetic Nanoplatforms in Biomedical Applications, in: In Topics in Current Chemistry, Vol. 378, Springer, 2020, https://doi.org/10.1007/s41061-019-0277-9.

[64] M. Suciu, C.M. Ionescu, A. Ciorita, S.C. Tripon, D. Nica, H. Al-Salami, L. Barbu-Tudoran, Applications of superparamagnetic iron oxide nanoparticles in drug and therapeutic delivery, and biotechnological advancements, Beilstein J. Nanotechnol. Vol. 11 (2020) 1092–1109, https://doi.org/10.3762/BJNANO.11.94.

[65] K. Sundarraj, V. Manickam, A. Raghunath, M. Periyasamy, M.P. Viswanathan, E. Perumal, Repeated exposure to iron oxide nanoparticles causes testicular toxicity in mice, Environ. Toxicol. *32* (2) (2017) 594–608, https://doi.org/10.1002/tox.22262.

[66] Y. Tang, B. Chen, W. Hong, L. Chen, L. Yao, Y. Zhao, Z.P. Aguilar, H. Xu, ZnO nanoparticles induced male reproductive toxicity based on the effects on the endoplasmic reticulum stress signaling pathway, Int. J. Nanomed. *14* (2019) 9563–9576, https://doi.org/10.2147/IJN.S223318.

[67] C. Toocheck, T. Clister, J. Shupe, C. Crum, P. Ravindranathan, T.K. Lee, J.M. Ahn, G.V. Raj, M. Sukhwani, K.E. Orwig, W.H. Walker, Mouse spermatogenesis requires classical and nonclassical testosterone signaling, Biol. Reprod. *94* (1) (2016), https://doi.org/10.1095/biolreprod.115.132068.

[68] E. Tvrda, R. Peer, S.C. Sikka, A. Agarwal, Iron and copper in male reproduction: a double-edged sword, J. Assist. Reprod. Genet. *32* (1) (2015) 3–16, https://doi.org/10.1007/s10815-014-0344-7.

[69] R. Vakili-Ghartavol, A.A. Momtazi-Borojeni, Z. Vakili-Ghartavol, H.T. Aiyelabegan, M.R. Jaafari, S.M. Rezayat, S. Arbabi Bidgoli, Toxicity Assessment of Superparamagnetic Iron Oxide Nanoparticles in Different Tissues, in: In Artificial Cells, Nanomedicine and Biotechnology, Vol. 48, Taylor and Francis Ltd, 2020, pp. 443–451, https://doi.org/10.1080/21691401.2019.1709855.

[70] N.V.S. Vallabani, S. Singh, A.S. Karakoti, Magnetic nanoparticles: current trends and future aspects in diagnostics and nanomedicine, Curr. Drug Metab. *20* (6) (2018) 457–472, https://doi.org/10.2174/1389200220666181122124458.

[71] T. Vangijzegem, D. Stanicki, S. Laurent, Magnetic iron oxide nanoparticles for drug delivery: applications and characteristics, Expert Opin. Drug Deliv. *16* (1) (2019) 69–78, https://doi.org/10.1080/17425247.2019.1554647.

[72] M. Vassal, S. Rebelo, M. de L. Pereira, Metal oxide nanoparticles: evidence of adverse effects on the male reproductive system, Int. J. Mol. Sci. Vol. 22 (Issue 15) (2021), https://doi.org/10.3390/ijms22158061.

[73] M. Vassallo, D. Martella, G. Barrera, F. Celegato, M. Coïsson, R. Ferrero, E. S. Olivetti, A. Troia, H. Sözeri, C. Parmeggiani, D.S. Wiersma, P. Tiberto, A. Manzin, Improvement of hyperthermia properties of iron oxide nanoparticles by surface coating, ACS Omega (2022), https://doi.org/10.1021/acsomega.2c06244.

[74] Wahajuddin, S. Arora, Superparamagnetic iron oxide nanoparticles: magnetic nanoplatforms as drug carriers, Int. J. Nanomed. Vol. 7 (2012) 3445–3471, https://doi.org/10.2147/IJN.S30320.
[75] W.H. Walker, Testosterone signaling and the regulation of spermatogenesis, Spermatogenesis *1* (2) (2011) 116–120, https://doi.org/10.4161/spmg.1.2.16956.
[76] C. Wang, L. Feng, X. Yang, F. Wang, W. Lu, Folic acid-conjugated liposomal vincristine for multidrug resistant cancer therapy, Asian J. Pharm. Sci. *8* (2) (2013) 118–127, https://doi.org/10.1016/j.ajps.2013.07.015.
[77] F. Wang, C.H. Lu, I. Willner, From Cascaded Catalytic Nucleic Acids to Enzyme-Dna Nanostructures: Controlling Reactivity, Sensing, Logic Operations, and Assembly of Complex Structures, in: In Chemical Reviews, Vol. 114, American Chemical Society, 2014, pp. 2881–2941, https://doi.org/10.1021/cr400354z.
[78] W. Wang, S. Wei, L. Li, X. Su, C. Du, F. Li, B. Geng, P. Liu, G. Xu, Proteomic analysis of murine testes lipid droplets, Sci. Rep. *5* (2015), https://doi.org/10.1038/srep12070.
[79] H. Wei, Y. Hu, J. Wang, X. Gao, X. Qian, M. Tang, Superparamagnetic Iron Oxide Nanoparticles: Cytotoxicity, Metabolism, and Cellular Behavior in Biomedicine Applications, in: In International Journal of Nanomedicine, Vol. 16, Dove Medical Press Ltd, 2021, pp. 6097–6113, https://doi.org/10.2147/IJN.S321984.
[80] Wise, T., Lunstra, D.D., Rohrer, G.A., & Ford, J.J. (2003). Relationships of Testicular Iron and Ferritin Concentrations with Testicular Weight and Sperm Production in Boars. In J. Anim. Sci (Vol. 81). https://academic.oup.com/jas/article-abstract/81/2/503/4789825.
[81] L. Wu, W. Wen, X. Wang, D. Huang, J. Cao, X. Qi, S. Shen, Ultrasmall iron oxide nanoparticles cause significant toxicity by specifically inducing acute oxidative stress to multiple organs, Part. Fibre Toxicol. *19* (1) (2022), https://doi.org/10.1186/s12989-022-00465-y.
[82] H. Yang, H. Wang, C. Wen, S. Bai, P. Wei, B. Xu, Y. Xu, C. Liang, Y. Zhang, G. Zhang, H. Wen, L. Zhang, Effects of iron oxide nanoparticles as T 2-MRI contrast agents on reproductive system in male mice, J. Nanobiotechnology *20* (1) (2022), https://doi.org/10.1186/s12951-022-01291-2.
[83] S. Zanganeh, G. Hutter, R. Spitler, O. Lenkov, M. Mahmoudi, A. Shaw, J. S. Pajarinen, H. Nejadnik, S. Goodman, M. Moseley, L.M. Coussens, H.E. Daldrup-Link, Iron oxide nanoparticles inhibit tumour growth by inducing pro-inflammatory macrophage polarization in tumour tissues, Nat. Nanotechnol. *11* (11) (2016) 986–994, https://doi.org/10.1038/nnano.2016.168.

DISCUSSÃO GERAL

No contexto da saúde reprodutiva, embora o uso da nanotecnologia seja amplamente explorado no desenvolvimento de sistemas e dispositivos com vantagens proeminentes para utilização clínica, diagnóstico e tratamento de diversas patologias, muitas ainda são as lacunas relacionadas aos efeitos adversos que as NPs podem causar aos órgãos reprodutivos e à saúde humana (Barkalina et al., 2014; Remião et al., 2018; Luo et al., 2024). Uma compreensão intensa das vias moleculares envolvidas facilitará a tradução clínica eficaz destas ferramentas baseadas em nanotecnologia.

No Capítulo 1, analisamos e comparamos de forma detalhada, através de uma revisão sistemática da literatura, as causas e os impactos da interação de NPs inorgânicas com as células reprodutoras de roedores machos. Uma visão ampla da toxicidade de diferentes NPs inorgânicas foi encontrada nos artigos avaliados. Entretanto, a falta de padronização de protocolos quanto ao tamanho das NPs, concentrações/doses e vias de administração, mostraram resultados bastante variáveis.

Em geral, observamos que a toxicidade de diferentes NPs depende fortemente das características físico-químicas e propriedades intrínsecas, que as tornam vantajosas para o desenvolvimento de tecnologias voltadas para o tratamento e diagnóstico de doenças do trato reprodutivo. Estudos com diferentes NPs inorgânicas mostraram que os mecanismos de interações biológicas e os efeitos adversos como citotoxicidade, estresse oxidativo, danos ao DNA, comprometimento da função mitocondrial e inflamação podem ser determinados pelas características físico-químicas das mesmas, como tamanho, forma, especificidade área de superfície, carga, atividade catalítica e presença de grupos funcionais em suas superfícies (Asare et al., 2012; Kumar et al., 2014; Jia et al., 2020; Shandilya et al., 2020). A geração de EROs e/ou indução de resposta inflamatória tem sido apontada como um dos fatores primários

na toxicidade de diferentes NPs inorgânicas (Krawetz et al., 2009; Lan e Yang, 2012; Tang et al., 2019; Pinho et al., 2020; Dantas et al., 2022).

Devido às propriedades únicas das SPIONs, como o superparamagnetismo, a relação superfície-volume, maior área superficial e fácil metodologia de síntese, elas têm atraído a atenção de vários pesquisadores para o desenvolvimento de diversas aplicações biomédicas (Zanganeh et al., 2016; Suciu et al., 2020; Tsakmakidis et al., 2020). Além disso, são consideradas biocompatíveis para vários sistemas biológicos (Patil et al., 2015; Schemberg et al., 2022). Entretanto, apesar dessas inúmeras vantagens, poucos são os estudos relacionados à toxicologia reprodutiva das SPIONs. Neste contexto, nos Capítulos 2 e 3 focamos na avaliação da toxicidade de SPIONs *in vitro* e *in vivo* em células testiculares de modelos murinos, com o intuito de obter uma compreensão mais abrangente de como essas nanoestruturas poderiam afetar as células testiculares.

No Capítulo 2, iniciamos com a caracterização físico-química das Cit_SPIONs. A caracterização das nanopartículas é crucial para determinar a composição e a estrutura dos materiais, além de avaliar a eficácia do método de síntese utilizado (Mourdikoudis et al., 2018; Titus et al., 2018). Diferentes técnicas são utilizadas para caracterizar o tamanho, a forma, a composição elementar e várias outras propriedades físico-químicas das nanopartículas. Em alguns casos, algumas propriedades podem ser avaliadas por mais de uma técnica (Mourdikoudis et al., 2018; Titus et al., 2018). As técnicas de Microscopia Eletrônica de Transmissão (TEM), Difração de Raio-X (XRD), espectroscopia Raman, espectroscopia de Mössbauer, Magnetometria de amostra vibratória (VSM), Potencial Zeta e Espectroscopia de fotoelétrons excitados por raio-X (XPS), foram as técnicas utilizadas para caracterizar as Cit_SPIONs e demostraram claramente o tamanho das NPs, a natureza superparamagnética e a eficiência do revestimento com citrato de sódio.

Neste capítulo, avaliamos a toxicidade de Cit_SPIONs em células testiculares de camundongos usando modelos *in vitro*. Estudos *in vitro* fornecem informações importantes, rápidas e de baixo custo para uma compreensão básica dos principais mecanismos biológicos envolvidos em uma determinada condição/patologia (Moysidou et al., 2021; Savage et al., 2019). Além disso, testes *in vitro* são amplamente utilizados para prever os riscos potenciais ou a possível toxicidade dos nanomateriais antes da sua aplicação final. Eles servem como screening para identificação de possíveis efeitos agudos de nanopartículas potencialmente perigosas (Savage et al., 2019)..

Inicialmente avaliamos a toxicidade de Cit_SPIONs em cultura de células testiculares primárias de camundongos. Modelos e ensaios *in vitro*, baseados em células imortalizadas ou culturas primárias, facilitam a investigação e a compreensão de diversos eventos e processos biológicos específicos sob diferentes condições e são indispensáveis para uma ampla gama de estudos biomédicos (Piwocka et al., 2024), seja para testar a eficácia e toxicidade de novos medicamentos, ou na fabricação de vacinas, na tecnologia de reprodução assistida, dentre outros (Patil et al., 2020; Moysidou et al., 2021). A internalização das Cit_SPIONs nas células testiculares *in vitro* foi avaliada através da cultura organotípica de tecidos. Esse tipo de cultura representa uma ferramenta reprodutível e rápida para testar os efeitos dos agentes biológicos e químicos nos tecidos (Vaira et al., 2010). Além disso, toda a estrutura histológica e tridimensional (3D) é mantida, permanecendo intactas as interações inter- e extracelulares, os componentes da matriz celular e a capacidade metabólica no microambiente celular (Salas et al., 2020).

Resultados dos estudos *in vitro* (Capítulo 2) demonstraram alta suscetibilidade das células somáticas (Leydig e Sertoli) à exposição das Cit_SPIONs, destacando a internalização acentuada nas células de Leydig. Alterações relevantes também foram obtidas nos espermatozoides expostos às Cit_SPIONs, como diminuição da viabilidade, motilidade,

integridade do DNA, aumento de EROs, alterações na função mitocondrial e peroxidação lipídica. Esses resultados indicam que o aumento da geração de EROs desempenharam papel importante na toxicidade das células testiculares.

No Capítulo 3, avaliamos os efeitos da injeção intratesticular de Cit_SPIONs nas células de Leydig e nos espermatozoides de camundongos. Utilizamos modelos *in vivo* com o intuito de observar o acúmulo e os efeitos da exposição a longo prazo. Várias pesquisas demonstraram os efeitos de diversas NPs por diferentes vias de administração (Dantas et al., 2022). Entretanto, neste estudo, optamos pela injeção intratesticular para observar os impactos locais durante a exposição das células testiculares às Cit_SPIONs. Uma vez que, a administração sistêmica poderia subestimar os efeitos adversos, através do processo de metabolização. A introdução de NPs em fluidos biológicos pode resultar na formação do efeito corona, ou seja, na adsorção espontânea de proteínas, lipídios, porções de açúcar, ácidos nucléicos e metabólitos na superfície de NMs (Wan et al., 2015; Martel et al., 2016; Ke et al., 2017; Lima et al., 2020; Zhang et al., 2022; Mahmoudi et al., 2023). Devido às propriedades físico-químicas das NPs e das complexidades das matrizes biológicas, os efeitos das NPs, incluindo função, absorção, biodistribuição, respostas imunológicas e toxicidade podem alterar imprevisivelmente (Lesniak et al., 2012; Bertrand et al., 2017; Chen et al., 2017; Francia et al., 2019; Chetwynd et al., 2020; Fadare et al., 2020). A escolha da concentração das NPs foi baseada em estudos anteriores *in vitro* realizados por nosso grupo de pesquisa, que demonstraram a biocompatibilidade das Cit_SPIONs em células fibroblásticas (Ferraz et al., 2020).

Os resultados obtidos com o estudo *in vivo* (Capítulo 3) demonstraram que após a injeção intratesticular, as Cit_SPIONs apresentaram uma biodistribuição disseminada em diferentes regiões testiculares, após 56 dias da injeção intratesticular. Entretanto, observou-se uma maior concentração nas células de Leydig, com consequente diminuição da atividade esteroidogênica e redução dos níveis de testosterona. Além disso, alterações secundárias foram

observadas, como alterações dos túbulos seminíferos, perda de células germinativas, danos no DNA de espermátides alongadas e redução da produção de espermatozoides. Curiosamente, a distribuição de Cit_SPIONs foi específica no tecido testicular, não sendo observada a sua presença no parênquima renal, pulmonar ou hepático. Esses achados sugerem que o acúmulo de Cit_SPIONs nas células de Leydig, somado à diminuição da atividade esteroidogênica e redução dos níveis de testosterona, foram fundamentais para aumentar a vulnerabilidade das células germinativas e dos espermatozoides.

Apesar de ser um componente essencial para o desenvolvimento de diferentes tipos celulares, o ferro se torna tóxico em excesso (Kaplan, 2002; Leichtmann-Bardoogo et al., 2012; Tvrda et al., 2015a; Liu et al., 2022;). Nos testículos, o desenvolvimento e a alta taxa mitótica das células germinativas masculinas necessitam de altas taxas de ferro (Tvrda et al., 2015a; Liu et al., 2022;). O ferro é necessário para a síntese de DNA, crescimento celular e mitocondriogênese das células germinativas (Aitken e Curry, 2011; Leichtmann-Bardoogo et al., 2012; Tvrda et al., 2015b; Liu et al., 2022). Portanto, a espermatogênese é um processo altamente dependente de ferro (Liu et al., 2022; Tvrda et al., 2015a). Assim, os sistemas de transporte e absorção de ferro pelas células germinativas são fortemente regulados pela barreira hematotesticular que protege as células germinativas meióticas e pós-meióticas (Aitken e Curry, 2011). Além disso, as espermátides e os espermatozoides em maturação são extremamente vulneráveis ao estresse oxidativo, implicando na necessidade de uma homeostase de ferro bem equilibrada no TS (Aitken e Curry, 2011).

Leichtmann-Bardoogo et al. (2012) avaliaram a deposição e as proteínas de transporte de ferro em testículos de camundongos com sobrecarga do elemento. Observaram que o ferro se acumulou principalmente ao redor dos túbulos seminíferos (TS), com pequenas quantidades localizadas no interior deles. Dessa forma, esses resultados sugerem que a localização preferencial das Cit_SPIONs nas células de Leydig estão diretamente relacionados com a

regulação pela barreira hematotesticular. Além disso, com relação às alterações observadas nos espermatozoides em nosso estudo especulamos que, a sobrecarga de ferro testicular, a inativação de enzimas antioxidantes e os distúrbios do metabolismo lipídico podem ter causado a morte oxidativa substancial (ferroptose) das células.

Dados preliminares de estudos *in vitro* usando fibroblastos humanos, realizados em nosso laboratório, mostraram que essas NPs apresentaram rápida e alta eficiência de internalização celular, baixa citotoxicidade e alta indução de morte celular (apoptose) após hipertermia magnética (Ferraz et al., 2020). Nossos dados, obtidos nos estudos *in vitro* e *in vivo*, demonstraram que as células testiculares, principalmente as células de Leydig e os espermatozoides são sensíveis às SPIONs. Assim, esses resultados com as SPIONs abrem perspectivas para o desenvolvimento de tecnologias voltadas para esterilização/contracepção masculina. Uma dessas possibilidades é o desenvolvimento de uma técnica baseada em nanopartículas magnéticas (NPMs) de magnetita (Fe_3O_4) associadas a um campo magnético, que tem como princípio promover a hipertermia testicular e interrupção da espermatogênese. Além disso, nossas descobertas abrem novas perspectivas para o desenvolvimento de terapias utilizando SPIONs para modular a função das células de Leydig como, por exemplo, terapias anti-androgênicas para combater cânceres do sistema reprodutor masculino dependentes de andrógenos.

CONCLUSÕES

Artigo 1: Male reproductive toxicity of inorganic nanoparticles in rodent models: A systematic review

- Os resultados mostraram uma boa correlação dos efeitos encontrados *in vitro* e *in vivo*;

- A funcionalização da superfície das nanopartículas demonstrou ser uma forma eficiente para a redução dos efeitos tóxicos;
- Os artigos avaliados apresentaram resultados totalmente variados, devido à falta de padronização do tamanho das NPs, das concentrações/doses e das vias de administração;
- Os efeitos das NPs à longo prazo, a exposição materna e a toxicidade fetal foram pouco explorados;
- A maioria dos estudos não fornecem informações detalhadas sobre as vias de toxicidade celular;
- O aumento de EROs e o estresse oxidativo mostrou-se como um dos principais mecanismos de toxicidade das NPs inorgânicas;
- As IONPs foram pouco estudadas quanto à toxicidade reprodutiva.
- Esses resultados mostram a necessidade de implantação de uma regulamentação, com protocolos padronizados para prever os efeitos toxicológicos, agudos e crônicos, das NPs na saúde e no meio ambiente.

Artigo 2: The toxicity of superparamagnetic iron oxide nanoparticles induced on the testicular cells: *in vitro* study

- As Cit_SPIONs foram eficientemente caracterizadas físico-quimicamente em relação ao seu tamanho, forma, composição e magnetização;
- As células somáticas testiculares (Leydig e Sertoli) e os espermatozoides mostraram-se sensíveis aos efeitos das Cit_SPIONs;
- A internalização acentuada de Cit_SPIONs nas células de Leydig contribuíram para suas alterações morfológicas;

- O aumento de EROs nas células espermáticas contribuíram para as alterações morfofuncionais observadas;
- As Cit_SPIONs apresentam toxicidade relevante para as células testiculares, através da indução de estresse oxidativo;

Artigo 3: Effects of superparamagnetic iron oxide nanoparticles (SPIONs) testicular injection on Leydig cell function and sperm production in a murine model

- O acúmulo preferencial de Cit_SPIONs nas células de Leydig levou à diminuição da atividade esteroidogênica e do suporte androgênico;
- Esse estudo destaca a suscetibilidade das células de Leydig e das células espermáticas às Cit_SPIONs;
- A vulnerabilidade das células germinativas, os danos no DNA de espermátides alongadas e a diminuição da produção diária de espermatozoides devem se tanto ao acúmulo de Cit_SPIONs no compartimento tubular, quanto à diminuição dos níveis de testosterona plasmática;
- A exposição às Cit_SPIONs não alterou a viabilidade, a morfologia dos espermatozoides e o ritmo da espermatogênese;
- A modulação da função das células de Leydig pelas Cit_SPIONs abrem novas possibilidades para o desenvolvimento de terapias anti-androgênicas e métodos de contracepção masculina.

REFERÊNCIAS

Abbasi Kajani, A., Haghjooy Javanmard, S., Asadnia, M., Razmjou, A., 2021. Recent Advances in Nanomaterials Development for Nanomedicine and Cancer. ACS Appl Bio Mater 4, 5908-5925 . https://doi.org/10.1021/acsabm.1c00591

Ahamed, M., 2013. Silica nanoparticles-induced cytotoxicity, oxidative stress and apoptosis in cultured A431 and A549 cells. Hum Exp Toxicol 32, 186–195. https://doi.org/10.1177/0960327112459206

Aitken, R.J., Curry, B.J., 2011. Redox Regulation of Human Sperm Function: From the Physiological Control of Sperm Capacitation to the Etiology of Infertility and DNA Damage in the Germ Line. Antioxidants & Redox Signaling 14, 367–381. https://doi.org/10.1089/ars.2010.3186

Aminabad, N.S., Farshbaf, M., Akbarzadeh, A., 2018. Recent Advances of Gold Nanoparticles in Biomedical Applications: State of the Art. Cell Biochem Biophys 77, 123–137. https://doi.org/10.1007/s12013-018-0863-4

Anselmo, A.C., Mitragotri, S., 2015. A Review of Clinical Translation of Inorganic Nanoparticles. AAPS Journal 17, 1041–1054. https://doi.org/10.1208/s12248-015-9780-2

Asare, N., Instanes, C., Sandberg, W.J., Refsnes, M., Schwarze, P., Kruszewski, M., Brunborg, G., 2012. Cytotoxic and genotoxic effects of silver nanoparticles in testicular cells. Toxicology 291, 65–72. https://doi.org/10.1016/j.tox.2011.10.022

Barkalina, N., Charalambous, C., Jones, C., Coward, K., 2014. Nanotechnology in reproductive medicine: Emerging applications of nanomaterials. Nanomedicine 10, e921-e938. https://doi.org/10.1016/j.nano.2014.01.001

Bayda, S., Adeel, M., Tuccinardi, T., Cordani, M., Rizzolio, F., 2020. The history of nanoscience and nanotechnology: From chemical-physical applications to nanomedicine. Molecules 25, 112. https://doi.org/10.3390/molecules25010112

Bertrand, N., Grenier, P., Mahmoudi, M., Lima, E.M., Appel, E.A., Dormont, F., Lim, J.M., Karnik, R., Langer, R., Farokhzad, O.C., 2017. Mechanistic understanding of in vivo protein corona formation on polymeric nanoparticles and impact on pharmacokinetics. Nat Commun 8. https://doi.org/10.1038/s41467-017-00600-w

Chen, P.C., Mwakwari, S.C., Oyelere, A.K., 2008. Gold nanoparticles: From nanomedicine to nanosensing, Nanotechnology, Science and Applications 2008, 45-66. https://doi.org/10.2147/NSA.S3707

Chen, Z., Zhang, A., Wang, X., Zhu, J., Fan, Y., Yu, H., Yang, Z., 2017. The Advances of Carbon Nanotubes in Cancer Diagnostics and Therapeutics. J Nanomater 2017, 13. https://doi.org/10.1155/2017/3418932

Chetwynd, A.J., Zhang, W., Thorn, J.A., Lynch, I., Ramautar, R., 2020. The Nanomaterial Metabolite Corona Determined Using a Quantitative Metabolomics Approach: A Pilot Study. Small 16, 000295. https://doi.org/10.1002/smll.202000295

Contera, S., de La Serna, J.B., Tetley, T.D., 2021. Biotechnology, nanotechnology and medicine. Emerg Top Life Sci. 4, 551–554. https://doi.org/10.1042/ETLS20200350

Cypriyana P J, J., S, S., Angalene J, L.A., Samrot, A. v., Kumar S, S., Ponniah, P., Chakravarthi, S., 2021. Overview on toxicity of nanoparticles, it's mechanism, models used in toxicity studies and disposal methods – A review. Biocatal Agric Biotechnol. 36, 102117. https://doi.org/10.1016/j.bcab.2021.102117

Dantas, G.P.F., Ferraz, F.S., Andrade, L.M., Costa, G.M.J., 2022. Male reproductive toxicity of inorganic nanoparticles in rodent models: A systematic review. Chem Biol Interact. 363, 110023. https://doi.org/10.1016/j.cbi.2022.110023

Ding, W., Chen, Zhichuan, Gu, Y., Chen, Zhengru, Zheng, Y., Sun, F., 2021. Magnetic Testis Targeting and Magnetic Hyperthermia for Noninvasive, Controllable Male Contraception via Intravenous Administration. Nano Lett 21, 6289–6297. https://doi.org/10.1021/acs.nanolett.1c02181

Durfey, C.L., Swistek, S.E., Liao, S.F., Crenshaw, M.A., Clemente, H.J., Thirumalai, R.V.K.G., Steadman, C.S., Ryan, P.L., Willard, S.T., Feugang, J.M., 2019. Nanotechnology-based approach for safer enrichment of semen with best spermatozoa. J Anim Sci Biotechnol 10, 14. https://doi.org/10.1186/s40104-018-0307-4

Egbuna, C., Parmar, V.K., Jeevanandam, J., Ezzat, S.M., Patrick-Iwuanyanwu, K.C., Adetunji, C.O., Khan, J., Onyeike, E.N., Uche, C.Z., Akram, M., Ibrahim, M.S., el Mahdy, N.M., Awuchi, C.G., Saravanan, K., Tijjani, H., Odoh, U.E., Messaoudi, M., Ifemeje, J.C., Olisah, M.C., Ezeofor, N.J., Chikwendu, C.J., Ibeabuchi, C.G., 2021. Toxicity of Nanoparticles in Biomedical Application: Nanotoxicology. J Toxicol. 2021, 21. https://doi.org/10.1155/2021/9954443

Fadare, O.O., Wan, B., Liu, K., Yang, Y., Zhao, L., Guo, L.H., 2020. Eco-Corona vs Protein Corona: Effects of Humic Substances on Corona Formation and Nanoplastic Particle Toxicity in Daphnia magna. Environ Sci Technol 54, 8001–8009. https://doi.org/10.1021/acs.est.0c00615

Fatima, H., Kim, K.S., 2018. Iron-based magnetic nanoparticles for magnetic resonance imaging. Advanced Powder Technology 29, 2678–2685. https://doi.org/10.1016/j.apt.2018.07.017

Ferraz, F.S., López, J.L., Lacerda, S.M.S.N., Procópio, M.S., Figueiredo, A.F.A., Martins, E.M.N., Guimarães, P.P.G., Ladeira, L.O., Kitten, G.T., Dias, F.F., Domingues, R.Z., Costa, G.M.J., 2020. Biotechnological approach to induce human fibroblast apoptosis using superparamagnetic iron oxide nanoparticles. J Inorg Biochem 206, 111017. https://doi.org/10.1016/j.jinorgbio.2020.111017

Feugang, J.M., 2017. Novel agents for sperm purification, sorting, and imaging. Mol Reprod Dev. 84:832–841. https://doi.org/10.1002/mrd.22831

França, L.R., Hess, R.A., Dufour, J.M., Hofmann, M.C., Griswold, M.D., 2016. The Sertoli cell: one hundred fifty years of beauty and plasticity. Andrology 4, 189–212. https://doi.org/doi:10.1111/andr.12165.

Francia, V., Yang, K., Deville, S., Reker-Smit, C., Nelissen, I., Salvati, A., 2019. Corona Composition Can Affect the Mechanisms Cells Use to Internalize Nanoparticles. ACS Nano 13, 11107–11121. https://doi.org/10.1021/acsnano.9b03824

Habas, K., Demir, E., Guo, C., Brinkworth, M.H., Anderson, D., 2021. Toxicity mechanisms of nanoparticles in the male reproductive system. Drug Metab Rev. 53, 604-617. https://doi.org/10.1080/03602532.2021.1917597

Hadrup, N., Lam, H.R., 2014. Oral toxicity of silver ions, silver nanoparticles and colloidal silver - A review. Regulatory Toxicology and Pharmacology 68, 1–7. https://doi.org/10.1016/j.yrtph.2013.11.002

Heinrich, A., DeFalco, T., 2020a. Essential roles of interstitial cells in testicular development and function. Andrology 8, 903–914. https://doi.org/10.1111/andr.12703

Heinrich, A., DeFalco, T., 2020b. Essential roles of interstitial cells in testicular development and function. Andrology 8, 903–914. https://doi.org/10.1111/andr.12703

Jia, J., Wang, Z., Yue, T., Su, G., Teng, C., Yan, B., 2020. Crossing biological barriers by engineered nanoparticles. Chem Res Toxicol 33, 1055–1060. https://doi.org/10.1021/acs.chemrestox.9b00483

Jivago, J.L.P.R., Brito, J.L.M., Capistrano, G., Vinícius-Araújo, M., Verde, E.L., Bakuzis, A.F., Souza, P.E.N., Azevedo, R.B., Lucci, C.M., 2021. New prospects in neutering male animals using magnetic nanoparticle hyperthermia. Pharmaceutics 13, 1465. https://doi.org/10.3390/pharmaceutics13091465

Kaplan, J., 2002. Strategy and tactics in the evolution of iron acquisition. Semin Hematol 39, 219–226. https://doi.org/10.1053/shem.2002.35631

Ke, P.C., Lin, S., Parak, W.J., Davis, T.P., Caruso, F., 2017. A Decade of the Protein Corona. ACS Nano. 11, 11773 – 11776. https://doi.org/10.1021/acsnano.7b08008

Khalid, K., Tan, X., Mohd Zaid, H.F., Tao, Y., Lye Chew, C., Chu, D.T., Lam, M.K., Ho, Y.C., Lim, J.W., Chin Wei, L., 2020. Advanced in developmental organic and inorganic nanomaterial: a review. Bioengineered. 11, 328–355. https://doi.org/10.1080/21655979.2020.1736240

Kim, T.S., Lee, S.H., Gang, G.T., Lee, Y.S., Kim, S.U., Koo, D.B., Shin, M.Y., Park, C.K., Lee, D.S., 2010. Exogenous DNA uptake of boar spermatozoa by a magnetic nanoparticle vector system. Reproduction in Domestic Animals 45, e201– e206 https://doi.org/10.1111/j.1439-0531.2009.01516.x

Kinnear, C., Moore, T.L., Rodriguez-Lorenzo, L., Rothen-Rutishauser, B., Petri-Fink, A., 2017. Form Follows Function: Nanoparticle Shape and Its Implications for Nanomedicine. Chem Rev. 117, 11476−11521. https://doi.org/10.1021/acs.chemrev.7b00194

Kolosnjaj-Tabi, J., Wilhelm, C., 2017. Magnetic nanoparticles in cancer therapy: How can thermal approaches help? Nanomedicine. 12, 573–575. https://doi.org/10.2217/nnm-2017-0014

Kong, L., Hu, W., Lu, C., Cheng, K., Tang, M., 2019. Mechanisms underlying nickel nanoparticle induced reproductive toxicity and chemo-protective effects of vitamin C in male rats. Chemosphere 218, 259–265. https://doi.org/10.1016/j.chemosphere.2018.11.128

Krawetz, S.A., De Rooij, D.G., Hedger, M.P., 2009. Molecular aspects of male fertility. International Workshop on Molecular Andrology. EMBO Rep 10, 1087–1092. https://doi.org/10.1038/embor.2009.211

Kumar, A., Kumar, P., Anandan, A., Fernandes, T.F., Ayoko, G.A., Biskos, G., 2014. Engineered nanomaterials: Knowledge gaps in fate, exposure, toxicity, and future directions. J Nanomater 2014, 16. https://doi.org/10.1155/2014/130198

Lan, Z., Yang, W.X., 2012. Nanoparticles and spermatogenesis: How do nanoparticles affect spermatogenesis and penetrate the blood-testis barrier. Nanomedicine 7, 579–596. https://doi.org/10.2217/nnm.12.20

Leichtmann-Bardoogo, Y., Cohen, L.A., Weiss, A., Marohn, B., Schubert, S., Meinhardt, A., Meyron-Holtz, E.G., 2012. Compartmentalization and regulation of iron metabolism proteins protect male germ cells from iron overload. Am J Physiol Endocrinol Metab 302, E1519-E1530. https://doi.org/10.1152/ajpendo.00007.2012

Lesniak, A., Fenaroli, F., Monopoli, M.P., Åberg, C., Dawson, K.A., Salvati, A., 2012. Effects of the presence or absence of a protein corona on silica nanoparticle uptake and impact on cells. ACS Nano 6, 5845–5857. https://doi.org/10.1021/nn300223w

Li, X., Wang, L., Fan, Y., Feng, Q., Cui, F.Z., 2012. Biocompatibility and toxicity of nanoparticles and nanotubes. J Nanomater. 2012, 19. https://doi.org/10.1155/2012/548389

Lima, T., Bernfur, K., Vilanova, M., Cedervall, T., 2020. Understanding the Lipid and Protein Corona Formation on Different Sized Polymeric Nanoparticles. Sci Rep 10, 1129. https://doi.org/10.1038/s41598-020-57943-6

Liu, Y., Cao, X., He, C., Guo, X., Cai, H., Aierken, A., Hua, J., Peng, S., 2022. Effects of Ferroptosis on Male Reproduction. Int J Mol Sci. 23, 7139. https://doi.org/10.3390/ijms23137139

Liu, Y., Li, X., Xiao, S., Liu, X., Chen, X., Xia, Q., Lei, S., Li, H., Zhong, Z., Xiao, K., 2020. The effects of gold nanoparticles on leydig cells and male reproductive function in mice. Int J Nanomedicine 15, 9499–9514. https://doi.org/10.2147/IJN.S276606

Luo, X., Jia, K., Xing, J., Yi, J., 2024. The utilization of nanotechnology in the female reproductive system and related disorders. Heliyon 10, e25477. https://doi.org/10.1016/j.heliyon.2024.e25477

Mahmoudi, M., Landry, M.P., Moore, A., Coreas, R., 2023. The protein corona from nanomedicine to environmental science. Nat Rev Mater 8, 422–438. https://doi.org/10.1038/s41578-023-00552-2

Malik, S., Muhammad, K., Waheed, Y., 2023. Nanotechnology: A Revolution in Modern Industry. Molecules 2, 661. https://doi.org/10.3390/molecules28020661

Manke, A., Wang, L., Rojanasakul, Y., 2013. Mechanisms of nanoparticle-induced oxidative stress and toxicity. Biomed Res Int. 2013, 15. https://doi.org/10.1155/2013/942916

Mansoori, G.A., Soelaiman, T.A.F., 2005. Nanotechnology-An Introduction for the Standards Community, Journal of ASTM International 2, 1-22. https://doi.org/10.1520/JAI1311

Martel, J., Wu, C.Y., Hung, C.Y., Wong, T.Y., Cheng, A.J., Cheng, M.L., Shiao, M.S., Young, J.D., 2016. Fatty acids and small organic compounds bind to mineralo-organic nanoparticles derived from human body fluids as revealed by metabolomic analysis. Nanoscale 8, 5537–5545. https://doi.org/10.1039/c5nr08116e

Meena, R., Kajal, K., R, P., 2014. Cytotoxic and Genotoxic Effects of Titanium Dioxide Nanoparticles in Testicular Cells of Male Wistar Rat. Appl Biochem Biotechnol 175, 825–840. https://doi.org/10.1007/s12010-014-1299-y

Mima, M., Greenwald, D., Ohlander, S., 2018. Environmental Toxins and Male Fertility. Curr Urol Rep. 19, 50. https://doi.org/10.1007/s11934-018-0804-1

Mourdikoudis, S., Pallares, R.M., Thanh, N.T.K., 2018. Characterization techniques for nanoparticles: Comparison and complementarity upon studying nanoparticle properties. Nanoscale 10, 12871. https://doi.org/10.1039/c8nr02278j

Moysidou, C.M., Barberio, C., Owens, R.M., 2021. Advances in Engineering Human Tissue Models. Front Bioeng Biotechnol. 8, 620962. https://doi.org/10.3389/fbioe.2020.620962

Mruk, D.D., Cheng, C.Y., 2015. The mammalian blood-testis barrier: Its biology and regulation. Endocr Rev. 36, 564–591. https://doi.org/10.1210/er.2014-1101

Odhiambo, J.F., DeJarnette, J.M., Geary, T.W., Kennedy, C.E., Suarez, S.S., Sutovsky, M., Sutovsky, P., 2014. Increased conception rates in beef cattle inseminated with nanopurified bull semen. Biol Reprod 91, 1-10. https://doi.org/10.1095/biolreprod.114.121897

O'Donnell, L., Smith, L.B., Rebourcet, D., 2022. Sertoli cells as key drivers of testis function. Semin Cell Dev Biol. 121, 2-9. https://doi.org/10.1016/j.semcdb.2021.06.016

Olugbodi, J.O., David, O., Oketa, E.N., Lawal, B., Okoli, B.J., Mtunzi, F., 2020. Silver nanoparticles stimulates spermatogenesis impairments and hematological alterations in testis and epididymis of Male rats. Molecules 25, 1063. https://doi.org/10.3390/molecules25051063

Patil, R., Kale, A., Mane, D., Patil, D., 2020. Isolation, culture and characterization of primary cell lines of human buccal mucosal fibroblasts: A combination of explant enzamytic technique. Journal of Oral and Maxillofacial Pathology 24, 68–75. https://doi.org/10.4103/jomfp.JOMFP_282_19

Patil, U.S., Adireddy, S., Jaiswal, A., Mandava, S., Lee, B.R., Chrisey, D.B., 2015. In vitro/in vivo toxicity evaluation and quantification of iron oxide nanoparticles. Int J Mol Sci. 16, 24417-24450. https://doi.org/10.3390/ijms161024417

Pham, H.N., Pham, T.H.G., Nguyen, D.T., Phan, Q.T., Le, T.T.H., Ha, P.T., Do, H.M., Hoang, T.M.N., Nguyen, X.P., 2017. Magnetic inductive heating of organs of mouse models treated by copolymer coated Fe3O4 nanoparticles. Advances in Natural Sciences: Nanoscience and Nanotechnology 8, 025013. https://doi.org/10.1088/2043-6254/aa5e23

Pinho, A.R., Rebelo, S., de Lourdes Pereira, M., 2020. The impact of zinc oxide nanoparticles on male (In)fertility. Materials 13, 1–18. https://doi.org/10.3390/ma13040849

Piwocka, O., Musielak, M., Ampuła, K., Piotrowski, I., Adamczyk, B., Fundowicz, M., Suchorska, W.M., Malicki, J., 2024. Navigating challenges: optimising methods for primary cell culture isolation. Cancer Cell Int 24, 28. https://doi.org/10.1186/s12935-023-03190-4

Ratner, B.D., 2019. Biomaterials: Been There, Done That, and Evolving into the Future. Annu. Rev. Biomed. Eng 21, 171–191. https://doi.org/10.1146/annurev-bioeng-062117

Remião, M.H., Segatto, N. V., Pohlmann, A., Guterres, S.S., Seixas, F.K., Collares, T., 2018. The potential of nanotechnology in medically assisted reproduction. Front Pharmacol 8. https://doi.org/10.3389/fphar.2017.00994

Sack, M., Alili, L., Karaman, E., Das, S., Gupta, A., Seal, S., Brenneisen, P., 2014. Combination of conventional chemotherapeutics with redox-active cerium oxide nanoparticles - A novel aspect in cancer therapy. Mol Cancer Ther 13, 1740–1749. https://doi.org/10.1158/1535-7163.MCT-13-0950

Salas, A., López, J., Reyes, R., Évora, C., de Oca, F.M., Báez, D., Delgado, A., Almeida, T.A., 2020. Organotypic culture as a research and preclinical model to study uterine leiomyomas. Sci Rep 10, 5212. https://doi.org/10.1038/s41598-020-62158-w

Savage, D.T., Hilt, J.Z., Dziubla, T.D., 2019. In vitro methods for assessing nanoparticle toxicity, in: Methods in Molecular Biology. Humana Press Inc., pp. 1–29. https://doi.org/10.1007/978-1-4939-8916-4_1

Schemberg, J., Abbassi, A. El, Lindenbauer, A., Chen, L.Y., Grodrian, A., Nakos, X., Apte, G., Khan, N., Kraupner, A., Nguyen, T.H., Gastrock, G., 2022. Synthesis of Biocompatible Superparamagnetic Iron Oxide Nanoparticles (SPION) under Different Microfluidic Regimes. ACS Appl Mater Interfaces 14, 48011–48028. https://doi.org/10.1021/acsami.2c13156

Schulz, R.W., Nóbrega, R.H., 2011. The reproductive organs and processes | Regulation of Spermatogenesis, in: Encyclopedia of Fish Physiology. Elsevier Inc., pp. 627–634. https://doi.org/10.1016/B978-0-12-374553-8.00269-0

Shandilya, R., Mishra, P.K., Pathak, N., Lohiya, N.K., Sharma, R.S., 2020. Nanotechnology in reproductive medicine: Opportunities for clinical translation. Clin Exp Reprod Med 47, 245–262. https://doi.org/10.5653/cerm.2020.03650

Shen, J., Yang, D., Zhou, X., Wang, Y., Tang, S., Yin, H., Wang, J., Chen, R., Chen, J., 2019. Role of autophagy in zinc oxide nanoparticles-induced apoptosis of mouse LEYDIG cells. Int J Mol Sci 20, 4042. https://doi.org/10.3390/ijms20164042

Sosa-Acosta, J.R., Iriarte-Mesa, C., Ortega, G.A., Díaz-García, A.M., 2020. DNA–Iron Oxide Nanoparticles Conjugates: Functional Magnetic Nanoplatforms in Biomedical Applications. Top Curr Chem 378, 1–29. https://doi.org/10.1007/s41061-019-0277-9

Souza, M.R., Mazaro-Costa, R., Rocha, T.L., 2021. Can nanomaterials induce reproductive toxicity in male mammals? A historical and critical review. Science of the Total Environment 769, 144354. https://doi.org/10.1016/j.scitotenv.2020.144354

Suciu, M., Ionescu, C.M., Ciorita, A., Tripon, S.C., Nica, D., Al-Salami, H., Barbu-Tudoran, L., 2020. Applications of superparamagnetic iron oxide nanoparticles in drug and therapeutic delivery, and biotechnological advancements. Beilstein Journal of Nanotechnology 11, 1092–1109. https://doi.org/10.3762/BJNANO.11.94

Svingen, T., Koopman, P., 2013. Building the mammalian testis: Origins, differentiation, and assembly of the component cell populations. Genes Dev. 27, 2409-2426. https://doi.org/10.1101/gad.228080.113

Tang, Y., Chen, B., Hong, W., Chen, L., Yao, L., Zhao, Y., Aguilar, Z.P., Xu, H., 2019. ZnO nanoparticles induced male reproductive toxicity based on the effects on the endoplasmic reticulum stress signaling pathway. Int J Nanomedicine 14, 9563–9576. https://doi.org/10.2147/IJN.S223318

Titus, D., James Jebaseelan Samuel, E., Roopan, S.M., 2018. Nanoparticle characterization techniques, in: Green Synthesis, Characterization and Applications of Nanoparticles. Elsevier, pp. 303–319. https://doi.org/10.1016/B978-0-08-102579-6.00012-5

Tsakmakidis, I.A., Samaras, T., Anastasiadou, S., Basioura, A., Ntemka, A., Michos, I., Simeonidis, K., Karagiannis, I., Tsousis, G., Angelakeris, M., Boscos, C.M., 2020. Iron oxide nanoparticles as an alternative to antibiotics additive on extended boar semen. Nanomaterials 10, 1–16. https://doi.org/10.3390/nano10081568

Tvrda, E., Peer, R., Sikka, S.C., Agarwal, A., 2015a. Iron and copper in male reproduction: a double-edged sword. J Assist Reprod Genet 32, 3–16. https://doi.org/10.1007/s10815-014-0344-7

Tvrda, E., Peer, R., Sikka, S.C., Agarwal, A., 2015b. Iron and copper in male reproduction: a double-edged sword. J Assist Reprod Genet 32, 3–16. https://doi.org/10.1007/s10815-014-0344-7

Vaira, V., Fedele, G., Pyne, S., Fasoli, E., Zadra, G., Bailey, D., Snyder, E., Faversani, A., Coggi, G., Flavin, R., Bosari, S., Loda, M., 2010. Preclinical model of organotypic culture for pharmacodynamic profiling of human tumors. Proc Natl Acad Sci U S A 107, 8352–8356. https://doi.org/10.1073/pnas.0907676107

Vallabani, N.V.S., Singh, S., Karakoti, A.S., 2018. Magnetic Nanoparticles: Current Trends and Future Aspects in Diagnostics and Nanomedicine. Curr Drug Metab 20, 457–472. https://doi.org/10.2174/1389200220666181122124458

Vangijzegem, T., Stanicki, D., Laurent, S., 2019. Magnetic iron oxide nanoparticles for drug delivery: applications and characteristics. Expert Opin Drug Deliv 16, 69–78. https://doi.org/10.1080/17425247.2019.1554647

Wan, S., Kelly, P.M., Mahon, E., Stöckmann, H., Rudd, P.M., Caruso, F., Dawson, K.A., Yan, Y., Monopoli, M.P., 2015. The “sweet” Side of the protein corona: Effects of glycosylation on nanoparticle-cell interactions. ACS Nano 9, 2157–2166. https://doi.org/10.1021/nn506060q

Wang, F., Gao, F., Lan, M., Yuan, H., Huang, Y., Liu, J., 2009. Oxidative stress contributes to silica nanoparticle-induced cytotoxicity in human embryonic kidney cells. Toxicology in Vitro 23, 808–815. https://doi.org/10.1016/j.tiv.2009.04.009

Wang, R., Song, B., Wu, J., Zhang, Y., Chen, A., Shao, L., 2018. Potential adverse effects of nanoparticles on the reproductive system. Int J Nanomedicine 13, 8487–8506. https://doi.org/10.2147/IJN.S170723

Wu, Y., Kong, L., 2020. Advance on toxicity of metal nickel nanoparticles. Environ Geochem Health 42, 2277–2286. https://doi.org/10.1007/s10653-019-00491-4

Yan Cheng, C., Mruk, D.D., 2012. The blood-testis barrier and its implications for male contraception. Pharmacol Rev 64, 16–64. https://doi.org/10.1124/pr.110.002790

Yang, H., Liu, C., Yang, D., Zhang, H., Xi, Z., 2009. Comparative study of cytotoxicity, oxidative stress and genotoxicity induced by four typical nanomaterials: The role of particle size, shape and composition. Journal of Applied Toxicology 29, 69–78. https://doi.org/10.1002/jat.1385

Zanganeh, S., Hutter, G., Spitler, R., Lenkov, O., Mahmoudi, M., Shaw, A., Pajarinen, J.S., Nejadnik, H., Goodman, S., Moseley, M., Coussens, L.M., Daldrup-Link, H.E., 2016. Iron oxide nanoparticles inhibit tumour growth by inducing pro-inflammatory macrophage polarization in tumour tissues. Nat Nanotechnol 11, 986–994. https://doi.org/10.1038/nnano.2016.168

Zhang, W., Chetwynd, A.J., Thorn, J.A., Lynch, I., Ramautar, R., 2022. Understanding the Significance of Sample Preparation in Studies of the Nanoparticle Metabolite Corona. ACS Measurement Science Au 2, 251–260. https://doi.org/10.1021/acsmeasuresciau.2c00003.

ANEXOS

Patente

INSTITUTO NACIONAL DA PROPRIEDADE INDUSTRIAL

09/09/2022 870220082311 16:20

29409161948459727

Pedido nacional de Invenção, Modelo de Utilidade, Certificado de Adição de Invenção e entrada na fase nacional do PCT

Número do Processo: BR 10 2022 018099 7

Dados do Depositante (71)

Depositante 1 de 2

Nome ou Razão Social: UNIVERSIDADE FEDERAL DE MINAS GERAIS

Tipo de Pessoa: Pessoa Jurídica

CPF/CNPJ: 17217985000104

Nacionalidade: Brasileira

Qualificação Jurídica: Instituição de Ensino e Pesquisa

Endereço: Av. Antônio Carlos, 6627 - Unidade Administrativa II - 2º andar- sala 2011

Cidade: Belo Horizonte

Estado: MG

CEP: 31270-901